AD_____

Award Number: DAMD17-02-1-0095

TITLE: Hyaluronic Acid and Hyaluronidase in Prostate Cancer: Evaluation of Their Therapeutic and Prognostic Potential

PRINCIPAL INVESTIGATOR: Vinata B. Lokeshwar, Ph.D.

CONTRACTING ORGANIZATION: University of Miami
Miami, FL 33136

REPORT DATE: January 2006

TYPE OF REPORT: Final

PREPARED FOR: U.S. Army Medical Research and Materiel Command
Fort Detrick, Maryland 21702-5012

DISTRIBUTION STATEMENT: Approved for Public Release;
Distribution Unlimited

The views, opinions and/or findings contained in this report are those of the author(s) and should not be construed as an official Department of the Army position, policy or decision unless so designated by other documentation.

20060508031

REPORT DOCUMENTATION PAGE

Form Approved
OMB No. 0704-0188

1. REPORT DATE	2. REPORT TYPE	3. DATES COVERED
01-01-2006	Final	1 Jan 2002 – 31 Dec 2005

4. TITLE AND SUBTITLE

Hyaluronic Acid and Hyaluronidase in Prostate Cancer: Evaluation of Their Therapeutic and Prognostic Potential

5a. CONTRACT NUMBER

5b. GRANT NUMBER
DAMD17-02-1-0095

5c. PROGRAM ELEMENT NUMBER

6. AUTHOR(S)

Vinata B. Lokeshwar, Ph.D.

5d. PROJECT NUMBER

5e. TASK NUMBER

5f. WORK UNIT NUMBER

7. PERFORMING ORGANIZATION NAME(S) AND ADDRESS(ES)

University of Miami
Miami, FL 33136

8. PERFORMING ORGANIZATION REPORT NUMBER

9. SPONSORING / MONITORING AGENCY NAME(S) AND ADDRESS(ES)
U.S. Army Medical Research and Materiel Command
Fort Detrick, Maryland 21702-5012

10. SPONSOR/MONITOR'S ACRONYM(S)

11. SPONSOR/MONITOR'S REPORT NUMBER(S)

12. DISTRIBUTION / AVAILABILITY STATEMENT
Approved for Public Release; Distribution Unlimited

13. SUPPLEMENTARY NOTES

14 ABSTRACT
Identification of accurate prognostic indicators could aid in individualization of treatment and better prediction of outcome or prostate cancer patients. Treatment modalities that target these molecules could effectively control CaP progression. The results of this project identify HYAL1 type hyaluronidase (HAase) as one such molecule. HA is a glycosaminoglycan and HAase is an enzyme that degrades HA into angiogenic fragments. Immunohistochemical analysis using archival radical prostatectomy CaP specimens from patients on whom there is 72 - 131 month follow-up show that HYAL1 and combined HA-HYAL1 inferences staining are independent predictors for biochemical recurrence. Studies on HYAL1 transfectants show that blocking HYAL1 expression in CaP cells, decreases growth by blocking cell cycle progression and invasive activity by 3-4-fold. HYAL1-AS transfectants show a 4-7-fold decrease in tumor growth, and generate tumors that are non-infiltrating and less vascularized. Transfectants expressing **high HYAL1 levels** also grow 4-fold slower and undergo apoptosis. **High HYAL1 producing transfectants** show either decreased tumor growth (3-fold) or **do not form tumors**. Microarray analysis data support the role of HYAL1 as molecular determinant of prostate cancer. Analysis of 21 HAase inhibitors identified some compounds that show higher specificity to inhibit HYAL1 activity.

15. SUBJECT TERMS

HA, HAase, HYAL1, Prognostic Indicator, Chemotherapy, Combination Drug Treatmenter

16. SECURITY CLASSIFICATION OF:

a. REPORT	b. ABSTRACT	c. THIS PAGE	17. LIMITATION OF ABSTRACT	18. NUMBER OF PAGES	19a. NAME OF RESPONSIBLE PERSON USAMRMC
U	U	U	UU	112	19b. TELEPHONE NUMBER (include area code)

Standard Form 298 (Rev. 8-98)
Prescribed by ANSI Std. Z39.18

Table of Contents

1. Lokeshwar, VB, Schroeder, GL, Carey, RI, Soloway, MS., and Iida. JBC 277:33654-33663, 2002

2. Franzmann, EJ, Schoreder, GL, Goodwin, WJ, Weed, DT, Fisher, P, and Lokeshwar, VB., Int. J. Cancer 106:438-445, 2003

3. Posey, TJ, Soloway, MS, Ekici, S, Sofer, M, Civantos, F, Duncan, RC, Lokeshwar, VB,. Cancer Research 63:2638-2644, 2003

4. Dandekar, DS, Lokeshwar, VB, Cevallos-Arellano, E, Soloway, MS, Lokeshwar, BL., Cancer Chemother Pharmacol 52:59-66, 2003

5. Ekici, S, Cerwinka, W H, Duncan, RC, Gomez, P, Civantos, F, Soloway, MS, Lokeshwar, VB., Int. J. Cancer 112:121-129, 2004

6. Lokeshwar, VB, Cerwinka WH, Lokeshwar BL., Cancer Research 65:2243-2250

7. Lokeshwar, VB, Cerwinka WH, Lokeshwar BL., Cancer Research 65:7782-7789

8. Isoyama T, Thwaites, D, Selzer, MG, Carey, RI, Barbucci, R, and Lokeshwar, VB., Differential selectivity of hyaluronidase inhibitors toward acidic and basic hyaluronidases. Glycobiology 16: 11-21, 2006

9. Cohen, BL, Gomez, P, Omori, Y, Duncan, RC, Soloway, MS, Lokeshwar, VB, and Lokeshwar, BL., Cyclooxygenase-2 (COX-2) expression is an independent predictor of prostate cancer recurrence. Int. J. Cancer (In Press)

Principal Investigator: Vinata B. Lokeshwar, Ph.D.

Project Title: Hyaluronic acid and hyaluronidase in prostate cancer: Evaluation of their therapeutic and prognostic potential.

1. A. INTRODUCTION AND OBJECTIVES: There are two overall objectives of this funded project. The first is to evaluate the independent prognostic potential of two tumor markers, identified in our laboratory, i.e., hyaluronic acid (HA) and HYAL1 type hyaluronidase (HAase). The second objective is to evaluate the effect of HYAL1 inhibition on prostate cancer (CaP) growth and metastasis using two complementary approaches, i.e., the antisense approach and the use of a HAase inhibitor, VERSA-TL 502. We also plan to examine the mechanism by which HYAL1 regulates CaP cell growth and metastasis.

The majority of the newly diagnosed prostate cancer (CaP) patients have clinically organ-confined disease. However, limited knowledge about which CaP is likely to progress, as well as, when it will recur severely impedes individualized selection of therapy and subsequent prediction of outcome (1-5). Advances in tumor biology have unraveled genes and their products that closely associate and function in CaP growth, metastasis and angiogenesis (1,6-8). Some of the molecules may serve as accurate prognostic indicators. Moreover, treatment modalities that target the functions of these molecules could effectively control CaP progression. In preliminary studies we identified that HA and HYAL1 type HAase may be such markers. HA is a glycosaminoglycan that is made up of repeating disaccharide units, D-glucuronic acid and N-acetyl-D-glucosamine. It is abundantly present in tissues and tissue fluids. In addition to its structural role, HA regulates several cellular processes (9-10). Concentrations of HA are elevated in several cancers including those of colon, breast and in bladder (11-19). In a published report that we had presented as the preliminary evidence at the time of submission of this funded project, we demonstrated that HA levels are 4-8-fold elevated in CaP tissues, when compared to the normal prostate and benign prostatic hyperplasia tissues (20). Immunohistochemical analysis demonstrated that HA present in CaP tissues mostly localizes to the tumor-associated stroma. Small fragments of HA are known to be anigogenic and we showed the presence of such angiogenic HA fragments in high-grade CaP tissues.

HAase is an endoglycosidase that cleaves internal β-N-acetyl-D-glucosaminic linkages in the HA polymer, yielding HA fragments (21). At present 6 HAase genes have been identified, which cluster into two tightly linked triplets on chromosomes 3p21.3 (HYAL1, HYAL2 and HYAL3) and 7q31.3 (HYAL4, PH20, HYALp1) (22). Using RT-PCR, cDNA cloning/sequencing, cell-culture, immunoblotting and pH activity profile studies, we confirmed that HYAL1 is the HAase that is expressed in CaP tissues and it is secreted by CaP cells (23). We also showed that HAase levels are elevated in CaP tissues when compared to the levels in NAP and BPH tissues. Furthermore, the increase in HAase levels correlates with CaP progression (metastatic > high-grade >> low-grade (Gleason 5/6) > NAP/BPH) (23). By immunohistochemical analysis, which was presented as the preliminary evidence during the submission of this funded project, we showed that the HYAL1 type HAase is exclusively expressed in CaP cells. Based on our immunoshistochemical studies we hypothesized that HA and HYAL1 may be potentially accurate prognostic indicators for CaP. To investigate the function of HYAL1 we had stably transfected DU145 cells with full-length HYAL1 cDNA in the sense and antisense orientation and planned to study the behavior of DU145, as well as, PC3-ML transfectants both *in vitro* and *in vivo*. In addition, we had identified a HAase inhibitor, VERSA-TL502 (24). This inhibitor inhibits the HAase activity secreted by CaP cells (IC_{50} 2 µg/ml). We had hypothesized that VERSA-TL 502 may also inhibit CaP cell growth and invasive behavior, both *in vitro* and *in vivo*.

The following is a succinct report of the progress in achieving our objectives in the grant period.

B. (BODY): Progress related to Aim 1: To correlate HA and HYAL1 staining intensity and its pattern in CaP tissues with clinical outcome.

<u>Rationale and background</u>: Two studies were conducted under this aim. The first study involved evaluation of the prognostic potential of HA and HYAL1 to predict biochemical recurrence within 64 months (i.e., within 5-years). Our results show that HYAL1 either alone or in combination with HA is an independent predictor of biochemical recurrence in CaP patients. This study was presented in detail in the first year's progress report and has been published (25; Appendix 1). Out of the 70 patients that were included in that study follow-up of ≥ 72 months (72 to 131 months) was available on 66 patients. In the study described below, we compared the prognostic ability of HA and HYAL1 with two other potential prognostic indicators of CaP (i.e., CD44v6 and microvessel density (MVD)) to predict biochemical recurrence up to 131 months.

We chose to compare CD44v6 and MVD with HA and HYAL1 since all of these molecules are biologically related. For example, CD44 denotes a family of cell surface transmembrane glycoproteins which serve as the cell surface receptor for HA (26,27). Alternative splicing of CD44 mRNA in 10 of the 20 exons generates several variant CD44 isoforms (27,28). The correlation between tumor progression and CD44s and/or its isoforms is controversial. We and others have shown that the androgen insensitive CaP line PC-3 and primary PCa cells express CD44s and CD44 variants (e.g., CD44v3 and CD44v6), however, the androgen sensitive poorly metastatic line LNCaP does not express CD44 (29-31). Contrary to these findings, it has been shown that the over-expression of CD44v6 in a rat CaP line decreases metastasis (32). Recently, Ekici et al showed that decreased expression of CD44v6 could be a predictor of poor prognosis in clinically localized CaP (33). Aaltomaa et al also reported similar results (34).

Angiogenesis is an essential process for tumor growth and metastasis (35-37). As discussed above, degradation of HA by HAase generates angiogenic HA fragments. Clinical significance of angiogenesis, measured as microvessel density (MVD), has been demonstrated for several tumor types, including, gastrointestinal, breast, bladder and renal cell carcinomas (38-41). Studies that compared various endothelial cell markers (i.e., CD31, CD34 and Factor VIII) have shown that CD34 is a sensitive endothelial cell marker for measuring MVD (42,43). At the present time, the clinical significance of MVD, as an independent predictor of pathological stage and recurrence in PCa remains controversial (42-45).

Since HYAL1 degrades HA and generates angiogenic fragments and CD44 acts as a cell-surface receptor for both HA and HA fragments, it is interesting to examine whether these biologically linked molecules are accurate prognostic indicators for PCa, and whether they influence each other's prognostic capabilities.

Experimental procedures:
Specimens and study individuals: We initially chose 150 archival specimens from CaP patients who underwent retropubic prostatectomy for clinically localized CaP between 1992 and 1996. Out of these 150 patients, on 66 patients, a minimum available follow-up of 72 months was available. Of the 66 patients, 25 patients had biochemical or clinical recurrence before 72 months (mean time to recurrence: 21.3 months; range: 3 to 61 months), and 41 patients were free of disease recurrence (mean follow-up: 103 months; range: 72 - 131 months). Biochemical recurrence was defined as a PSA level ≥ 0.4 ng/ml in 2 successive measurements after the operation, in which case the first date of elevated PSA level was considered as the

date of failure. The patient characteristics with respect to age, preoperative PSA, and tumor (i.e., Gleason sum, stage, margin, extraprostatic extension (EPE) and seminal vesicle invasion) are shown in Table 1.

Table 1: Distribution of pre- and post-operative parameters among study patients. Note that biochemical recurrence with post-operative PSA levels ≥ 0.4 ng/ml within 72 months was used a cut point for defining progression. Thus, any CaP patient who showed a biochemical recurrence within 72 months was included in the progressed category.

Preoperative parameters				Postoperative parameters			
Progression	Age (yrs)	PSA (ng/ml)	Clinical Stage	Gleason sum	EPE	Margin	Seminal vesicle invasion
Biochemical recurrence (n = 25)	Median: 64 Mean: 65.1	Median: 9.0 Mean: 14.04	T1c: 10 T2a: 5 T2b: 10	6 = 2 7 = 14 8 = 6 9 = 3	(+) = 21 (-) = 4	(+)=18 (-)=7	(+) = 14 (-) = 11
No biochemical or clinical recurrence (n = 41)	Median: 65 Mean: 62.98	Median: 6 Mean: 8.1	T1c: 22 T2a: 5 T2b: 14	5 = 7 6 = 9 7 = 20 8 = 5	(+) = 4 (-) = 37	(+)=9 (-)=32	(+) = 3 (-) = 38

HA and HYAL1 staining: IHC localization of HA and HYAL1 in CaP tissues was carried out as described previously (20). For all specimens, paraffin-embedded blocks containing CaP tissues representing the majority of the Gleason sum were selected by the study's pathologist (Dr. Francisco Civantos). The blocks were cut into 3-μm thick sections and placed on positively charged slides. The specimens were deparafinized, rehydrated and treated with an Antigen-retrieval solution (Dako Laboratories). For each specimen, two slides were prepared, one for HA and the other for HYAL1 staining. For HA staining, the slides were incubated with 2 μg/ml of a biotinylated bovine nasal cartilage protein at room temperature for 35 min (20). The specificity of HA staining was established as described previously (20). Following incubation with the HA-binding protein, the slides were washed in phosphate buffered saline (PBS) and sequentially incubated with streptavidin peroxidase at room temperature for 30 min and 3,3'-diaminobenzidine (DAB) chromogen substrate solution (Dako Laboratories). The slides were counterstained with hematoxylin, dehydrated and mounted.

For HYAL1 staining, the slides were incubated with 3.7 μg/ml of anti-HYAL1 IgG at 4⁰ C for 16 hr. Rabbit polyclonal anti-HYAL1 IgG was generated against a peptide sequence present in HYAL1 protein (amino acids 321 to 338) and its specificity for IHC was confirmed as described previously (20, 25). Following incubation with anti-HYAL1 IgG, the slides were washed in PBS and incubated with a linking solution containing a biotinylated goat anti-rabbit IgG (Dako LSAB kit) at room temperature for 30 min. The slides were then treated with streptavidin peroxidase and DAB chromogen. The slides were counterstained with hematoxylin, dehydrated and mounted.

Slide grading for HA and HYAL1: Two readers independently evaluated all slides in a blinded fashion. Any discrepancy in assigning staining intensity was resolved by both readers reexamining those slides simultaneously. The staining for HA and HYAL-1 was graded as 0 (no staining), 1+, 2+, and 3+. For HA staining, both the tumor-associated stroma and tumor cells

were graded in each slide. The overall staining grade for each slide was assigned based on the staining intensity of the majority of the tumor tissue in the specimen. However, if ~ 50% of the tumor tissue stained as 1+ and the other 50% as 3+, the overall staining grade was 2+. If the staining distribution was ~ 50% of the tumor staining 2+ and the remaining staining as 3+, the overall staining inference was assigned as 3+. The staining scale was further subcategorized into low grade and high grade. For HA staining, low-grade staining included 0, 1+ and 2+ staining, and high-grade staining included 3+ intensity. In those cases (n = 2) where the stromal tissues were evaluated as low-grade staining but the tumor cells stained as 3+, the overall HA staining was considered as high grade. For HYAL1, high-grade staining represented 2+ and 3+ staining, whereas low-grade staining included 0 and 1+ staining intensities. For the combined HA-HYAL-1 staining, a positive result was indicated only when both HA (stromal, tumor cells, or both) and HYAL-1 staining intensities were of high grade. Any other combination was considered negative. All slides were reviewed out of order to prevent direct comparison of individual cases for HA and HYAL1.

CD34 staining: Following the antigen retrieval step (as described above), the slides were incubated with a mouse monoclonal anti-human hematopoietic progenitor cell CD34 antibody (dilution of 1:20; DAKO, Denmark) at 4°C for 15 hours. The slides were then incubated with a biotinylated anti-mouse antibody and an avidin-peroxidase conjugate solution (Vectastain ABC Kit, Vector Laboratories, Burlingame, CA). To visualize peroxidase binding sites, the slides were incubated with a 3,3'-diaminobenzidine (DAB) chromogen substrate solution (Dako Laboratories) for 10 minutes. The slides were counterstained with hematoxylin, dehydrated and mounted.

The method described by Weidner et al (42) was used for scoring of the microvessels stained with CD34. The area of the highest MVD in each tissue specimen was localized under 40X magnification and was designated as "hot spot". The microvessels in the hot spots were counted under 400X-magnification. Any vessel with lumen and endothelial cell or endothelial cell cluster stained positively for CD34 was considered to be a single countable microvessel. MVD count was defined as the mean value of the counts obtained in 3 separate, contiguous but not overlapping areas within the hot spot. A cutoff value was determined using the receiver operating characteristic (ROC) curve and according to this value two groups of low and high MVD were assigned. Microvessels were examined and counted by the three readers (S.E., V.B.L. and W.H.C.) independently and without the knowledge of the clinical and pathological status of the patients. The sections were reviewed out of order to prevent direct comparison of individual cases for CD34.

CD44v6 staining: Following antigen retrieval, the slides were incubated with a mouse monoclonal anti-human CD44v6 antibody (dilution of 1:50; Bender Med systems, Vienna, Austria) at 4°C for 15 hours. The sections were then incubated with a biotinylated secondary antibody and an avidin-peroxidase conjugate solution (Vectastain ABC Kit, Vector Laboratories, Burlingame, CA). To visualize peroxidase binding sites, the slides were incubated with a 3,3'-diaminobenzidine (DAB) chromogen substrate solution (Dako Laboratories) for 10 minutes. The slides were counterstained with hematoxylin, dehydrated and mounted.

The slides for CD44v6 were scored as described by Ekici et al (33). All sections included normal prostate tissue and/or benign prostatic hyperplasia glands as internal controls. Intensity of staining was graded as 0 for no staining, 1 for weak intensity, 2 for moderate intensity and 3 for strong intensity. A combined staining score based on an estimate of the percentage of tumor cells stained and the intensity of staining was developed. The areas of tumor cells stained with maximum intensity (primary area) and the other tumor cells stained with lesser intensity (secondary area) were determined in percentage values. The combined score is obtained by adding the scores of the primary and secondary areas. Staining intensities were examined and

scored by two readers (S.E. and V.B.L.), independently and in a blinded fashion. A cutoff value was determined from the ROC curve and according to this value two groups of low and high CD44v6 staining were assigned.

Statistical Analysis:

The inter-assay variability regarding staining intensity was determined by Pearson's correlation analysis. The Spearman's bivariate correlation coefficients were 0.85, 0.9, 0.98 and 0.95 for HA, HYAL1, CD34 and CD44v6 staining, respectively. For all the markers, a high-grade staining was considered as a true positive if the patient had biochemical recurrence. Consequently, low-grade staining was considered as a true negative, if the patient had no biochemical recurrence. The sensitivity, specificity, positive predictive value (PPV), and negative predictive value (NPV) for HA, HYAL1, HA-HYAL1, CD34 and CD44v6 staining inferences were calculated using the 2 x 2 contingency table (high-grade/low-grade staining and progressed/non-progressed CaP patients) at 72, 84, 100 and 112 month cut-off limits. For CD44v6 and MVD, Receiver Operating Characteristic curves were developed for determining the optimal cut-off limits that yielded the best possible sensitivity and specificity values. The cut-off limits for CD44v6 and MVD were 180 and 41, respectively. The sensitivity is defined as: true positive (i.e., No. of recurred patients predicted by a marker) ÷ total no. of recurred patients. Specificity: true negatives (i.e., No. of non-recurred patients predicted by a marker) ÷ total no. of non-recurred patients. Accuracy: No. of True positive + No. of true negatives ÷ total no. of CaP patients in the study. PPV: No. of true positive ÷ No. of true positive + No. of false positive. NPV: No. of true negative ÷ No. of true negative + No. of false negative. The data on various, biochemical, surgical, and pathologic parameters, as well as HA, HYAL1, HA-HYAL1, CD34 and CD44v6 staining inferences, were analyzed by Cox Proportional Hazard model, using single variable analysis (univariate analysis) or step-wise selection analysis. Stratified Kaplan-Meier analyses were performed on the variables that were found to be significant in the multivariate Cox Proportional Hazard model. Statistical analysis was carried out under the direction of project's statistician, Dr. Robert Duncan, using the SAS Software Program (version 8.02; SAS Institute, Cary, NC).

Results:
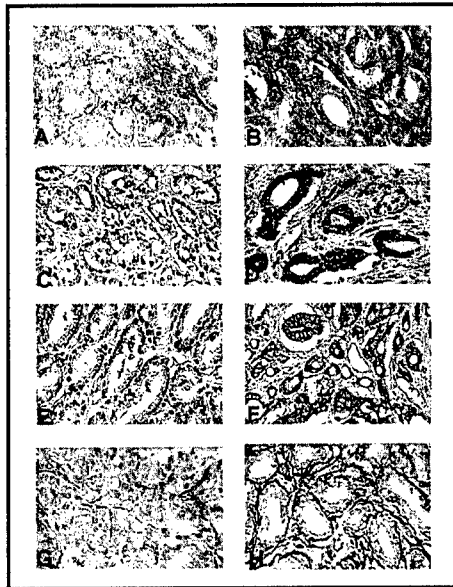## Immunohistochemistry of the tissue markers:

Fig 1. Localization of HA, HYAL1, CD44v6 and MVD in CaP tissues: A non-recurred patient (panels A, C, E, G) and a recurred patient (panels B, D, F, H). Panels A and B: HA; Panels C and D: HYAL1; Panels E and F: CD44v6; Panels G and H: MVD

Fig. 1 shows immunohistochemical localization of HA, HYAL1, CD44v6 and MVD in 2 Gleason 7 PCa specimens, one each from a non-recurred (panels A, C, E, G) and a recurred (panels B, D, F, H) patient, respectively. As shown in Fig. 1 panel A, very little HA staining is seen in PCa tissue from a patient who did not progress within 72 months. Among the 41 PCa specimens from non-recurred patients, 25 showed low-grade staining. Panel B shows high-grade HA staining in PCa specimen from a patient who had biochemical recurrence in < 72 months (median time to recurrence: 19 months; mean time to recurrence: 21.3 months). The HA staining is seen mainly in tumor-associated stroma.

However, high-grade HA staining was also seen in tumor cells in 8 out of 25 patients who had biochemical recurrence. Out of the 25 patients who had recurred, 24 showed high-grade HA staining.

As shown in Fig. 1 panel C, little HYAL1 staining is seen in the PCa tissue from a non-recurred patient. Out of the 41 non-recurred patients, PCa specimens from 33 had low-grade staining. In the PCa specimen from a patient who later recurred, high-grade HYAL1 staining is seen (Fig. 1, panel D). The HYAL1 expression is seen exclusively in tumor cells. Out of the 25 patients who recurred within 72 months, 21 had high-grade HYAL1 staining. Contrary to some earlier reports (33,34), low-grade CD44v6 staining is observed in the PCa specimen from a non-recurred patient (Fig. 1, panel E) and high-grade CD44v6 staining is observed in the PCa tissue from a recurred patient (Fig. 1, panel F). CD44v6 staining is mostly associated with the plasma membrane of tumor cells. We also observed CD44v6 in non-neoplastic epithelial cells in normal prostate and benign prostatic hyperplasia glands. However, the staining intensity of CD44v6 in non-neoplastic cells was less than that in tumor cells. Using a cut-off limit of 180 on the scoring scale, 23 out of 41 PCa specimens from non-recurred patients showed low-grade staining, whereas, out of the 25 patients who recurred, 17 showed high-grade staining.

As shown in Fig. 1 panel G, MVD is low in the PCa tissue from a non-recurred patient. As determined from the Receiver Operating Characteristic curve, a cut-off limit of 41 was set to score low or high MVD. Out of the 41 non-recurred patients, PCa tissues from 25 patients had low MVD. However, the MVD was high in 19 out of 25 PCa tissues obtained form patients who had a recurrence. Fig. 1 panel H shows high MVD in the PCa specimen from a patient who later recurred.

Determination of sensitivity, specificity, accuracy: We determined sensitivity, specificity, accuracy of HA, HYAL1, combined HA-HYAL1, CD44v6 staining inferences and MVD at 72-, 84-, 100- and 112-months of follow-up. Data on 72 and 112 months is shown here (For details please see Appendix 2; ref. 46). As shown in Table 2, the sensitivity of HA, HYAL1, combined HA-HYAL1, CD44v6, and MVD for predicting CaP recurrence is 96%, 84%, 84%, 76% and 68%, respectively within 72 months. The specificity, of HA (61%), CD44v6 (56.1%), and MVD (61%) was lower than that of HYAL1 (80.5%) and combined HA-HYAL1 (87.8%). The

Parameter	HA (%) 72 months	112 months	HYAL1 (%) 72 months	112 months	HA- 72 months	HYAL1 (%) 112 months
Sensitivity	96	92.6	84	85.2	84	81.5
Specificity	61 (25/41)	80.6	80.5	94.4	87.8	94.4
Accuracy	74.2	91.1	81.8	88.9	86.4	86.7
Parameters	CD44v6 (%) 72 months	112 months	MVD (%) 72 months	112 months		
Sensitivity	72 months	112 months	72 months	112 months		
Specificity	76	77.8	68	62.9		
Accuracy	61	77.8	56.1	61.1		

Table 2: 72 and 112 months were used a cut point for determining biochemical recurrence.

accuracy of the HA-HYAL1 (86.4%) was the highest, followed by HYAL1 (81.8%), HA (74.2%), MVD (66.7%), and CD44v6 (57.6%). Follow-up information of ≥112 month was available on 45 patients (mean follow-up 121 months; median 120.2; range 112 – 131 months). At 112 month, the sensitivity of HA, HYAL1, HA-HYAL1, MVD and CD44v6 was 92.6%, 85.2%, 81.5%, 77.8% and 62.9% respectively. At final analysis, both HYAL1 and combined HA-HYAL1 had the best specificity (94.4%, 94.4%) and accuracy (88.9%, 86.7%), followed by HA, MVD and CD44v6 (Table 2).

Evaluation of the prognostic capabilities of pre-operative and post-operative parameters and histological markers:

Univariate analysis:

Since the study patients in this cohort had variable follow-up between 72 and 131 months, we used Cox Proportional Hazard model and single parameter analysis to determine the prognostic significance of each of the pre-operative (i.e., age, PSA and clinical stage) and post-operative parameters (i.e., Gleason sum, margin +/-, EPE +/-, seminal vesicle invasion +/-), as well as, staining inferences of HA, HYAL1, combined HA-HYAL1, CD44v6 and MVD. In the univariate analysis, age ($p = 0.5104$; hazard ratio = 1.019), clinical stage ($p = 0.2683$, hazard ratio = 1.2620) and CD44v6 staining ($p = 0.131$ hazard ratio = 1.826) were not significant in predicting biochemical recurrence. However, pre-operative PSA ($p = 0.0006$, hazard ratio/unit PSA change = 1.048), Gleason sum overall ($p = 0.0002$; hazard ratio = 2.5), margin status ($p = 0.0003$; hazard ratio = 4.5), EPE ($p<0.0001$; hazard ratio = 12.781), seminal vesicle invasion ($p<0.0001$; hazard ratio = 6.56), HA staining ($p=0.0008$; hazard ratio = 12.091), HYAL1 staining ($p<0.0001$; hazard ratio = 13.192), HA-HYAL1 staining ($p<0.0001$; hazard ratio = 10.749) and MVD ($p = 0.0015$; hazard ratio = 4.36) significantly predicted biochemical recurrence. (Please see Appendix 2 for details, ref. 46).

Parameter	P Value	Hazard Ratio
PSA	< 0.0001*	1.068
EPE	0.0016*	6.222
HYAL1	0.0009*	8.196
HA-HYAL1	0.0021*	5.191

Table 3: HA and HYAL1 or HA-HYAL1were included in the multivariate analysis; *: Statistically significant

Multivariate analysis:
To determine the smallest number of variables that could jointly predict biochemical recurrence in this cohort of study patients, we used Cox Proportional Hazard model and step-wise selection analysis. When age, pre-operative PSA, clinical stage, Gleason sum (overall or ≥ 7), EPE, seminal vesicle invasion and staining inferences of HA, HYAL1, CD44v6, and MVD were included in the model, only pre-operative PSA ($p < 0.0001$, hazard ratio/unit PSA change = 1.086), EPE ($p = 0.0016$, hazard ratio = 6.222) and HYAL1 ($p = 0.0009$, hazard ratio = 8.1896) reached statistical significance in predicting biochemical recurrence (Table 3).

The inclusion of the combined HA-HYAL1 staining inference instead of HA and HYAL1 staining inferences, in the multiple regression model again showed that pre-operative PSA ($p = 0.0002$, hazard ratio/unit PSA change 1.077), EPE ($p = 0.0009$, hazard ratio = 6.906) and HA-HYAL1 ($p = 0.0021$, hazard ratio = 5.191) were significant in predicting biochemical recurrence (Table 3 B). None of the other pre-operative (PSA, clinical stage) and post-operative parameters (Gleason sum and seminal veicle) or CD44v6 and MVD staining inferences reached statistical significance in the multivariate model ($P > 0.05$, in each case).

Fig. 2: Kaplan-Meier analysis: Data on parameters significant in multivariate analysis (Table 3) were stratified to perform Kaplan-Meier analysis.

Kaplan-Meier analysis: The joint effect of HYAL1 and EPE or HYAL1 and PSA on biochemical analysis was evaluated using stratified Kaplan-Meier analysis. As shown in **Fig. 2 A,** the probability of biochemical recurrence was highest when HYAL1 and was high and EPE was positive and a patient had the lowest probability of
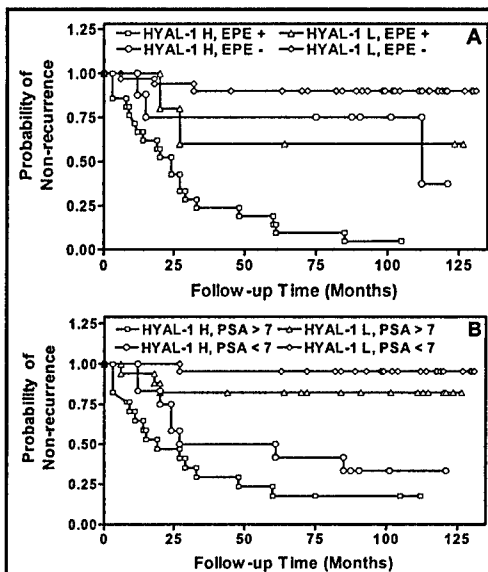
recurrence when HYAL1 was low and EPE was negative. Since PSA was a continuous estimate, with values ranging between 0.5 and 62 ng/ml for the entire study cohort (n = 66), the cohort was divided into those with PSA < 7 and > 7 ng/ml. PSA > 7 ng/ml was used as a cut-off limit, since that was the median value for the entire cohort. As shown in **Fig 2 B**, individuals with high HYAL1 and PSA 7 ng/ml had the highest probability of recurrence, followed HYAL1 high, PSA < 7 ng/ml individuals. CaP patients with low HYAL1 staining and PSA < 7 ng/ml had the lowest probability of recurrence. Identical results were obtained with HA-HYAL1 staining inferences were included in the Kaplan-Meier analysis instead of HYAL1 inferences. These data confirm the multivariate analysis results (as discussed above), which selected HYAL1 (or HA-HYAL1), pre-operative PSA and EPE as independent prognostic indicators.

Summary: The results, which we have obtained, demonstrate that HYAL1 and HA-HYAL1 are independent prognostic indicators for predicting biochemical recurrence of CaP. An additional point that deserves attention is that in this study we had long follow-up on each patient (minimum follow-up 72 months), which was sufficient to detect any biochemical recurrence. This long follow-up makes a strong case that HYAL1 and HA-HYAL1 are potentially useful prognostic indicators for CaP.

C. (BODY): Progress related to Aim 2: To evaluate the effect of HYAL1 inhibition on CaP growth and metastasis.

Rationale and background: When we submitted the above referenced grant we had generated DU145 transfectants that either over produced (HYAL1 sense) or under produced (HYAL1-antisense) HYAL1-type HAase. Contrary to our hypothesis that HYAL1 enhances CaP growth, when we injected these transfectants in athymic nude mice to study the effect of HYAL1 on tumor growth, we found that both the HYAL1-sense and HYAL1-antisense transfectants did not generate palpable tumors in 30 days, whereas, the vector only transfectants (i.e., wild type) generated palpable tumors in 7 days. As a result, we generated DU145 transfectants again and12 this time we selected two different types of HYAL1-sense transfectant clones: 1. Moderately HYAL1 over-producing 2. Highly HAase over-producing. Since PC3-ML cells express little HYAL1, we generated only HYAL1-sense transfectants and again selected moderately HAase-overproducing and highly HAase-overproducing clones. Both the *in vitro* and *in vivo* analysis of these clones demonstrates that both, the over and under production of HYAL1 decreases CaP growth and its invasive potential.

Experimental procedures:

Generation of DU145 and PC3-ML transfectants: The entire HYAL1 cDNA coding region (nucleotides 618 – 1925 GenBank # HSU03056) was amplified by RT-PCR analysis as described previously (47). The amplified cDNA was directly cloned into pcDNA 3.1/v5/His-TOPO eukaryotic expression vector, using a TOPO-TA cloning kit (Invitrogen). This vector allows bi-directional cloning of PCR products, i.e., the cDNA has a 50:50 chance of insertion into the vector either in the sense or antisense orientation with respect to the CMV promoter. HYAL1-sense (HYAL1-S) and HYAL1-antisense (HYAL1-AS) constructs were used for transfection studies. Since DU145 cells produce high levels of HAase, we generated both HYAL1-S and HYAL1-AS transfectants. However, for PC3-ML cells, we generated only HYAL1-S transfectants since these produce very little HAase (1-3 mU/10^6 cells). CaP cells (2 x 10^5) were transfected with 5-µg DNA of HYAL1-S, HYAL1-AS or pcDNA3.1/v5-His vector constructs using Effectene™ transfection reagent and a protocol supplied by the manufacturer (Qiagen).

The transfectants were selected in geneticin (400-µg/ml for DU145 and 300-µg/ml for PC3-ML). 25 to 30 transfectant clones for each construct were analyzed and data on 2 representative clones are presented.
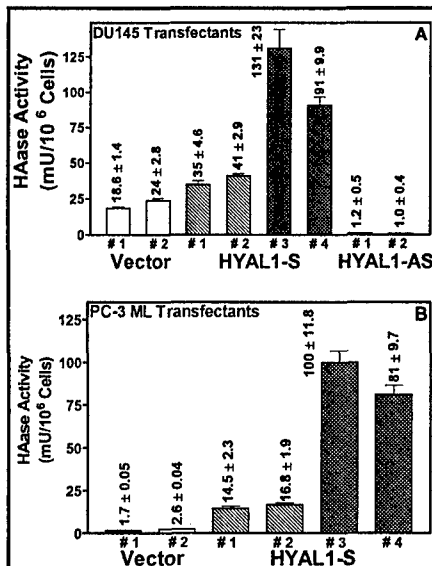

Figure 3: Analysis of HAase activity. Data: mean ± SD (Triplicates in 3 experiments).

Analysis of HYAL1 expression in transfectants: HAase test: To measure HAase activity secreted by different transfectant clones, actively growing cultures of transfectants (~ 10^5 cells/24-well plates) were incubated for 48 hr in RPMI 1640 containing insulin, selenium and transferrin (RPMI+ITS) and the conditioned media (CM) were assayed for HAase activity using the HAase test. Briefly, microtiter plates coated with 200 µg/ml HA were incubated with transfectant CM in a HAase assay buffer (48) at 37^0 C for 12-15 h. Following incubation, the degraded HA was washed off and HA remaining on the wells was detected using the biotinylated HA binding protein and an avidin-biotin detection system. HAase activity (mU/ml) was normalized to cell number. As shown in **Fig. 3 A**, DU145 HYAL1-S clones # 1 and # 2 secrete 1.5-2.3-fold more HAase activity and HYAL1-S # 3 and # 4 clones secrete 3.8-7.3-fold more HAase activity, when compared to vector # 1 and # 2 clones. There is > 90% reduction in HAase secretion in HYAL1-AS clones. PC-3 ML HYAL1-S clones # 1 and # 2 secrete HAase activity similar to that secreted by DU145 vector clones, and it is about 10-fold more than that secreted by PC-3 ML vector clones **(Fig. 3 B)**. HYAL1-S # 3 and # 4 clones secrete HAase activity similar to that secreted by DU145 # 3 and # 4 clones.
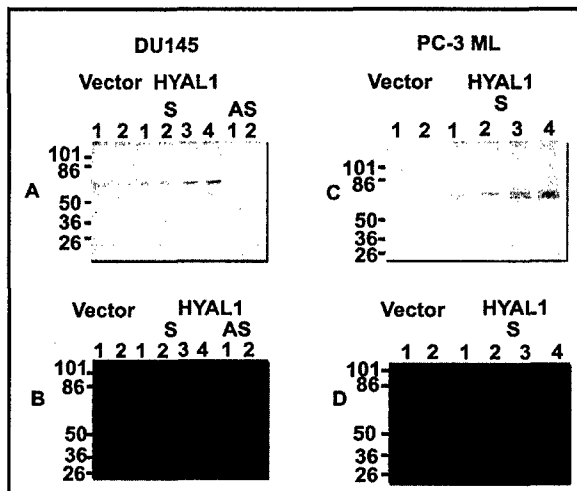

Figure 4: Detection of HYAL1 expression in DU145 and PC-3 ML transfectants. A & C. HYAL1 immunoblot analysis: **B & D:** Substrate (HA)-gel assay.

Anti-HYAL1 immunoblotting: To detect HYAL1 expression, CM (10-µg protein) were immunoblotted using the anti-HYAL1 IgG. A ~ 60-kDa HYAL1 protein is secreted in the CM of DU145 vector and HYAL1-S clones but not in HYAL1-AS clones. **(Fig 4 A, photo-image Appendix A)**. In PC-3 ML clones, HYAL1 protein is detected in the CM of HYAL1-S transfectants but not in vector clones. The amount of HYAL1 protein detected in HYAL1-S clones # 3 and # 4 is higher than that detected in HYAL1-S # 1 and # 2 clones **(Fig 4 B)**.

Substrate (HA)-gel analysis: To confirm the expression of active HAase, we separated the CM of DU145 and PC-3 ML transfectants a SDS-polyacrylamide gel containing HA and the gel was incubated in the HAase assay buffer. Following incubation, the gel was stained and destained to visualize active HAase (Appendix 1). As shown in **Fig 4 C and D**, a ~ 60-kDa active HAase species is detected in the CM of DU145 vector and HYAL1-S clones and in PC-3 ML HYAL1-S clones. As expected from HAase activity and HYAL1 immunoblotting results, the ~

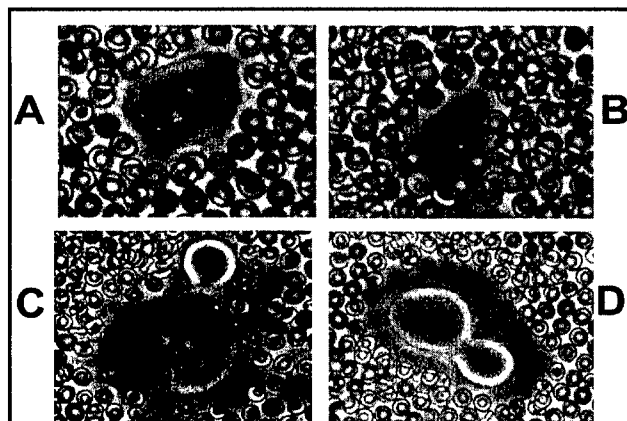60-kDa active HAase species is absent in CM of DU145 HYAL1-AS and PC-3 ML vector clones (Fig 4 C, D).

Fig 5: Examination of pericellular matrix. A: Vector # 1; **B:** HYAL1-S # 1; **C:** HYAL1-S # 4; **D:** HYAL1-AS # 2.

Effect of HYAL1 expression on pericellular matrix formation: We next determined whether HYAL1 expression regulates pericellular matrix that surrounds CaP cells and whether HA is an important component it. 24-h cultures of DU145 transfectant clones (1×10^4 cells/6-cm dish) were overlaid with formaldehyde fixed human erythrocytes and observed under a phase contrast microscope. Cells showing a bright region around the entire periphery with width $\geq$ the diameter of an erythrocyte (i.e., pericellular matrix) were counted in 10 fields (49, 50). Results were expressed as % cells with pericellular matrix ± S.D. As shown in **Figure 5**, vector #1 and HYAL1-S clones (# 1 and # 3) do not exhibit pericellular matrices as the erythrocytes closely abut the surface of each cell. However, HYAL1-AS cells (clone # 1) exhibit a clear pericellular matrix. There was a 3- and 4.6-fold increase in the percentage of cells with pericellular matrix for HYAL1-AS transfectants when compared to vector, moderate HYAL1 over-producing and high HYAL1 over-producing transfectants, respectively (P < 0.001). Thus, HA is an important component of the pericellular matrix of prostate cancer cells and it is degraded by HYAL1.
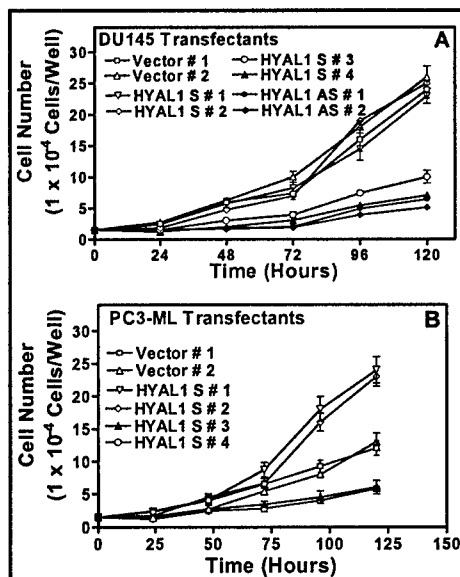

Figure 6: Determination of proliferation rate of transfectants. Data: mean ± SD from duplicate measurements in 3 experiments.

Effect of HYAL1 expression on cell proliferation, cell cycle and apoptosis:

Cell proliferation: Vector, HYAL1-S and HYAL1-AS clones of CaP cells (2×10^4/well) were plated on 24-well culture plates in growth medium. Cells were counted in duplicate wells every 24-h for a total period of 120-h, in 2 independent experiments. As shown in **Fig 6 A**, the growth rate o f DU145 vector and HYAL1-S # 1 and # 2 transfectant is comparable (doubling time ~ 26-28 hr). However, both HYAL1-AS clones and also HYAL1-S # 3 and # 4 clones (which secrete $\geq$ 100 mU/10^6 HAase activity) grow 4-5-fold slower than vector clones (doubling time ~ 90-96 hr). PC-3 ML HYAL1-S # 1 and HYAL1-S # 2 clones grow 1.5-2-fold faster than the vector clones, however, the high HYAL1 producer clones, HYAL1-S # 3 and # 4 grow 2-2.5-fold slower than the vector clones (Fig. 6 B).

Cell-cycle analysis: Cultures of transfectants (10^6 cells/ml) were lysed in a hypotonic solution containing 0.1% NP40 and 50 μg/ml propidium iodide and analyzed using an EPICS XL flow cytometer equipped with a long pass red filter, FL3 (630 nm). FL3 histograms were analyzed by Modfit Easy (Lite) Program (Veritas Software, ME). As shown in **Table 4**, decreased growth rate of HYAL1-AS transfectants is due to cell-cycle arrest in the G2-M phase. There is a 200% - 300% increase in the number of HYAL1-AS #1 cells in G2-M phase when compared to vector

and all HYAL1-S transfectant clones. Correspondingly, the % of HYAL1-AS cells in S-phase is decreased when compared to vector and HYAL1-S cells. The increase in the G2-M phase of

Name	G0-G1	S	G2-M
Vector # 1	52.6%	35.9%	11.5%
Vector # 2	50.4%	37.2%	12.4%
HYAL1-S # 1	52.3%	36.4%	11.3%
HYAL1-S # 2	49.4%	38.5%	12.1%
HYAL1-S # 3	50.9%	37.6%	11.5%
HYAL1-S # 4	53.4%	36.9%	9.7%
HYAl1-AS # 1	48.9%	28.8%	22.3%
HYAL1-AS # 2	43.9%	24.8%	31.3%

Table 4: Cell cycle Analysis of DU145 transfectants. Shaded area: G2-M block

cell cycle in HYAL1-AS transfectants was statistically significant (P < 0.001; Tukey's test). Interestingly, for HYAL1-S # 3 and # 4, we observed an extra peak to the left of the G0-G1 peak, possibly representing apoptotic cells. In PC3-ML transfectants, HYAL1 expression also increased the number of cells in the S-phase with a corresponding decrease in the number of cells in G2-M phase (data not shown).
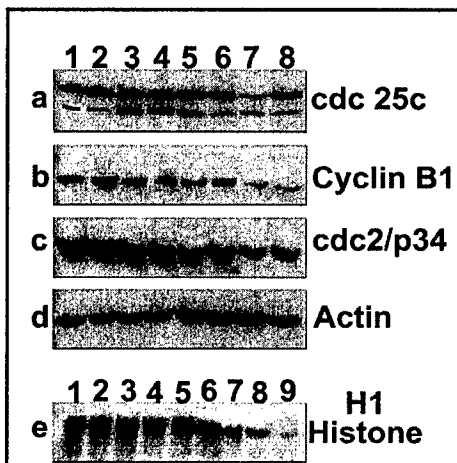
Analysis of G2-M regulators: We analyzed the expression of G2-M regulators, i.e., cdc25c, cyclin B1, and cdc2/p34 proteins in various clones by immunoblot analysis, using commercially available antibodies (49,50). As shown in **Fig. 7**, both cdc25c bands, plausibly representing active (phosphorylated) and native forms, are detected in all DU145 transfectants. There is ~ 3-fold decrease in the expression of active cdc25c in HYAL1-AS transfectants when compared to the vector and HYAL1-S transfectant clones. There is also ~ 3-fold and 2-fold decrease in the expressions of cyclin B1 and cdc2/p34 in HYAL1-AS transfectants when compared to vector and HYAL1-S clones (**Fig 7**). We also examined cdc2/p34 kinase activity, which is elevated upon binding of cyclin B1 to cdc2/p34 during G2-M transition. The kinase

Figure 7: Analysis of G2-M cell cycle regulators. Lanes 1 & 2: vector clones # 1 & 2; lanes 3-6: HYAL1-S clones 1 - 4; lanes 7 & 8: HYAL1-AS clones # 1 & 2. e: Lanes 1 - 8 are the same as above: lane 9: negative control.

activity assay was performed by immunoprecipitating the cell lysates of DU145 transfectant clones with cdc2/p34 using a mouse anti-cdc2/p34 IgG and protein-A agarose. The immunoprecipitates were incubated in a kinase assay buffer containing H1 histone (2.5-µg), 5-µM ATP, 5-µCi γ-^{32}P-ATP. Histone H1 was analyzed by SDS-PAGE and autoradiography (Appendix 4). As shown in **Fig 7, a** ~ 2.5- and 3-fold decrease in cdc2/p34-associated H1 histone kinase activity is observed in HYAL1-AS transfectant clones when compared to vector and all HYAL1-S transfectants. These results show that the slow proliferation rate of HYAL1-AS transfectants is due to G2-M arrest.

Analysis of apoptosis: We determined whether the reduced cell growth observed in high HYAL1 producing clones of CaP transfectants (i.e., HYAL1-S # and # 4 clones) was due to increased apoptosis, using free nucleosome release assay. Briefly, 96-h cultures of transfectants (10^5 cells/24-well plate) were lysed and the cell lysates were tested for free nucleosome release using the Cell Death ELISA kit (Roche Diagnostics). As shown in **Fig. 8 A**, there is a 3-fold increase in the intracellular levels of free nucleosomes in HYAL1-S # 3 and HYAL1-S # 4 cells when compared to vector, HYAL1-S #1 and #2, as well as, HYAL1-AS clones. Apoptotic activity was also high in HYAL1-S # 3 and # 4 transfectant clones. We also found that partially purified HYAL1 at concentrations > 80 mU/ml induced apoptosis in DU145 vector, HYAL1- S # 1 and # 2 and HYAL1-AS clones (Data not shown). These results show that CaP cells which either do not express or moderately over-express HYAL1 can be induced to undergo apoptosis by exposing them to > 80 mU/ml HYAL1 concentration.
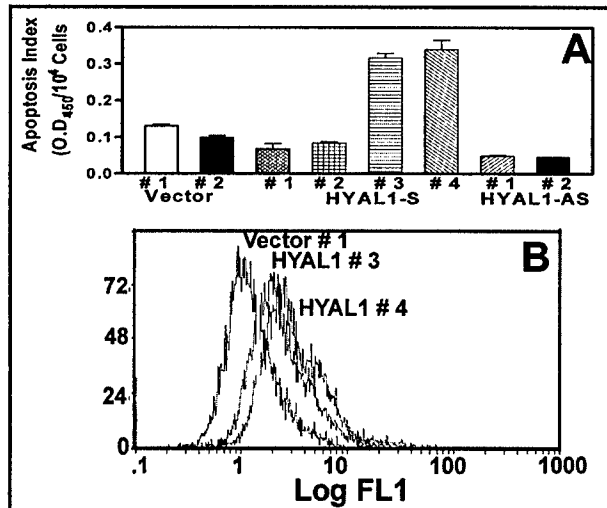
Figure 8: Examination of apoptosis. A: Apoptotic activity. Data: Mean ± S.D. (3 measurements each in 2 experiments). **B:** EGFP-Annexin V binding. Expt. was repeated twice.

To confirm the induction of apoptosis, we measured the outward translocation of plasma membrane phosphyatidyl serine by Annexin-V binding assay. Annexin-V binding was examined in 96-h cultures of HYAL1 vector and HYAL1-S # 3 and # 4 clones using the ApoAlert™ Annexin V-EGFP kit (BD-Clontech Laboratories, Inc.) and flow-cytometry. The median fluorescence intensity (Annexin V binding to PS) was compared among transfectants in the green fluorescence channel (log FL1). As shown in **Fig 8 B**, there is a distinct increase in EGFP-Annexin V binding to HYAL1-S # 3 and # 4 cell surface when compared to vector control (Median peak LogFL1: vector: 1.21; HYAL1-S # 3, 2.37; HYAL1-S # 4, 2.83). Therefore, the decreased cell growth observed in high HYAL1 producers is due to induction of apoptosis.
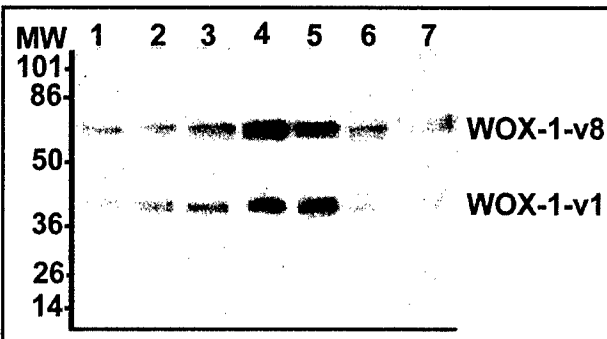

Fig 9: WOX1 expression. Lanes 1: Vector # 1; lanes 2 - 5: HYAL1-S # 1-4; lanes 6 & 7: HYAL1-AS 1 & 2

Analysis of WOX-1 expression in DU145 transfectants. To determine whether HYAL1-mediated apoptosis might involve WOX-1, we analyzed the expression of all WOX-1 isoforms by immunobloting using a WOX1 monoclonal antibody (EMD Biosciences). This antibody detects all of the 8 WOX1 isoforms, that are generated by mRNA splicing. As shown in **Fig 9**, DU145 cells express 2 WOX-1 isoforms (v1: 46 kDa and v8: 60 kDa). Expression of both of these isoforms is elevated ~ 3-fold in HYAL1-S # 3 and # 4 clones when compared to vector, moderate HYAL1 overproducers (HYAL1-S # 1) and HYAL1-AS transfectants. Both WOX1 v1 and v8 isoforms contain all of the function domains required for inducing apoptosis, as demonstrated in the L929 fibroblast system. (51).
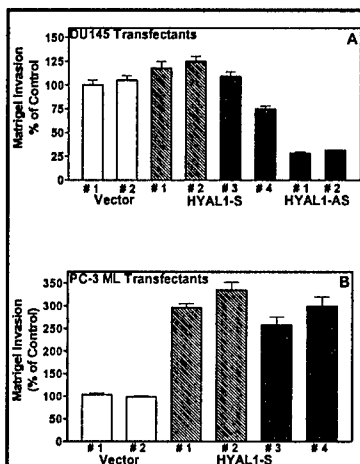
Effect of HYAL1 expression on *in vitro* invasion: Matrigel invasion assay was performed to study the effect of HYAL1 expression on the invasive activity of HYAL1 transfectants. Briefly, membranes in 12-well Transwell plates were coated with Matrigel (100-µg/cm²). Transfectants (3x10⁵ cells/well) were plated on the upper chamber in a serum-free medium and the bottom chamber contained growth medium. Following 48-h incubation, invasion of cells through Matrigel into the bottom chamber was quantified using the MTT assay (49,50). To normalize the differences in the rate of cell proliferation among various transfectants, invasion

Fig 10: Invasion assay: Data: mean ± SD; n=2 measurements in 3 experiments.

results were calculated as cells in the bottom chamber ÷ cells in upper + bottom chambers) x 100. The invasive activity of vector clones was considered as 100%. As shown in **Fig. 10 A**, the invasive activity of DU145 HYAL1-S clo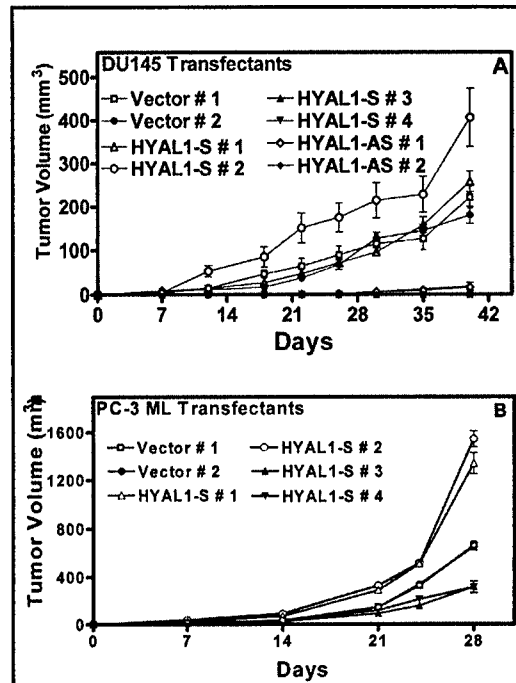nes (both moderate and high producers) is similar to that of vector clones. However, the invasive activity of HYAL1-AS clones is 3-fold less when compared to vector clones (P < 0.001; Tukey's test). As shown in **Fig. 10 B**, HYAL1 expression in PC3-ML cells increases their invasive activity by 3-3.5-fold (P < 0.001). These results show that HYAL1 expression increases the invasive activity of CaP cells.

Effect of HYAL1 expression on tumor xenografts: Transfectants (2 x 10^6 cells) were subcutaneously implanted on the dorsal flank of 5-week old male athymic mice (10 mice/clone). After tumors became palpable, tumor size was measured 2x weekly. Tumor volume was calculated assuming an ellipsoid shape (38). Following euthanasia (DU145: 42 day; PC-3 ML: 28 day), tumors were weighed.

As shown in **Fig. 11 A**, there is a 4-5-fold delay in the generation of palpable tumors in animals injected with DU145 HYAL1-AS transfectants (33 ± 4 days) when compared to vector and moderate HYAL1 overproducing transfectants (6 – 8 days) (P < 0.001; Tukey's multiple comparison's test). Interestingly, **high HYAL1 producers did not form palpable tumors even on day 40 when necropsy was performed**. The weight (g) of vector (# 1: 0.17 ± 0.05; # 2: 0.14 ± 0.04) and moderate HYAL1 overproducers (HYAL1-S # 1: 0.21 ± 0.06; # 2: 0.27 ± 0.14) tumors was 4- and 7-fold more than HYAL1-AS tumors (#1: 0.03 ± 0.01; 0.04 ± 0.01) (P < 0.001). While **no animals injected with HYAL1-S # 3 or # 4 transfectants had visible evidence of tumor**, in some animals Matrigel™ plug-like material was visible. High HYAL1 producing transfectants generated in a 2nd transfection experiment also did not form tumors (data not shown).

Moderate HYAL1 producing PC-3 ML tumors (HYAL1-S # 1 and # 2) grow about 2-fold faster, whereas, high HYAL1 producing tumors grow 2-2.5-fold slower than vector tumors (**Fig. 11 B**). At day 28, the weights (g) of moderate HYAL1 producing tumors (#1: 0.57 ± 0.12; # 2: 0.6 ± 0.14) were 2-fold higher than vector tumors (# 1: 0.28 ± 0.06; # 2: 0.29 ± 0.04) and 3.5-fold higher than high HYAL1 producing tumors (# 3: 0.16 ± 0.03; # 4: 0.14 ± 0.05) (P < 0.001).

Fig 11: DU145 and PC-3 ML transfectant tumor growth. Data: mean ± SD.

Tumor histology, HA, HYAL1 localization and MVD determination: Histology of tumor xenografts was performed at Charles River Laboratories. As shown in **Fig. 12,** histology reports and photomicrographs show that while DU145 vector and moderate HYAL1 producing tumors show high mitotic figures, invade skeletal muscle and lymph nodes and infiltrate lymphatic and blood vessels HYAL1-AS tumors are non-invasive (tumor does not invade muscle panel E). The Matrigel™ plug-like material removed from HYAL1-S # 3 and # 4 animals is ≥ 99% free of tumor cells and no mitotic figures are observed (Fig 12 A panel, F).

To confirm that transfectants retained their phenotype regarding HYAL1 expression, HYAL1 (and also HA) was localized in tumor xenografts using the methods described in section C.a. As shown in **Fig. 13 A**, tumor cells in vector, and HYAL1-S # 1 and # 2 xenografts express significant levels of HYAL1 but HYAL1-AS cells do not secrete HYAL1 (Fig 16). Interestingly, HA production increased in the tumor-associated stroma of vector and HYAL1-S # 1 tumor

specimens when compared to HYAL1-AS # 1 tumor specimens (Fig 16). Since HYAL1-S # 3 and # 4 specimens contained only Matrigel, they were not evaluated for HA, HYAL1 or MVD determinations.
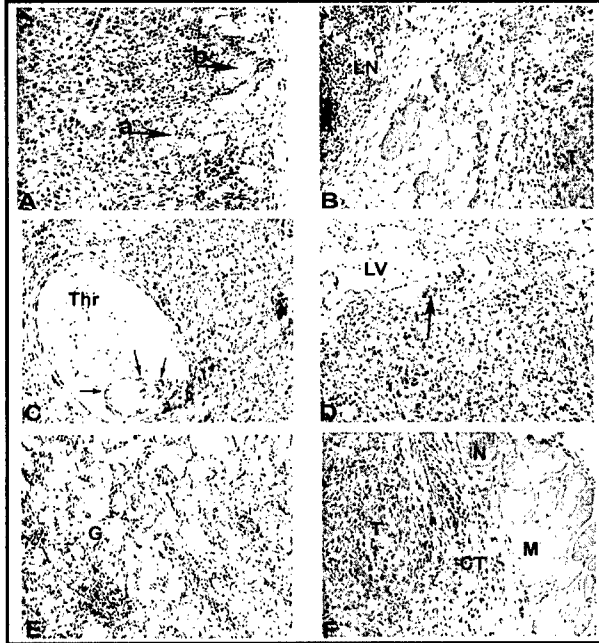
MVD was determined as described in section C.a using rat anti-mouse CD34 monoclonal antibody. MVD in vector was only 1.4-fold higher than HYAL1-AS tumors (P > 0.05). However, the length of capillaries in vector (817.4 ± 141.5 µm) and HYAL1-S (# 1: 1031 ± 262.5; # 2: 817.9 ± 305.3) tumors was 4-5-fold higher than of capillaries in HYAL1-AS tumors (# 1: 218.1 ± 103.4; # 2: 247.1 ± 96.1) **(Fig. 13 B)**.

Fig 12: Tumor histology: A & B: Vector # 1, # 2; C & D: HYAL1-S # 1, # 2; E: HYAL1-S # 3; F: HYAL1-AS # 4

D (Body): Progress related to Aim 3:
Rationale and background: Data presented in the above section show that HYAL1 is a molecular determinant of CaP growth and progression. This is the **first report** that demonstrates that depending upon the concentration, HYAL1 can act both as a tumor promoter and a suppressor. Since this is a novel finding the mechanisms by which HYAL1 can act as a tumor promoter and as a suppressor are unknown. To understand the mechanisms by which HYAL1 regulates both of these processes we performed cDNA microarray analysis on DU145 transfectants.

Experimental procedures:
D. Gene expression analysis: To examine the mechanisms by which HYAL1 (i.e., either its over-expression and inhibiton) may inhibit CaP growth, invasion and angiogenesis, microarray and bioinformatics analyses were performed in the DNA microarray facility of University of Miami. Briefly, total RNA was isolated from DU145 vector, HYAL1-S #3, HYAL1-S #4 and HYAL1-AS #1, #2 transfectants. The RNA was reverse transcribed and the cDNAs were labeled with either Cy-5 or Cy-3. Labeled cDNAs from 2 independent experiments were hybridized as pairs (vector: HYAL-S # 3 or vector : HYAL1-S # 4), to the 20K human oligo microarrays (Agilent Tech) as per the manufacturer's instructions. For each biological replicate

Figure 13: A: HYAL1 and HA localization: Panels a,b,c: HYAL1; Panels d,e,f: HA. Panels a & d: vector # 1; panels b & e: HYAL1-S # 1; panels c & f: HYAL1-AS # 1. **B: Localization of microvessels.** Panel a: vector # 1; panel b: HYAL1-S # 1; panel c: HYAL1-S # 2; panel d: HYAL1-AS # 1.

we performed two technical sub-replicates for dye-swap. The microarrays were scanned using GenePix 4000A (Axon Instruments, Inc.). The microarrays were scanned at 10-□m resolution
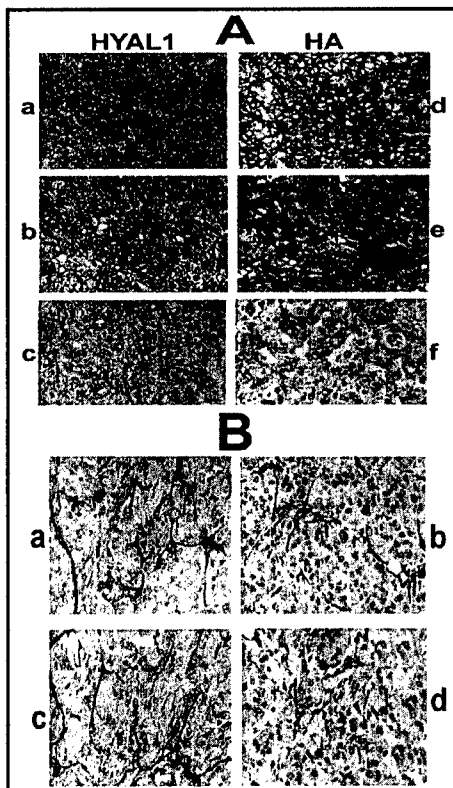
using a GenePix 4000A scanner (Axon Instruments; Molec. Devices). Resulting images were analyzed with the software package GenePix Pro 5.1 (Axon Instruments). Data extracted from the images were transferred to the software package Acuity 4.0 (Axon Instruments) for normalization and statistical analysis. Data from each array were normalized using both color normalization across the whole array and Lowess normalization. Only those genes, which showed differential expression in both clones, were selected for further analysis. To identify significantly expressed genes we used one class SAM (Significant Analysis of Microarray, http://www-

Gene name	HYAL1-S #3 & #4	HYAL1-AS #1 & #2
Cell growth		
Cyclin B1		2.6 ± 0 .87, 2.0 ± 0.53 ↓
DUSP1		2.0 ± 0.55, 1.9 ± 0.4↑
CKS2		2.8 ± 0.73, 2.0 ± 0.21↓
Apoptosis		
BAG1	2.0 ± 0.46, 3.1± 1.3 ↓	
IL 24	3.1 ± 0.75, 4.8 ± 0.82↑	
Clusterin	1.7 ± 0.32, 2.6 ± 0.35 ↑	
BAG5	2.4± 0.26, 2.7± 0.52 ↑	
JNK pathway		
CRKL	1.8 ± 0.25, 2.9 ± 0.61↑	
MAP4K5 (KHS1)	2.4 ± 0.37, 1.8 ± 0.28 ↑	
Angiogenesis		
CXCL1		2.0 ± 0.19, 3.4 ± 0.59 ↓
CXCL2		1.6 ± 0.14, 1.8 ± 0.37 ↓
b-FGF 2		2.4, 2.1 ↓
Invasion/metastasis		
Collagen type IV	2.4 ± 0.43, 3.3± 0.94 ↑	
MMP-1		46.0± 9.5, 28±8.6 ↓
CD44		3.8±0.78, 4.7±1.1 ↓
uPA		4.1±0.52, 2.8±0.63 ↓
Autocrine motility factor		1.7±0.33, 1.6±0.41 ↓

Table 5: Gene expression analysis. ↑: up-regulation; ↓: down-regulation

stat.stanford.edu/~tibs/SAM) analysis and NIA Array Analysis ANOVA tool (http://lgsun.grc.nia.nih.gov/ANOVA). The selected genes were classified according to Gene Ontology category "biological process" using Onto-Express (http://vortex.cs.wayne.edu/Projects.html). Among the differentially expressed genes, we focused on genes related to cell cycle, apoptosis, invasion and angiogenesis.

As shown in **Table 5**, HYAL1 expression regulates the expression of several genes involved in cell cycle, apoptosis, angiogenesis and invasion/metastasis pathways. We used the software (52,53) to perform pathway analysis. **Fig. 14** shows our working model regarding HYAL1 functions. In the cell cycle pathway, HYAL1 may influence the G2-M progression by modulating cyclin B1 and CKS2 expression and/or by activating the JNK pathway through regulation of CRKL and KHS1 gene expression. At the present time, there is no experimental evidence whether HYAL1 also influences the MEK-7-JNK-c-jun and induces ERK1/2 (similar to bovine testicular HAase) pathway for promoting G2-M transition. Over-expression of HYAL1 may induce apoptosis through a mitochondria-mediated pathway that involves WOX1, IL24,

BAG1, BAG5 and/or JNK (please see section B.a). It is noteworthy that although we observed increased expression of WOX1 v1 and v8 proteins in HYAL1-S # 3 and #4 transfectants (section C.c.4), no over-expression of WOX1 was observed in the microarray analysis. However, the human oligo microarrays from Agilent include only WOX1 v2, v4 and v7 oligo arrays, thus, no

Fig 14
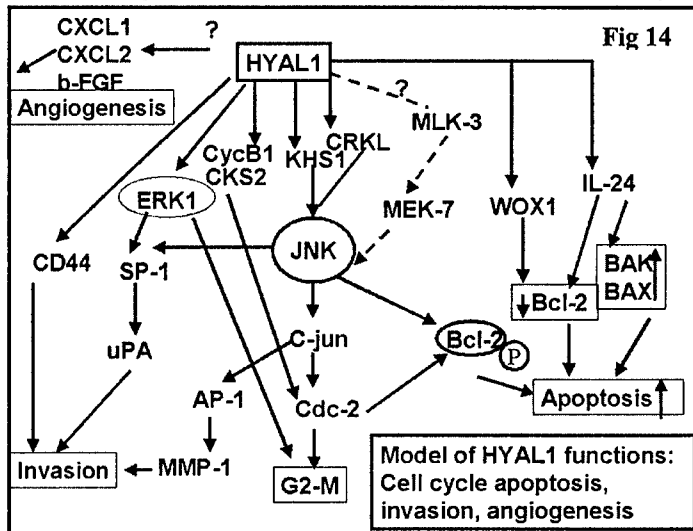
information on WOX1 v1 and v8 differential expression could be obtained using by these microarrays. Induction of ERK1 and JNK pathways by HYAL1 may be responsible for the observed increase in the expression of MMP-1 and uPA genes, and thereby increasing the invasive activity of CaP cells.

It is also noteworthy that HYAL1 increases the expression of the gene for CD44, which is a HA receptor. CD44 is a family of glycoproteins made up of several isoforms, some of which are associated with metastasis (e.g., CD44-v6). For example, DU145 and PC-3 ML cells express both CD44 standard form (~ 85-90 kDa) and CD44-v6 isoform. We have shown that CD44 v6 is over-expressed in CaP tissues (section B). If HYAL1 indeed regulates the expression of CD44 and its isoforms, it may explain why CD44 v6 was not found to be a prognostic indicator of biochemical recurrence when HYAL1 staining was included in the analysis (section C.b.2, Appendix 3).

At the present time it is unknown how HYAL1 induces the expression of genes that encode CD44, autcrine motility factor and angiogenesis promoting genes (i.e., CXCL1, CXCL2 and b-FGF), however, autocrine motility factor induces JNK1 and JNK2 expression. We plan to test the validity the working model of HYAL1 function by examining the expression of the protein products of genes that are differentially expressed under high-HYAL1 and no-HYAL1 conditions.
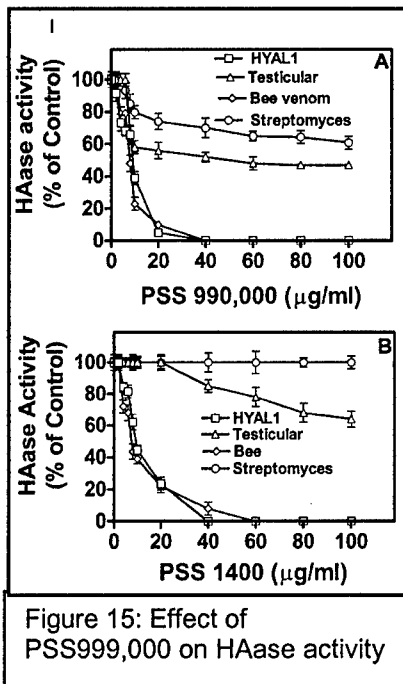
Figure 15: Effect of PSS999,000 on HAase activity

Screening of HAase inhibitors: To identify the most effective inhibitors of HYAL1 that are also somewhat selective, we screened 21 HAase inhibitors against HYAL1 and 3 other HAases, including bovine testicular HAase. The inhibitors included polymers of poly (styrene-4-sulfonate) (mol. wt. 1400 to 9.9×10^5 Dalton i.e., PSS1400 to PSS990,000; Fluka Biochem.) and O-sulfated HA derivative containing 2, 3, or 4 sulfonate groups (sHA 2.0; sHA 2.5; sHA 2.75), heparin and gossypol. sHA derivatives were synthesized using a method described by Barbucci et al. Briefly, tributylamine salt of human umbilical cord HA- sodium salt was suspended in anhydrous dimethyl formamide and mixed with various amounts of anhydrous SO_3^- pyridine under a stream of nitrogen. The amount of SO_3^- pyridine determines the number of O-sulfated groups on the HA. Sulfated HA was then precipitated, dialyzed against water and lyophilized. sHA compounds were analyzed by elemental analyses to confirm the degree of sulfation (54).

As shown in Fig. 15 A, PSS 990,000 inhibits the activity of all 4 HAases in a dose-dependent manner. However, HYAL-1 and bee HAases are more sensitive to inhibition by PSS 990,000 than testicular and Streptomyces HAases. From the inhibition curves we determined the IC_{50} values for each inhibitor. The IC_{50} values of PSS 990,000 for testicular HAase (0.042 μM) and Streptomyces HAase (0.39 μM) are 4.2-fold and 40-fold higher than the IC_{50} values for

Inhibitors	HYAL1 IC_{50} (μM)	Bee venom HAase IC_{50} (μM)	Bovine PH20 IC_{50} (μM)	Strep. HAase IC_{50} (μM)
PSS 990,000	0.0096	0.0091	0.042*	0.39*
PSS 17,000	0.89	1.0	0.89	NI
PSS 1400	8.2	6.6	67.6*	NI
PSS 210	NI	NI	NI	NI
sHA 2.0	0.03	0.029	0.12*	NI
sHA 3.0	0.028	0.03	0.08	NI
sHA 4.0	0.014	0.02	0.064*	NI
Heparin	0.39	0.41	1694*	NI
Gossypol	NI	NI	NI	NI
1-Tetradecane sulfonic acid	63*	NI	NI	NI
Glycerrhizic acid	39.4*	NI	NI	NI

Table 6: IC_{50} values of HAase inhibitors for HYAL-1, bee, testicular and Streptomyces HAases. The IC_{50} value for each inhibitor was calculated by generating an inhibition curve. NI: No inhibition; *: Significant differences. Note: PSS 990,000 is same as VERSA-TL 502

HYAL-1 (0.0096 μM) and bee HAase (0.0091 μM), respectively (Table 6). VERSA-TL 502 is the sodium salt of PSS of mol. wt. ~ 10^6 Dalton, which was used by Anderson et al to demonstrate that PSS inhibits testicular HAase activity and blocks fertilization (6). As shown in Table 1, IC_{50} values of VERSA-TL 502 for HYAL-1 (0.0088 μM), bee (0.0081 μM), testicular HAase (0.042 μM) and Streptomyces HAase (0.32 μM) mirror those for PSS 990,000.
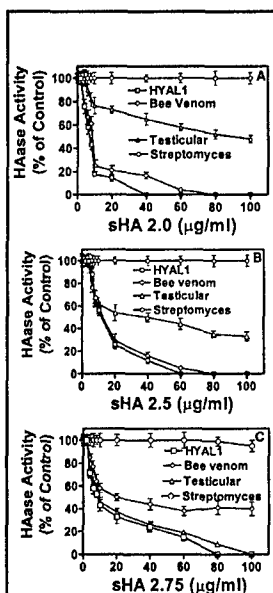

Fig 16: Effect of sHA on HAase activity

We next tested the effects of sHA2.0, sHA 2.5 and sHA 2.75 on HAase activity using the HAase ELISA-like assay. As shown in Fig 16 A, sHA2.0 inhibits the activity of HYAL-1, bee and testicular HAases in a dose-dependent manner. However, the activity of Streptomyces HAase is not inhibited by sHA2.0. The IC_{50} value of sHA2.0 to inhibit testicular HAase (0.078 μM) is 4-times higher than that for HYAL-1 (0.019 μM) and bee HAase (0.019 μM), respectively (Table 6). sHA2.5 has similar inhibition profile as that for sHA2.0, i.e., HYAL-1 and bee HAases are inhibited to a greater degree than the testicular HAase (Fig 16 B and Table 6). Streptomyces HAase is not inhibited by sHA2.5 even at a concentration of 100-μg/ml (Fig 16 B). sHA2.75 is slightly more inhibitory to HYAL-1, bee and testicular HAase than sHA2.0 and sHA2.5 (Fig 16 C). In fact, Streptomyces HAase is slightly inhibited (~ 5%) by sHA2.75 at the 100 μg/ml concentration. The IC_{50} values for HYAL-1 (0.0083 μM) and bee (0.012 μM) HAases are ~ 2.8-4.6-fold higher than the IC_{50} values for testicular HAase (0.038 μM), respectively (Table 6). It is noteworthy that in the same assay system, HA alone even at high concentration (i.e., 100 μg/ml) did not inhibit the activity of any of the 4 HAases (data not shown). Since sHA derivatives are hygroscopic and the mol. wt. of sHA2.0 (774,000 Dalton), sHA2.5 (818,000 Dalton) and sHA2.75 (848,000 Dalton) are estimates, the IC_{50} values presented in Table 6 for each sHA compound may be off by a factor of 2 (or 50% error).

By enzyme kinetic analysis, we found that both PSS and sHA compounds inhibit activity of various HAases by a mixed inhibition mechanism, i.e., competitive and non-competitive (55).

Effect of HAase inhibitors on the growth of DU145, LNCaP and PC3-ML cells. In addition to testing the effect of VERSA-TL 502 on the growth of CaP cells, which was proposed in the application, we also tested the effect of lower mol. wt. PSS compounds (PSS17,000, 6,800 and 1400) on the growth of DU145, PC-3 ML and LNCaP. Briefly, CaP cells (1.5 x 10^4 cells/well) were plated on 24-well plates in growth medium in the presence of various concentrations (0-20 µg/ml) of VERSA-TL 502, PSS 17,000, 6,800 and PSS1400. Every 24-hr for 96-hr, cells were stained with trypan blue and counted. As shown in Fig. 17 and 18, HAase inhibitors inhibit the growth of DU145 and LNCaP cells, both of which secrete HAase and express HYAL1. However, the HAase inhibitors do not inhibit the growth of PC-3 ML cells which do not secrete HAase (fig 19). These results show that PSS compounds inhibit the growth of CaP cells by inhibiting tumor-derived HAase.

Summary: The results obtained by performing the work proposed under Aims 2 and 3 demonstrate that HYAL1 is a molecular determinant of prostate cancer growth, progression and angiogenesis. In the no-cost extension year, we were able to study 21 HAase inhibitors to find those which are effective and specific inhibitors of HYAL1. We are planning to use these inhibitors to test their potential as treatments for controlling prostate cancer growth and progression.
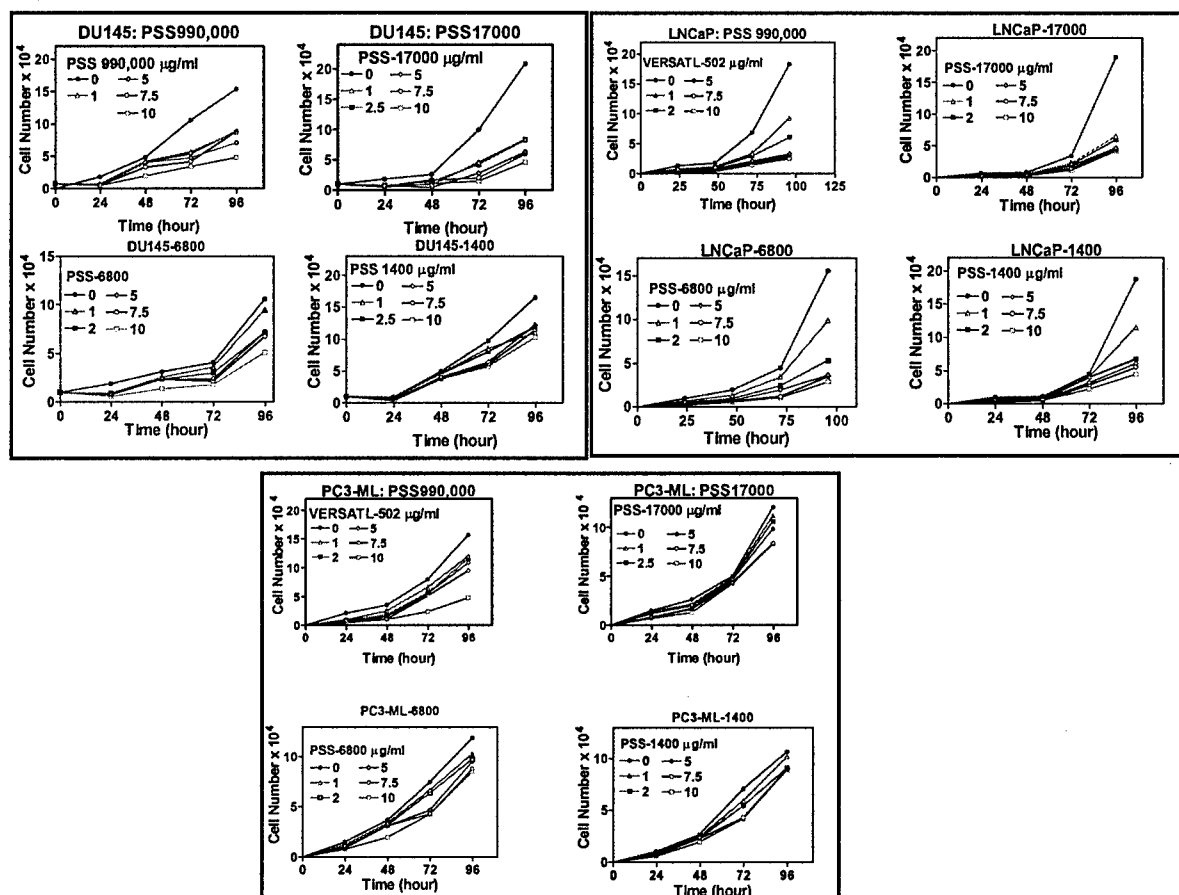

Figure 17,18,19: Effect of PSS compounds on the proliferation of DU145 (Fig 17), LNCaP (Fig 18) and PC3-ML (Fig 19)

2 Key Research accomplishments:
A. Establishment of HYAL1 and combined HA-HYAL1 staining inferences as potentially accurate predictors of biochemical recurrence. The studies presented here are **the first**, which demonstrate the prognostic potential of HYAL1 in any type of cancer.

B. This is the **first demonstration** HYAL1 (or any other HAase) acts as both a tumor promoter and a suppressor depending upon the concentration to which tumor cells are exposed.
HYAL1 induces G2-M transition in CaP cells, stimulates CaP cell growth, invasion and angiogenesis.
At concentration > 100 mU/ml, HYAL1 acts as a **novel apoptotic protein** and high HYAL1 expression inhibits tumor generation.

C. Our findings that HYAL1 in general) can act both as a tumor promoter and a suppressor **resolve the controversy** regarding the role of HAases in cancer. These findings form the basis for testing potential of anti-HAase and high-HYAL1 treatment modalities to control CaP growth and progression

D. Synthetic HAase inhibitors inhibit HYAL1 activity secreted by CaP cells and also inhibit the growth of CaP cells. The growth inhibitory activity of HAase inhibitors correlates with their ability to inhibit HAase activity.

3. Reportable outcomes:
A. Database of CaP patients with long-term follow-up (72 – 131 months).

B. Generation of HYAL1-sense (both moderately producing and overproducing) and HYAL1-antisense (under producing) stable cell lines of DU145 and PC3-ML cells.

C. Identification of intracellular pathways and signaling molecules involved in HYAL1-induced CaP growth and progression.

D. Identification of HAase inhibitors that may be used for controlling CaP growth.

E. I have applied for a NIH RO1 application based on the work performed because of the funding that I received from the CDMRP/PCRP.

F. The University of Miami has selected some of the work carried out under this award to file a US patent on, "Hyaluronidase Inhibitors As Anti-Cancer Agents"

F. Publications:
1. Lokeshwar, V.B. Schroeder, G.L., Carey, R.I. Soloway, M.S., Iida, N. Regulation of hyaluronidase activity by alternative mRNA splicing. J. Biol. Chem. 277: 33654-33663, 2002.

2. Posey, J.T., Soloway, M.S., Ekici, S., Sofer, M., Civantos, F., Duncan, R.C., Lokeshwar, V.B. Evaluation of the prognostic potential of hyaluronic acid and hyaluronidase (HYAL1) for prostate cancer. Cancer Res. 63: 2638-2644, 2003.

3. Franzmann, E., Schroeder, G.L., Goodwin, G.J., Weed, D., and **Lokeshwar, V.B.** Expression of tumor markers, hyaluronic acid and hyaluronidase, in head and neck tumors. Int. J. Cancer 106: 438-445, 2003.

4. Dandekar, D.S., Lokeshwar V.B., Cevallos-Ariello, E., Soloway, M.S., and Lokeshwar B.L.

(2003) An orally active amazonian plant extract (birm) inhibits prostate cancer growth and metastasis. Cancer Chemother. Pharmacol. 52: 59-66.

5. Ekici S., Cerwinka, W.H., Duncan, R. C. Gomez, P., Civantos, F., Soloway, M.S., Lokeshwar, V.B. Comparison of the prognostic potential of hyaluronic acid, hyaluronidase (HYALI-1), CD44v6 and Microvessel density for prostate cancer . Int J Cancer 112: 121-129, 2004

6. Lokeshwar, V.B. Cerwinka, W. H., Lokeshwar, B.L. HYAL1 hyaluronidase: A molecular determinant of bladder cancer growth and progression. Cancer Res. 65: 2243-2250, 2005

7. Lokeshwar, V.B. Cerwinka, W. H., Lokeshwar, B.L. HYAL1 hyaluronidase in prostate cancer: A tumor promoter and a suppressor. Cancer Res. 65: 7782 – 7789.

8. Isoyama T, Thwaites D, Selzer MG, Carey RI, Barbucci R, Lokeshwar VB. Differential selectivity of hyaluronidase inhibitors toward acidic and basic hyaluronidases. Glycobiology 16: 11-21; 2006.

9. Cohen, B.L., Gomez, P., Omori, Y., Duncan, R.C., Soloway, M.S., Lokeshwar, V.B., Lokeshwar, B.L. (2005) Cyclooxygenase-2 (COX-2) expression is an independent predictor of prostate cancer recurrence. Int. J. Cancer (In Press).

E. Abstracts:

1. Lokeshwar, V.B.*, Posey, J.T., Schroeder, G.L. (2002) HA and HAase in prostate cancer: molecular markers with function. Fourth International Innovators in Urology Meeting, Miami, Florida. Prostate cancer and Prostatic Diseases 5: suppl. 1., S19.

2. Lokeshwar, V.B.*, Posey, J.T., Schroeder, G.L. (2002) HA and HAase in prostate cancer: molecular markers with function. Sylvester Comprehensive Cancer Center Poster Presentation (Annual Zubrad Lecture/Poster Meeting; First Prize in Faculty category).

3. Dandekar DS, **Lokeshwar, VB**, Cevallos E, Lokeshwar BL. (2003) Plant extract "BIRM" induces G0/G1 Arrest and caspase-mediated apoptosis in vitro and inhibits in vivo tumor growth and metastasis of prostate cancer. AACR Proceedings Vo 44, #648, p148.

5. Dandekar DS, Lokeshwar, VB, Cevallos E, Lokeshwar BL. (2003)Induction of caspase-mediated apoptosis and inhibition of prostate tumor grwoth and metastasis by a plant extract - BIRM.Miami Nature Biotechnology Short Reports. vol 14:106.

6. Ekici S., Cerwinka, W.H., Duncan, R. C. Gomez, P., Civantos, F., Soloway, M.S., Lokeshwar, V.B. Comparison of the prognostic potential of hyaluronic acid, hyaluronidase (HYALI-1), CD44v6 and Microvessel density for prostate cancer (AUA 2004; Discussed Poster session).

7. Cerwinka, W.H., Lokeshwar, B.L., Lokeshwar, V.B. HYAL1 hyaluronidase in prostate cancer: A tumor promoter or a suppressor (AUA 2005, Discussed Poster session).

F. Patents: Lokeshwar V.B., "Hyaluronidase Inhibitors As Anti-Cancer Agents" (Provisional Patent Application will be filed by March 1, 2006).

G. Gen Bank Citations:

1. Lokeshwar, V.B*. Schroeder, G.L., and Iida, N. (2002) Homsapiens hyaluronidase 1 variant 1 (HYAL1) mRNA, complete cds; alternatively spliced. Accession # AF502904.

2. Lokeshwar, V.B*. Schroeder, G.L., and Iida, N. (2002) Homsapiens hyaluronidase 1 variant 2 (HYAL1) mRNA, complete cds; alternatively spliced. Accession # AF502905.

3. Lokeshwar, V.B*. Schroeder, G.L., and Iida, N. (2002) Homsapiens hyaluronidase 1 variant 3(HYAL1) mRNA, complete cds; alternatively spliced. Accession # AF502906.

4. Lokeshwar, V.B*. Schroeder, G.L., and Iida, N. (2002) Homsapiens hyaluronidase 1 variant 4 (HYAL1) mRNA, complete cds; alternatively spliced. Accession # AF502907.

5. Lokeshwar, V.B*. Schroeder, G.L., and Iida, N. (2002) Homsapiens hyaluronidase 1 variant 5 (HYAL1) mRNA, complete cds; alternatively spliced. Accession # AF502908.

6. Lokeshwar, V.B*. Schroeder, G.L., and Iida, N. (2002) Homsapiens hyaluronidase 3 variant 1 (HYAL3) mRNA, complete cds; alternatively spliced. Accession # AF502909.

7. Lokeshwar, V.B*. Schroeder, G.L., and Iida, N. (2002) Homsapiens hyaluronidase 3 variant 2 (HYAL3) mRNA, complete cds; alternatively spliced. Accession # AF502910.

8. Lokeshwar, V.B*. Schroeder, G.L., and Iida, N. (2002) Homsapiens hyaluronidase 3 variant 3 (HYAL3) mRNA, complete cds; alternatively spliced. Accession # AF502911.

9. Lokeshwar, V.B*. Schroeder, G.L., and Iida, N. (2002) Homsapiens hyaluronidase 3 (HYAL3) mRNA, complete cds; Accession # AF502912.

H. Clinical translational research: No clinical trials were undertaken.

I. Personnel and training provided: This award has allowed the P.I. to provide research training to two attending urologists. Dr. Sinan Ekici was a fellow of the Turkish Research Council and worked on Aim 1 of the project. Dr. Tadahiro Isoyama worked on Aims 2 and 3. In addition, the award has allowed the P.I. to provide research training to a total of 6 urology residents in the Department of Urology at University of Miami. However they were not paid by the grant. Personnel paid by the grant are: Lokeshwar Vinata, Grethchen Schroeder, Marie Selzer, Barbara Lopez, Roozbeh Golshani, Veronica Estrella and Luis Lopez.

4. Conclusions: Results derived from the experiments performed under Aim 1, demonstrate that HYAL1 and HA-HYAL1 are sensitive and specific markers for predicting biochemical recurrence for CaP patients who undergo radical prostatectomy. The multivariate analysis and long-term follow-up information establishes **for the first time**, the independent prognostic potential of HYAL1 type HAase for any type of cancer, in general, and for CaP in particular. The

results derived from experiments performed under Aims 2 and demonstrate **for the first time** that tumor-derived HAase in general and HYAL1 in particular act as both a tumor promoter and a suppressor, depending upon the concentration to which tumor cells are exposed. These results demonstrate that **both anti-HAase and high-HYAL1 treatments may have merit** in controlling CaP growth and progression.

5. REFERENCES:

1. Pettaway, C.A. Prognostic markers in clinically localized prostate cancer. Tech. Urol., 4: 35-42, 1998.

2. Blute, M.L. Bergstralh, E.J., Iocca, A., Scherer, B., Zincke, H. Use of Gleason score, prostate specific antigenm seminal vesicle and margin status to predict biochemical failure after radical prostatectomy. J. Urol., 165: 119-125, 2001.

3. Muzzonigro, G., Galosi, A.B. Biological selection criteria for radical prostatectomy. Ann N Y Acad Sci. 963:204-212, 2002.

4. Small, E.J., Roach M 3rd. Prostate-specific antigen in prostate cancer: a case study in the development of a tumor marker to monitor recurrence and assess response. Semin Oncol. 29: 264-73, 2002.

5. Palisaan, R.J., Graefen, M., Karakiewicz, P.I., Hammerer, P.G., Huland, E., Haese, A., Fernandez, S., Erbersdobler, A., Henke, R.P., Huland, H. Assessment of clinical and pathologic characteristics predisposing to disease recurrence following radical prostatectomy in men with pathologically organ-confined prostate cancer. Eur Urol. 41:155-161, 2002.

6. Isaacs W, De Marzo A, Nelson W. Focus on prostate cancer. Cancer Cell. 2:113-116, 2002.

7. Muzzonigro, G., Galosi, A.B. Biological selection criteria for radical prostatectomy. Ann N Y Acad Sci. 963:204-212, 2002.

8. Partin, A.W., Murphy, G.P., Brawer, M.K. Report on Prostate Cancer Tumor Marker Workshop 1999. Cancer, 88: 955- 963, 2000.

9.Tool, BP. Hyaluronan is not just a gloo! J. Clin. Invest. 106: 335-336, 2000.

10. Delpech, B., Girard, N., Bertrand, P., Courel, N.M., Chauzy, C., Delpech, A. Hyaluronan: Fundamental principles and applications in cancer. J. Intern. Med. 242: 41-48, 1997.

11.Hautmann, S.H., Lokeshwar, V.B., Schroeder, G.L., Civantos, F., Duncan, R.C., Friedrich, M.G., Soloway, M.S. Elevated tissue expression of hyaluronic acid and hyaluronidase validate HA-HAase urine test for bladder cancer. J. Urol., 165: 2068-2074, 2000.

12. Setala, L.P., Tammi, M.I., Tammi, R.H., Eskelin, M.J., Lipponen, P.R., Argen, U.M., Parkkinen, J., Alhava, E.M., Kosma, V.M., Hyaluronan expression in gastric cancer cells is associated with local and nodal spread and reduced survival rate. Br. J. Cancer, 79: 1133-1138, 1999.

13. Auvinen, P., Tammi, R., Parkkinen, J., Tammi, M., Agren, U., Johansson, R., Hirvikoski, P., Eskelinen, M., Kosma, V.M., Hyaluronan in peritumoral stroma and malignant cells associates with breast cancer spreading and predicts survival. Am. J. Pathol., 156: 529-536, 2000.

14. Pirinen, R., Tammi, R., Tammi, M., Hirvikoski, P., Parkkinen, J.J., Johansson, R. Prognostic value of hyaluronan expression in non-small-lung cancer: increased stromal expression indicates unfavorable outcome in patients with adenocarcinoma. Int J Cancer 95: 12-27, 2001.

15. Knudson, W. Tumor associated hyaluronan: providing an extracellular matrix that facilitates invasion. Am. J. Pathol., 148: 1721-1726, 1996.

16. Ropponen, K., Tammi, M., Parkkinen, J., Eskelinen, M., Tammi, R., Iipponen, P., Argen, V., Alhava, E., Kosma, V.M. Tumor-associated hyaluronan as an unfavorable prognostic factor in colorectal cancer. Cancer Res., 58:342-347, 1998.

17. Lipponen, P., Aaltomaa, S., Tammi, R., Tammi, M., Agren, U., Kosma, V.M. High stromal hyaluronan level is associated with poor differentiation and metastasis in prostate cancer. Eur. J. Cancer 37: 849-856, 2001.

18. Lokeshwar, V.B., Obek, C., Pham, H.T., Wei, D.C., Young, M.J., Duncan, R.C, Soloway, M.S., Block, N.L. Urinary hyaluronic acid and hyaluronidase: Markers for bladder cancer detection and evaluation of grade. J. Urol., 163: 348-356, 2000.

19. Lokeshwar, V.B., Obek, C., Soloway, M.S., Block, N.L. Tumor-associated hyaluronic acid: A new sensitive and specific urine marker for bladder cancer. Cancer Res., 57: 773-777, 1997.

20. Lokeshwar, V.B., Rubinowicz, D., Schroeder, G.L., Forgacs, E., Minna, J.D., Block, N.L. Nadji, M., Lokeshwar, B.L. Stromal and epithelial expression of tumor markers hyaluronic acid and hyaluronidase in prostate cancer. J. Biol. Chem. 276: 11922-11932, 2001.

21. Roden, L., Campbell, P., Fraser, J.R.E., Laurent, T.C., Petroff, H., Thompson, J.N. Enzymatic pathways of hyaluronan catabolism. In: The biology of hyaluronan. Whelan, E, (ed), Wiley, Chichister, Ciba Foundation Symp., 143, pp-60-86, 1989.

22. Csoka, A.B., Frost, G.I., Stern, R. The six hyaluronidase-like genes in the human and mouse genomes. Matrix Biol. 20: 499-508, 2001.

23. Lokeshwar, V.B., Lokeshwar, B.L., Pham, H.T., Block, N.L. Association of hyaluronidase, a matrix-degrading enzyme, with prostate cancer progression. Cancer Res., 56: 651-657, 1996.

24. Anderson, A.R., Feathergill, K., Diao, X., Cooper, M., Kirpatrick, R., Spear, P., Waller, D.P., Chany, C., Doncel, G.E., Herold, B., Zaneveld, L.J.D. Evaluation of poly(styrene-4-sulfonate) as a preventive agent for conception and sexually transmitted diseases. J. Androl., 21: 862-875, 2000.

25. Posey, J.T., Soloway, M.S., Ekici, S., Sofer, M., Civantos, F., Duncan, R.C., Lokeshwar, V.B. Evaluation of the prognostic potential of hyaluronic acid and hyaluronidase (HYAL1) for prostate cancer. Cancer Res. 63: 2638-2644, 2003.

26. Lesley, J, Hascall, VC, Tammi, M, Hyman, R. Hyaluronan binding by cell surface CD44. J Biol Chem. 2000 275: 26967-26975.

27. Cichy, J, Pure, E. The liberation of CD44. J Cell Biol. 2003, 161: 839-843.

28. Naor, D, Nedvetzki, S, Golan, I, Melnik, L, Faitelson, Y. CD44 in cancer. Crit Rev Clin Lab Sci. 2002, 39: 527-579.

29. Lokeshwar, BL, Lokeshwar, VB, Block, NL. Expression of CD44 in prostate cancer cells: association with cell proliferation and invasive potential. Anticancer Res. 1995, 15: 1191-

30. Welsh, CF, Zhu, D, Bourguignon, LY. Interaction of CD44 variant isoforms with hyaluronic acid and the cytoskeleton in human prostate cancer cells. J Cell Physiol. 1995, 64: 605-612.

31. Iczkowski, KA, Bai, S, Pantazis, CG. Prostate cancer overexpresses CD44 variants 7-9 at the messenger RNA and protein level. Anticancer Res. 2003 234: 3129-3140.

32. Gao, AC., Lou, W., Sleeman, JP, Isaacs, JT. Metastasis suppression by the standard CD44 isoform does not require the binding of prostate cancer cells to hyaluronate. Cancer Res. 1998, 58: 2350-2352.

33. Ekici, S, Ayhan, A, Kendi, S, Ozen, H. Determination of prognosis in patients with prostate cancer treated with radical prostatectomy: prognostic value of CD44v6 score. J Urol, 167: 2037-2041, 2002.

34. Aaltomaa, S, Lipponen, P, Ala-Opas, M. Kosma, VM. Expression and prognostic value of CD44 standard and variant v3 and v6 isoforms in prostate cancer. Eur Urol., 2001 39:138-144.

35. Folkman, J, Browder, T, Palmblad, J. Angiogenesis research: guidelines for translation to clinical application. Thromb Haemost. 2001, 86: 23-33.

36. Sauer, G, Deissler, H. Angiogenesis: prognostic and therapeutic implications in gynecologic and breast malignancies. Curr Opin Obstet Gynecol. 2003, 15: 45-49.

37. Goddard, JC, Sutton, CD, Furness, PN, O'Byrne, KJ, Kockelbergh, R.C. Microvessel density at presentation predicts subsequent muscle invasion in superficial bladder cancer. Clin Cancer Res. 2003, 9: 2583-2586.

38. Poon, RT, Fan, ST, Wong, J. Clinical significance of angiogenesis in gastrointestinal cancers: a target for novel prognostic and therapeutic approaches. Ann Surg. 2003, 238: 9-28.

39. Zhang, X, Yamashita, M, Uetsuki, H, Kakehi, Y. Angiogenesis in renal cell carcinoma: Evaluation of microvessel density, vascular endothelial growth factor and matrix metalloproteinases. Int J Urol. 2002, 9: 509-514.

40. De La Taille, A, Katz, AE, Bagiella, E, Buttyan, R, Sharir, S, Olsson, CA, Burchardt, T, Ennis, RD, Rubin, MA. Microvessel density as a predictor of PSA recurrence after radical prostatectomy : A comparison of CD34 and CD31. Am J Clin Pathol 2000, 113: 555-562.

41. Bono, AV, Celato, N., Cova, V., Salvadore, M., Chinetti, S., Novario, R. Microvessel density in prostate carcinoma. Prostate Cancer Prostatic Dis. 2002, 5: 123-127.

42. Weidner, N., Carroll, P.R., Flax, J., Blumenfeld, W., Folkman, J. Tumor angiogenesis correlates with metastasis in invasive prostate carcinoma. Am J Pathol 1993, 143: 401-409.

43. Silberman, M.A., Partin, A.W., Veltri, R.W., Epstein, J.I. Tumor angiogenesis correlates with progression after radical prostatectomy but not with pathologic stage in Gleason sum 5 to 7 adenocarcinoma of the prostate. Cancer 1997, 79: 772-779.

44. Gettman, M.T., Bergstralh, E.J., Blute, M., Zincke, H., Bostwick, D.G. Prediction of patient outcome in pathologic stage T2 adenocarcinoma of the prostate: Lack of significance for microvessel density analysis. Urology 1998, 51:79-85.

45. Rubin, M.A., Buyyounouski, M., Bagiella, E., Sharir, S., Neugut, A., Benson, M., De La Taille, A., Katz, A.E., Olsson, C.A., Ennis, R.D. Microvessel density in prostate cancer : Lack of correlation with tumor grade, pathologic stage, and clinical outcome. Urology 1999, 53: 542-547.

46. Ekici S., Cerwinka, W.H., Duncan, R. C. Gomez, P., Civantos, F., Soloway, M.S., Lokeshwar, V.B. Comparison of the prognostic potential of hyaluronic acid, hyaluronidase (HYALI-1), CD44v6 and Microvessel density for prostate cancer Int J Cancer 2004, 112: 121-129.

47. Lokeshwar, V.B., Schroeder, G.L., Carey, R.I., Soloway, M.S., Iida, N. Regulation of hyaluronidase activity by alternative mRNA splicing. J Biol Chem. 277: 33654-33663, 2002.

48. Lokeshwar, V.B., Young M.J., Goudarzi, G., Iida, N., Yudin, A.I., Cherr, G.N., Selzer, M.G. Identification of bladder tumor-derived hyaluronidase: Its similarity to HYAL1. Cancer Res., 59: 4464-4470, 1999.

49. Lokeshwar, V.B., Cerwinka, W.H., Lokeshwar, B.L. HYAL1 hyaluronidase in bladder cancer: A molecular determinant of bladder cancer growth and progression. Cancer Res., 2005, In Press.

50. Lokeshwar, V.B., Cerwinka, W.H., Lokeshwar, B.L. HYAL1 hyaluronidase in prostate cancer: A tumor promoter and a suppressor (To be submitted to Proc. Natl. Acad. Sci, USA).

51. Chang, N.S., Doherty, J., Ensign, A. JNK1 physically interacts with WW domain-containing oxidoreductase (WOX1) and inhibits WOX1-mediated apoptosis. J Biol Chem. 2003; 278: 9195-202.

52. Khatri, P., Draghici, S., Ostermeier, G.C., and Krawetz, S.A. Profiling gene expression using onto-express. Genomics, 2002, 79: 266–70.

53. Draghici, S., Khatri, P., Martins, R.P., Ostermeier, G.C., and Krawetz, S.A. Global functional profiling of gene expression. Genomics, 2003, 81: 98–104.

54. Barbucci, R., Lamponi, S., Magnani, A., Poletti, L.F., Rhodes, N.P., Sobel, M., Williams, D.F. Influence of Sulfation on Platelet Aggregation and Activation with Differentially Sulfated Hyaluronic Acids. J Thromb Thrombolysis. 1998, 6: 109-115.

55. Isoyama T, Thwaites D, Selzer MG, Carey RI, Barbucci R, Lokeshwar VB. Differential selectivity of hyaluronidase inhibitors toward acidic and basic hyaluronidases. Glycobiology 16: 11-21; 2006.

Regulation of Hyaluronidase Activity by Alternative mRNA Splicing*

Vinata B. Lokeshwar‡§¶‖, Grethchen L. Schroeder‡, Robert I. Carey‡, Mark S. Soloway‡, and Naoko Iida‡¶

From the Departments of ‡Urology and §Cell Biology and Anatomy, University of Miami School of Medicine, Miami, Florida 33101

Hyaluronidase is a hyaluronic acid-degrading endoglycosidase that is present in many toxins and the levels of which are elevated in cancer. Increased concentration of HYAL1-type hyaluronidase correlates with tumor progression and is a marker for grade (G) 2 or 3 bladder cancer. Using bladder tissues and cells, prostate cancer cells, and kidney tissues and performing reverse transcription-PCR, cDNA cloning, DNA sequencing, and in vitro translation, we identified splice variants of HYAL1 and HYAL3. HYAL1v1 variant lacks a 30-amino acid (aa) sequence (301–330) present in HYAL1 protein. HYAL1v1, HYAL1v2 (aa 183–435 present in HYAL1 wild type), HYAL1v3 (aa 1–207), HYAL1v4 (aa 260–435), and HYAL1v5 (aa 340–435) are enzymatically inactive and are expressed in normal tissues/cells and G1 bladder tumor tissues. However, HYAL1 wild type is expressed in G2/G3 tumors and in invasive tumor cells. Stable transfection and HYAL1v1-specific antibody confirmed that the HYAL1 sequence from aa 301 to 330 is critical for hyaluronidase activity. All tumor cells and tissues mainly express HYAL3 variants. HYAL3v1 lacks a 30-aa sequence (299–328) present in HYAL3 protein, that is homologous to the 30-aa HYAL1 sequence. HYAL3v1, HYAL3v2 (aa 251–417 present in HYAL3 wild type), and HYAL3v3 (aa 251–417, but lacking aa 299–328), are enzymatically inactive. Although splicing of a single independent exon generates HYAL1v1 and HYAL3v1, internal exon splicing generates the other HYAL1/HYAL3 variants. These results demonstrate that alternative mRNA splicing controls cellular expression of enzymatically active hyaluronidase and may explain the elevated hyaluronidase levels in bladder/prostate cancer.

Hyaluronidases (HAases)[1] are a family of enzymes that are crucial for the spread of bacterial infections, toxins present in

various venoms, and possibly, cancer progression (1–6). In humans, six HAase genes have been identified. These genes occur in clusters of three at two chromosomal locations (Ref. 7 and human genome blast search). HYAL1, HYAL2, and HYAL3 occur on chromosome 3p21.3, and PH20, HYAL4, and HYALP1 occur on chromosome 7q31.3. With the possible exception of HYAL4 and HYALP1, all other HAases degrade hyaluronic acid (HA) (7).

HA is a nonsulfated glycosaminoglycan made up of repeating disaccharide units, D-glucuronic acid, and N-acetyl-D-glucosamine. HA is present in body fluids, tissues, and the extracellular matrix (8–10). It keeps tissues hydrated and maintains osmotic balance and cartilage integrity (8, 10). HA also actively regulates cell adhesion, migration, and proliferation by interacting with specific cell surface receptors such as CD44 and RHAMM (11). The concentrations of HA are elevated in several inflammatory diseases and various carcinomas (e.g. bladder, prostate, breast, lung, colon, and so forth; Refs. 9 and 12–19). For example, we have shown that urinary HA concentration is a highly sensitive and specific marker for detecting bladder cancer, regardless of its grade (18, 19). In tumor tissues, HA may promote tumor growth and metastasis probably by actively supporting tumor cell migration and offering protection against immune surveillance (20–22). Small fragments of HA, generated by HAases, stimulate angiogenesis (23–25). We recently showed that HA fragments of ~10–15 disaccharide units stimulate endothelial cell proliferation by acting through cell surface HA receptor, RHAMM, and activating the mitogen-activated protein kinase pathway (26). We have also shown that elevated levels of HYAL1-type HAase coincide with the presence of angiogenic HA fragments in prostate tumor tissues and in the urine of bladder cancer patients (17, 27).

Among the six HAases, HYAL1, HYAL2, and PH20 are well characterized. HYAL1 type HAase was originally purified from human plasma and urine (28, 29). However, we have shown that HYAL1 is the major tumor-derived HAase expressed in bladder and prostate cancer tissues (17, 30). It has a optimum pH range of 4.0–4.3, and the enzyme is 50–80% active at pH 4.5 (17). Triggs-Raine et al. (31) have shown that a lack of functional HYAL1 results in a disorder called mucopolysaccharidosis IX. In this study the authors identified that aa Glu^{268} is crucial for HYAL1 activity. HYAL2 was originally designated as the lysosomal HAase, and it cleaves high molecular mass HA into ~20-kDa HA fragments (32). It has a pH optimum of ~4.0 and is possibly less active than other HAases. HYAL-2 may also be exposed to the cell surface through a GPI anchor (32). The third HAase gene in the 3p21.3 locus is HYAL3. Although

tumor; RT, reverse transcription; ELISA, enzyme-linked immunosorbent assay; TIM, triose phosphate isomerase.

HYAL3 transcripts have been detected in brain and liver tissues, its protein product is uncharacterized (31). Based on the sequence information deposited in GenBank™ HYAL3 is predicted to be made up of either 463 aa (accession number AF040710 (gi number 2935327)) or 417 aa (accession number BC012892 (gi number 15277616)).

Besides acidic HAases, PH20 (*i.e.* testicular HAase) is well characterized. PH20 is a sperm surface HAase that has a broad pH activity profile (pH 3.2–9.0) (33). In addition to being a HA-degrading enzyme, PH20 may also interact with HA to increase internal calcium, possibly by binding HA through aa 205–235 (34). This study also revealed that *N*-glycosylation and intrachain disulfide linkages are important for the HAase activity of PH20 (34).

Recently, the crystal structure of the bee venom HAase has been documented (35). The bee HAase shares ~30% sequence identity with human HAases. The crystal structure of bee HAase reveals a classical TIM barrel topology, where the catalytic site corresponds to Asp^{143} and Glu^{145} (aa numbering according to GenBank™ accession number AAA27730.1). Glu^{145} is involved the cleavage of the β-1,4 glycosidic bond between *N*-acetyl-D-glucosamine and D-glucuronic acid through an acid-base catalytic mechanism. These Asp and Glu residues are conserved in all mammalian HAases (32). For example, in HYAL1, the putative catalytic site residues are Asp^{131} and Glu^{133}, respectively, and in HYAL3, they are Asp^{127} and Glu^{129}, respectively (according to GenBank™ accession numbers AAD09137.2 and AAH12892.1). Based on the amino acid homology between bee HAase and mammalian HAases and conservation of several aa residues involved in both HA binding (*i.e.* substrate binding groove) and its catalysis (*i.e.* active site), a TIM barrel topology and a similar mechanism for the catalytic cleavage of HA are likely for the mammalian HAases (32).

In this study, we have identified several mRNA splice variants of HYAL1 and HYAL3 expressed in bladder and prostate cancer cells and in bladder and kidney tissues. These splice variants were characterized in terms of their protein product and HAase activity. We also identified a 30-aa region that is crucial for the HAase activity of HYAL1 and HYAL3 proteins.

EXPERIMENTAL PROCEDURES

Tissue Specimens—Normal bladder specimens were obtained from organ donors (20–50 years old), and the urothelial layer from these specimens was flash frozen after separation from the underlying muscle. Bladder tumor tissues (~1 g), bladder specimens with no evidence of disease (NED), and specimens of involved lymph node (*i.e.* local extension of tumor into lymph node) were obtained from bladder cancer patients undergoing cystectomy or transurethral resection of bladder tumor. The tissue specimens were split, and the mirror segment was examined by histology following fixation in formalin. In this study, we have included data from only those specimens that were histologically confirmed as normal and tumor (with grade information). All of the tissues were flash frozen and stored at −70 °C until use.

Tissue Culture—Established bladder cancer cell lines (*i.e.* HT1376, RT4, and UMUC-3) and prostate cancer cell lines (*i.e.* DU145 and LNCaP) were obtained from the American Type Culture Collection. Dr. Mark E. Stearns (Medical College of Pennsylvania, Philadelphia, PA) kindly provided the prostate cancer line PC3-ML (36). Bladder cancer cell lines 253J-Lung and 253J-parent were gifts from Dr. Colin Dinney (M. D. Anderson Cancer Center, University of Texas, Houston, TX) (37). All of these cell lines were cultured in RPMI 1640, 10% fetal bovine serum, and gentamicin. Primary normal bladder cell cultures were set up from the normal urothelium. The urothelial cells were gently scrapped from the bladder urothelium in RPMI 1640 containing 40% fetal bovine serum. The cell suspension (2 ml) was added to T-25 tissue culture flasks, and the cells were allowed to attach overnight. The following day, the nonadherent cells were washed off, and the cells were cultured in keratinocyte growth medium (Clonetics/BioWhitaker, San Diego, CA) until 80% confluence. The epithelial growth was confirmed by cytokeratin staining. Total RNA was extracted from the urothelial cultures on either the first or the second passage.

RT-PCR, cDNA Cloning, and Sequence Analyses—Total RNA was extracted from bladder/prostate cells, bladder tissues, and lymph node specimens using a RNA extraction kit (Qiagen). Total RNA from kidney tissues was purchased from BD Biosciences/CLONTECH (Palo Alto, CA). Total RNA (~1 μg) was subjected to first strand cDNA synthesis using a Superscript™ preamplification system and oligo(dT) primers (Invitrogen). The entire HYAL1 coding sequence was amplified from the first strand cDNA using a HYAL1-L3/HYAL1-R2 primer pair that we have used previously (17). HYAL1-L3 primer sequence is as follows: 5'-CTTCCTCCAGGAGTCTCTGGT-3'. The HYAL1-R2 primer sequence is as follows: 5'-ATCACCACATGCTCTTCCGC-3'. This primer pair should amplify a 1926-bp HYAL1 cDNA that contains the entire coding region of HYAL1 (618–1925). When compared with the HYAL1 clone HSU03056 that is deposited in GenBank™, HYAL1 cDNA amplified by the HYAL1-L3/HYAL1-R2 primer pair will contain an extra C at the 5' terminus. This C is present in the human LUCA13 cosmid clone from the chromosome region 3p21.3 (GenBank™ accession number ACC002425). Thus, in this study, as compared with the HYAL1 clone HSU03056, the numbering of nucleotides in HYAL1wt and HYAL1 variant cDNAs is offset by 1.

To amplify HYAL3 cDNA, we used the following primer pair: 1) HYAL3-L2: The sequence of this primer corresponds to nucleotides 157–176 in the HYAL3 clone AF040710. This sequence is not present in the HYAL3 clone BC012892. HYAL3-L2 primer sequence is as follows: 5'-CCAGAGGCCAGCATCAACAT-3'. 2) HYAL3-R2: The sequence of this primer (5'-GACTCACATGATCTCAGAGG-3') is reverse complementary to the sequence between nucleotides 1629 and 1648 in the HYAL3 clone AF502912, nucleotides 1628 and 1647 in the clone AF040710, and nucleotides between 1464 and 1483 in the clone BC012892. The HYAL3-L2/HYAL3-R2 primer pair should amplify a 1491-bp HYAL3 product. The amplification of HYAL1 and HYAL3 cDNAs was carried out by PCR as described previously (17). PCR products were analyzed by agarose gel electrophoresis and ethidium bromide staining.

The PCR products were directly cloned into the eukaryotic expression vector pcDNA3.1/v5/His-TOPO using a TOPO cloning kit (Invitrogen). This expression vector contains a strong cytomegalovirus promoter for eukaryotic expression, a neomycin resistance gene for selecting stable mammalian cell transfectants, and an ampicillin resistance gene for bacterial selection. All of the cloned HYAL1 and HYAL3 cDNAs were sequenced in an automated DNA sequencer in the DNA core facility at the University of Miami.

Generation of RT4 Stable Transfectants—RT4 cells (2 × 10^5 cells/ 6-cm dish) were transfected with 5 μg of either HYAL1 wild type (HYAL1wt) or HYAL1v1 (one of the HYAL1 variants) or pcDNA3.1/v5/His-TOPO vector using the Effectene™ transfection agent (Qiagen). Following 48 h of incubation in the growth medium (RPMI 1640, 10% fetal bovine serum, gentamicin), the transfectants were selected in neomycin (100 μg/ml)-containing growth medium. The RT4 clones resistant to neomycin were expanded and tested for HAase activity and HYAL1 protein expression using an HAase activity ELISA-like assay and immunoblot analysis, respectively, as described below.

In Vitro Translation—HYAL1 and HYAL3 cDNAs were *in vitro* translated using the TNT® Quick coupled transcription/translation system (Promega, Madison, WI). For generating [^{35}S]methionine-labeled product, 1 μg of cDNA (vector, HYAL1, or HYAL3) was mixed with TNT® Quick master mix and 20 μCi of Amersham Biosciences Redivue™ L-[^{35}S]methionine. The reaction was carried out at 30 °C for 90 min. Following incubation, 5-μl aliquots of each sample were mixed with 20 μg of bovine serum albumin and precipitated with equal volume of ice-cold 20% tricholoroacetic acid. The precipitates were centrifuged, washed twice in 10% tricholoroacetic acid, and washed once with 80% ice-cold ethanol. The precipitates were dissolved in SDS sample buffer and analyzed by 12% SDS-PAGE under reducing/nonreducing conditions.

Alternatively, the HYAL1/HYAL3 cDNAs or vector DNA were mixed with TNT® Quick master mix and 20 μM unlabeled L-methionine. The reaction was carried out at 30 °C for 90 min. The unlabeled *in vitro* translated products were analyzed for HAase activity by the ELISA-like assay.

HAase ELISA-like Assay—HAase ELISA-like assay has been described previously (17, 18, 38, 39). To assess HAase activity secreted by RT4 transfectants and bladder cancer cells, at ~60% confluence, various cultures were washed three times in phosphate-buffered saline and incubated in RPMI 1640 containing insulin, transferrin, and selenium solution (ITS supplement, Sigma-Aldrich). Following a 48-h incubation, the serum-free conditioned media were collected. For the HAase activity ELISA-like assay, various aliquots (0.5, 1.0, 2.5, 5.0, 7.5, and 10 μl)

of either *in vitro* translated samples, serum-free culture-conditioned media of different cells/transfectants or urine from bladder cancer patients or normal individuals were incubated with 96-well HA-coated microtiter plates in the presence of HAase assay buffer. Following incubation, the degraded HA was washed off, and the HA remaining on the wells was detected using a biotinylated HA-binding protein and an avidin-biotin detection system. The HAase present in each sample was calculated using a standard graph, which was prepared by plotting $A_{405\ nm}$ *versus* HAase concentration (units $\times$ 10^{-4}/ml) (18, 39). In the *in vitro* translated samples, the $A_{405\ nm}$ of each HYAL1/HYAL3 sample was subtracted from the $A_{405\ nm}$ of the vector sample, and the difference was used to determine the HAase activity.

Generation of Anti-HYAL1v1 Peptide Antibody—A 13-aa HYAL1v1 peptide (NH_2-TNHFLPLESCQAI-COOH) was synthesized, conjugated to keyhole limpet hemocyanin, and injected in New Zealand rabbits. The anti-HYAL1v1 antibody was purified using the HYAL1v1 peptide-conjugated affinity chromatography. The synthesis of HYAL1v1 peptide, generation of rabbit polyclonal antibody, and affinity purification were carried out by ResGen™ Invitrogen Corp. (Huntsville, AL).

Immunoblot Analysis—Conditioned media of bladder cancer cells and stable transfectants and urine specimens were separated by 8.5% SDS-PAGE under nonreducing conditions. The gels were blotted on to polyvinylidene difluoride membranes. The blots were probed with either anti-HYAL1 peptide IgG (30) or anti-HYAL1v1peptide affinity-purified IgG at 4 °C for 16 h. The blots were developed using an alkaline phosphatase detection system, as described previously (30).

RESULTS

Detection of HYAL1 Splice Variants by RT-PCR, cDNA Cloning, and Sequence Analysis—Based on the Human Genome Blast search, HYAL1 gene contains three exons separated by two introns (NT_006014.7/HS3_6171, *Homo sapiens* chromosome 3 working sequence). It has been previously shown that the untranslated region in exon 1 between nucleotides 110 and 596 is alternatively spliced (GenBank™ accession number AF173154). To detect the expression of HYAL1 in various cancer cells, tumor tissues, and normal kidney tissue, we performed RT-PCR analysis using a HYAL1-specific primer pair. This primer pair should amplify the entire HYAL1 coding region (bp 618–1926), an untranslated region in exon 1 that is alternatively spliced (nucleotide 110 joining 596), and the first 110 bp. Thus, the length of the expected PCR product is 1926 nucleotides. Fig. 1 (*A* and *B*) shows two gels in which PCR products from various samples were analyzed. The different tissue specimens are numbered (*e.g.* NBL-1 to NBL-4; G1-BT-1 to G1-BT-3; G2-BT-1 and G2-BT-2; G3-BT-1 to G3-BT-3; NED1-1; NED-2; LN-1 and LN-2). An approximately 1.4-kb product is amplified from bladder cancer cells (*i.e.* HT1376, 253J-Lung, 253J-parent, and UMUC-3), prostate cancer cells (*i.e.* DU145, LNCaP, and PC3-ML), G2 and G3 bladder tumor tissues (G3-BT-1, G2-BT-1, G2-BT-2, G3-BT-2, and G3-BT-3), lymph node specimens invaded with bladder tumor (LN-1 and LN-2) and normal kidney tissue (Fig. 1, *A* and *B*). RT4 RNA sample showed negligible amplification of any HYAL1-related PCR products. A smaller ~1.3-kb PCR product is also amplified from 253J-Lung and HT1376 RNA samples (Fig. 1*A*). The same ~1.3-kb PCR product was also detected in the kidney tissue and some bladder tumor tissue specimens when electrophoresis was carried out for a longer period of time to allow separation between ~1.4- and ~1.3-kb PCR products (data not shown). As shown in Fig. 1 (*A* and *B*), an approximately 500-bp PCR product is amplified from RNA samples isolated from a primary normal bladder cell culture (NBL cells), normal bladder tissues (NBL-1, NBL-2, NBL-3, and NBL-4), kidney tissue, and G1 bladder tumor tissues (G1-BT-2 and G1-BT-3). An approximately 650-bp PCR product is also amplified from two G1 bladder tumor tissues (G1-BT-1 and G1-BT-3), NBL2 tissue, normal kidney tissue, and an LN-2 specimen (Fig. 1, *A* and *B*). An approximately 1.0-kb PCR product is amplified from a G3 bladder tumor tissue (G3-BT-1) and an LN-1 specimen (Fig. 1
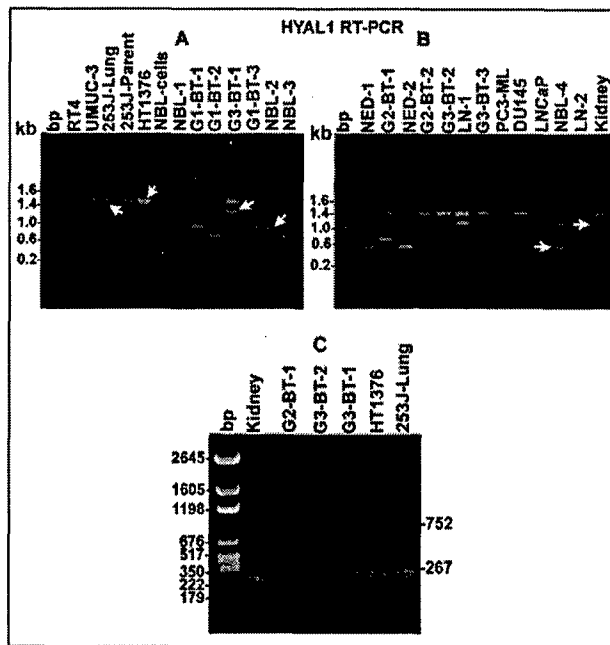

FIG. 1. **Examination of HYAL1 expression in tissues and cells.** Total RNA extracted from bladder tissues, bladder cells (tumor cells: RT4, UMUC-3, 253J-Lung, and 253J-parent and HT1376; NBL cells: normal bladder cells), prostate cancer cells (PC3-ML, DU145, and LN-CaP) was subjected to RT-PCR analysis using HYAL1-specific primers as described under "Experimental Procedures." The PCR products were analyzed by agarose gel electrophoresis. Six PCR products of different lengths are marked. PCR products expressed in each of these tissues or cells were cloned and sequenced. The tissue specimens in each category are numbered (*e.g.* NBL-1, NBL-2, G1-BT-1, G3-BT-1, LN-1, etc.). *A* and *B*, RT-PCR analysis using primer pair HYAL1-L3 and HYAL1-R2. This primer pair should amplify an approximately 1.9-kb HYAL cDNA (*i.e.* 1–1926 bp) that contains the HYAL1 coding region (618–1925 bases). A 200-bp ladder (Promega) was used as a bp marker. *C*, RT-PCR analysis using the primer pair HYAL1-L3 and HYAL1-R3. This primer pair should amplify a 267- or 752-bp PCR product depending upon the splicing status of the HYAL1 transcript related to the untranslated region between nucleotides 110–596. pGEM markers (Promega) were used as a bp ladder.

A and *B*). A slightly larger PCR product (~1.1-kb) was detectable in NBL-4 and kidney tissue samples (Fig. 1*B*).

Because the RT-PCR analysis described above does not result in the amplification of an approximately 1.9-kb PCR product that is expected based on the primer pair design, there could be two possibilities. First, such a product may have been missed because of the large size of the PCR product, and second, bladder tissues/cells contain only the HYAL1 transcript in which the bp between 110 and 596 are spliced out. The second possibility is based on the sequences deposited in GenBank™, which show that the 5′-untranslated region between nucleotides 110 and 596 is alternatively spliced (*e.g.* accession numbers HSU03056 and AF173154). To test these possibilities we performed RT-PCR analysis using a HYAL1 primer pair (*i.e.* HYAL1-L3/HYAL1-R3) that lies outside the boundaries of the spliced region. This primer pair would generate a 267-bp PCR product if the region between nucleotides 110 and 596 is spliced out, and a 752-bp PCR product will be generated if the HYAL1 transcript is unspliced. We have previously used this primer pair to demonstrate the presence of HYAL1 splicing in this region in prostate cancer cells (17). As shown in Fig. 1*C*, a major 267-bp PCR-amplified product is present in all samples, which include kidney, G2-BT-1, G3-BT-2, G3-BT-1, HT1376, and 253J-Lung. However, a minor 752-bp product is visible in bladder cancer cells and bladder tumor tissues. The presence and absence of the region between nucleotides 110 and 596 was
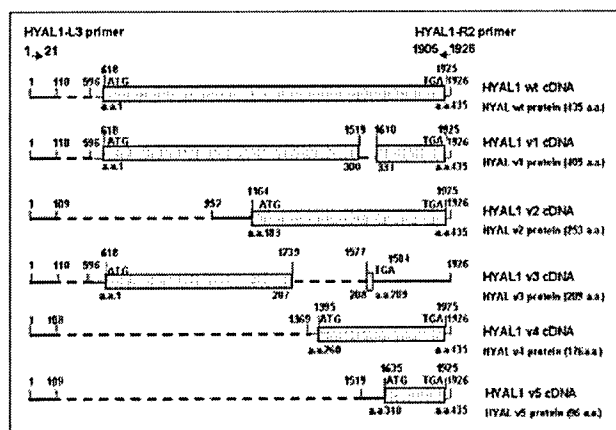
FIG. 2. **A schematic representation of the HYAL1 splice variants.** The figure shows HYAL1wt and different splice variant cDNAs. The numbering is based on the sequence of cDNA clone HSU03056 that is deposited in GenBank™. However, the numbering is offset by 1. This is because HSU03056 clone lacks the nucleotide C that is present in the 5′ terminus of all HYAL1 clones described in this study. The coding region is shown as a *dotted block.* The *dashed line* shows the region that is spliced out, and *solid line* represents untranslated regions. Each splice junction is marked by the nucleotides at the 5′ and 3′ boundaries that are joined because of splicing. The translation initiation and termination codons for HYAL1wt and HYAL1 variants are marked. The figure also shows the position of the forward (*i.e.* HYAL1-L3) and the reverse complementary (*i.e.* HYAL1-R2) primer pair used to amplify HYAL1 cDNA. The sequences of these primers are given under "Experimental Procedures."

confirmed by cDNA cloning and sequencing of the 267- and 752-bp PCR products as we described before (17). These results indicate that it is very likely that the HYAL1 transcripts in which the region between nucleotides 110 and 596 is unspliced are not the major HYAL1 transcripts expressed in bladder tumor tissues and cells. Furthermore, lack of amplification of an approximately 1.9-kb PCR product in tissue/cell specimens may be due to some technical difficulty associated with the amplification of large PCR products.

All of the different PCR products from each sample were gel-isolated and directly cloned into the eukaryotic expression vector pcDNA3.1/v5/His-TOPO. The sequence analyses revealed that various PCR products represent HYAL1 mRNA splice variants. The cDNA and amino acid sequences of each of the five HYAL1 splice variants described in this study have been deposited in GenBank™. As shown in Fig. 2, the ~1.4-kb product is actually 1441 bases in length and is generated by splicing of the region from nucleotides 109 to 595 and, thus, joining nucleotides 110–596. This HYAL1 splice variant that arises from an internal splicing event in exon 1 has been identified previously (GenBank™ accession number AF173154 (gi number 5825510)). For the purpose of this study, we have designated the 1441-bp HYAL1 cDNA as HYAL1wt. The cloned HYAL1wt cDNA encodes the intact wild type HYAL1 protein consisting of 435 aa, the sequence of which is identical to that deposited in GenBank™ (accession number AAD09137.2)

The actual length of the ~1.3-kb product is 1351 bases. It lacks the region in Exon 1 between nucleotides 110 and 596 and, in addition, contains a deletion that joins nucleotides 1519 and 1610 (*i.e.* nucleotides 1520–1609 are deleted; Fig. 2). This cDNA, designated as HYAL1v1 (HYAL1 variant 1; GenBank™ accession number AF502904), can encode a protein that is 405 aa in length. When compared with the HYAL1wt protein sequence, the HYAL1v1 protein lacks 30 aa from aa 301–330. Thus, in the putative HYAL1v1 protein, aa 300 is joined to aa 331 (Fig. 2).

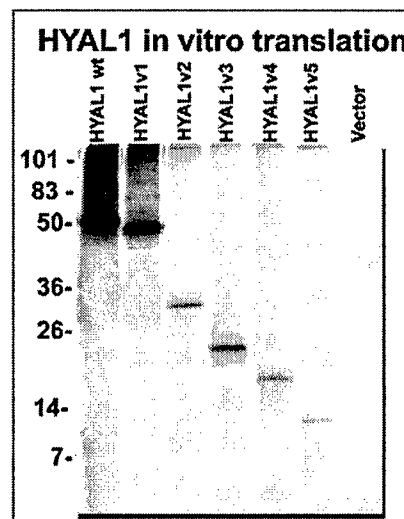The HYAL1v2 cDNA consists of 1084 bases (Fig. 2). In this

FIG. 3. *In vitro* **transcription/translation of HYAL1wt and HYAL1 variant cDNAs.** Various HYAL1 cDNAs and plasmid vector DNA were transcribed and translated *in vitro* using a coupled transcription/translation system and ^{35}S-labeled methionine, as described under "Experimental Procedures." The ^{35}S-labeled proteins were analyzed by SDS-PAGE along with molecular mass markers as described under "Experimental Procedures."

variant, nucleotide 109 is joined to nucleotide 952, *i.e.* the sequence from nucleotides 110 to 951 is deleted (GenBank™ accession number AF502905). If the HYAL1v2 variant is translated, using an ATG at position 1164 as the start codon, it will generate a protein consisting of 253 aa. The sequence of the putative HYAL1v2 protein is identical to the HYAL1wt protein sequence from aa 183 to 435.

The slightly larger ~1.1-kb HYAL1 variant is designated as HYAL1v3, and it is 1104 bases in length (Fig. 2). HYAL1v3 contains two spliced regions; in the first, nucleotide 110 joins nucleotide 596, and in the second, nucleotide 1239 joins nucleotide 1577 (*i.e.* bases from 1240 to 1576 are deleted; GenBank™ accession number AF502906). If HYAL1v3 is translated, it will utilize ATG[618] as the start codon and generate a protein consisting of 209 aa (Fig. 2). The first 207 aa of the putative HYAL1v3 protein are identical to the first 207 aa of the HYAL1wt protein.

The ~0.65-kb PCR product originates from a HYAL1v4 variant whose actual length is 666 bases (Fig. 2). The HYAL1v4 cDNA contains a deletion starting from nucleotide 109 and ending at nucleotide 1368. Thus, in the HYAL1v4 cDNA, nucleotide 108 is joined to nucleotide 1369 (GenBank™ accession number AF502907). The HYAL1v4 cDNA contains an open reading frame starting at ATG[1395] that allows translation of a polypeptide consisting of 176 aa. The aa sequence of the putative HYAL1v4 protein is identical to the aa sequence of HYAL1wt starting with aa 260–435 (Fig. 2).

The splice variant HYAL1v5 consists of 517 bases, and this variant is generated by splicing of nucleotides 109 and 1519 (GenBank™ accession number AF502908). If ATG[1635] is used as the start codon, the HYAL1v5 variant will encode a protein made up of 96 aa, the sequence of which is identical to the HYAL1wt protein sequence from aa 340 to 435 (Fig. 2).

In Vitro Translation and Analysis of HAase Activity of HYAL1 Variant Proteins—To determine whether various HYAL1 variants encode HAase activity, we used a coupled *in vitro* transcription/translation system and ^{35}S-labeled L-methionine to generate HYAL1wt and HYAL1 variant proteins. As shown in Fig. 3, the *in vitro* translated HYAL1wt and HYAL1 variant (v1–v5) proteins are of molecular mass ~50, ~47, ~30,
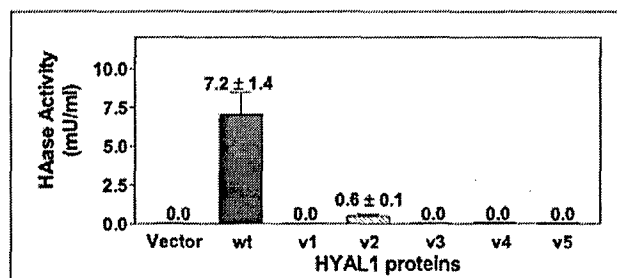
FIG. 4. **Analysis of HAase activity of HYAL1wt and HYAL1 variant proteins.** *In vitro* translated, unlabeled HYAL1wt and HYAL1 variant proteins, as well as vector-only control were analyzed for HAase activity using the HAase activity ELISA-like assay as described under "Experimental Procedures." Each sample was assayed at five different concentrations in duplicate. The results represent milliunits/ml ± S.E. Each experiment was repeated twice and independently.

~20, and ~10 kDa. The molecular mass of these proteins is similar to the expected molecular mass of the HYAL1wt and various HYAL1 variant polypeptides, based on their deduced aa sequences. The reduced intensities of the ^{35}S-labeled HYAL1v2, HYAL1v3, HYAL1v4, and HYAL1v5 proteins are most likely not due to reduced synthesis but to the reduced number of methionine residues present in these polypeptides. Based on the deduced aa sequence, HYAL1wt and HYAL1v1 proteins contain 9 methionines, whereas HYAL1v2, HYAL1v3, HYAL1v4, and HYAL1v5 proteins contain 6, 4, 4, and 3 methionines, respectively.

The HAase activity of *in vitro* translated HYAL1 variant proteins was measured using an ELISA-like assay (30, 39). Because we have previously shown that HYAL1 type HAase has a pH optimum at 4.2 (range 4.0–4.3; Ref. 30), the HAase ELISA-like assay was carried out at pH 4.2. As shown in Fig. 4, no HAase activity is detected in the vector only sample. However, the *in vitro* translated HYAL1wt protein has measurable HAase activity (7.2 ± 1.4 milliunits/ml). Interestingly, the HYAL1v1 protein that lacks only 30 aa (aa 301–330) has no HAase activity (Fig. 4). It is noteworthy that the HYAL1v1 protein contains both the putative HAase catalytic site (Asp[131] and Glu[133]) and Glu[268], which are critical for HAase activity of HYAL1 (Figs. 2 and 4 and Ref. 31). The HYAL1v2 protein that lacks the putative catalytic site but retains Glu[268] and the 30-aa sequence shows less than 90% of HAase activity (0.6 ± 0.1 milliunits/ml) when compared with the HYAL1wt protein. No HAase activity is detected in HYAL1v3, HYAL1v4, and HYAL1v5 proteins. We also conducted the HAase ELISA-like assay at pH 3.7, 5.0, and 7.0, and none of the HYAL1 variants showed any activity at these pH levels (data not shown). These results demonstrate that although the catalytic site in HYAL1 may lie in the amino-terminal third of the protein, a 30-aa sequence from aa 301 to 330 is also critical for HAase activity.

Evaluation of HAase Expression in Stable Transfectants Expressing HYAL1wt and HYAL1v1 cDNA Constructs—It is possible that when translated *in vitro*, the HYAL1v1 protein does not fold correctly and/or lacks some post-translational modifications that are necessary for HAase activity. To test this possibility, we stably transfected RT4 bladder cancer cells with plasmid vector DNA, HYAL1wt, or HYAL1v1 cDNA constructs. We have previously shown that HYAL1 is not expressed in RT4 cells and that these cells do not secrete any HAase activity in their culture-conditioned media. We analyzed 10 stable clones of RT4 cells/construct (*i.e.* vector, HYAL1wt, and HYAL1v1) for HAase activity and HYAL1-related protein expression. The data on two representative clones/construct are shown in Figs. 5 and 6. Fig. 5A shows immunoblot analysis of culture-condi-
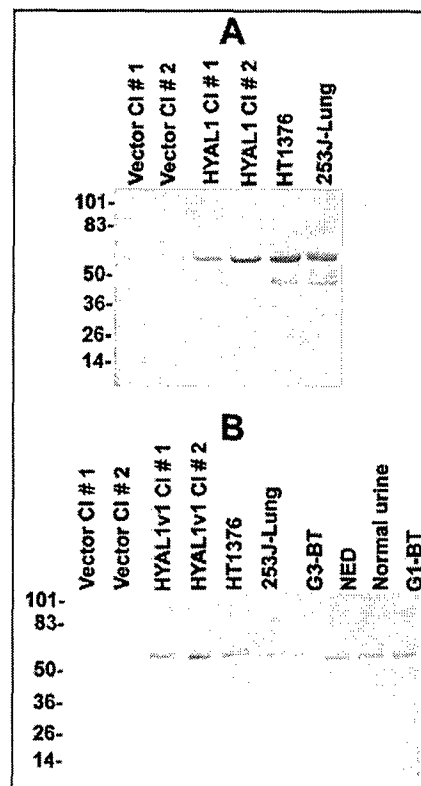

FIG. 5. **Immunoblot analysis of HYAL1 and HYAL1v1 expression.** Serum-free culture-conditioned media of RT4 stable transfectant (*i.e.* vector only, HYAL1wt, and HYAL1v1; two clones/construct), bladder cancer cells, and patient urine were subjected to either anti-HYAL1 or anti-HYAL1v1 peptide IgG immunoblot analysis as described under "Experimental Procedures." *A*, immunoblot analysis using anti-HYAL1 peptide IgG. *HYAL1* indicates HYAL1wt. *B*, immunoblot analysis using an affinity-purified anti-HYAL1v1 IgG. *G3-BT*, urine specimen obtained from a patient with G3 bladder tumor; *G1-BT*, urine specimen obtained from a patient with G1 bladder tumor; *NED*, urine specimen obtained from a patient with a history of bladder cancer but no disease at the time of specimen collection.

tioned media of RT4 clones and HT1376 and 253J-lung cells using an anti-HYAL1 peptide IgG (30). The anti-HYAL1 peptide IgG was generated against a peptide sequence in HYAL1 between aa 321 and 338 (30). Thus, this antibody will be able to recognize HYAL1wt and variant proteins HYAL1v2 and HYAL1v4. However, it will not detect other variant proteins (*i.e.* HYAL1v1, HYAL1v3, and HYAL1v5) that either partially or completely lack this sequence. Although no expression of HYAL1-related protein is observed in the vector only clones, an approximately 60-kDa HYAL1 protein is detected in the conditioned media of HYAL1wt clones and HT1376 and 253J-lung cells. The molecular mass of the HYAL1wt protein detected in the conditioned media is higher than that generated by *in vitro* translation (~50 kDa), indicating that HYAL1 protein is glycosylated or modified by other post-translational modifications. It is noteworthy that the anti-HYAL1 peptide IgG was able to immunoprecipitate [35S]methionine-labeled HYAL1wt polypeptide generated by *in vitro* translation (data not shown). The smaller product observed in the conditioned media of HT1376 and 253J-Lung cells is most likely a degradation product. This is because these cells do not express HYAL1 v2 and HYAL1v4 transcripts (as seen in Fig. 1A), and furthermore, the molecular mass of this product (~45 kDa) is larger than those of the expected HYAL1 v2 and HYAL1 v4 products.

Fig. 5B shows immunoblot analysis of conditioned media of HYAL1 v1 transfectants of RT4, HT1376, and 253J-Lung cells
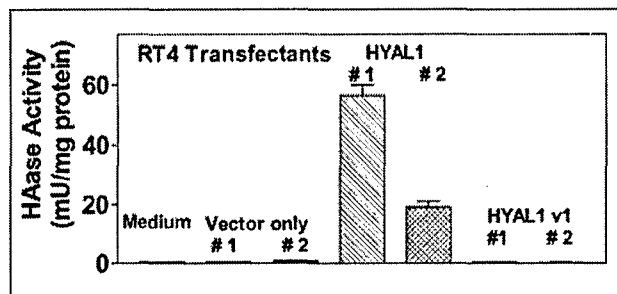
FIG. 6. **Analysis of HAase activity secreted by RT4 stable trans-fectants.** Serum-free culture-conditioned media of two clones each of vector only, HYAL1wt, and HYAL1v1 RT4 transfectants were assayed for HAase activity using the ELISA-like assay as described under "Experimental Procedures." Five concentrations of each sample were assayed in duplicate in each experiment, and each experiment was independently repeated three times. The HAase activity was normalized to total protein (mg/ml) and expressed as milliunits/mg protein ± S.E.

FIG. 7. **Examination of HYAL3 expression in tissues and cells.** Total RNA extracted from bladder tissues, bladder cells (RT4, UMUC-3, 253J-Lung, 253J-parent, and HT1376), and lymph node specimens invaded with bladder tumor was subjected to RT-PCR analysis using HYAL3 specific primers as described under "Experimental Procedures." The PCR products were analyzed by agarose gel electrophoresis. Four PCR products of different lengths are marked. PCR products expressed in each of these tissues or cells were cloned and sequenced. A 200-bp ladder (Promega) was used a bp marker.

and urine specimens using an anti-HYAL1v1 affinity-purified peptide IgG. The anti-HYAL1v1 antibody was generated against a 13-aa peptide in which the 300th aa present in the HYAL1 sequence is juxtaposed with 331st aa Such a peptide can occur only in the HYAL1v1 protein, in which the aa 300 is joined to aa 331 because of mRNA splicing. Therefore, this antibody is specific for HYAL1v1 and does not detect other HYAL1 proteins. As expected, no HYAL1v1 protein is detected in the conditioned media of vector only clones. However, an approximately 57-kDa protein is detected in the conditioned media of HYAL1v1 clones. Interestingly, the protein detected by anti-HYAL1v1 peptide IgG is also present in the conditioned media of HT1376 and 253J-Lung cells and in the urine of bladder cancer patients (G3-BT and G1-BT), a patient with bladder cancer history but no disease at the time of urine collection, and normal individual (Fig. 5*B*). The faint smaller bands that are observed in some samples are possibly degradation products that may be generated during sample storage. The fact that the molecular mass of the HYAL1v1 protein is larger than the HYAL1v1 polypeptide generated by *in vitro* translation suggests that the HYAL1v1 protein is also post-translationally modified. The secretion of both the cloned and naturally occurring HYAL1v1 protein in the culture-conditioned media suggests that the HYAL1v1 protein is folded and processed correctly. It should be noted that the ~57-kDa protein detected by anti-HYAL1v1 IgG in the immunoblot analysis is HYAL1v1, because the affinity-purified anti-HYAL1v1 IgG was able to immunoprecipitate HYAL1v1 polypeptide generated by *in vitro* translation (data not shown).

We next measured the HAase activity secreted in the conditioned media of various RT4 transfectants, and the activity was normalized to total protein in the conditioned media. As shown in Fig. 6, there is no detectable HAase activity in the medium control and in the conditioned media of the vector only clones. However, the two HYAL1wt clones secrete high levels of HAase activity (*i.e.* clone number 1: 56.5 ± 3.5 milliunits/mg protein and clone number 2: 27 ± 4 milliunits/mg protein). However, no HAase activity is detected in the conditioned media of RT4 clones that express and secrete HYAL1v1 protein. These results demonstrate that the HYAL1v1 protein is enzymatically inactive and that the sequence from aa 301 to 330 is critical for the activity of HYAL1 protein.

Detection of HYAL3 Splice Variants, cDNA Cloning, and Sequencing—Because the chromosomal locations are similar in HYAL1, HYAL2, and HYAL3 genes (7, 32, 40), we examined whether HYAL3 might also be similarly spliced and generate splice variants. The Human Genome Blast search reveals that
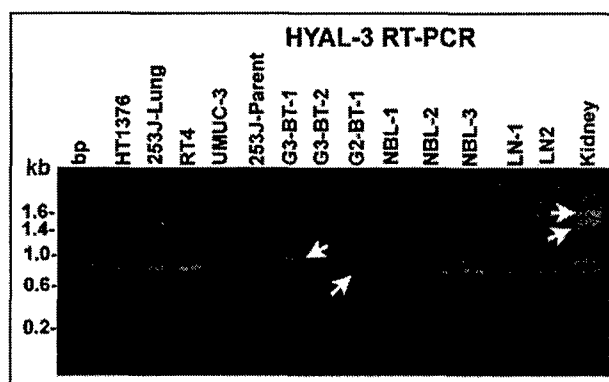
HYAL3 gene contains four exons separated by three introns (NT_006014.7/HS3_6171, *H. sapiens* chromosome 3 working sequence). To HYAL3 expression, we performed RT-PCR analysis on RNA extracted from bladder cancer lines (*i.e.* HT1376, 253J-Lung, RT4, UMUC-3, and 253J-parent), bladder tissues (*i.e.* normal and tumor), lymph node positive for tumor, and normal kidney tissue. The primer pair that we used for PCR analysis was designed to amplify a full-length HYAL3 cDNA, 1.5-kb in length. As shown in Fig. 7, an approximately 1.5-kb product is amplified from normal kidney tissue RNA. A smaller ~1.4-kb product is also visible in the kidney tissue sample that is detectable in many bladder cancer cell lines. The major PCR amplification product that is present in all bladder cancer cells, tissues, and lymph node specimens is ~600 bp in length (Fig. 7). This product is also present in the kidney tissue sample, along with an approximately 700-bp product. In addition, the 700-bp product is amplified from RNA extracted from G3 bladder tumor tissue (*i.e.* G3-BT-1), normal bladder tissue (*i.e.* NBL-3), and normal kidney tissue.

The ~1.5, ~1.4, ~0.7, and 0.6-kb PCR products were gel-isolated and directly cloned into the eukaryotic expression vector pcDNA3.1/v5/His-TOPO. The sequence analyses revealed that different PCR products represent HYAL3 splice variants. As shown in Fig. 8, the ~1.5-kb splice variant is actually 1492 bases in length. The sequence of this cDNA is 100% homologous to the HYAL3 clone AF040710 from nucleotides 157 to 1647, except that our cDNA has an extra G at position 1422 (GenBank[TM] accession number AF502912). This G is present in other HYAL3 cDNA clones (*e.g.* BC012892) and in the cosmid clone LUCA14 from 3p21.3, sequences of which are deposited in GenBank[TM] (accession numbers gi16164953, gi15208650, gi13543476, and AF036035). The G at position 1422 is also present in all of the HYAL3 splice variants identified in this study. Because of the presence of this G, translation of the HYAL3 polypeptide terminates at position 1447 (TAA termination codon position 1445–1447) and generates a 417-aa protein (Fig. 8).

The ~1.4-kb PCR product contains 1402 bases. As shown in Fig. 8, this sequence contains a 90-base deletion that joins nucleotides 1089 and 1180 (*i.e.* nucleotides 1090–1179 are deleted). This cDNA is designated as HYAL3v1 and can encode a protein made up of 387 aa (GenBank[TM] accession number AF502909). The putative HYAL3v1 protein contains a 30-aa deletion that involves aa 299–328. Thus, in the HYAL3v1
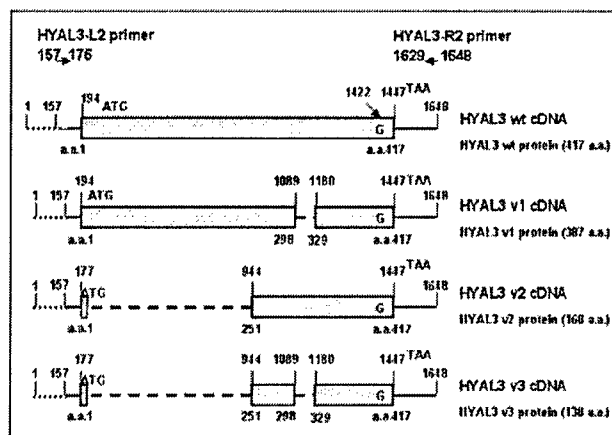
FIG. 8. **A schematic representation of the HYAL3 splice variants.** The figure shows HYAL3wt and different splice variant cDNAs. The numbering is based on the sequence of cDNA clone AF040710 that is deposited in GenBank™. However, the numbering is offset by 1 after nucleotide 1422. This is because the AF040710 is missing a G at position 1422. The coding region is shown as a *dotted block*. The *dashed line* shows the region that is spliced out, and the *solid line* represents untranslated regions. The *dotted line* between nucleotides 1 and 157 indicates the portion missing in our cDNAs. Each splice junction is marked by the nucleotides at the 5' and 3' boundaries that are joined because of splicing. The translation initiation and termination codons for HYAL1wt and HYAL1 variants are marked. The figure also shows the position of the forward (*i.e.* HYAL3-L2) and the reverse complementary (*i.e.* HYAL3-R2) primer pair used to amplify HYAL3 cDNA. The sequences of these primers are given under "Experimental Procedures," and the numbering is according to HYAL3 clone deposited in GenBank™ (accession number AF502912).

protein, aa 298 is joined to aa 329. The ~0.7-kb HYAL3 PCR product is actually 726 bases in length. The sequence analysis reveals that this variant (designated as HYAL3v2) is generated by a 766-base deletion that joins nucleotides 177 and 944 (Fig. 8; GenBank™ accession number AF502910). The HYAL3v2 variant would encode a 168-aa polypeptide in which aa 2–168 are identical to aa 251–417 in HYAL3wt protein. The smallest HYAL3 variant, HYAL3v3, is 636 bases in length. It is generated by two splicing events; in the first event, nucleotides 177 and 944 join, and in the second, the 90 bases between nucleotides 1089 and 1180 are deleted (as observed in HYAL3v1, Fig. 8; GenBank™ accession number AF502911). As shown in Fig. 8, the HYAL3v3 cDNA would encode a 138-aa protein, which like the HYAL3v2 protein is 100% homologous to aa 251–417 in the HYAL3wt sequence, except that it lacks the 30 aa sequence from aa 299 to 328.

In Vitro Translation and Examination of HAase Activity of HYAL3wt and Variant Proteins—Various HYAL3 cDNAs were *in vitro* translated using the coupled transcription/translation system and ^{35}S-lableled methionine. As shown in Fig. 9, HYAL3wt, HYAL3v1, HYAL3v2, and HYAL3v3 cDNAs upon *in vitro* transcription and translation generate polypeptide chains with molecular masses ~48, ~45, ~20, and ~16 kDa, respectively. The molecular masses of these proteins are comparable with the expected molecular masses based on the number of aa present in HYAL3wt and variant polypeptide chains. No protein is detected with vector only (Fig. 9, *Vector*).

We next measured the HAase activity of *in vitro* translated HAYL3 proteins. Because the HYAL3 gene is located in the same chromosomal location as the HYAL1 and HYAL2 genes, we assumed that like the HYAL1 and HYAL2 proteins, the HYAL3 protein may also have an acidic pH optimum (32). Therefore, we assayed the HAase activity of *in vitro* translated HAYL3 proteins at pH 4.2, using the HAase activity ELSA-like assay (17). As shown in Fig. 10, no HAase activity is detected
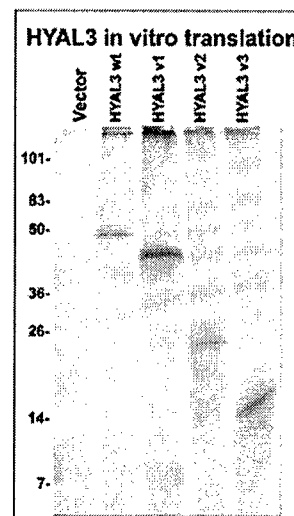

FIG. 9. *In vitro* **transcription/translation of HYAL3wt and HYAL3 variant cDNAs.** Various HYAL3 cDNAs and plasmid vector DNA were transcribed and translated *in vitro* using a coupled transcription/translation system and ^{35}S-labeled methionine, as described under "Experimental Procedures." The ^{35}S-labeled proteins were analyzed by SDS-PAGE along with molecular mass markers as described in "Experimental Procedures."

with vector only. However, HYAL3wt protein has measurable HAase activity (7.4 ± 1.4 milliunits/ml). The HYAL3v1 variant that lacks the 30-aa sequence from aa 299 to 328 but retains the putative enzyme catalytic site (Asp[127] and Glu[129]; Ref. 32) and Glu[266], which may also be important for HAase activity (31), has no HAase activity (Fig. 10). The HYAL3v2 variant that retains the 30-aa sequence and Glu[266] but lacks the putative enzyme catalytic site is also enzymatically inactive (Fig. 10). The HYAL3v3 variant that contains only Glu[266] and lacks both the putative enzyme catalytic site and the 30-aa sequence has no HAase activity. These results demonstrate that in addition to the putative catalytic site and possibly Glu[266], the 30-aa sequence from aa 299 to 328 is critical for HAase activity of the HYAL3 protein.

Comparison of the 30-aa Sequence between HYAL1, HYAL3, and Other HAases—Because in both HYAL1 and HYAL3 proteins a 30-aa sequence appears to be critical for HAase activity, we compared this sequence present in both proteins. As shown in Fig. 11, the 30-aa sequence present in HYAL1 (aa 301–330) and HYAL3 (aa 299–328) appears to be similarly situated in both proteins. In this 30-aa sequence, 17 aa among the first 22 are either identical or conserved substitutions. When a comparable 30-aa sequence among other human HAases (*i.e.* HYAL2, HYAL4, and PH20) is aligned, 17 of the first 22 aa are highly conserved (*i.e.* identical or conserved substitutions). Furthermore, the conserved aa occur at positions 2, 3, 6–8, 10–12, and 14–22. In addition, at position 29, either a Ser or a Thr residue is present in all HAases. In HYALP1, which is possibly a pseudogene (7), the 30-aa region also appears to be conserved, and of the first 22 aa in this sequence, 16 are conserved. In HYALP1, a Ser residue is present at position 29. We also compared a similarly positioned 30-aa sequence in bee HAase. As shown in Fig. 11, of the first 22, 12 are conserved (either identical or conserved substitutions) that occur at positions 2, 3, 6, 7 14, 15, and 17–22. In addition, Thr at position 29 is also conserved. The high sequence homology among mammalian and invertebrate HAases with respect to the 30-aa sequence suggests that this sequence is critical for HAase structure and activity.
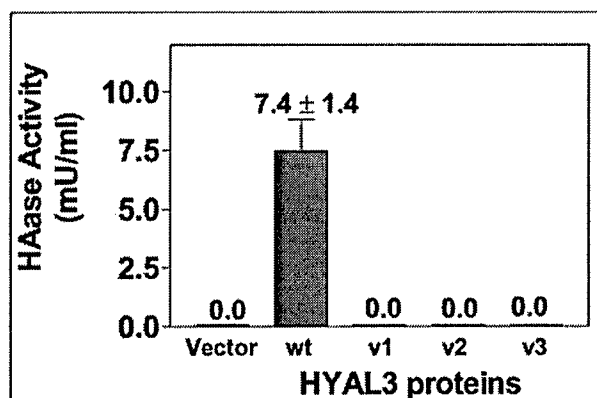
FIG. 10. **Analysis of HAase activity of HYAL3wt and HYAL3 variant proteins.** *In vitro* translated, unlabeled HYAL3wt and HYAL3 variant proteins, as well as vector-only control were analyzed for HAase activity using the HAase activity ELISA-like assay as described under "Experimental Procedures." Each sample was assayed at five different concentrations in duplicate. The results represent milliunits/ml ± S.E. Each experiment was repeated twice and independently.
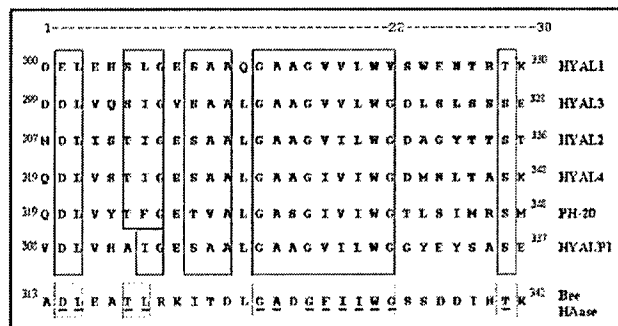

FIG. 11. **Comparison of a 30-aa sequence in various human and bee HAases.** The 30-aa sequences identified in HYAL1 and HYAL3 type HAases were compared with each other and with the corresponding 30-aa sequences in other human and bee HAases. The *numbers* indicate the positions of this sequence in various HAases. The *boxes* highlight the conserved (*i.e.* identical or conserved substitutions) aa between various HAases.

DISCUSSION

In this study we have identified a 30-aa sequence that is well conserved in several HAases and is required for enzyme activity of at least two human HAases (*i.e.* HYAL1 and HYAL3). The nucleotide sequence of HYAL1 gene reveals this gene contains three exons and two introns. Exons 1 (~1.5 kb) and 3 (0.9 kb) are relatively large compared with exon 2 (90 bp). The HYAL1 genomic sequence shows that the 90-bp sequence (nucleotides 1520–1609) that is missing in HYAL1v1 is the entire exon 2. Other HYAL1 variants appear to be generated by internal exon splicing events that usually involve exon 1. For example, the HYAL1wt described in this study is generated by an internal exon 1 splicing event, involving nucleotides 110 and 596. This splice variant has been described previously (GenBank™ accession number AF173154). HYAL1v2 appears to be generated by internal exon splicing involving nucleotides 109 and 952 as donor/acceptor sites, respectively, both of which are present in exon 1. Generation of HYAL1v3 variant is interesting in that it involves 2 splicing events. The first is the same internal exon 1 splicing involving nucleotides 110 and 596. The second splicing involves splicing of nucleotide 1239 present in exon 1 to nucleotide 1577 that is present in exon 2. Generation of HYAL1v4 again involves an internal exon splicing event involving exon 1; both the donor (nucleotide 108) and acceptor (nucleotide 1369)

sites are present in exon 1. Generation of HYAL1v5 involves internal exon 1 splicing that starts at nucleotide 109 and ends nearly at the end of exon 1 (nucleotide 1519). Thus, the analysis of HYAL1 variants demonstrates that exon 1 in HYAL1 gene has several internal donor and acceptor sites suitable for alternative mRNA splicing resulting in the generation of various HYAL1 splice variants. In addition, exon 2 can be alternatively spliced. It is interesting to note that each of these splicing events (either internal exon splicing or splicing of two exons) maintain the same open reading frame as the HYAL1 protein, resulting in different HYAL1 variant proteins.

Our study on HYAL3 splice variants confirms that the 30-aa sequence that is important for enzyme activity is encoded by an independent exon. The nucleotide sequence of HYAL3 gene reveals that this gene contains four exons separated by three introns. Exon 3 is 90 bp in length and corresponds to the 90-bp v1 region (nucleotides 1090–1179). Thus, splicing out of the independent exon 3 generates HYAL3v1. As observed for HYAL1 variants, HYAL3v2 and HYAL3v3 splice variants are generated by an internal exon splicing events that involve exons 2 and 3. For example, HYAL3v2 variant is generated by an internal splicing event involving exon 2 (nucleotides 178–943 are deleted), and HYAL3v3 is generated by the same internal splicing event involving exon 2 and also splicing of the independent exon 3.

It is interesting to note that different bladder and lymph node specimens and cells show differences in the pattern and types of HYAL1 and HYAL3 splice variant that are expressed. The reason for this heterogeneity is unknown at present. It is noteworthy that bladder tumors show heterogeneity in their ability to progress and recur. This heterogeneity in turn relates to the differences in the biological behavior of different bladder tumors (41). It is possible that the heterogeneous expression of the HYAL1 or HYAL3 variant may be related to the different biological behavior of different bladder tumors. Because in both HYAL1 and HYAL3 proteins the loss of the 30-aa sequence results in the loss of HAase activity and because the 30-aa sequence is coded by one single independent exon, the 90-bp-long independent exon in both genes seems to encode an aa sequence that is critical for HAase activity.

Other studies involving site-directed mutagenesis of PH20, identification of a naturally occurring mutation in HYAL1, and the crystal structure of bee HAase have identified several aa present in different parts of HAase that are conserved and are important for activity (31, 35, 42). The crystal structure of bee HAase reveals that the insect and possibly mammalian HAases have a classical $(\beta/\alpha)_8$ TIM barrel structure (35). The dominant feature of the HAase structure is a large groove that extends perpendicular to the barrel axis. In bee HAase, loops following the β strands 2, 3, and 4 form one wall of the groove, and those of 1, 5, 6, and 7 form the other wall. This groove is large enough to accommodate a hexasaccharide (35). Co-crystallization of bee HAase with a hexasaccharide shows that the catalytic site that cleaves the glycosidic bond between *N*-acetyl-D-glucosamine and D-glucuronic acid lies in aa residues Asp[143] and Glu[145] (numbering according to GenBank™ accession number AAA27730.1). In a substrate-assisted acid-base catalytic mechanism, Glu[145] acts as the proton donor, and the *N*-acetyl group of the substrate acts as the nucleophile. In all human HAases, this Glu residue is conserved along with Asp and is believed to be responsible for substrate cleavage (32). In the HYAL1 sequence this Glu is aa 131 (numbering according to GenBank™ accession number AAD09137.2), and in HYAL3 it is aa 129 (numbering according to GenBank™ accession number AAH12892.1). Thus, the 30-aa sequence that we have identi-

fied in HYAL1 (aa 301–300) and in HYAL3 (aa 299–328) most likely is not a part of the catalytic site.

Based on the bee HAase crystal structure, the 30-aa sequence from aa 313 to 342 (Fig. 11), that is homologous to the 30-aa sequences in HYAL1 and HYAL3, forms β sheets 6 and 7, α-helix 8, and the loops in between (35). Because the loops following β strands 6 and 7 are involved in forming one of the walls of the substrate binding groove, loss of the 30-aa sequence in HYAL1 and HYAL3 proteins may result in the loss of substrate binding. The substrate-associated catalytic cleavage of the glycosidic bond between N-acetyl-D-glucosamine and D-glucuronic acid requires accurate positioning of the N-acetyl side chain of the substrate with respect to the catalytic site (35). This is achieved by two hydrogen bonding interactions and a hydrophobic interaction. The crystal structure shows that in bee HAase, Trp^{333} is involved in hydrophobic interaction with the N-acetyl side chain (35). This Trp^{333} corresponds to Trp^{321} in HYAL1 and Trp^{319} in HYAL3, both of which are present in the respective 30-aa sequences (Fig. 11). This Trp residue is also conserved in all HAases and other chitinolytic enzymes (43, 44). Thus, the absence of this Trp residue in HYAL1v1 and HYAL3v1 mutant proteins may lead to improper positioning of the substrate resulting in no catalysis. It remains to be determined why this 30-aa sequence is so well conserved in various HAases and what role other conserved residues play in terms of substrate binding and catalysis. It should be noted that the loss of β sheets 6 and 7, α-helix 8, and the loops in between, because of the 30-aa deletion in HYAL1v1 and HYAL3v1, may also result in complete loss of the TIM barrel structure, making these proteins enzymatically inactive.

Other HYAL1 and HYAL3 variant proteins also illustrate the importance of various structural domains for HAase activity. For example, HYAL1v3 variant, which contains the putative catalytic site (*i.e.* Asp^{129} and Glu^{131}) but lacks aa 208–435, has no HAase activity. It is likely that the HYAL1v3 protein does not form a proper TIM barrel structure, and at the very least, it lacks the substrate-binding groove. HYAL1v2 (aa 183–435) and HYAL1v4 (aa 260–435) proteins retain the 30-aa sequence and also Glu^{268}, which has been shown to be critical for HAase activity. However, these variants are enzymatically inactive, because they lack the putative catalytic site as well as parts of the substrate-binding groove. A similar situation may hold true for HYAL3v2 variant (aa 251–435), which also does not have any HAase activity. The variants HYAL1v5 (aa 340–435) and HYAL3v3 (aa 251–435 but lacking aa 299–328) lack more than two-thirds of the respective molecules and hence will not fold properly, lack the HAase catalytic site, and have no substrate binding groove. Thus, this study illustrates the involvement of several structural domains that are conserved in various HAases and are important for enzyme activity.

Detection of various HYAL1/HYAL3 variants in bladder and prostate cancer lines, bladder tumor tissues, as well as normal kidney tissue suggest that the expression of functionally active HAase in various cells and tissues may be regulated by alternative mRNA splicing. We have previously shown that HAase levels are elevated (3–7-fold) in the urine of bladder cancer patients who have high grade (*i.e.* G2/G3) disease (39). Furthermore, in a study of 504 patients, we demonstrated that the HAase level serves as a highly sensitive (82%) and specific (83%) marker for detecting G2/G3 bladder cancer (18). Urinary HAase levels together with HA levels (*i.e.* HA-HAase test) are sensitive and specific in detecting bladder cancer and monitoring its recurrence (18, 45). We have also shown that both invasive bladder and prostate cancer cells secrete high levels of HAase activity, and HYAL1 is the major HAase expressed in these carcinomas (17, 30, 46). Consistent with these observa-

tions, in this study we observed that the full-length HYAL1wt transcript that encodes a functional HAase is expressed only in bladder and prostate cancer cells, G2/G3 bladder tumor tissues, and lymph node specimens showing tumor invasion. In normal bladder and G1 bladder tumor tissues, in a normal bladder primary culture, and in bladder tissues showing no evidence of tumor, the major HYAL1 transcript that is expressed is the HYAL1v5 variant. Because this transcript or other HYAL1 variant transcripts (*i.e.* HYAL1v2-v4) that are also expressed in some of these specimens do not encode a functional HAase, it may explain why in these tissues or cells no HAase activity and wild type HYAL1 protein are detected (30, 46, 47).

HAase protein has been shown to be associated with tumor angiogenesis and/or invasion (48). However, because HYAL1 (and also HYAL2 and HYAL3) is present on chromosome 3p 21.3 locus, and this region is a critical tumor homozygous deletion region in lung and breast cancers, it has been suggested that HYAL1 may be a tumor suppressor (7, 49). A recent study clearly demonstrates that the RASSF1 gene and not HYAL1 is the tumor suppressor gene present in that locus (50). Thus, several observations, including elevation of HAase levels in bladder and prostate tumors (18, 30), suggest that HYAL1 may have a role in promoting tumor progression. Normal cells may suppress the HAase activity of HYAL1 by generating HYAL1 splice variants that encode an inactive enzyme. It remains to be determined why the normal bladder cells/tissues, G1 bladder tumor tissues, and normal kidney tissues express different splice variants that encode inactive HYAL1 proteins.

The expression of HYAL3 protein has been previously detected in prostate cancer cells by RT-PCR analysis (51). Our results show that in all bladder tumor cells and prostate cancer cells,[2] and in all of the bladder tumor tissues that we have tested, the major HYAL3 transcript appears to be HYAL3v3 variant. This variant is enzymatically inactive. In fact we were unable to clone HYAL3wt from various cancer cells and tissues. The minor ~1.4-kb transcript expressed in cancer cells/tissues is HYAL3v1. Once again it remains unclear what is the function of these enzymatically inactive HYAL3 variant proteins.

This study identifies a 30-aa sequence that is highly conserved among all human and insect HAases and is critical for HAase activity. This study also identifies alternative mRNA splicing as the likely mechanism of regulating the expression of enzymatically active HAase in various tissues and cells. The expression of HYAL1wt mRNA that encodes the functional HYAL1 protein in high grade bladder tumor tissues and in invasive bladder/prostate cancer cells provides an insight into why HAase levels are elevated and serve as a marker for tumor progression.

REFERENCES

1. Kreil, G. (1995) *Protein Sci.* **4**, 1666–1669
2. Roden, L., Campbell, P., Fraser, J. R. E., Laurent, T. C., Petroff, H., and Thompson, J. N. (1989) *CIBA Found. Symp.* **143**, 60–86
3. Tu, A. T., and Hendon, R. R. (1983) *Comp. Biochem. Physiol. B. Comp. Biochem.* **76**, 377–383
4. Gmachl, M., and Kreil, G. (1993) *Proc. Natl. Acad. Sci. U. S. A.* **90**, 3569–3573
5. Henrissat, B. (1991) *Biochem. J.* **280**, 309–316
6. Henrissat, B., and Bairoch, A. (1996) *Biochem. J.* **316**, 695–696
7. Csoka, A. B., Frost G. I., and Stern, R. (2001) *Matrix Biol.* **20**, 499–508

8. Laurent, T. C., and Fraser, J. R. E. (1992) *FASEB J.* **6**, 2397–2404
9. Delpech, B., Girard, N., Bertrand, P., Chauzy, C., and Delpech, A. (1997) *J. Intern. Med.*, **242**, 41–48
10. Tammi, M. I., Day, A. J., and Turely, E. A. (2002) *J. Biol. Chem.* **277**, 4581–4584
11. Turley, E. A., Noble, P. W., and Bourguignon, L. Y. W. (2002) *J. Biol. Chem.* **277**, 4589–4592
12. Toole, B. P., Wight, T. N., and Tammi, M. I. (2002) *J. Biol. Chem.* **277**, 4593–4596
13. Ropponen, K., Tammi, M. I., Parkkinen, J., Eskelinen, M. J., Tammi, R. H., Lipponen, P. R., Argen, U. M., Alhava, E. M., and Kosma, V. M. (1998) *Cancer Res.*, **58**, 342–347
14. Setala, L. P., Tammi, M. I., Tammi, R. H., Eskelinen, M. J., Lipponen, P. R., Argen, U. M., Alhava, E. M., and Kosma, V. M. (1999) *Br. J. Cancer* **79**, 1133–1138
15. Auvinen, P., Tammi, R. H., Parkkinen, J., Tammi, M. I., Argen, U. M., Johansson, R., Hirvikoski, P., Eskelinen, M. J., and Kosma, V. M. (2000) *Am. J. Pathol.*, **156**, 529–536
16. Pirinen, R., Tammi, R., Tammi, M., Hirvikoski, P., Parkkinen, J. J., Johansson, R., Bohm, J., Hollmen, S., and Kosma V. M. (2001) *Int. J. Cancer* **95**, 12–17
17. Lokeshwar, V. B., Rubinowicz, D., Schroeder, G. L., Forgacs, E., Minna, J. D., Block, N. L., Nadji, M., and Lokeshwar, B. L. (2001) *J. Biol. Chem.* **276**, 11922–11932
18. Lokeshwar, V. B., Obek, C., Pham, H. T., Wei, D., Young, M. J., Duncan, R. C., Soloway, M. S., and Block, N. L. (2000) *J. Urol.* **163**, 348–356
19. Lokeshwar, V. B., and Block, N. L. (2000) *Urol. Clin. North Am.* **27**, 53–60
20. Liu, N., Lapcevich, R. K., Underhill, C. B., Han, Z., Gao, F., Swartz, G., Plum, S. M., Zhang, L., and Gree S. J. (2001) *Cancer Res.* **61**, 1022–1028
21. Hayen, W., Goebeler, M., Kumar, S., Riessen, R., and Nehls, V. (1999) *J. Cell Sci.* **112**, 2241–2251
22. Hobarth, K., Maier, U., and Marberger, M. (1992) *Eur. Urol.* **21**, 206–210
23. Slevin, M., Krupinski, J., Kumar, S., and Gaffney, (1998) *J. Lab. Invest.* **78**, 987–1003
24. Trochon, V., Mabilat-Pragnon, C., Bertrand, P., Legrand, Y., Soria, J., Soria, C., Delpech, B., and Lu, H. (1997) *FEBS Lett.* **418**, 6–10
25. Rooney, P., Kumar, S., Ponting, J., and Wang M. (1995) *Int. J. Cancer* **60**, 632–636
26. Lokeshwar, V. B., and Selzer, M. G. (2000) *J. Biol. Chem.* **265**, 27641–27649
27. Lokeshwar, V. B., Obek, C., Soloway, M. S., and Block N. L. (1997) *Cancer Res.* **57**, 773–777; Correction (1998) *Cancer Res.* **58**, 3191
28. Frost, G. I., Csoka, T. B., Wong, T., and Stern, R. (1997) *Biochem. Biophys. Res. Commun.* **236**, 10–15
29. Csoka, T. B., Frost, G. I., Wong, T., and Stern, R. (1997) *FEBS Lett.* **417**, 307–310
30. Lokeshwar, V. B., Young, M. J., Gouddarzi, G., Iida, N., Yudin, A. I., Cherr, G. N., and Selzer, M. G. (1999) *Cancer Res.* **59**, 4464–4470
31. Triggs-Raine, B., Salo, T. J., Zhang, H., Wicklow, B. A., and Natowicz, M. R. (1999) *Proc. Natl. Acad. Sci. U. S. A.* **96**, 6296–6300
32. Lepperdinger, G., Mullegger, J., and Kreil, G. (2001) *Matrix Biol.* **20**, 509–514
33. Cherr, G. N., Yudin, A. I., and Overstreet, J. W. (2001) *Matrix Biol.* **20**, 515–525
34. Vines, C. A., Li, M. W., Deng, X., Yudin, A. I., Cherr, G. N., and Overstreet, J. W. (2000) *Mol. Reprod. Dev.* **60**, 542–552
35. Markovic-Housley, Z., Miglierini, G., Soldatova, L., Rizkallah, P. J., and Muller, U. (2000) *Structure* **8**, 1025–1035
36. Wang, M., and Stearns, M. E. (1991) *Differentiation.* **48**, 115–125
37. Dinney, C. P. N., Fishback, R., Singn, R. K., Eve, B., Pathak, S., Brown, N., Xie, B., Fan, D., Bucana, C. D., Fidler, J. J., and Killion, J. J. (1995) *J. Urol.* **143**, 1532–1538
38. Stern, M., and Stern, R. (1992) *Matrix* **12**, 397–403
39. Pham, H. T., Block, N. L., and Lokeshwar, V. B. (1997) *Cancer Res.* **57**, 778–783; Correction (1997) *Cancer Res.* **57**, 1662
40. Shuttleworth, T. L., Wilson, M. D., Wicklow, B. A., Wilkins, J. A., and Triggs-Raine, B. L. (2002) *J. Biol. Chem.* **277**, 23008–23018
41. Lee R., Droller, M. J. (2000) *Urol. Clin. North Am.* **27**, 1–13, vii
42. Arming, S., Strobl, B., Wechselberger, C., and Kreil, G. (1997) *Eur. J. Biochem.* **247**, 810–814
43. Tews, I., Perrakis, A., Oppenheim, A., Dauter, Z., Wilson, K. S., and Vorgias, C. E. (1996) *Nat. Struct. Biol.* **3**, 638–648
44. Tews, I. Terwisscha van Scheltinga, A. C., Perrakis, A., Wilson, K. S., and Dijkstra, B. W. (1997) *J. Am. Chem. Soc.* **119**, 7954–7959
45. Lokeshwar, V. B., Schroeder, G. L., Selzer, M. G., Hautmann, S. H., Posey, J. T., Duncan, R. C., Watson, R., Rose, L., Markowitz, S., and Soloway, M. S. (2002) *Cancer* **95**, 61–72
46. Lokeshwar, V. B., Soloway, M. S., and Block, N. L. (1998) *Cancer Lett.* **131**, 21–27
47. Hautmann, S. H., Lokeshwar, V. B., Schroeder, G. L., Civantos, F., Duncan, R. C., Gnann, R., Friedrich, M. G., and Soloway, M. S. (2001) *J. Urol.* **165**, 2068–2074
48. Liu, D., Pearlman, E., Diacnou, E., Guo, K., Mori, H., Haqqi, T., Markowitz, S., Wilson, J., and Sy, M. S. (1996) *Proc. Natl. Acad. Sci. U. S. A.* **93**, 7832–7837
49. Frost, G. I., Mohapatra, G., Wong, T. M., Csoka, A. B., Gray, J. W., and Stern, R. (2000) *Oncogene* **19**, 870–877
50. Ji, L., Nishizaki, M., Gao, B., Burbee, D., Kondo, M., Kamibayashi, C., Xu, K., Yen, N., Atkinson, E. N., Fang, B., Lerman, M. I., Roth, J. A., and Minna, J. D. (2002) *Cancer Res.* **262**, 2715–2720
51. Patel, S., Turner, P. A., Stubberfield, C., Barry, E., Rohlff, C. R., Stamps, A., Tyson, K., Terrett, J., Box, G., Eccles, S., and Page, M. J. (2002) *Int. J. Cancer* **97**, 416–424

EXPRESSION OF TUMOR MARKERS HYALURONIC ACID AND HYALURONIDASE (HYAL1) IN HEAD AND NECK TUMORS

Elizabeth J. Franzmann[1,2], Grethchen L. Schroeder[3], William Jarrard Goodwin[1,2], Donald T. Weed[1,2], Penelope Fisher[1] and Vinata B. Lokeshwar[2–4]*

[1]*Department of Otolaryngology, University of Miami School of Medicine, Miami, FL, USA*
[2]*Sylvester Comprehensive Cancer Center, University of Miami School of Medicine, Miami, FL, USA*
[3]*Department of Urology, University of Miami School of Medicine, Miami, FL, USA*
[4]*Department of Cell Biology and Anatomy, University of Miami School of Medicine, Miami, FL, USA*

Characteristic behaviors of head and neck squamous cell carcinoma (HNSCC) include a propensity to occur as multiple synchronous and metachronous tumors, frequent recurrence and metastasis. Early detection of HNSCC and monitoring its recurrence are necessary to improve prognosis. Hyaluronic acid (HA), a component of extracellular matrix, promotes metastasis. Small fragments of HA stimulate angiogenesis. HA fragments are generated when hyaluronidase (HAase), an endoglycosidase, degrades the HA polymer. Using the HA test (an ELISA-like assay) we found that saliva HA levels are 4.9-fold elevated in 11 HNSCC patients (2841 ± 887 ng/mg protein) when compared to 6 normal controls (579.3 ± 122.6 ng/mg protein; $p = 0.00238$). HNSCC patients included in our study were patients with cancers of the oral cavity ($n = 4$), pharynx ($n = 7$) and larynx ($n = 1$). The HA levels were also elevated in MDA-1483, FaDu and HEp-2 cell lines when compared to the transformed keratinocyte line HEK-001. Saliva HAase levels measured using the HAase test (an ELISA-like assay) were 3.7-fold elevated in HNSCC patients (10.4 ± 1.4 mU/mg protein) when compared to normal controls (2.8 ± 0.7 mU/mg protein; $p = 0.0028$). MDA-1483 and HEp-2 cells secreted 7- to 11-fold higher levels of HAase in their conditioned media (CM) when compared to FaDu cells, and the latter secreted 1.5-fold more HAase than HEK-001 cells. Reverse transcriptase (RT)-PCR analysis detected the expression of full-length HYAL1 type HAase transcript in tumor cells. None of the cells exhibited the expression of PH20 in RT-PCR analysis. Immunoblot analysis confirmed the expression of a ~55 kDa HYAL-related protein in tumor cell CM and in patients' saliva. The pH activity profile and optimum (pH 4.4) of the HAase activity present in HNSCC patients' or normal saliva and that secreted in the CM of tumor cells closely resembled that of the partially purified HYAL1 type HAase. The profiles of HA species in HNSCC patients' and normal saliva are different. The high-stage HNSCC patients' saliva contains a high-molecular-mass HA species and HA fragments, in addition to the HA species present in the normal individual's saliva. These results show that HYAL1 is the major tumor-derived HAase expressed in HNSCC. Furthermore, HA and HAase may be sensitive and specific markers for detecting HNSCC and monitoring its recurrence. Further studies are needed to confirm these preliminary studies.
© *2003 Wiley-Liss, Inc.*

Key words: *head and neck tumors; hyaluronic acid; hyaluronidase; HA-HAase test; HYAL1*

Head and neck squamous cell carcinoma (HNSCC) accounts for most of the 500,000 worldwide incident cancers of the mouth, pharynx and larynx.[1,2] According to the American Cancer Society Cancer Facts and Figures 2002, approximately half of the estimated 38,000 new cases of HNSCC in the United States are oral cavity cancers; cancers of the pharynx and larynx make up the rest. The prognosis of HNSCC patients depends upon the site at which the cancer originates, as well as tumor stage.[1,3–5] Head and neck cancer is generally staged I–IV, based upon the American Joint Committee on Cancer Staging System (AJCC) TMN (tumor, metastasis, node) classification.[4] Over 80% of stage I and 60% of stage II patients can be cured after treatment.[4] However, patients with more advanced disease (i.e., stages III and IV) have less than

a 30% chance of cure.[4] Similarly, patients with node-positive disease, regardless of the site of origin of the cancer, have poor prognosis.[4–6] Because of the complexity of the head and neck, therapy often results in facial disfigurement, speech and swallowing problems and substantial health care costs.

The most important predisposing factors for the development of HNSCC are tobacco and alcohol.[1,4,5] Since the entire mucosal surface of the upper aerodigestive tract is exposed to carcinogens in tobacco and alcohol, multiple sites are at risk for the development of synchronous and metachronous lesions.[3–6] In addition to disease progression and metastasis, HNSCC has a propensity to recur. For example, a recurrent tumor at the primary site occurs in approximately 20–30% of patients and remains the most common cause of failure for patients treated for head and neck tumors.[7] Regional recurrence in the neck occurs in 10–15% of patients and remains the most common cause of disease-related death in these patients.[7] Therefore, patients' prognosis is bleak with later-stage recurrence.[7] The detection of HNSCC and monitoring its recurrence can be improved if molecules that associate with the development, growth and invasion and metastasis of HNSCC are identified.[8–10] Since hyaluronic acid (HA) and hyaluronidase (HAase) have been shown to be involved in tumor progression and serve as highly sensitive and specific markers in the detection of and making prognostic predictions for some tumors, these molecules may function in HNSCC.

HA is a nonsulfated glycosaminoglycan (GAG) made of repeating disaccharide units, D-glucuronic acid and N-acetyl-D-glucosamine.[11–13] HA is present in body fluids, tissues and extracellular matrix. It performs several functions in normal physiology such as keeping tissues hydrated, maintaining osmotic balance and supporting cartilage integrity.[12–14] It also interacts with cell surface receptors (e.g., CD44, RHAMM, etc.) and, through these interactions, regulates cell adhesion, migration and proliferation.[15,16] Concentrations of HA are elevated in several cancers, including

colon, breast, prostate, bladder and lung.[17-25] Tissue expression of HA in tumors such as colon and breast predicts poor prognosis.[18,19,21,22] Using an ELISA-like assay (HA test), we have previously demonstrated that urinary HA levels are elevated in bladder cancer patients, regardless of the tumor grade.[24] Depending upon the type of tumor, HA may be synthesized by stromal cells, tumor cells or both.[17-19,22,23,25] In tumor tissues, HA supports metastasis by promoting tumor cell migration, offering protection against immune surveillance and causing a partial loss of contact-medicated inhibition of cell growth and migration.[26-29]

HAase is an endoglycosidase that degrades HA into small angiogenic HA fragments.[30-32] HA and angiogenic HA fragments stimulate endothelial cell proliferation, adhesion and migration by activating the focal adhesion kinase and MAP kinase pathways.[33-35] We have previously detected these fragments in the urine of high-grade bladder cancer patients and high-grade prostate cancer tissues.[25,36] HAase has been shown to alter the expression of CD44 isoforms,[37] which may also be involved in tumor progression. In addition, HAase is associated with increased tumor cell cycling.[38] Of the 6 human HAases encoded by different genes, 3 are characterized at the protein level.[39-41] HYAL1 type HAase was originally purified from human plasma and urine.[39] However, we have shown that HYAL1 is the major tumor-derived HAase expressed in bladder and prostate cancer tissues and have characterized its expression at the mRNA and protein levels in tumor cells.[17,25,42] Furthermore, using an ELISA-like assay (i.e., HAase test) we have shown that the HAase levels serve as an accurate marker for detecting high-grade bladder tumors.[24]

HYAL1 type HAase has an optimum pH range of 4.0–4.3, and the enzyme is 50–80% active at pH 4.5.[25] The expression of PH20 mRNA has been detected by Reverse transcriptase (RT)-PCR analysis in some tumor tissues, including laryngeal cancer. However, the presence of PH20 protein has not been documented in these studies.[43,44] In another study, while HYAL1 transcripts were present, enzyme activity and protein were markedly reduced or absent in 6 of the 7 HNSCC cell lines tested.[45] In our study, using the HA and HAase tests, we investigated whether HA and HAase are useful tumor markers for HNSCC. Furthermore, we have characterized the type of HAase that is expressed in HNSCC cells and patients' saliva.

MATERIAL AND METHODS

Saliva collection

Approximately 1 cc of saliva was collected from 12 consecutive HNSCC patients (i.e., SCC1–SCC12) and 6 normal volunteers, according to the protocol approved by the Institutional Review Board at the University of Miami. Among the HNSCC patients, there was 1 laryngeal cancer patient, 4 patients with oral cavity cancer (oral tongue, $n = 1$; bucal mucosa, $n = 1$; retromolar trigone, $n = 2$) and 6 patients with pharyngeal cancer. Of the pharyngeal cancer patients, 4 were oropharyngeal (base of tongue, $n = 1$; tonsil, $n = 3$) and 2 were hypopharyngeal. In 1 of the patients, SCC1, saliva was collected after the tumor had been removed and there was no gross evidence of tumor at the time of saliva collection. In patient SCC12, saliva was collected prior to neck dissection to remove a 3.7 cm node containing squamous cell carcinoma. Although appropriate endoscopy and biopsies were performed, a primary site in the upper aerodigestive tract was never identified. Saliva specimens from all patients and normal controls were placed on ice for transport and stored at −20 to −70°C.

Cell culture

We obtained FaDu (hypopharyngeal cancer), HEp-2 (originally classified as laryngeal cancer, but now classified as a Hela contaminant) and HEK-001 (transformed keratinocyte) cell lines from the American Type Culture Collection (ATCC). MDA-1483, an oral squamous cell carcinoma line, was a gift from Dr. Mien-Chie Hung PhD, University of Texas M.D. Anderson Cancer Center.

HNSCC cells were maintained in RPMI-1640 medium supplemented with 10% fetal bovine serum and gentamycin. HEK-001 cells were grown in Keratinocyte Growth Medium (Cambrex Bioscience Walkersville, Inc., Walkersville, MD) supplemented with L-glutamine, epidermal growth factor and bovine pituitary extract. At approximately 60% confluence, cultures were washed and incubated in serum-free RPMI-1640 or Keratinocyte Growth Medium supplemented with insulin, transferrin and selenium. The cell-conditioned media (CM) were collected at 48–72 hr.

ELISA-like assay for HA (HA test)

HA concentration was measured using an ELISA-like assay originally described by Fosang et al.[46] and later modified by Lokeshwar et al.[24] for measuring HA levels in urine, tissue extracts and cell CM (HA test). The HA ELISA-like assay is based on a competition binding principle where the HA coated on a microtiter well competes with HA present in biologic specimens.[24,46] Ninety-six-well microtiter plates were coated with human umbilical cord HA (25 μg/ml; ICN Biomedicals, Aurora, OH). The HA-coated wells were incubated with various amounts (0.5–10 μl) of either saliva specimens or cell CM in the presence of a biotinylated bovine nasal cartilage HA-binding protein. The amount of the biotinylated HA-binding protein bound on the wells was determined using an avidin-biotin detection system (Vector Laboratories, Inc., Burlingame, CA). The amount of HA present in each sample (ng/ml) was determined using a standard graph. We routinely normalize HA levels (and HAase levels; see below) in biologic fluids, tissue extracts or cell CM to total protein to eliminate the influence of a patient's hydration status (for biologic fluids), losses during extraction (for tissue extracts) or differences in cell growth (for cell CM). The HA levels are expressed as ng/mg (i.e., ng HA/mg protein). For each sample, 3 different amounts, each in duplicate, were tested. The HA levels are expressed as mean ± SE

HAase ELISA-like assay (HAase test)

HAase levels present in CM of cell lines and saliva were measured using an ELISA-like assay similar to that developed by Stern and Stern[47] with several modifications to allow measuring of HAase levels in urine, tissue extracts and cell CM (HAase test).[24,48] Microtiter wells coated with 200 μg/ml HA were incubated with CM or saliva for 16 hr at 37°C in HAase assay buffer (0.1 M sodium formate, 0.15 M NaCl, pH 4.2, 0.2 mg/ml bovine serum albumin). After incubation, the plates were washed to remove degraded HA. The HA remaining on the wells was determined using the same biotinylated HA-binding protein and the avidin-biotin detection system as the HA test. HAase concentration (mU/ml) was determined using a standard graph and then normalized to total protein. The HAase levels were finally expressed as mU/mg (i.e., mU HAase/mg protein). For each sample, 3 different amounts, each in duplicate, were tested. The HAase levels are expressed as mean ± SE

The pH activity profile of HAase was determined in normal and HNSCC patients' saliva specimens, CM of a transformed keratinocyte (HEK-001) and 2 cell lines (HEp-2 and MDA-1483). Identical amounts of saliva specimens or CM were added to HA-coated plates containing HAase buffer at various pH values, increasing by 1.5 pH units from pH 3.0 to 8.0. To achieve effective buffering, we used formate-NaCl buffer between pH 3.0 and 5.0, 0.1 M sodium acetate-0.15 M NaCl buffer between pH 5.0 and 6.5 and 0.1 M phosphate buffer between pH 6.5 and 8.0. Partially purified HYAL1 from bladder cancer patients' urine[42] and bovine testicular HAase (Sigma Chemical Co., St. Louis, MO) were used as positive controls. The control wells received the buffers of specified pH, identical to those added in the sample wells. The results were expressed as O.D.$_{405 nm}$ (control sample).

RT-PCR analysis for HYAL1 and PH-20

Total RNA was extracted from cell lines and a normal oropharyngeal tissue (collected at uvulopalatopharyngoplasty from a pa-

tient with obstructive sleep apnea), using an RNA extraction kit (Qiagen, Valencia, CA). Total RNA (about 1 μg) was subjected to first-strand cDNA synthesis using the Superscript™ preamplification system and oligo (dT) primers (Life Technologies, Inc., Gaithersburg, MD). The cDNA was amplified for using Ampli-*Taq* Gold™ (Perkin-Elmer Life Sciences, Wellesley, MA) and a previously described strategy.[25] Specifically, primers for HYAL1 were as follows: HYAL1L2 (the sequence between the nucleotides 594 and 613, Genbank accession number HSU03056): L 5'-TT-GTCCTCGACCAGTCCCGT-3'; HYAL1R2 (the reverse complementary sequence between nucleotides 1906 and 1925, GenBank accession number HSU03056): 5'-ATCACCACATGCTCTTC-CGC-3'. Primers for PH-20 have been previously described[42] and were as follows: PH20L1 (the sequence between nucleotides 908 and 927, GenBank accession number S67798): 5'-CTTAGTCT-CACAGAGGCCAC-3'; PH20R1 (the reverse complementary sequence between nucleotides 1517 and 1536): 5'-TACACACTC-CTTGCTCCTGG-3'. PCR conditions were as follows: *(i)* 95°C for 10 min; *(ii)* 10 cycles of 94°C for 30 sec (70–60°C) for 30 sec, i.e., annealing temperature dropping by 1°C at each cycle, 72°C for 1 min; *(iii)* 30 cycles of 94°C for 30 sec, 60°C for 30 sec and 72°C for 1 min; and *(iv)* 72°C for 7 min, final extension. The PCR mixture for HYAL1 amplification contained 5% dimethyl sulfoxide. The PCR products were analyzed by 1.2% agarose gel electrophoresis and eithidium bromide staining. Plasmids containing HYAL1 cDNA and PH20 cDNA served as positive controls for respective PCRs.

Immunoblot analysis for HYAL1

Cell CM were concentrated 10-fold and protein was determined. Approximately equal amounts of protein from different CM or saliva specimens were separated on an 8.5% SDS-polyacrylamide gel, under nonreducing conditions, and then blotted onto a polyvinylidene difluoride membrane. The blot was blocked with 3% BSA in 20 mM Tris-HCl, pH 7.4, 0.15 M NaCl and 0.05% Tween 20. The blot was probed with 5 μg/ml of an anti-HYAL1 peptide IgG at 4°C for 16 hr. The anti-HYAL1 peptide IgG was generated against a 19-amino-acid sequence between HYAL1 (amino acids 321–338), and purified as described previously.[42] After incubation, the blot was washed and incubated with an alkaline phosphatase-conjugated goat anti-rabbit IgG (1:7,500 dilution; Sigma Chemical Co., St. Louis, MO) at room temperature for 2 hr. The blot was washed and developed using an alkaline phosphatase color detection system (Bio-Rad, Hercules, CA). The specificity of the anti-HYAL1 antibody has been previously determined.[42]

Determination of HA profile in saliva

Saliva specimens from normal individuals and HNSCC patients (stages I to IV) were applied to a Sephadex G-50 column (1.5 × 120 cm) equilibrated with phosphate-buffered saline. The column was eluted in the same buffer at 7 ml/hr and 3 ml fractions were collected. The fractions were assayed for HA by the HA test as described above. The column was calibrated using human umbilical cord HA and HA fragments, F1 (10–15 disaccharide units), F2 (2–3 disaccharide units) and F3 (~2 disaccharide units), respectively.[36]

RESULTS

Determination of HA and HAase levels in saliva specimens

HA levels in saliva. The HA test was used to determine the HA levels present in saliva specimens from 12 HNSCC patients and 6 normal individuals. Determination of HA concentration by an ELISA-like assay, its normalization to total protein and its expression as ng/mg has been designated as the HA test. It is noteworthy that in saliva specimens, regardless of whether these were from normal individuals or HNSCC patients, the protein concentration generally varied between 0.7 and 3 mg/ml. Thus, HNSCC patients secrete neither less nor aberrantly more protein in their saliva; rather, the variation in individual protein concentration is likely a reflection of the hydration status of the oral cavity. The HA test was originally designed to measure urinary HA levels in bladder cancer patients.[24] As shown in Table I, the HA levels in 6 of 6 normal individuals are below 1,000 ng/mg. The mean HA levels in the normal individuals' saliva are 579.3 ± 122.6 ng/mg. The HA levels are significantly elevated HNSCC patients with active disease. For example, in 8 of the 11 patients the HA levels are above 1,000 ng/mg (Table I). The mean HA levels among patients with active HNSCC are 2,841 ± 887.8 ng/mg. Thus, the mean saliva HA levels in HNSCC patients are 4.9-fold elevated when compared to the normal controls. It is noteworthy that the HA levels are comparable to those of normal controls in patient 1 (468 ± 14.5 ng/mg). This patient had an excisional biopsy performed elsewhere. At our institution the patient underwent saliva collection followed by resection of normal tissue margins around the tumor site. There was no microscopic tumor in the margin tissue on final pathology.

The difference between the saliva HA levels of HNSCC patients and those of normal individuals is statistically significant ($p = 0.0238$, 2-tailed p-value, Mann-Whitney test). Since the saliva HA

TABLE I – MEASUREMENT OF HA AND HAase LEVELS IN SALIVA SPECIMENS

Study Individuals	Site	Stage	HA Levels (ng/mg)	HAase Levels (mU/mg)
Normal 1	–	–	800 ± 50	3.7 ± 0.3
Normal 2	–	–	743 ± 120	3.6 ± 0.4
Normal 3	–	–	250 ± 27	4.0 ± 0.5
Normal 4	–	–	973 ± 123	4.3 ± 0.3
Normal 5	–	–	430 ± 70	0.5 ± 0.2
Normal 6	–	–	281 ± 20	0.6 ± 0.1
HNSCC patients				
1	OC	No Tumor	468 ± 14.5	1.7 ± 0.3
2	P	IV	3925 ± 223	17 ± 3.4
3	P	IV	9692 ± 177	19.5 ± 4
4	OC	III	3821 ± 200	15.4 ± 1.2
5	OC	III	1199 ± 109	8.9 ± 0.8
6	L	III	344 ± 23	10.9 ± 0.6
7	P	III	568 ± 66	5.6 ± 0.8
8	OC	III	2176 ± 340	7.4 ± 0.6
9	P	II	1126 ± 33	8.0 ± 1.0
10	P	IV	6451 ± 555	6.8 ± 0.8
11	P	III	1240 ± 88	7.5 ± 0.6
12	Unknown primary	IV	707 ± 99	7.6 ± 0.77

HA and HAase levels were measured in saliva specimens from 12 HNSCC patients and 6 normal individuals using the HA and HAase tests as described in Material and Methods. OC, oral cavity; P, pharynx; L, larynx. Bars: mean ± S.E. Patient 1 had no active disease at the time of saliva collection.

levels are elevated in patients with either oral cavity, pharyngeal or laryngeal HNSCC, as well as among patients with either stage II, III or IV disease, it is possible that the HA levels are elevated in HNSCC patients, regardless of the site and stage of the disease. However, due to a small number of patients included in this preliminary study, correlation between tumor stage and HA levels could not be determined.

HAase levels in saliva. Determination of HAase concentration by an ELISA-like assay, its normalization to total protein and its expression as ng/mg has been designated as the HAase test. The HAase test was originally designed to measure urinary HAase levels in bladder cancer patients.[24]

As shown in Table I the HAase levels in 6 of 6 normal individuals are below 5 mU/mg. The mean HAase levels in the normal individuals' saliva are 2.8 ± 0.71 mU/mg. The HAase levels are significantly elevated in HNSCC patients with active disease. For example, in 11 of the 11 patients, the HAase levels are above 5 mU/mg (Table I). The mean HAase levels among patients with active HNSCC are 10.42 ± 1.4 mU/mg. Thus, the mean saliva HAase levels in HNSCC patients are 3.7-fold elevated when compared to those of the normal controls. The HAase levels are comparable to those of normal controls in patient 1 (1.7 ± 0.3 mU/mg), who had no evidence of HNSCC at the time of saliva collection.

The difference between the saliva HAase levels of HNSCC patients and those of normal individuals is statistically significant (p = 0.0028, 2-tailed p-value, Mann-Whitney test). Since the saliva HAase levels are elevated in patients with either oral cavity, pharyngeal or laryngeal HNSCC, as well as among patients with either stage II, III or IV disease, it is possible that the HAase levels are elevated in HNSCC patients, regardless of the site and stage of the disease. However, due to a small number of patients included in this preliminary study, correlation between tumor stage and HAase levels could not be determined.

Determination of HA and HAase levels in cell CM

Both tumor cells and fibroblasts isolated from tumor tissues have been shown to produce HA *in vitro*.[17,23] We therefore compared HA production among HNSCC cell lines FaDu, MDA-1483, transformed keratinocyte HEK-001 and Hep-2 (a positive control). We found that all cell lines secrete measurable amounts of HA in their CM. However, both FaDu (2.2 ± 0.3 μg/mg) and MDA-1483 (4.3 ± 0.7 μg/mg) cells secrete higher amounts of HA in their CM when compared to HEK-001 (0.5 ± 0.04 μg/mg) and HEp-2 (0.9 ± 0.05 μg/mg) cells, respectively.

We next measured HAase levels in cell CM using the HAase test. The HAase assay was performed at pH 4.3. We found that HEp-2 (47.3 ± 6.7 mU/mg) and MDA-1483 (69.0 ± 7.9 mU/mg) cell lines secrete 7- to 11-fold higher levels of HAase in their CM than FaDu (6.4 ± 1.1 mU/mg) cells. FaDu cells secrete 1.5-fold more HAase in their CM than the HEK-001 cells (4.3 ± 0.7 mU/mg). These results indicate that HNSCC cells secrete both the HA and HAase in their CM and the transformed keratinocyte line secretes significantly less HA and HAase than the tumor cells.

Characterization of HAase in HNSCC cells and patients' saliva

We have previously shown that HYAL1 type HAase is the major HAase expressed in bladder and prostate cancer tissues and cells, as well as in the urine of bladder cancer patients.[17,25,42] However, PH20 mRNA expression has been detected in laryngeal cancer tissues.[43] We therefore examined the expression of HYAL1 and PH20 in HNSCC cell lines, tissues and saliva specimens.

RT-PCR analysis. We performed RT-PCR analysis on total RNA isolated from HEp-2, MDA-1483, FaDu and HEK-001 cells and a normal pharyngeal tissue specimen, using a HYAL1-specific primer pair that we have previously used to amplify the entire coding region of HYAL1 from bladder and prostate cancer cells.[25] As shown in Figure 1a, an expected 1.3 kb HYAL1-specific PCR product is amplified from HEp-2, FaDu and HEK-001 cells and the
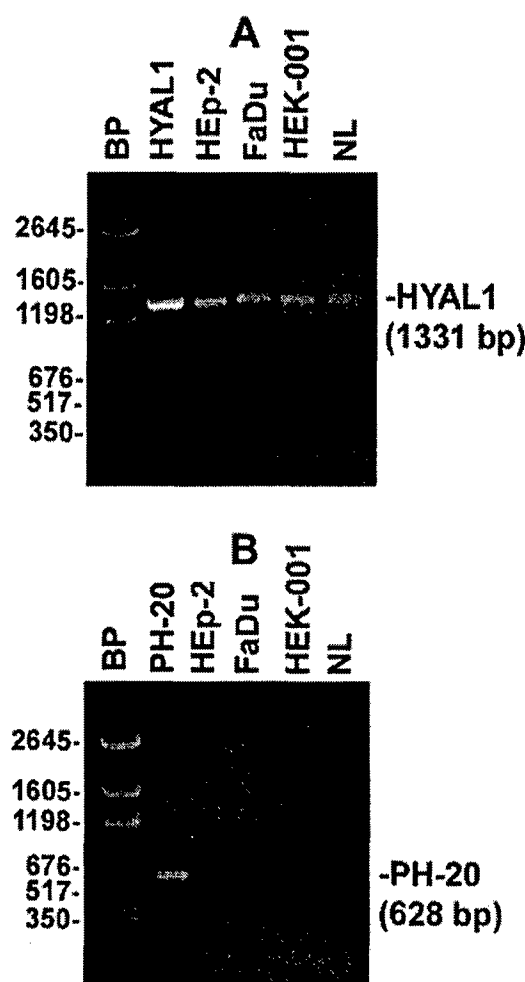

FIGURE 1 – Examination of HYAL1 and PH20 transcripts in cells and tissues: total RNA was isolated from HEp-2, FaDu and HEK001 cells and a normal oropharyngeal tissue specimen. The RNA was reverse transcribed and PCR amplified using HYAL1 and PH20 specific primer pairs as described in Material and Methods. Full-length HYAL1 and PH20 cDNAs served as positive controls for PCR. PCR products were analyzed by agarose gel electrophoresis.

normal tissue. The length and the sequence of this product are similar to those of the HYAL1 cDNA, which was used as a positive control in this RT-PCR analysis. This PCR product was not amplified in negative control samples, prepared by the omission of either first-strand cDNA or the Ampli-Taq Gold polymerase in the PCR mix (data not shown).

When the RT-PCR analysis was performed using a PH20-specific primer pair, an expected 628 bp PCR product is amplified from the DNA of a positive control plasmid that contains the entire PH20 coding sequence (Fig. 1b). However, none of the cell lines and the normal tissue showed expression of the PH20 mRNA (Fig. 1b).

Immunoblot analysis. We next examined the expression of HYAL1 protein in the cell CM and patients' saliva by immunoblot analysis using an anti-HYAL1 peptide IgG. This antibody is directed against the amino acid sequence containing amino acids 321–338 in the HYAL1 sequence and has been well characterized in terms of its specificity to detect HYAL1 in immunoblot and immunohistochemic analyses.[17,25] As shown in Figure 2a, a major ~55 kDa protein is detected in the CM of MDA-1483, HEp-2 and
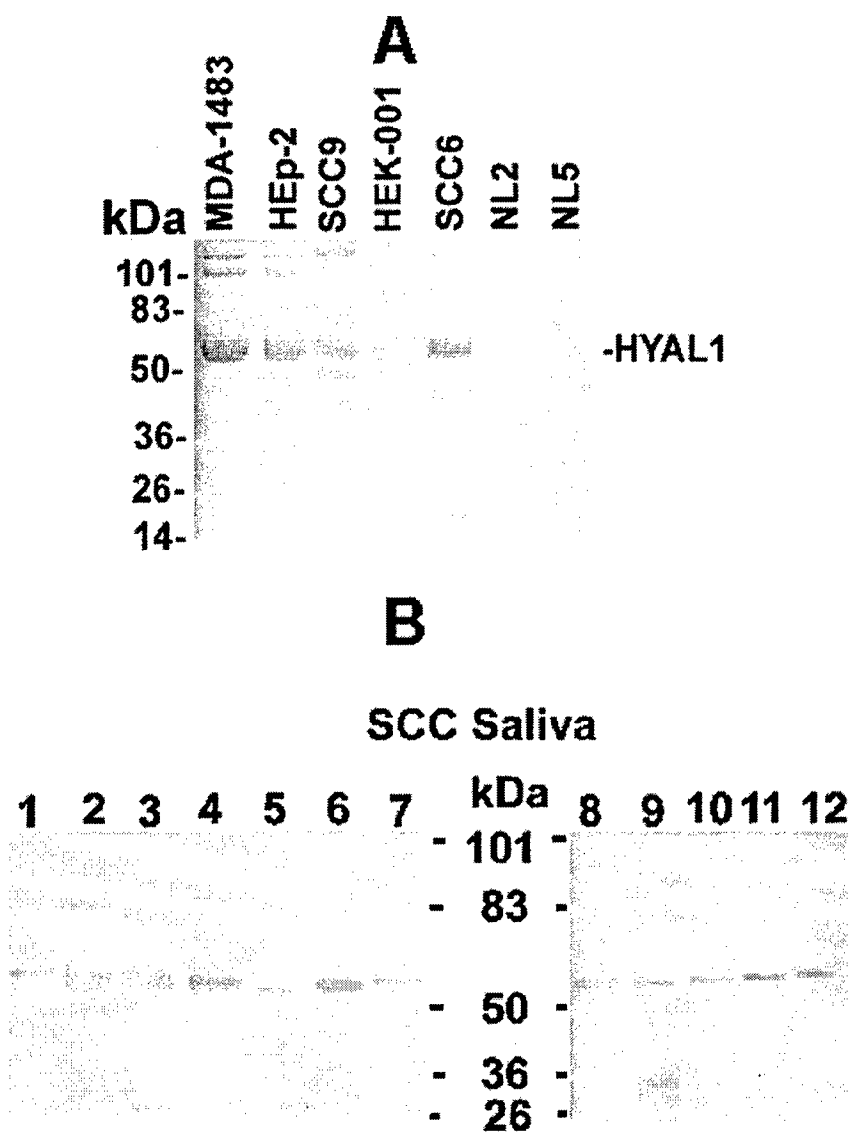
FIGURE 2 – Immunoblot analysis of saliva specimens and cell CM using anti-HYAL1 antibody. *(a)* Culture CM (~5 μg of total protein) and saliva specimens from SCC6 and SCC9 patients and NL2, and NL5 controls (~10 μg of total protein) were subjected to immunoblot analysis using an anti-HYAL1 peptide IgG, as described in Material and Methods. *(b)* Saliva specimens from all 12 HNSCC patients presented in Table I were subjected to HYAL1 immunoblot analysis using the anti-HYAL1 IgG, as described in Material and Methods.

HEK-001 cells. Furthermore, a ~55 kDa protein is also detected in saliva specimens from SCC6 and SSC9 patients. As shown in Figure 1, SSC6 and SSC9 patients have 10.9 and 8 mU/mg of HAase activity in their saliva. None to very weak expression of the 55 kDa HYAL1-related protein is observed in saliva specimens from NL2 and NL5 patients (Fig. 2*a*). These results demonstrate that a 55 kDa HYAL1-related protein is expressed in HNSCC patients' saliva and that its expression is consistent with the HAase activity that is detected in saliva specimens.

We next analyzed the presence of HYAL1 in saliva specimens from all 12 HNSCC patients using the anti-HYAL1 immunoblot analysis. As shown in Figure 2*b*, a major ~55 kDa protein is detected in the saliva of HNSCC patients. The minor bands in the saliva of patients 3 and 9 could be HYAL1 degradation products. The intensity of the HYAL1 band roughly corresponded to the amount of HAase activity present in the saliva of each patient as shown in Table I.

Determination of pH activity profile of HAase activity. We have recently shown that the HYAL1 type HAase has a pH optimum range between 4.1 and 4.3. Furthermore, the HAase expressed in bladder and prostate cancer tissues, cells and bladder cancer pa-

tients' urine has the same pH optimum. Moreover, the HYAL1 type HAase is 50% active at pH 4.5 and has no activity at pH 5.0.[25] On the contrary, PH20 is active between pH 3 and 9 and has a broad pH optimum in the neutral pH range.[49–52] We determined the pH activity profile of the HAase activity secreted in the CM of HEp-2, MDA-1483 and HEK-001 cells and saliva specimens from the SCC8 patient and NL3 control using the HAase ELISA-like assay, conducted at different pH values. A partially purified HYAL1 preparation and bovine testicular HAase were also assayed at different pH values to serve as positive controls. As shown in Figure 3*a*, the HAase activity present in saliva from a HNSCC patient (SCC8) and normal individual (NL3) has a single pH optimum at 4.4. The pH activity profile and the pH optimum of the HAase activity present in saliva closely resemble that of HYAL1 (pH optimum = 4.2–4.3, Fig. 3*a*). The testicular HAase has a broad pH activity profile with a pH optimum at 5.0. The enzyme is over 80% active at pH 6.5, ~ 65% active at pH 7.0 and 41% active at pH 8.0. These results show that the HAase activity present in saliva is distinct from the testicular type HAase activity, and it resembles the acidic type HAases such as HYAL1. As shown in Figure 3*b*, the HAase activity secreted CM of HEp-2,
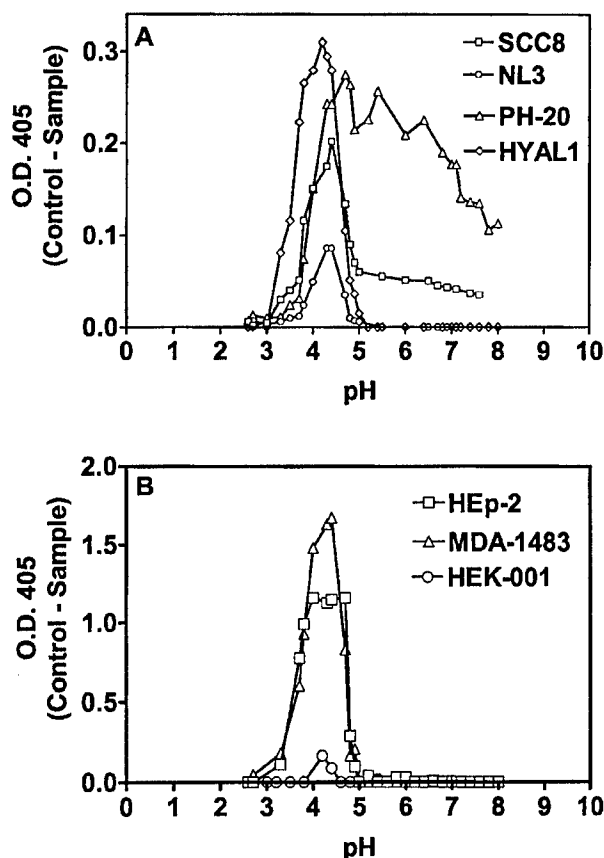
Figure 3 – Determination of pH activity profile of HAase activity present in CM and saliva specimens. Saliva specimens from SCC8 patient, NL3 control and culture CM from MDA-1483, Hep-2 and HEK-001 cells were assayed for HAase activity at different pH values as described in Material and Methods. (a) pH activity profile of saliva specimens. Partially purified HYAL1 and testicular HAase (PH-20) were also analyzed under same assay conditions. (b) pH activity profile of cell culture CM.

MDA-1483 and HEK-001 cells exhibits a single pH optimum at 4.3–4.4, suggesting the presence of an acidic type HAase, such as HYAL1, in the CM.

Analysis of HA species present in saliva

It has been shown that small HA fragments (3–25 disaccharide units) generated by HAase digestion of HA are angiogenic.[32] We have previously demonstrated the presence of such angiogenic fragments in the urine of bladder cancer patients and in prostate cancer tissues.[25,36] We analyzed the profile of HA species present in normal individuals and HNSCC patients by gel-filtration chromatography. As shown in Figure 4, 1 HA species that has intermediate size between the high-molecular-mass HA and the F1 fragment is present in the normal individual's saliva. The patient with stage T1N0 disease has a saliva HA profile similar to that of the normal individual. The stage T2N0 patient's saliva contains 2 HA peaks, a large HA peak that elutes before the HA peak present in the normal individual's saliva, suggesting that the size of this HA species is higher than that present in the normal individual's saliva. The smaller second HA peak elutes at a position similar to that of the F1 HA fragment, which is angiogenic.[25,36] The saliva HA profile of HNSCC patients with stage T3N1 and T4N0 reveals several HA peaks. These peaks correspond to HA (i.e., peaks I and II), the F1 fragment (peak III) and the F2 fragment (i.e., peak IV).
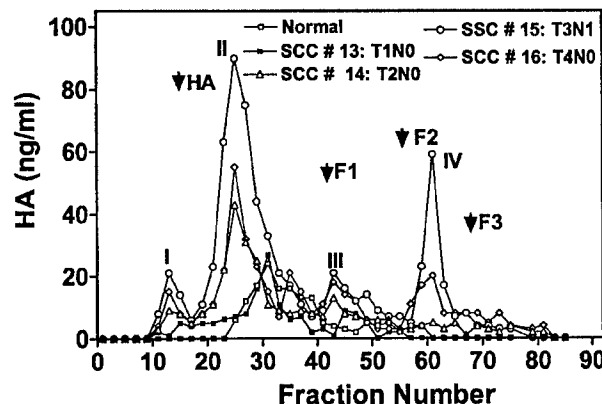

Figure 4 – Examination of saliva HA profiles of normal and HNSCC patients. The sizes of HA species in the saliva of a normal individual, and HNSCC patients (stages T1N0, T2N0, T3N1 and T4N0) were determined by gel-filtration chromatography on a Sephadex G-50 column, as described in Material and Methods. The column was standardized using high-molecular-mass HA and HA fragments F1 (10–15 disaccharide units), F2 (2–3 disaccharide units) and F3 (~2 disaccharide units).

These results show that the HNSCC patients with higher stage may contain both the high-molecular-mass and low-molecular-mass HA species. The low-molecular-mass HA species may result from HA degradation by HAase.

DISCUSSION

The management of HNSCC is challenging. Elimination of the initial tumor offers the best chance of cure, yet with current treatment modalities we succeed only 50% of the time.[52,53] Therapy fails most often due to recurrence at the primary site or in the neck, and less often from distant metastases.[52–54] Research in HNSCC focuses on the identification of molecular markers and their ability to accurately stage tumors and predict recurrence.[8–10,55] Identifying such markers will help to initiate effective treatment protocols promptly. Based on the findings reported here, we believe that HA and HAase are candidate tumor markers.

Pathologists have long recognized a mucin-like substance noted on gross examination of tumor specimens, which has since been identified as HA.[21] HA is potentially a useful marker for diagnosis and prognosis for many tumors.[17–25] For example, we have previously shown that urinary HA levels, measured using the HA test, have 83.1% sensitivity and 90.1% specificity to detect bladder cancer, regardless of its tumor grade.[24] The results of this pilot study using the HA test indicate that HA levels are ~5-fold elevated in the saliva of HNSCC patients when compared to normal controls. In 8 of 11 HNSCC patients with active disease, the HA levels were >1,000 ng/mg, whereas all 6 normal controls had HA levels of |< 1,000 ng/mg.| In tumor tissues depending upon tissue origin, either the tumor-associated stroma or tumor cells, or both, secretes elevated levels of HA.[17–20,22–25] Although at present the cellular origin of HA present in HNSCC tissues is unknown, under *in vitro* culture conditions both HNSCC cell lines and the HEp-2 line secrete higher amounts of HA in their CM than the keratinocyte line HEK-001.

Like HA, HAase levels are elevated in bladder and prostate cancer tissues.[17,24,25,48] In our study, HAase levels were elevated 3.7-fold in the saliva of HNSCC patients when compared to normal controls. While in all 6 normal individuals the HAase levels were <5 mU/mg, the HAase levels were above 5 mU/mg in all 11 HNSCC patients with active disease. Urinary HAase levels with a cutoff limit of 10 mU/mg are highly sensitive (81.5% sensitivity) and specific (83.8% specificity) markers for detecting

high-grade bladder tumors, which are invasive and metastatic.[24] In HNSCC, stage III and IV tumors represent advanced stage disease with poor prognosis.[4,43] It is noteworthy that in our study, saliva HAase levels are elevated in all of the stage III and IV patients when compared to normal controls. HAase levels are also elevated among HNSCC patients regardless of the site that is involved. Thus, HAase may be a potential marker for HNSCC. However, it remains to be determined whether HAase levels are also elevated in stage I HNSCC, which is less likely to metastasize.

We have previously shown that tumor cells under both *in vivo* and *in vitro* secrete HAase.[17,25,42] Consistent with these results, HNSCC line MDA-1483 and the HEp-2 cell line secrete 12- to 17-fold more HAase in their CM than the HEK-001 cell line. In tumor tissues, HAase degrades HA into angiogenic HA fragments. We have previously detected such angiogenic HA fragments in the urine of bladder cancer patients and in prostate cancer tissues.[25,36] Because HAase may be intricately involved in tumor progression, its levels may be elevated in high-grade bladder cancer and high-stage HNSCC.

Little is known about HAase expression in HNSCC. Using the HAase test we have shown that HAase is overproduced in the saliva of HNSCC patients and HNSCC cell lines when compared to normal controls. Using RT-PCR analysis we have shown that HYAL1 rather than PH20 is the major HAase transcript expressed in the cell lines. The pH activity profile and pH optimum of the HAase activity present in normal and patients' saliva, as well as that secreted in the CM of HNSCC cells, closely resembles that of HYAL1 and not PH20. Godin *et al.*[43] have previously reported the expression of PH20 mRNA in laryngeal cancers and suggested that detection of PH20 mRNA by RT-PCR analysis is a useful prognostic tool for laryngeal cancers. It is possible that unlike oral cavity and pharyngeal SCC, in laryngeal cancers, PH20 is the major HAase that is expressed. In our study, among the 12 HNSCC patients, 1 had laryngeal cancer (i.e., SCC6, Fig. 1a). This patient's saliva had elevated HAase activity (10.9 mU/mg) with pH optimum at 4.3. Furthermore, this patient's saliva showed the presence of HYAL1 protein (Fig. 4). Thus, in HNSCC it may be important to characterize HAase expression at mRNA, protein and activity levels.

Frost *et al.*[45] have previously reported the presence of HYAL1 transcript in HNSCC cell lines. However, they did not detect any HAase activity and HYAL1 protein in the CM of HNSCC cells and suggested that an alternative splicing event was responsible for inhibiting protein translation. In a recent study, we have characterized 5 alternatively spliced variants of HYAL1, all of which synthesize truncated HYAL1 proteins that are enzymatically inactive.[56] However, since both HYAL1 protein and HAase activity are detected in HNSCC patients' saliva and HNSCC cell CM demonstrate that HNSCC patients' saliva contains functional HYAL1, which is most likely secreted by tumor cells. It is possible that the HNSCC cell lines described by Frost *et al.* are unable to secrete HAase activity, as has been reported previously for some bladder cancer cell lines.[45] We have previously shown that invasive tumor cells, and not the noninvasive tumor cells, secrete high

levels of HAase.[42,57] This is the most likely reason why HAase serves as a marker for detecting high-grade tumors.[24,48]

Among the 12 HNSCC patients included in our study, 1 patient (patient 11, Fig. 1a) was initially diagnosed with an unknown primary at an outside hospital and was referred to our institution. An unknown primary presents as a lymph node in the neck containing squamous cell carcinoma in a patient with no evidence of disease in the upper aerodigestive tract. On direct laryngoscopy, a suspicious area on the tonsil was identified and biopsied. Pathology came back positive for HNSCC. This patient had saliva HA levels of 1,240 ng/mg and HAase levels of 7.5 mU/mg, indicating positive HA and HAase tests. Patient SCC12 also was diagnosed with an unknown primary tumor. The primary tumor in this patient was not identified prior to treatment. This patient had saliva HA levels of 707 ng/mg and HAase levels of 7.6 mU/mg, indicating a borderline HA test and a positive HAase. This finding suggests that even microscopic disease may be identified using the HA-HAase test. These results are also consistent with our previous finding that the HA-HAase test can detect bladder tumor recurrence ~5 months before its clinical detection.[58]

At the present time it is unknown whether HA and HYAL-1 serve as independent markers for predicting the prognosis of HNSCC and whether the HA and/or HAase levels correlate with HNSCC stage. This is because in this preliminary study of 12 HNSCC patients, except for 1 stage II patient, others had stage III or IV disease and the patients were not followed for disease progression and/or recurrence. We have previously shown that the HA levels are elevated in bladder cancer patients, regardless of tumor grade, whereas the HAase levels are preferentially elevated in G2 and G3 bladder cancer patients.[24] In a recent study on prostate cancer we found that HYAL1 and not HA is an independent predictor of biochemic recurrence/disease progression as measured by increases in the levels of prostate-specific antigen after radical prostatectomy.[59] However, in other studies, HA has been shown to be an independent predictor of tumor metastasis.[22,23,60] Since in HNSCC patients both HA and HAase levels are elevated, the expression of these 2 may be linked; i.e., as cells upregulate HA-synthase, the expression of HAase is also increased. Future studies based on our preliminary studies could test this possibility.

In conclusion, in this preliminary study we have shown that tumor markers HA and HAase are overexpressed in the saliva of HNSCC patients when compared to normal controls. These markers also appear to be elevated in most of the tumor cell lines studied. HYAL1 is likely the main HAase expressed in HNSCC. Similar work using more samples and appropriate statistical analysis is warranted to determine if HA and HAase are useful markers for HNSCC.

REFERENCES

1. Funk GF, Karnell LH, Robinson RA, Zhen WK, Trask DK, Hoffman HT. Presentation, treatment, and outcome of oral cavity cancer: a National Cancer Data Base report. Head Neck 2002;24:165–80.
2. Parkin DM, Pisani P, Ferlay J. Estimates of the worldwide incidence of 25 major cancers in 1990. Int J Cancer 1999;80:827–41.
3. Patel U, Spitznagel E, Piccirillo J. Multivariate analyses to assess treatment effectiveness in advanced head and neck cancer. Arch Otolaryngol Head Neck Surg 2002;128:497–503.
4. Vokes EE, Weichselbaum RR, Lippman SM, Hong WK. Head and Neck Cancer. N Engl J Med 1993;328:184–94.
5. Sloan D, Goepfert H. Conventional therapy of head and neck cancer. Hematol Oncol Clin North Am 1991;5:601–25.
6. Slaughter DP, Southwick HW, Smejkal W. "Field cancerization" in

oral stratified squamous epithelium clinical implications of multicentric origin. Cancer 1953;3:963–8.
7. Goodwin WJ. Salvage surgery for patients with recurrent squamous cell carcinoma of the upper aerodigestive tract: when do the ends justify the means? Laryngoscope 2000;110:S1–18.
8. Forastiere A, Koch W, Trotti A, Sidransky D. Head and Neck Cancer. N Engl J Med 2001;345:1890–1900.
9. Braakhuis BJ, Tabor MP, Leemans CR, van der Waal I, Snow GB, Brakenhoff RH. Second primary tumors and field cancerization in oral and oropharyngeal cancer: molecular techniques provide new insights and definitions. Head Neck 2002;24:198–206.
10. Helliwell TR. Molecular markers of metastasis in squamous carcinomas. J Pathol 2001;194:289–93.

11. Toole BP, Wight TN, Tammi MI. Hyaluronan-cell interactions in cancer and vascular disease. J Biol Chem 2002;277:4593–6.
12. Tammi MI, Day AJ, Turley EA. Hyaluronan and homeostasis: a balancing act. J Biol Chem 2002;277:4581–4.
13. Laurent TC, Fraser JRE. Hyaluronan. FASEB J 1992;6:2397–404.
14. Delpech B, Girard N, Bertrand P, Courel NM, Chauzy C, Delpech A. Hyaluronan: fundamental principles and applications in cancer. J Intern Med 1997;242:41–8.
15. Turley EA, Noble PW, Bourguignon LY. Signaling properties of hyaluronan receptors. J Biol Chem 2002;277:4589–92.
16. Knudson W, Chow G, Knudson CB. CD44-mediated uptake and degradation of hyaluronan. Matrix Biol 2002;21:15–23.
17. Hautmann SH, Lokeshwar VB, Schroeder GL, Civantos F, Duncan, RC, Friedrich MG, Soloway MS. Elevated tissue expression of hyaluronic acid and hyaluronidase validate HA-HAase urine test for bladder cancer. J Urol 2000;165:2068–74.
18. Setala LP, Tammi MI, Tammi RH, Eskelin MJ, Lipponen PR, Argen UM, Parkkinen J, Alhava EM, Kosma VM. Hyaluronan expression in gastric cancer cells is associated with local and nodal spread and reduced survival rate. Br J Cancer 1999;81:1133–8.
19. Auvinen P, Tammi R, Parkkinen J, Tammi M, Agren U, Johansson R, Hirvikoski P, Eskelinen M, Kosma VM. Hyaluronan in peritumoral stroma and malignant cells associates with breast cancer spreading and predicts survival. Am J Pathol 2000;156:529–36.
20. Pirinen R, Tammi R, Tammi M, Hirvikoski P, Parkkinen JJ, Johansson R. Prognostic value of hyaluronan expression in non-small-lung cancer: increased stromal expression indicates unfavorable outcome in patients with adenocarcinoma. Int J Cancer 2001;95:12–27.
21. Knudson W. Tumor associated hyaluronan: providing an extracellular matrix that facilitates invasion. Am J Pathol 1996;148:1721–6.
22. Ropponen K, Tammi M, Parkkinen J, Eskelinen M, Tammi R, Lipponen P, Argen V, Alhava E, Kosma VM. Tumor-associated hyaluronan as an unfavorable prognostic factor in colorectal cancer. Cancer Res 1998;58:342–7.
23. Lipponen P, Aaltomaa S, Tammi R, Tammi M, Agren U, Kosma VM. High stromal hyaluronan level is associated with poor differentiation and metastasis in prostate cancer. Eur J Cancer 2001;37:849–56.
24. Lokeshwar VB, Obek C, Pham HT, Wei DC, Young MJ, Duncan RC, Soloway MS, Block NL. Urinary hyaluronic acid and hyaluronidase: markers for bladder cancer detection and evaluation of grade. J Urol 2000;163:348–56.
25. Lokeshwar VB, Rubinowicz D, Schroeder GL, Forgacs E, Minna, JD, Block NL, Nadji M, Lokeshwar BL. Stromal and epithelial expression of tumor markers hyaluronic acid and hyaluronidase in prostate cancer. J Biol Chem 2001;276:11922–32.
26. Liu N, Lapcevich RK, Underhill CB, Han Z, Gao F, Swartz G, Plum SM, Zhang L, Gree SJ. Metastatin: a hyaluronan-binding complex from cartilage that inhibits tumor growth. Cancer Res 2001;61:1022–8.
27. Hayen W, Goebeler M, Kumar S, Riessen R, Nehls V. Hyaluronan stimulates tumor cell migration by modulating the fibrin fiber architecture. J Cell Sci 1999;112:2241–51.
28. Hoborth K, Maier, U, Marberger M. Topical chemoprophylaxis of superficial bladder cancer by mitomycin C and adjuvant hyaluronidase. Eur Urol 1992;21:206–10.
29. Itano N, Atsumi F, Sawai T, Yamada Y, Miyaishi O, Senga T, Hamguchi M, Kimata K. Abnormal accumulation of hyaluronan matrix diminishes contact inhibition of cell growth and promotes cell migration. Proc Natl Acad Sci USA 2002;99:3609–14.
30. Roden L, Campbell P, Fraser JRE, Laurent TC, Petroff H, Thompson JN. Enzymatic pathways of hyaluronan catabolism. In: Whelan E, ed. The biology of hyaluronan. Chichester, UK: Wiley, 1989. 60–86.
31. Jedrzejas MJ. Structural and functional comparison of polysaccharide-degrading enzymes. Crit Rev Biochem Mol Biol 2000;35:221–51.
32. West DC, Kumar S. Hyaluronan and angiogenesis. Ciba Found Symp 1989;143:187–201 [discussion, 201–7, 281–5].
33. West DC, Kumar S. The effect of hyaluronate and its oligosaccharides on endothelial cell proliferation and monolayer integrity. Exp Cell Res 1989;183:179–96.
34. Lokeshwar VB, Selzer MG. Differences in hyaluronic acid-mediated functions and signaling in arterial, microvessel, and vein-derived human endothelial cells. J Biol Chem 2000;275:27641–9.
35. Savani RC, Cao G, Pooler PM, Zaman A, Zhou Z, DeLisser HM. Differential involvement of the hyaluronan (HA) receptors CD44 and receptor for HA-mediated motility in endothelial cell function and angiogenesis. J Biol Chem 2001;276:36770–8.
36. Lokeshwar VB, Obek C, Soloway MS, Block NL. Tumor-associated

37. Tanabe KK, Nishi T, Saya H. Novel variants of CD44 arising from alternative splicing: changes in the CD44 alternative splicing pattern of MCF-7 breast carcinoma cells treated with hyaluronidase. Mol Carcinog 1993;7:212–20.
38. Lin G, Stern R. Plasma hyaluronidase (Hyal-1) promotes tumor cell cycling. Cancer Lett 2001;163:95–101.
39. Csoka AB, Frost GI, Stern R. The six hyaluronidase-like genes in the human and mouse genomes. Matrix Biol 2001;20:499–508.
40. Lepperdinger G, Mullegger J, Kreil G. Hyal2—less active, but more versatile? Matrix Biol 2001;20:509–14.
41. Cherr GN, Yudin AI, Overstreet J. The dual functions of GPI-anchored PH-20: hyaluronidase and intracellular signaling. Matrix Biol 2001;20:515–25.
42. Lokeshwar VB, Young MJ, Goudarzi G, Iida N, Yudin AI, Cherr GN, Selzer MG. Identification of bladder tumor-derived hyaluronidase: its similarity to HYAL1. Cancer Res 1999;59:4464–70.
43. Godin DA, Fitzpatrick PC, Scandurro AB, Belafsky PC, Woodworth BA, Amedee RG, Beech DJ, Beckman BS. PH20: a novel tumor marker for laryngeal cancer. Arch Otolaryngol Head Neck Surg 2000;126:402–4.
44. Beech DJ, Madan AK, Deng N. Expression of PH-20 in normal and neoplastic breast tissue. J Surg Res 2002;103:203–7.
45. Frost GI, Mohapatra G, Wong TM, Csoka AB, Gray JW, Stern R. HYAL1LUCA-1, a candidate tumor suppressor gene on chromosome 3p21.3, is inactivated in head and neck squamous cell carcinomas by aberrant splicing of pre-mRNA. Oncogene 2000;19:870–7.
46. Fosang AJ, Hey NJ, Carney SL, Hardingham TE. An ELISA plate-based assay for hyaluronan using biotinylated proteoglycan G1 domain (HA-binding region). Matrix 1990;10:306–13.
47. Stern M, Stern R. An ELISA-like assay for hyaluronidase and hyaluronidase inhibitors. Matrix 1992;12:397–403.
48. Pham HT, Block NL, Lokeshwar VB. Tumor-derived hyaluronidase: a diagnostic urine marker for high-grade bladder cancer. Cancer Res 1997;57:778–83.
49. Li M, Cherr GN, Yudin AI, Overstreet JW. Biochemical characterization of the PH-20 protein on the plasma membrane and inner acrosomal membrane of cynomolgus macaque spermatazoa. Mol Reprod Dev 1997;48:356–66.
50. Hunnicutt GR, Mahan K, Lathrop WF, Ramarao CS, Myles DG, Primakoff P. Structural relationship of sperm soluble hyaluronidase to the sperm membrane protein PH-20. Biol Reprod 1996;54:1343–9.
51. Cherr GN, Meyers SA, Yudin AI, Vandevoort CA, Myles DG, Primakoff P, Overstreet JW. The PH-20 protein in cynomolgus macaque spermatozoa: identification of two different forms exhibiting hyaluronidase activity. Dev Biol 1996;175:142–53.
52. Jesse RH, Sugarbaker EV. Squamous cell carcinoma of the oropharynx: why we fail. Am J Surg 1976;132:435–8.
53. Shah JP, Cendon RA, Farr HW, Strong EW. Carcinoma of the oral cavity. Am J Surg 1976;132:504–7.
54. Mukherji SK, Armao D, Joshi VM. Cervical nodal metastases in squamous cell carcinoma of the head and neck: what to expect. Head Neck 2001;23:995–1005.
55. Patel V, Leethanakul C, Gutkind JS. New approaches to the understanding of the molecular basis of oral cancer. Crit Rev Oral Biol Med 2001;12:55–63.
56. Lokeshwar VB, Schroeder GL, Carey RI, Soloway MS, Iida N. Regulation of hyaluronidase activity by alternative mRNA splicing. J Biol Chem 2002;277:33654–63.
57. Lokeshwar VB, Soloway MS, Block NL. Secretion of bladder tumor-derived hyaluronidase activity by invasive bladder tumor cells. Cancer Lett 1998;131:21–7.
58. Lokeshwar VB, Schroeder GL, Selzer MG, Hautmann SH, Posey JT, Duncan RC, Watson R, Rose L, Markowitz S, Soloway MS. Bladder tumor markers for monitoring recurrence and screening comparison of hyaluronic acid-hyaluronidase and BTA-stat tests. Cancer 2002;95: 61–72.
59. Posey JT, Soloway MS, Ekici E, Sofer M, Civantos F, Duncan RC, Lokeshwar VB. Evaluation of the prognostic potential of hyaluronic acid and hyaluronidase (HYAL1) for prostate cancer. Cancer Res, in press.
60. Hiltunen EL, Anttila M, Kultti A, Ropponen K, Penttinen J, Yliskoski M, Kuronen AT, Juhola M, Tammi R, Tammi M, Kosma VM. Elevated hyaluronan concentration without hyaluronidase activation in malignant epithelial ovarian tumors. Cancer Res 2002;62:6410–3.

hyaluronic acid: a new sensitive and specific urine marker for bladder cancer. Cancer Res 1997;57:773–7.

APPENDIX 3

Evaluation of the Prognostic Potential of Hyaluronic Acid and Hyaluronidase (HYAL1) for Prostate Cancer[1]

J. Timothy Posey, Mark S. Soloway, Sinan Ekici, Mario Sofer, Francisco Civantos, Robert C. Duncan, and Vinata B. Lokeshwar[2]

Departments of Urology [J. T. P., M. S. S., S. E., M. S., F. C., V. B. L.], Department of Epidemiology [R. C. D.], and Cell Biology and Anatomy [V. B. L.], University of Miami School of Medicine, Miami, Florida 33101

ABSTRACT

Despite the development of nomograms designed to evaluate the prognosis of a patient with prostate cancer (CaP), the information has been limited to prostate-specific antigen (PSA), clinical stage, Gleason score, and tumor volume estimates. To improve our ability to predict prognosis, information regarding the molecular properties of CaP is needed. Hyaluronic acid (HA) is a glycosaminoglycan that promotes tumor metastasis. Hyaluronidase (HAase) is an enzyme that degrades HA into angiogenic fragments. We recently showed that in CaP tissues, whereas HA is localized mostly in the tumor-associated stroma, HYAL1 type HAase is exclusively localized in CaP cells (Lokeshwar *et al.* J. Biol. Chem., *276:* 11922–11932, 2001). We evaluated the prognostic potential of HA and HYAL1 in CaP by immunohistochemistry.

Archival CaP specimens were obtained from patients who underwent radical retropubic prostatectomy for clinically localized CaP. Group 1 ($n = 25$) included patients who showed biochemical recurrence (PSA >0.4 ng/ml; mean recurrence: 21.3 months). Group 2 included patients with no clinical or biochemical recurrence ($n = 45$; mean follow-up: 80.9 months). For HA and HYAL1 staining, a biotinylated HA-binding protein and an anti-HYAL1 antibody were used. The staining was evaluated on the basis of intensity (0 to 3+) and as dense or sparse (for HA staining only) and then grouped as low grade and high grade.

In CaP specimens, HYAL1 was exclusively expressed in tumor cells. Although the stroma was stained positive for HA, 40% of tumor cells also expressed HA. HA, HYAL1, and combined HA-HYAL1 staining predicted progression with 96%, 84%, and 88% sensitivity, 55.5%, 80%, and 84.4% specificity, and 70%, 81.4%, and 85.7% accuracy, respectively. In the univariate analysis, preoperative PSA, Gleason sum, stage, margin, seminal vesicle, extra-prostatic extension (EPE), HA, HYAL1, and HA-HYAL1 were significant in predicting progression ($P < 0.05$). However, in the multiple logistic regression analysis, only EPE [odds ratio (OR) = 33.483; $P = 0.002$], HYAL1 (OR = 12.42; $P = 0.009$), HA-HYAL1 (OR = 18.048; $P = 0.0033$), and margin (OR = 26.948; $P = 0.006$)] were significant. Thus, in this 5-year follow-up study, HYAL1, together with EPE and margin, was found to be an independent prognostic indicator.

INTRODUCTION

In the last decade, because of the increased public awareness of serum PSA[3] screening, the number of CaP cases has steadily increased. PSA screening has resulted in the detection of more clinically localized CaP, which has the potential to be cured by radical prostatectomy or radiation therapy (1–4). However, within the first 10 years after surgery, CaP recurs [defined as PSA failure (biochemical re-

lapse), local/systemic recurrence] in ~10–50% of cases, depending on a variety of prognostic factors (5–7). Treatment failure may be attributable to a local recurrence or distant metastasis. Existing preoperative indicators (*i.e.,* PSA levels, clinical stage, biopsy Gleason sum) or their combination in nomograms, as well as surgical and pathologic parameters (*i.e.,* prostatectomy Gleason sum, margin +/−, node status, seminal vesicle, and EPE), provide a limited estimate of the prognosis for CaP (8, 9). Identifying molecules that are expressed in clinically localized CaP but associate with CaP invasion and metastasis might significantly improve the prognostic capabilities and management of CaP patients after a curative approach. We have recently shown the expression of two tumor markers, HA and HAase, in CaP (10, 11).

HA is a glycosaminoglycan made up of repeated disaccharide units, D-glucuronic acid and *N*-acetyl-D-glucosamine (12–14). HA is a component of tissue matrix and tissue fluids. HA keeps the tissues hydrated and maintains the osmotic balance (12–14). In addition, by interacting through cell surface receptors (*e.g.,* CD44 and RHAMM), it regulates cell adhesion, migration, and proliferation (15). Concentrations of HA are elevated in several cancers, including colon, breast, prostate, bladder, and lung, and serve as highly sensitive and specific markers for detecting bladder cancer, regardless of the tumor grade (16–24). In tumor tissues, HA promotes tumor metastasis by opening up spaces for tumor cells to migrate and actively supports tumor cell migration by interacting with cell surface HA receptors (12, 14, 15). An HA coat around tumor cells may offer some protection against immune system surveillance and cause a partial loss of contact-mediated inhibition of cell growth and migration (25–28). Localization of HA either in tumor-associated stroma or tumor cells depends on the tissue origin. For example, in colon and stomach cancers, most of the tumor cells express HA (17, 21). In bladder cancer, HA expression is equally distributed in tumor-stroma and tumor cells (16). However, in CaP, HA is mostly localized in tumor stroma (22).

HAase is an endoglycosidase that degrades HA into small angiogenic fragments of 3–25 disaccharide units (29, 30). Angiogenic HA fragments induce endothelial cell proliferation, adhesion, and migration by activating focal adhesion kinase and mitogen-activated protein kinase pathways (31, 32). We have shown previously the presence of angiogenic HA fragments in high Gleason sum (≥ 7) CaP tissues (10). Six HAase genes have been identified in humans. Among these, products of HYAL1, HYAL2, and PH20 are well characterized (33–35). We have shown that HYAL1 type HAase is the major HAase expressed in prostate and bladder cancer tissues and have characterized the expression of HYAL1 at the mRNA and protein levels in prostate and bladder tumor cells (11, 36, 37). The HAase expressed by CaP cells has the same pH activity profile as that of HYAL1 (10). The expression of PH20 mRNA has been detected by reverse-transcription PCR analysis in some tumor tissues including CaP; however, the presence of PH20 protein has not been documented in these studies (38, 39). Because our recent observations show that the HAase family of genes are extensively alternatively spliced, which, in turn, regulates the generation of enzymatically active HAases, characterization of HAase expression in tumor tissues at the protein level may be nec-

essary (40). By immunohistochemical techniques, we have shown previously that the HYAL1 type HAase is localized in tumor epithelial cells and the expression increases with higher grades of CaP (10). In this study, we examined the prognostic potential of HA and HYAL1 for predicting CaP progression by immunohistochemically localizing these markers in archival CaP tissues and correlating the staining intensity with PSA biochemical recurrence as an indicator of CaP progression.

MATERIALS AND METHODS

Specimens and Study Individuals. Seventy-three CaP specimens were obtained from patients who underwent radical retropubic prostatectomy for clinically localized CaP and were followed for recurrence/disease progression. Three of the total 73 specimens were not included in the final analysis because the patients from whom the those specimens were obtained had positive lymph nodes. On all of the patients, a minimum follow-up of 64 months was available. This study was conducted under a protocol approved by the Institutional Review Board of the University of Miami. The progressed group (group 1) of patients ($n = 25$) included those who had biochemical recurrence (PSA >0.4 ng/ml) within 64 months (mean time to recurrence: 21.3 months; range: 3 to 61 months). The nonprogressed group (group 2) included patients ($n = 45$) who were disease free (*i.e.*, no clinical or biochemical recurrence) for a minimum of 64 months (mean follow-up: 80.6 months; range: 64–114 months). The patient characteristics with respect to age, preoperative PSA, and tumor (*i.e.*, Gleason, stage, margin, EPE, seminal vesicle invasion) are shown in Table 1.

IHC. IHC localization of HA and HYAL1 in CaP tissues was carried out as described previously (10). For all specimens, paraffin-embedded blocks containing CaP tissues representing the majority of the Gleason sum were selected by the pathologist (F. C.) of the study. The blocks were cut into 3-μm thick sections and placed on positively charged slides. The specimens were deparaffinized, rehydrated, and treated with an antigen-retrieval solution (Dako Laboratories). For each specimen, two slides were prepared, one for HA and the other for HYAL1 staining. For HA staining, the slides were incubated with 2 μg/ml of a biotinylated bovine nasal cartilage protein at room temperature for 35 min (10). The specificity of HA staining was established as described previously (10). After incubation with the HA-binding protein, the slides were washed in PBS and sequentially incubated with streptavidin peroxidase at room temperature for 30 min and DAB chromogen substrate solution (Dako Laboratories). The slides were counterstained with hematoxylin, dehydrated, and mounted.

For HYAL1 staining, the slides were incubated with 3.7 μg/ml of anti-HYAL1 IgG at 4°C for 16 h. Rabbit polyclonal anti-HYAL1 IgG was generated against a peptide sequence present in the HYAL1 protein (amino acids 321 to 338), and its specificity for IHC was confirmed as described previously (10, 37). After incubation with anti-HYAL1 IgG, the slides were washed in PBS and incubated with a linking solution containing a biotinylated goat antirabbit IgG (Dako LSAB kit; Dako Laboratories) at room temperature for 30 min. The slides were then treated with streptavidin peroxidase and DAB

chromogen. The slides were counterstained with hematoxylin, dehydrated, and mounted.

Slide Grading. Two readers (J. T. P. and V. B. L.) independently evaluated all slides in a blinded fashion. Any discrepancy in assigning staining intensity was resolved by both readers reexamining those slides simultaneously. The staining for HA and HYAL1 was graded as 0 (no staining), 1+, 2+, and 3+. For HA staining, both the tumor-associated stroma and tumor cells were graded separately in each slide for staining intensity. In the case of HA staining, the stromal staining was also evaluated as dense or sparse. The overall staining grade for each slide was assigned based on the staining intensity of the majority of the tumor tissue in the specimen. However, if ~50% of the tumor tissue stained as 1+ and the other 50% as 3+, the overall staining grade was 2+. If the staining distribution was ~50% of the tumor staining 2+ and the remaining staining as 3+, the overall staining inference was assigned as 3+. The staining scale was further subcategorized into low grade and high grade.

For HA staining, low-grade staining included 0, 1+ sparse, and 2+ sparse/dense staining, and high-grade staining included 3+ sparse and 3+ dense staining. In those cases ($n = 2$) where the stromal tissues were evaluated as low-grade staining but the tumor cells stained as 3+, the overall HA staining was considered as high grade. For HYAL1, high-grade staining represented 2+ and 3+ staining, whereas low-grade staining included 0 and 1+ staining intensities. For the combined HA-HYAL1 staining, a positive result was indicated only when both HA (stromal, tumor cells, or both) and HYAL1 staining intensities were of high grade. Any other combination was considered negative.

High-grade staining was considered as a true-positive result and the low-grade staining indicated a false-negative result if the patient had biochemical recurrence. If the patient had no clinical/biochemical recurrence, the low-grade staining indicated a true-negative result, and the high-grade staining was taken as a false-positive result.

Statistical Analysis. The consistency of staining was determined by staining 89% of the specimen for HA and HYAL1 staining twice on two separate occasions. The staining of these specimens was recorded independently. It is noteworthy that the interassay variability regarding staining intensity was determined by Pearson's correlation analysis. The Pearson's correlation coefficient (r) was 0.85 for HA staining and 0.9 for HYAL1 staining. Similarly, ~90% of the slides were recorded independently by each observer to determine consistency in grading. The sensitivity, specificity, accuracy, PPV, and NPV for HA, HYAL1, and HA-HYAL1 staining inferences were calculated using the 2 × 2 contingency table (high-grade/low-grade staining and progressed/nonprogressed CaP patients). The data on various, biochemical, surgical, and pathologic parameters, as well as HA, HYAL1, and HA-HYAL1 staining inferences, were analyzed by univariate logistic regression analysis. The data were also analyzed by a forward stepwise multiple logistic regression analysis beginning with all of the potential predictor variables. Statistical analysis was carried out by the statistician (R. C. D.) of the project using SAS Software Program (version 8.02; SAS Institute, Cary, NC).

Table 1 *Distribution of pre- and postoperative parameters among study patients*

Note that biochemical recurrence with postoperative PSA levels ≥0.4 ng/ml within 64 months was used as a cut point for defining progression. Thus, any CaP patient who showed a biochemical recurrence within 64 months was included in the progressed category. For the progressed group, median time for recurrence was 19 months and mean time for recurrence was 21.3 months. For the nonprogressed group, median follow-up time was 79 months; mean follow-up time was 80.6 months.

	Preoperative parameters			Postoperative parameters			
Progression	Age (yrs)	PSA (ng/ml)	Clinical stage	Gleason sum	EPE	Margin	Seminal vesicle invasion
Biochemical recurrence ($n = 25$)	Median: 64	Median: 9.0	T1 C = 10	6 = 2	(+) = 21	(+) = 18	(+) = 14
	Mean: 65.1	Mean: 14.04	T2 A = 5	7 = 14	(−) = 4	(−) = 7	(−) = 11
	Range: 51–74	Range: 2–62	T2 B = 10	8 = 6			
				9 = 3			
No biochemical or clinical recurrence ($n = 45$)	Median: 65	Median: 6.0	$T_{1C} = 24$	5 = 8	(+) = 6	(+) = 10	(+) = 3
	Mean: 63.5	Mean: 7.9	$T_{2A} = 6$	6 = 9	(−) = 39	(−) = 35	(−) = 42
	Range: 40–75	Range: 0.5–23	$T_{2B} = 15$	7 = 22			
				8 = 6			

RESULTS

HA Localization. HA was localized in 70 archival CaP specimens obtained from patients who underwent radical retropubic prostatectomy for clinically localized disease. These patients were being monitored for disease progression. An increase in PSA of ≥ 0.4 ng/ml was taken as an indicator of biochemical recurrence (either local recurrence or systemic progression). A minimum follow-up of 64 months was available for all patients. HA was localized in CaP tissues using a biotinylated HA binding protein. Shown in Fig. 1 are HA staining in Gleason sum 6 (A and B), 7 (C and D), and 8 (E and F) CaP specimens from nonprogressed (A, C, and E) and progressed (B, D, and F) patients. In all of the CaP specimens, HA was localized mostly in the tumor-associated stroma, although some tumor cells also showed HA staining in CaP specimens from patients who progressed (Fig. 1, B and F).

As shown in Fig. 1 A, C, and E, the CaP specimens from nonprogressed patients had low-grade HA staining, regardless of the Gleason sum. Of the 45 patients free of recurrence, 26 had low-grade HA staining. However, the CaP specimens from the patients who progressed in <64 months (median time to recurrence: 19 months; mean time to recurrence: 21.3 months) showed high-grade HA staining (Fig. 1, B, D, and F). Of the 25 CaP specimens from progressed patients, 22 showed high-grade staining in tumor stroma; 8 of these 22 also showed high-grade HA staining in tumor cells. In addition, 2 of the 25 CaP specimens showed high-grade staining only in tumor cells. Shown in Fig. 2 is an example of tumor cells that are positive for high-grade HA staining. Tumors cells appear to stain for HA equally, both in the cytoplasm and plasma membrane (Fig. 2B, *magnified*

view). Thus, of the 25 CaP specimens from progressed patients, 24 showed high-grade HA staining either in tumor stroma or tumor cells or both. Thus, high-grade HA staining (stroma, tumor cells, or both) had 96% sensitivity, 55.5% specificity, 70% accuracy, 54.5% PPV, and 96.2% NPV for predicting the biochemical recurrence (Table 2).

HYAL1 Localization. An anti-HYAL1 peptide IgG was used to localize HYAL1 in the archival CaP specimens. Shown in Fig. 3 are HYAL1 localization in Gleason 6 (A and B), 7 (C and D), and 8 (E and F) CaP tissues from patients who did not (A, C, and E) and who did (B, D, and F) progress. As shown in Fig. 3, low-grade HYAL1 staining was seen in all three CaP specimens from patients who did not progress, regardless of their Gleason sum (Fig. 3, A–E). Among the 45 nonprogressed patients, CaP specimens of 36 patients showed low-grade HYAL1 staining. In CaP specimens from progressed patients, tumor cells, and not tumor-stroma, stained for HYAL1. All three CaP specimens from progressed patients showed high-grade HYAL1 staining (Fig. 3, B, D, and F), regardless of their Gleason sum. Of the 25 progressed patients, CaP specimens from 21 patients showed high-grade HYAL1 staining. Thus, in this cohort of 70 patients, the HYAL1 localization in CaP specimens had 84% sensitivity, 82.2% specificity, 82.9% accuracy, 70% PPV, and 90.2% NPV for predicting biochemical recurrence within 64 months (Table 2).

Combined HA-HYAL1 Staining. We next determined the ability of combined high-grade HA and HYAL1 staining to predict biochemical recurrence. The combined HA-HYAL1 staining has 84% sensitivity, 86.7% specificity, 85.7% accuracy, 77.8% PPV, and 90.7% NPV for predicting progression. When 64 months was used as a cutoff limit to evaluate progression, there were seven false-positive cases,

Fig. 1. HA staining of CaP specimens from nonprogressed and progressed patients. HA was localized in CaP tissues using a biotinylated HA-binding protein and a streptavidin peroxidase DAB-chromogen detection system. A, C, and E, HA staining in specimens from nonprogressed patients. B, D, and F, HA staining in specimens from progressed patients. A and B, Gleason 6 CaP; C and D: Gleason 7 CaP; E and F, Gleason 8 CaP. Each *panel* represents ×400 magnification.

Fig. 2. A Gleason 8 CaP specimen with tumor cells showing HA staining. Gleason 8 specimen from a progressed patient where tumor cells show high-grade HA staining. *A*, ×100 magnification; *B*, ×400 magnification.
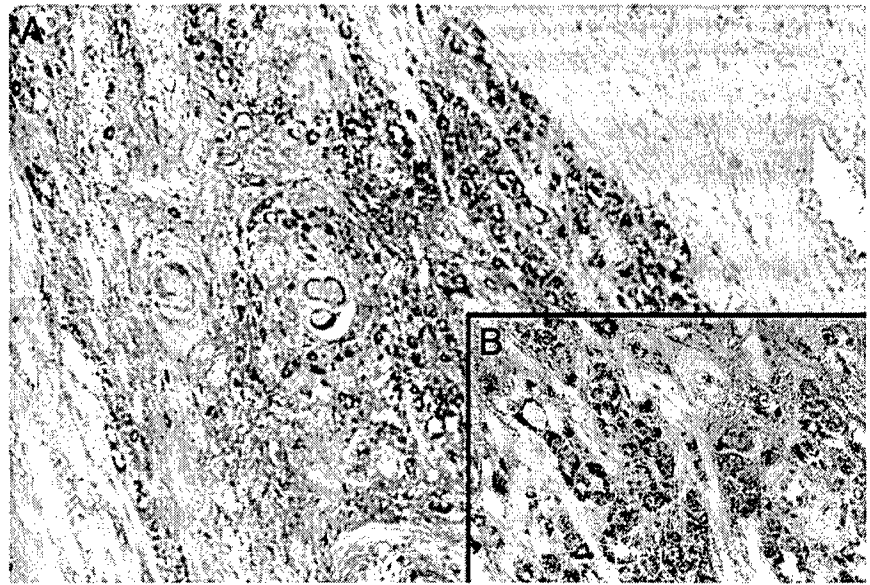
i.e., the specimens showed high-grade HA and HYAL1 staining, but the patients had no disease recurrence within 64 months. However, among these seven false-positive cases, two had a biochemical recurrence at 70 months (Table 2).

Evaluation of the Prognostic Capabilities of Preoperative, Postoperative Parameters, and HA and HYAL1 Staining Inferences: Univariate Analysis

We performed a univariate logistic regression analysis to determine the prognostic significance of preoperative parameters (*i.e.,* age, PSA, and clinical stage), postoperative surgical and pathologic parameters (*i.e.,* Gleason sum, margin +/−, EPE, seminal vesicle invasion +/−), as well as inferences of HA, HYAL1, and combined HA-HYAL1 staining. As shown in Table 3, both age ($P = 0.297$; OR = 1.041) and stage ($P = 0.287$; OR = 1.714) were not significant in predicting biochemical recurrence in the univariate analysis. However, preoperative PSA ($P = 0.0174$; OR = 1.10), Gleason sum ($P = 0.0023$; OR = 3.062), positive margin ($P = 0.0001$; OR = 9.0), EPE ($P < 0.0001$; OR = 34.125), seminal vesicle invasion ($P < 0.0001$; OR = 17.818), HA staining ($P = 0.0014$, OR = 30), HYAL1 staining ($P < 0.0001$; OR = 24.28), and combined HA-HYAL1 staining ($P < 0.0001$; OR = 34.125) were found to be significant in predicting biochemical recurrence. Patients with a Gleason sum ≥7 have been shown to have a greater risk of progression (41). In the univariate analysis, patients with a Gleason sum ≥7 had 2.3-fold greater odds of developing biochemical recurrence ($P = 0.015$; OR = 6.982) than when CaP tissues of all Gleason sums were analyzed together (Table 3).

Table 2 *Sensitivity, specificity, accuracy, PPV, and NPV of HA, HYAL1 and combined HA-HYAL1 staining inferences for predicting biochemical recurrence in CaP patients*

Note that 64 month follow-up was used a cut point for determining biochemical recurrence. Please note that 2 of the CaP patients who had a biochemical recurrence at 70 months and showed high-grade HA, HYAL1, and combined HA-HYAL1 staining were considered false positives and were included in the specificity calculation.

Parameters	HA	HYAL1	HA-HYAL1
Sensitivity	96% (*n* = 24/25)	84% (*n* = 21/25)	84% (*n* = 21/25)
Specificity	55.5% (*n* = 25/45)	82.2% (*n* = 37/45)	86.7% (*n* = 39/45)
Accuracy	70% (*n* = 49/70)	82.9% (*n* = 58/70)	85.7% (*n* = 60/70)
PPV	54.5% (*n* = 24/44)	70% (*n* = 21/30)	77.8% (*n* = 21/27)
NPV	96.2% (*n* = 25/26)	90.2% (*n* = 37/41)	90.7% (*n* = 39/43)

Evaluation of the Prognostic Capabilities of Preoperative, Postoperative Parameters, and HA and HYAL1 Staining Inferences: Forward Stepwise Multiple Logistic Regression Analysis.

To determine the smallest number of variables that could jointly predict biochemical recurrence in this cohort of study patients, we performed the forward stepwise multiple logistic regression analysis. Initially, when age, preoperative PSA, clinical stage, Gleason sum, EPE, seminal vesicle invasion, HA staining, and HYAL1 staining were included in the model, only EPE ($P = 0.0023$; OR = 33.483), positive margin ($P = 0.0059$; OR = 26.948), and HYAL1 staining ($P = 0.0094$; OR = 12.423) reached statistical significance in predicting biochemical recurrence (Table 4*A*). Gleason sum did not reach statistical significance in the multiple logistic regression analysis even after the patients were stratified according to Gleason ≥7 and <7 (data not shown).

The inclusion of the combined HA-HYAL1 staining inference instead of the individual HA and HYAL1 staining inferences, in the multiple regression model, again showed that EPE ($P = 0.0023$; OR = 35.944), margin ($P = 0.0086$; OR = 24.438), and HA-HYAL1 staining ($P = 0.0033$; OR = 18.047) were significant in predicting biochemical recurrence (Table 4*B*). None of the other routine prognostic parameters [*i.e.,* age, PSA, clinical stage, Gleason sum (or Gleason stratification as Gleason ≥7 and <7 and seminal vesicle invasion) that were included in the model reached statistical significance (*i.e.,* $P > 0.05$ in each case)].

DISCUSSION

In this study, we demonstrate for the first time that HYAL1 and combined HA-HYAL1 staining inferences provide independent prognostic information for predicting CaP recurrence/progression over and above the prognostic information provided by the standard pre- and postoperative parameters. Radical prostatectomy for organ-confined disease is performed with the idea of disease cure (42, 43). However, disease relapses in a high percentage of cases despite careful selection of patients for surgery based on individual preoperative parameters or their combination in algorithms and nomograms (6). Certain genes and their products that associate with CaP growth and metastasis have shown a potential in predicting biochemical recurrence after surgery (8, 44). Because both HA and HYAL1 are likely to be involved in
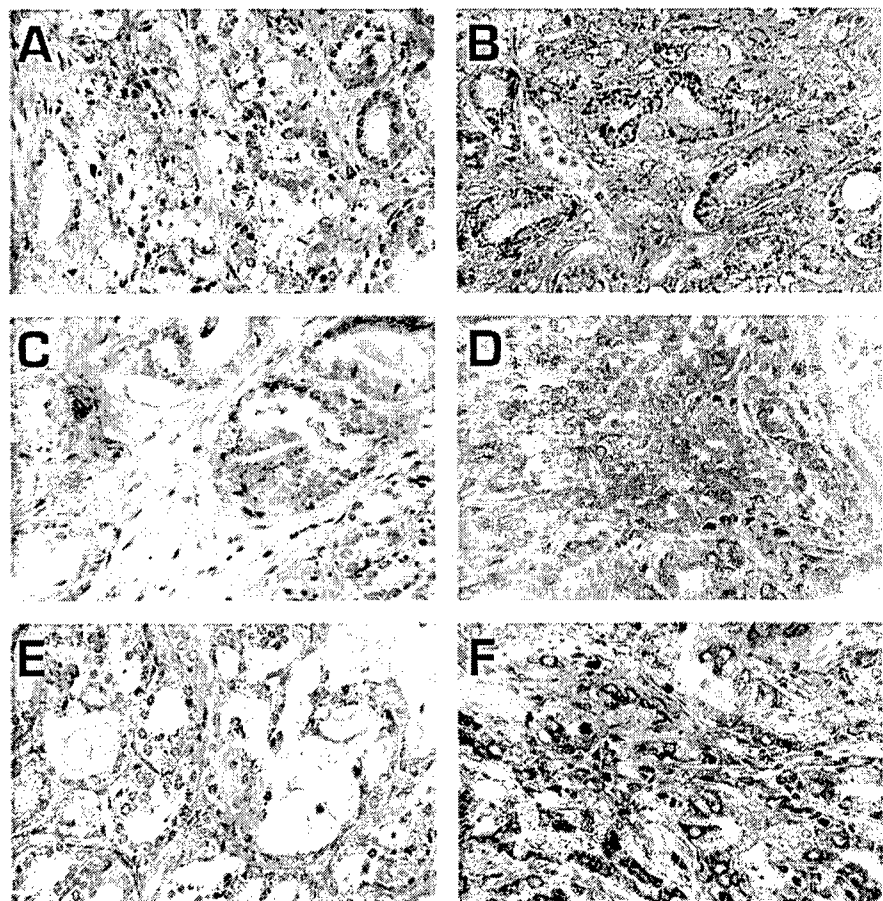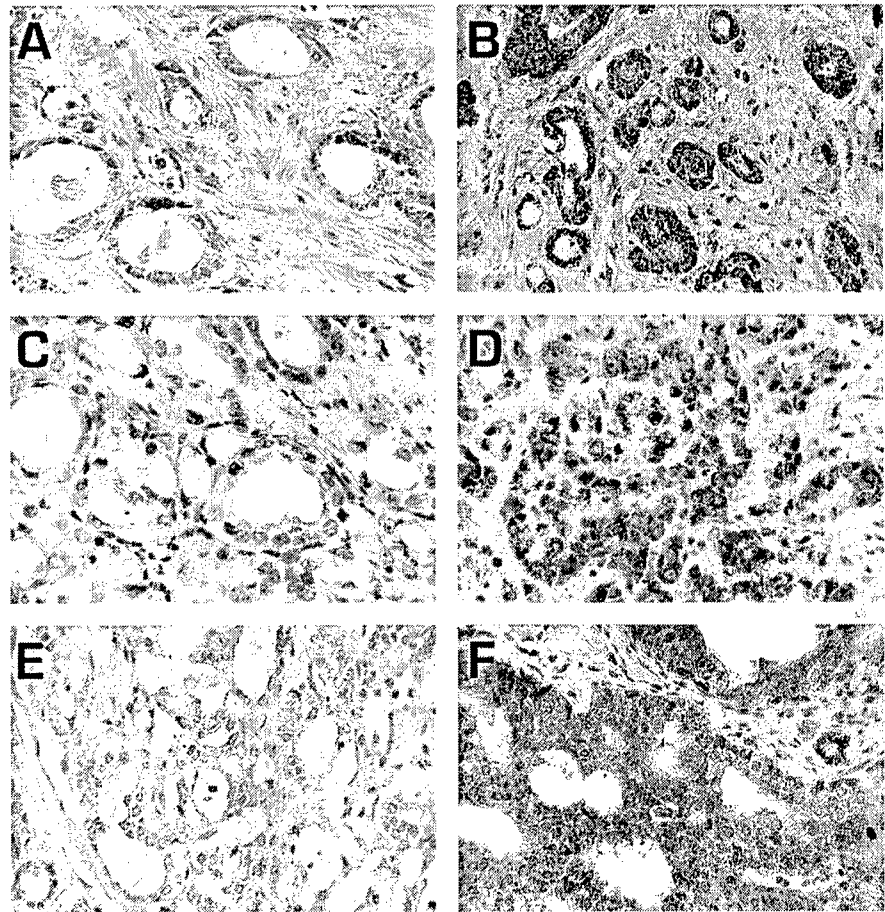
Fig. 3. HYAL1 staining of CaP specimens from nonprogressed and progressed patients. HYAL1 was localized in CaP tissues using an anti-HYAL1 antibody and a streptavidin peroxidase DAB-chromogen detection system. *A, C,* and *E,* HYAL1 staining in specimens from nonprogressed patients. *B, D,* and *F,* HYAL1 staining in specimens from progressed patients. *A* and *B,* Gleason 6 CaP; *C* and *D,* Gleason 7 CaP; *E* and *F,* Gleason 8 CaP. Each *panel* represents ×400 magnification.

tumor metastasis and angiogenesis (3, 45–49), it is not surprising that we found HA, HYAL1, and combined HA-HYAL1 staining inferences to have prognostic significance in predicting biochemical recurrence. In this study, we focused on CaP patients with clinically localized disease because such patients pose a dilemma for clinicians in terms of whether the cancer will metastasize; does the patient need additional treatment after surgery and what is the prognosis of the patient? Thus, in this patient population, accurate prognostic indicators will have clinical applicability. Nonetheless, although we eliminated from this study three CaP specimens from patients who had positive lymph nodes, all showed high-grade HA and HYAL1 staining, suggesting again that these molecules are associated with CaP progression.

In this study, HA staining in CaP tissues had high sensitivity

(96%) but low specificity (55.5%) in predicting biochemical recurrence. Consequently, although in the univariate analysis, HA staining showed prognostic significance (Table 3), in the forward stepwise multiple logistic regression analysis, it had no additional prognostic significance when standard biochemical, surgical, and pathologic parameters, as well as HYAL1 staining, were included in the model (Table 4). Consistent with this observation, Lipponen *et al.* (22) reported previously that HA expression in tumor-stroma of CaP specimens has no additional prognostic significance over the standard prognostic indicators (*i.e.,* Gleason sum, stage, and node status). The combination of HA with HYAL1 did increase the specificity, accuracy, and PPV of the combination when compared with that of HYAL1 or HA alone (Table 2). Similarly, the OR of the HA-HYAL1 combination (18.047) was slightly better than that of HYAL1 (12.423) alone. Thus, based on our study and that by Lipponen *et al.* (22), HA staining of CaP tissues generally has low specificity and is probably not of clinical significance.

Lipponen *et al.* (22) also reported that 39% of the CaP specimens expressed HA in tumor cells in addition to the expression in tumor-stroma. However, the presence of HA in tumor cells did not have independent prognostic significance. In our study, although we found 40% of the CaP specimens from progressed patients showed high-grade HA staining in tumor cells, it did not have any independent prognostic significance. In contrast to these observations, in gastrointestinal, colon, and breast cancers, HA expression in tumor cells correlates with poor survival (17, 18, 21). Thus, although HA expression is elevated in many types of cancers, the clinical significance of

Table 3 *Univariate analysis of pre- and postoperative prognostic parameters and HA, HYAL1, and combined HA-HYAL1 staining inferences*

Parameter	χ^2	P value	OR	95% CI[a]
Age	1.088	0.297	1.041	0.965–1.122
PSA	5.652	0.0174[b]	1.1	1.017–1.192
Clinical stage	0.539	0.287	1.741	0.636–4.621
Gleason sum (Overall)	9.266	0.0023[b]	3.062	1.49–6.294
Gleason sum ≥7	5.919	0.015[b]	6.982	1.459–33.411
Margin	14.764	0.0001[b]	9.0	2.934–27.603
EPE	25.435	<0.0001[b]	34.125	8.655–134.545
Seminal vesicle invasion	15.969	<0.0001[b]	17.818	4.339–73.175
HA	10.222	0.0014[b]	30.0	3.729–241.337
HYAL1	22.627	<0.0001[b]	24.281	6.524–90.375
HA-HYAL1	25.435	<0.0001[b]	34.125	8.655–134.545

[a] CI, confidence interval.
[b] Statistically significant.

Table 4 *Forward stepwise multiple logistic regression analysis of pre- and postoperative prognostic parameters and HA, HYAL1, and combined HA-HYAL1 staining inferences*

The significant parameters ($P < 0.05$) selected by the model are shown. *A*, in the analysis, HA and HYAL1 staining inferences were included separately, along with other pre- (*i.e.*, age, PSA, and clinical stage) and post- [*i.e.*, Gleason sum (or stratified Gleason as ≥ 7 and <7), EPE, margin $+/-$, and seminal vesicle invasion] surgery parameters. *B*, combined HA-HYAL1 staining inference was included in the analysis, together with the above-mentioned pre- and postoperative parameters.

Parameter	A				B			
	χ^2	P value	OR	95% CI[a]	χ^2	P value	OR	95% CI
EPE	15.20	0.0023[b]	33.483	3.493–320.912	9.271	0.0023[b]	35.944	3.583–360.565
Margin	7.573	0.0059[b]	26.948	2.58–281.463	6.895	0.0086[b]	24.438	2.249–265.55
HYAL1	6.846	0.0094[b]	12.423	1.856–83.158	NA	NA	NA	NA
HA-HYAL1	NA	NA	NA	NA	8.628	0.0033[b]	18.047	2.619–124.378

[a] CI, confidence interval; NA, not applicable.
[b] Statistically significant.

this expression, in terms of predicting prognosis, varies with the tissue of origin of each cancer.

We have shown that HAase levels, measured using an ELISA-like assay, correlate with CaP progression and serve as accurate urine markers for detecting intermediate- and high-grade bladder cancer (11, 50). HYAL1 is expressed in invasive CaP and bladder cancer cells (11, 36, 37). The present study is the first to demonstrate the prognostic significance of HYAL1 expression in cancer. In this study, HYAL1 staining in CaP specimens had high sensitivity (84%), specificity (82.2%), and accuracy (82.9%) in predicting biochemical recurrence after radical prostatectomy. Among all of the pre- and postoperative prognostic parameters included in the forward stepwise multiple logistic regression analysis, only EPE and margin had additional prognostic significance if HYAL1 is included in the model (Table 4).

In contrast with our observation that HYAL1 expression correlates with biochemical in CaP, Hiltunen *et al.* (51) have shown that in malignant epithelial ovarian tumors, the concentration of HA and not HAase is elevated. These observations suggest that the clinical significance of HA and HYAL1 expression may be different in tumors of different tissue origins. This notion is corroborated by the observations that although HA expression correlates with malignant tumor progression in gastric, breast, and colorectal cancers (17, 18, 21), HA expression has no prognostic significance in CaP (results from this study and Ref. 22). In bladder cancer, the HYAL1 expression correlates with tumor grade, *i.e.*, high-grade tumors, which have a propensity to invade and metastasize express high levels of HYAL1 (16, 23). The differences in the clinical significance of HA and HAase expression in tumors of different origins is further supported by the observations that although HYAL1 expression in a transplantable rat colon carcinoma cell tumor suppresses tumor growth, the overexpression of HYAL1 induces metastasis in a human xenograft model involving PC3-M CaP cells (52, 53). Taken together, HYAL1 is a tumor cell-derived HAase, the expression of which associates with cancer progression.

In this study, all of the patients had a minimum follow-up of 64 months and a median follow-up of 79 months in the nonprogressed group. A follow-up duration of >5 years was long enough if any of the CaP patients placed in the nonprogressed category were to have a biochemical recurrence. Therefore, based on this first report, with sufficiently long follow-up, HYAL1 expression merits further investigation and HA expression is of limited clinical value in predicting biochemical recurrence after radical prostatectomy. Most CaP patients with clinically localized disease have preoperative PSA values between 4 and 10 ng/ml, stage T_{1C} disease, and a biopsy Gleason sum between 5 and 7 (8). Such similarity limits the prognostic capability of these preoperative parameters. Further studies on HYAL1 and HA-HYAL1 staining in biopsy specimens should reveal whether these markers could improve our ability to predict prognosis for patients who choose a curative approach involving radical prostatectomy.

REFERENCES

1. Etzioni, R., Penson, D. F., Legler, J. M., di Tommaso, D., Boer, R., Gann, P. H., and Feuer, E. J. Overdiagnosis due to prostate-specific antigen screening: lessons from U.S. prostate cancer incidence trends. J. Natl. Cancer Inst., *94:* 981–990, 2002.
2. Yao, S. L., and Lu-Yao, G. Understanding and appreciating overdiagnosis in the PSA era. J. Natl. Cancer Inst., *94:* 958–960, 2002.
3. Muzzonigro, G., and Galosi, A. B. Biological selection criteria for radical prostatectomy. Ann. NY Acad. Sci., *963:* 204–212, 2002.
4. Small, E. J., and Roach M., III. Prostate-specific antigen in prostate cancer: a case study in the development of a tumor marker to monitor recurrence and assess response. Semin. Oncol., *29:* 264–273, 2002.
5. Palisaan, R. J., Graefen, M., Karakiewicz, P. I., Hammerer, P. G., Huland, E., Haese, A., Fernandez, S., Erbersdobler, A., Henke, R. P., and Huland, H. Assessment of clinical and pathologic characteristics predisposing to disease recurrence following radical prostatectomy in men with pathologically organ-confined prostate cancer. Eur. Urol., *41:* 155–161, 2002.
6. Waltregny, D., de Leval, L., Coppens, L., Youssef, E., de Leval, J., and Csatronovo, V. Detection of the 67-kD laminin receptor in prostate cancer biopsies as a predictor of recurrence after radical prostatectomy. Eur. Urol., *40:* 495–503, 2002.
7. Pound, C. R., Partin, A. W., Epstein, J. I., and Walsh, P. C. Prostate-specific antigen after anatomic radical retropubic prostatectomy. Patterns of recurrence and cancer control. Urol. Clin. North Am., *24:* 395–406, 1997.
8. Pettaway, C. A. Prognostic markers in clinically localized prostate cancer. Tech. Urol., *4:* 35–42, 1998.
9. Blute, M. L. Bergstralh, E. J., Iocca, A., Scherer, B., and Zincke, H. Use of Gleason score, prostate specific antigen seminal vesicle and margin status to predict biochemical failure after radical prostatectomy. J. Urol., *165:* 119–125, 2001.
10. Lokeshwar, V. B., Rubinowicz, D., Schroeder, G. L., Forgacs, E., Minna, J. D., Block, N. L. Nadji. M., and Lokeshwar, B. L. Stromal and epithelial expression of tumor markers hyaluronic acid and hyaluronidase in prostate cancer. J. Biol. Chem., *276:* 11922–11932, 2001.
11. Lokeshwar, V. B., Lokeshwar, B. L., Pham, H. T., and Block, N. L. Association of hyaluronidase, a matrix-degrading enzyme, with prostate cancer progression. Cancer Res., *56:* 651–657, 1996.
12. Tammi, M. I., Day, A. J., and Turley, E. A. Hyaluronan and homeostasis: a balancing act. J. Biol. Chem., *277:* 4581–4584, 2002.
13. Tool, B. P. Hyaluronan is not just a goo! J. Clin. Investig., *106:* 335–336, 2000.
14. Delpech, B., Girard, N., Bertrand, P., Courel, N. M., Chauzy, C., and Delpech, A. Hyaluronan: fundamental principles and applications in cancer. J. Intern. Med., *242:* 41–48, 1997.
15. Turley EA, Noble PW, and Bourguignon LY. Signaling properties of hyaluronan receptors. J. Biol. Chem., *277:* 4589–4592, 2002.
16. Hautman, S. H., Lokeshwar, V. B., Schroeder, G. L., Civantos, F., Duncan, R. C., Friedrich, M. G., and Soloway, M. S. Elevated tissue expression of hyaluronic acid and hyaluronidase validate HA-HAase urine test for bladder cancer. J. Urol., *165:* 2068–2074, 2000.
17. Setala, L. P., Tammi, M. I., Tammi, R. H., Eskelin, M. J., Lipponen, P. R., Argen, U. M., Parkkinen, J., Alhava, E. M., and Kosma, V. M. Hyaluronan expression in gastric cancer cells is associated with local and nodal spread and reduced survival rate. Br. J. Cancer, *79:* 1133–1138, 1999.
18. Auvinen, P., Tammi, R., Parkkinen, J., Tammi, M., Agren, U., Johansson, R., Hirvikoski, P., Eskelinen, M., and Kosma, V. M. Hyaluronan in peritumoral stroma and malignant cells associates with breast cancer spreading and predicts survival. Am. J. Pathol., *156:* 529–536, 2000.
19. Pirinen, R., Tammi, R., Tammi, M., Hirvikoski, P., Parkkinen, J. J., and Johansson, R. Prognostic value of hyaluronan expression in non-small-lung cancer: increased stromal expression indicates unfavorable outcome in patients with adenocarcinoma. Int. J. Cancer, *95:* 12–27, 2001.
20. Knudson, W. Tumor associated hyaluronan: providing an extracellular matrix that facilitates invasion. Am. J. Pathol., *148:* 1721–1726, 1996.

21. Ropponen, K., Tammi, M., Parkkinen, J., Eskelinen, M., Tammi, R., Lipponen, P., Argen, V., Alhava, E., and Kosma, V. M. Tumor-associated hyaluronan as an unfavorable prognostic factor in colorectal cancer. Cancer Res., 58: 342–347, 1998.

22. Lipponen, P., Aaltomaa, S., Tammi, R., Tammi, M., Agren, U., and Kosma, V. M. High stromal hyaluronan level is associated with poor differentiation and metastasis in prostate cancer. Eur. J. Cancer, 37: 849–856, 2001.

23. Lokeshwar, V. B., Obek, C., Pham, H. T., Wei, D. C., Young, M. J., Duncan, R. C., Soloway. M. S., and Block, N. L. Urinary hyaluronic acid and hyaluronidase: markers for bladder cancer detection and evaluation of grade. J. Urol., 163: 348–356, 2000.

24. Lokeshwar, V. B., Obek, C., Soloway, M. S., and Block, N. L. Tumor-associated hyaluronic acid: a new sensitive and specific urine marker for bladder cancer. Cancer Res., 57: 773–777, 1997.

25. Liu, N., Lapcevich, R. K., Underhill, C. B., Han, Z., Gao, F., Swartz, G., Plum, S. M., Zhang, L., and Gree, S. J. Metastatin: a hyaluronan-binding complex from cartilage that inhibits tumor growth. Cancer Res., 61: 1022–1028, 2001.

26. Hayen, W., Goebeler, M., Kumar, S., Riessen, R., and Nehls, V. Hyaluronan stimulates tumor cell migration by modulating the fibrin fiber architecture. J. Cell Sci., 112: 2241–2251, 1999.

27. Hoborth, K., Maier, U., and Marberger, M. Topical chemoprophylaxis of superficial bladder cancer by mitomycin C and adjuvant hyaluronidase. Eur. Urol., 21: 206–210, 1992.

28. Itano, N., Atsumi, F., Sawai, T., Yamada, Y., Miyaishi, O., Senga, T., Hamguchi, M., and Kimata, K. Abnormal accumulation of hyaluronan matrix diminishes contact inhibition of cell growth and promotes cell migration. Proc. Natl. Acad. Sci. USA, 99: 3609–3614, 2002.

29. Roden, L., Campbell, P., Fraser, J. R. E., Laurent, T. C., Petroff, H., and Thompson, J. N. Enzymatic pathways of hyaluronan catabolism. In: E. Whelan (ed.), The Biology of Hyaluronan. Ciba Foundation Symp. No. 143, pp. 60–86. Chichester, New York: Wiley, 1989.

30. Jedrzejas, M. J. Structural and functional comparison of polysaccharide-degrading enzymes. Crit. Rev. Biochem. Mol. Biol., 35: 221–251, 2000.

31. West, D. C., Hampson, I. N., Arnold, F., and Kumar, S. Angiogenesis induced by degradation products of hyaluronic acid. Science (Wash. DC), 228: 1324–1326, 1985.

32. Lokeshwar, V. B., and Selzer, M. G. Differences in hyaluronic acid-mediated functions and signaling in arterial, microvessel, and vein-derived human endothelial cells. J. Biol. Chem., 275: 27641–27649, 2000.

33. Csoka, A. B., Frost, G. I., and Stern, R. The six hyaluronidase-like genes in the human and mouse genomes. Matrix Biol., 20: 499–508, 2001.

34. Lepperdinger, G., Mullegger, J., and Kreil, G. Hyal2–less active, but more versatile? Matrix Biol., 20: 509–514, 2001.

35. Cherr, G. N., Yudin, A. I., and Overstreet, J. W. The dual functions of GPI-anchored PH-20: hyaluronidase and intracellular signaling. Matrix Biol., 20: 515–525, 2001.

36. Lokeshwar, V. B., Soloway, M. S., and Block, N. L. Secretion of bladder tumor-derived hyaluronidase activity by invasive bladder cancer cells. Cancer Lett., 131: 21–27, 1998.

37. Lokeshwar, V. B., Young, M. J., Goudarzi, G., Iida, N., Yudin, A. I., Cherr, G. N., and Selzer, M. G. Identification of bladder tumor-derived hyaluronidase: its similarity to HYAL1. Cancer Res., 59: 4464–4470, 1999.

38. Godin, D. A., Fitzpatrick, P. C., Scandurro, A. B., Belafsky, P. C., Woodworth, B. A., Amedee, R. G., Beech, D. J., and Beckman, B. S. PH20: a novel tumor marker for laryngeal cancer. Arch. Otolaryngol. Head Neck Surg., 126: 402–404, 2000.

39. Beech, D. J., Madan, A. K., and Deng, N. Expression of PH-20 in normal and neoplastic breast tissue. J. Surg. Res., 103: 203–207, 2002.

40. Lokeshwar, V. B., Schroeder, G. L., Carey, R. I. Soloway, M. S., and Iida, N. Regulation of hyaluronidase activity by alternative mRNA splicing. J. Biol. Chem., 277: 33654–33663, 2002.

41. Sweat, S. D., Bergstralh, E. J., Slezak, J., Blute, M. L., and Zincke, H. Competing risk analysis after radical prostatectomy for clinically nonmetastatic prostate adenocarcinoma according to clinical Gleason score and patient age. J. Urol., 168: 525–529, 2002.

42. Fradet, Y. Role of radical prostatectomy in high-risk prostate cancer. Can. J. Urol., 9: 8–13, 2002.

43. Klein, E. A., and Kupelian, P. A. Localized prostate cancer. Curr. Treat. Options Oncol., 1: 433–445, 2000.

44. Isaacs, J., De Marzo, A., and Nelson, W. Focus on prostate cancer. Cancer Cell, 2: 113–116, 2002.

45. Feroze-Merzoug, F., Schober, M. S., and Chen, Y. Q. Molecular profiling in prostate cancer. Cancer Metastasis Rev., 20: 165–171, 2001.

46. Claudio, P. P., Zamparelli, A., Garcia, F. U., Claudio, L., Ammirati, G., Farina, A., Bovicelli, A., Russo, G., Giordano, G. G., McGinnis, D. E., Giordano, A., and Cardi, G. Expression of cell-cycle-regulated proteins pRb2/p130, p107, p27(kip1), p53, mdm-2, and Ki-67 (MIB-1) in prostatic gland adenocarcinoma. Clin. Cancer Res., 8: 1808–1815, 2002.

47. Asmann, Y. W., Kosari, F., Wang, K., Cheville, J. C., and Vasmatzis, G. Identification of differentially expressed genes in normal and malignant prostate by electronic profiling of expressed sequence tags. Cancer Res., 62: 3308–3314, 2002.

48. Vis, A. N., van Rhijn, B. W., Noordzij, M. A., Schroder, F. H., and van der Kwast, T. H. Value of tissue markers p27(kip1), MIB-1, and CD44s for the pre-operative prediction of tumour features in screen-detected prostate cancer. J. Pathol., 197: 148–154, 2002.

49. Ross, J. S., Sheehan, C. E., Fisher, H. A., Kauffman, R. A., Dolen, E. M., and Kallakury, B. V. Prognostic markers in prostate cancer. Expert. Rev. Mol. Diagn., 2: 129–142, 2002.

50. Pham, H. T., Block, N. L., and Lokeshwar, V. B. Tumor derived hyaluronidase: a diagnostic urine marker for high-grade bladder cancer. Cancer Res., 57: 778–783, 1997.

51. Hiltunen, E. L., Anttila, M., Kultti, A., Ropponen, K., Penttinen, J., Yliskoski, M., Kuronen, A. T., Juhola, M., Tammi, R., Tammi, M., and Kosma, V. M. Elevated hyaluronan concentration without hyaluronidase activation in malignant epithelial ovarian tumors. Cancer Res., 62: 6410–6413, 2002.

52. Jacobson, A., Rahmanian, M., Rubin, K., and Heldin, P. Expression of hyaluronan synthase 2 or hyaluronidase 1 differentially affect the growth rate of transplantable colon carcinoma cell tumors. Int. J. Cancer, 102: 212–219, 2002.

53. Patel, S., Turner, P. R., Stubberfield, C., Barry, E., Rohlff, C. R., Stamps, A., McKenzie, E., Young, K., Tyson, K., Terrett, J., Box, G., Eccles, S., and Page, M. J. Hyaluronidase gene profiling and role of hyal-1 overexpression in an orthotopic model of prostate cancer. Int. J Cancer, 97: 416–424, 2002.

ORIGINAL ARTICLE

Devendra S. Dandekar · Vinata B. Lokeshwar
Edwin Cevallos-Arellano · Mark S. Soloway
Balakrishna L. Lokeshwar

An orally active Amazonian plant extract (BIRM) inhibits prostate cancer growth and metastasis

Abstract *Purpose*: Poor efficacy of conventional chemotherapeutic drugs against metastatic hormone-refractory prostate cancer (CaP) drives patients to try "alternative medicine". The antitumor activity of one such agent, "BIRM" (biological immune response modulator; "Simple Ecuadorian Oral Solution: an extract of an Amazonian plant"), was characterized in vitro and in vivo using established CaP cell lines and a tumor model. *Methods*: The cytotoxicity of BIRM in four human and one rat CaP cell line was evaluated using cell proliferation-inhibition and clonogenic survival assays. BIRM-induced apoptosis, alterations in cell cycle phase progression and inhibition of the extracellular matrix-degrading enzyme hyaluronidase were also investigated in these cells. The in vivo efficacy of BIRM was evaluated in rats with subcutaneous tumor implants of Dunning EGFP-MAT LyLu cells. The active species in BIRM were characterized by gel filtration chromatography. *Results*: BIRM inhibited cell proliferation and clonogenic growth of the CaP cells (IC_{50} about 8.0 µl/ ml). It increased cell accumulation in the G_0/G_1 phase by 33.8% and decreased the proportion of cells in S phase by 54.6%. Apoptotic cell death in BIRM-treated cells was associated with activation of cell death-associated caspases. BIRM inhibited the activity of hyaluronidase, a hyaluronic acid-degrading enzyme, at 1 µl/ml. Treatment of MAT LyLu tumor-bearing rats with BIRM by oral gavage resulted in a significant decrease in tumor incidence (50%), tumor growth rate (18.6 ± 1.3 days for 1 cc tumor growth in control rats and 25.7 ± 2.6 days in BIRM-treated rats), and only one out of six BIRM-treated rats versus four out of six in the control group developed lung metastasis. Three active ingredients in BIRM with a relative molecular mass (Mr) of ≥ 3500 were identified by ultracentrifugation and gel filtration chromatography and were found to be resistant to proteinase and heat (100°C). *Conclusion*: The plant extract BIRM contains antitumor compounds of Mr ≥ 3500 with potent antiproliferative activity in vitro and in vivo against prostate cancer cells.

Abbreviations *CaP* Prostate cancer/cancer of the prostate · *EGFP* Enhanced green fluorescence protein · *HA* Hyaluronic acid · *HAase* Hyaluronidase · *MTT* Methyl thiozolyl tetrazolium bromide [(3-[4,5-demethylthiozol-2-y]-2,5-diphenyl tetrazolium bromide]

D. S. Dandekar · V. B. Lokeshwar · M. S. Soloway
B. L. Lokeshwar (✉)
Department of Urology,
McKnight Vision Research Building,
University of Miami School of Medicine,
Miami, Florida, 33101, USA
E-mail: BLOKESHW@med.miami.edu
Tel.: +1-305-2431012
Fax: +1-305-2436893

D. S. Dandekar · V. B. Lokeshwar · M. S. Soloway
B. L. Lokeshwar
Sylvester Comprehensive Cancer Center,
University of Miami School of Medicine,
Miami, Florida, 33101, USA

E. Cevallos-Arellano
Instituto de Tumores, Quito, Ecuador

Introduction

Cancer of the prostate (CaP) is the most frequently diagnosed malignant cancer in American men with an estimated 189,000 new cases in 2002 [13]. The majority of CaP-related deaths, estimated to be 30,200 in 2002, are likely the result of failure of all currently available conventional treatments. Besides undergoing conventional therapy, CaP patients often seek treatment by unproven therapeutic approaches [12]. It is estimated that 30–40%

of men with CaP experiment with one or more complementary therapies which include high-dose vitamins and minerals, herbal preparations and supplements of soy, saw palmetto etc. [14]. Moreover, there is a dramatic increase in the number of patients moving towards complementary and alternative medicine and consuming plant extracts from "folklore medicine" [26]. We have come across one such natural herbal medicine "BIRM" (biological immune response modulator; "Simple Ecuadorian Oral Solution: an extract of an Amazonian plant") formulated by a physician (E.C.-A.), promoted in South America, and based on the local folklore of the Ecuadorian native population. The formulation is dispensed as a natural remedy for a variety of maladies including HIV-1 infection and cancer [1, 3, 4]. Very little systematic information is currently available on BIRM, and no studies have been undertaken to investigate the structure-function correlations in the ingredients of BIRM. Therefore, we decided to evaluate the efficacy and antiproliferative effects of BIRM in a CaP model.

Materials and methods

Test compound

BIRM was a gift from BIRM Inc. (Quito, Ecuador). BIRM is an aqueous extract of dried roots of a plant of the genus *Dulcamara* (family Solanaceae) grown in Ecuador, and marketed as a greenish-brown suspension with a mild bittersweet smell. The inactive ingredients in BIRM comprise 16% solid particles, likely root fibers, and the remainder, a lipid-free liquid. BIRM is prepared by aqueous extraction of dried roots followed by oxidation/reduction of the extract. During this process, the amount of roots and the timing of oxidation/reduction are carefully controlled to minimize batch-to-batch variation. Prior to initiation of this project, the efficacy of BIRM samples from five different batches were selected randomly and tested in two different cell lines (PC-3ML and LNCaP) by the MTT assay to determine the degree of interbatch variation. We found no interbatch variation in the potency of BIRM for induction of cytotoxicity. In the present study, BIRM samples from lot number 011-2000 were used. For all the studies reported here, BIRM clarified by centrifugation at 10,000 g was used.

Cells and tumor lines

Established human CaP cell lines (LNCaP and DU-145) were obtained from the ATCC (Rockville, Md.). A recently established bone metastatic PSA$^+$ CaP line (VCaP) was generously provided by Drs. Pienta and Cooper (Karmanos Cancer Center, University of Michigan, Ann Arbor, Mich.) [11, 17, 23]. A metastatic variant of a PC-3 cell line, PC-3ML, was a gift from Dr. M.E. Stearns (Allegheny University Hospitals, Philadelphia, Pa.) [15, 27]. All cultures were maintained in a complete medium containing RPMI-1640 basal medium, 10% fetal bovine serum (Atlanta Biologicals, Atlanta, Ga.), and 10 µg/ml gentamicin. The EGFP-MAT LyLu cell line was generated by stable transfection of Dunning MAT LyLu rat CaP cells with pEGFP-1 plasmid DNA (Clontech, Palo Alto, Calif.) and was maintained in complete medium with 250 nM dexamethasone as described previously [19, 28].

Growth inhibition assay

A ^{3}H-thymidine incorporation assay was performed as described previously [8]. Following incubation in medium containing BIRM or without BIRM, the cells were pulse-labeled with ^{3}H-thymidine (1 µCi/ml) for 2 h. Incorporation of ^{3}H-thymidine into cellular DNA was stopped by the addition of 10% trichloroacetic acid and the acid-precipitable radioactivity was determined by liquid scintillation counting [8]. Clonogenic survival of CaP cells exposed to BIRM for 24 h was assayed by the colony assay as described previously [8].

Determination of apoptotic activity

BIRM-induced apoptosis was assayed using a cell death ELISA kit (Cell Death ELISA-Plus kit; Roche Molecular Biochemicals, Mannheim, Germany). The assay measured the amount of free nucleosomes in cell lysate resulting from programmed cell death [9]. The relative amount of free nucleosomes present in cell lysates from cultures incubated with BIRM for 4 h or 24 h was estimated according to the supplier's instructions.

Cell cycle analysis

CaP cells (1×10^5) were cultured in 60-mm culture dishes. After an overnight culture, the cells were treated with 10 or 25 µl/ml of BIRM for 24 h. BIRM-treated and untreated cells were harvested and stained with 50 µg/ml propidium iodide. The amount of propidium iodide bound to DNA was profiled in an EPICS XL flow cytometer as described previously [19]. The fraction of dead cells at the time of harvesting was about 16% as determined by trypan blue exclusion. The majority of these cells were floating, so were discarded at the time of washing. The remaining dead cells were gated out using the forward angle light scatter and side scatter gatings during flow cytometry. About 20,000 propidium iodide-stained cells were analyzed in the flow cytometer from each sample. The MODFIT LT program (Verity Software House, Topsham, Me.) was used for the cell cycle phase analysis [29].

Determination of activation of cell death caspases

Caspase activation in CaP cells treated with BIRM was determined using a kit (Homogeneous Caspases Assay, fluorimetric; Roche) which determined collectively activated caspases nos. 2, 3, 6, 7, 8, 9 and 10. The assay measured the free rhodamine 110 (R110) resulting from the cleavage of a common caspase substrate, DEVD, conjugated with R110. The amount of free R110 was determined fluorimetrically at an excitation wavelength of 499 nm and an emission wavelength of 528 nm, and is expressed as relative fluorescence units (RFU) [25].

HAase assay

We tested whether BIRM affects HAase activity secreted in DU-145 culture-conditioned medium and partially purified HYAL1 using a HAase activity ELISA-like assay [20, 22]. HYAL1-type HAase was partially purified from the urine of patients with high-grade bladder cancer as described previously [20]. The assay was performed in a 96-well microtiter plate coated with HA (200 µg/ml, ICN Biomedicals). Wells were incubated with various concentrations of BIRM or column fractions from a Sephadex G-50 gel-filtration column (see below) in a HAase assay buffer at 37°C for 15 h [20]. Following incubation, HA degraded by HAase was washed off and the HA remaining in the microtiter wells was estimated using a biotinylated bovine nasal cartilage HA-binding protein, and an avidin-biotin detection system (Vector Laboratories, Burlingame, Calif.) [21].

Biochemical characterization of cytotoxic activity in BIRM

To study heat inactivation, BIRM was heated at 100°C for 5 min in a water bath. BIRM was digested with proteinase K (10 U/ml) at

37°C for 18 h. For size fractionation studies, clarified BIRM was loaded into ultrafiltration mini-Centriprep tubes (Millipore, Bedford, Mass.) with membrane barriers with different molecular weight cut-off points (i.e. about 3.5, 10 and 30 kDa). Following three cycles of centrifugation and separation of the low molecular weight fractions, both the filtrate and the retentate were assayed for cytotoxic activity. BIRM solution was also treated with charcoal-dextran (50 mg/ml) at 4°C for 12 h to remove lipids and steroids (if any). Following the various treatments, BIRM was centrifuged and various concentrations of the supernatant were added to PC3-ML cells cultured in 24-well plates (2×10^4 cells/well). BIRM-induced cytotoxicity was estimated using the MTT reduction assay following a 24-h treatment [19].

Fig. 1 Cytotoxicity of BIRM against prostate tumor cell lines. CaP cells cultured in growth medium (1×10^4 cells/well, 48-well plates) were exposed to various concentrations of BIRM. Following incubation for 24 h, DNA synthesis was determined by measuring ^{3}H-thymidine incorporation in the proliferating cells (*vertical bars* means ± SEM from three independent assays)

Gel filtration chromatography

Particle-free BIRM was loaded onto a G-50 Sephadex column (1.5×120 cm) equilibrated with 20 mM Tris-HCl, pH 7.4, containing 150 mM NaCl buffer (Tris/NaCl buffer) [20]. The column was eluted in Tris/NaCl buffer at 7 ml/h and 3-ml fractions were collected. Each fraction was assayed for protein (BCA-BioRad), uronate [2], inhibition of cell growth (MTT assay) [19] and inhibition of HAase activity (HAase ELISA-like assay).

Tumor generation and BIRM administration

This experiment was performed according to a protocol approved by the University of Miami Animal Care and Use Committee and as stipulated in the NIH Guide to the Humane Care and Use of Laboratory Animals. A suspension (1×10^5 cells, 0.5 ml) of growing EGFP-MAT LyLu cells was implanted subcutaneously into the dorsal flank of adult (about 250 g) male Copenhagen rats (Harlan Sprague Dawley, Indianapolis, Ind.) under mild anesthesia [19]. The rats were housed in a room under a 12-h light/12-h dark cycle and provided with food and water ad libitum throughout the experiment. Following implantation, the rats were randomly divided into two groups of six animals and gavaged with 1 ml of either distilled water (vehicle control, group 1) or BIRM (group 2) using a 3-inch stainless-steel intubation cannula on day 1 of tumor implantation and then daily for 30 days. Tumor growth was examined by palpating the skin around the site of injection. After the tumors became palpable (about day 5), they were measured three times a week using calipers, and the volumes calculated assuming approximation to an ellipsoid (length×height×width×0.524). Animals were euthanized when the tumor volume was about 10 cc or the tumor became significantly necrotic. At necropsy, lungs were collected and viewed under a Nikon stereomicroscope with a fluorescence attachment (SMZ 1500) to examine the presence of fluorescent metastatic tumor foci.

Statistical analysis

Triplicate samples were assayed in all in vitro experiments. Statistical analysis was performed using parametric and nonparametric Student's t-tests.

Results

BIRM inhibits cell proliferation in CaP cells

BIRM inhibited cell proliferation in all the CaP cell lines tested in a dose-dependent manner (Fig. 1). The concentration of BIRM causing 50% growth inhibition
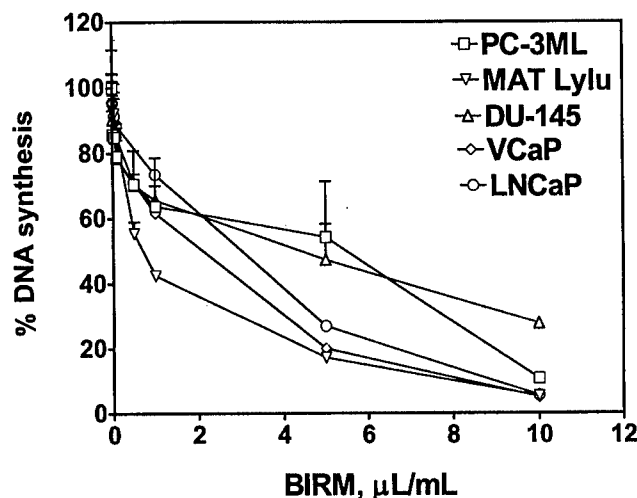
(IC_{50}) was 8 µl/ml (i.e. 0.8% v/v). Furthermore, the inhibitory activity of BIRM was comparable among all CaP cell lines regardless of their androgen sensitivity (androgen-sensitive LNCaP and VCaP cells versus androgen-resistant PC-3ML and DU-145 cells). Similar results were obtained by cell counting and Trypan blue exclusion assays (data not shown). The results presented in Fig. 1 and similar observation from other assays suggested that BIRM-induced inhibition of cell proliferation led to either cell death (cytotoxicity) or arrest of cell proliferation (cytostasis). To distinguish between these mechanisms, we investigated the colony-forming efficiency of CaP cells treated with BIRM. The clonogenic assay revealed a dose-dependent inhibition of colony formation in BIRM-treated CaP cells. Neither cell colonies nor cell clusters were observed in cultures exposed to BIRM at doses of 10 µl/ml and above for 24 h (Fig. 2A). The IC_{50} of BIRM for inhibiting clonogenic survival was also 8 µl/ml, the same as the value obtained in the ^{3}H-thymidine assay (Fig. 2B).

BIRM causes cell cycle arrest in CaP cells

As shown in Table 1, the proportion of cells in G_0/G_1 phase increased significantly from 56.4 ± 0.9% in control to 75.5 ± 2.2% in cultures treated with BIRM at 25 µl/ml. The increase in the G_0/G_1 phase fraction in the BIRM-treated cells was contrasted with a decrease in the S-phase fraction. The S-phase fraction in BIRM-treated cells was 13.1 ± 2.9% compared to 28.9 ± 2.1% in the control. A small decrease of 15–22% in the G_2/M fraction was also observed in BIRM-treated cells.
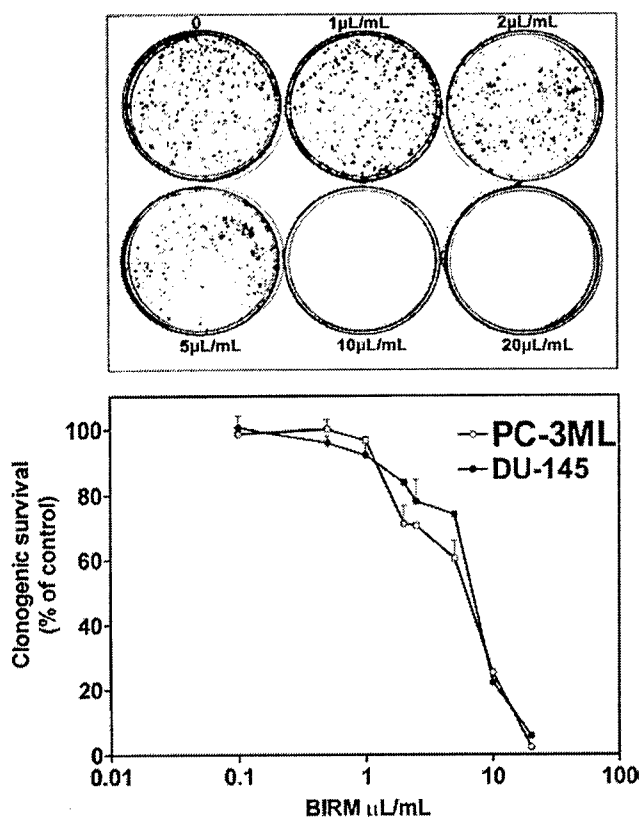
Fig. 2a, b Effect of BIRM on the growth of CaP cells. Cells cultured at low density in 60-mm culture dishes were exposed to BIRM for 24 h. Surviving cells at the end of incubation were allowed to form adherent cell colonies during the next 7–10 days. Cell colonies stained with 0.1% crystal violet and colonies containing > 50 cells were counted manually using a hand-held electronic counter in a blinded fashion. **a** Colonies of surviving PC3-ML cells exposed to BIRM for 24 h. **b** Clonogenic survival of CaP cells cultured with BIRM. The results are presented as means ± SEM from three independent experiments

BIRM induces apoptosis in CaP cells

We did not observe a significant difference in the levels of free nucleosomes in BIRM-treated cells during 4 h of treatment, but after 24 h of treatment the intracellular levels of free nucleosomes showed a two- to threefold dose-dependent increase (Fig. 3).

Activation of cell death-associated caspases

As shown in Fig. 4, the activities of one or more of caspases 2, 3, 7, 8, 9 and 10 were increased significantly in BIRM-treated cells as compared to the activities in control cells. We initially detected a time-dependent increase in combined caspase activity, beginning at 4 h of exposure to BIRM and peaking at 18 h. The dose-dependent increase in caspase activities showed a 50% increase in cells treated at 5 µl/ml BIRM over the activity in control cells following incubation for 18 h or longer (Fig. 4).

BIRM inhibits tumor growth and metastasis

As shown in Fig. 5, following tumor implantation, oral administration of BIRM (4 ml/kg body weight) to rats resulted in slow tumor growth. While the tumor incidence was 100% in the control group, only four out of six BIRM-treated animals (67%) developed tumors. The tumor growth rate estimated using non-linear regression analysis of tumor volumes over time for each animal confirmed a decreased growth rate in BIRM-treated animals. The time taken for tumors to reach 1 cc was 18.6 ± 1.3 days in control animals and 25.7 ± 2.6 days in BIRM-treated animals (mean ± SE from four animals). A 38% delay in tumor growth was observed in BIRM-treated animals compared with control animals. The difference in the growth rate between control and BIRM-treated animals was statistically significant (unpaired t-ctest: $P = 0.03$, $t = 2.773$, df $= 6$, 95% CI 0.835–13.36). Fluorescence imaging of the lungs at necropsy revealed that only one out of six BIRM-treated animals had metastatic lung foci, whereas five out of six control animals had tumor metastasis to the lungs. Furthermore, the tumor foci in the lungs of the BIRM-treated animal were significantly smaller than those in control animals (Fig. 6). These results indicate that ingredients in BIRM either delay or block spontaneous lung metastasis.

BIRM inhibits the activity of HYAL1-type HAase

Investigation of inhibition of matrix metalloproteinase activity by BIRM using a ^{3}H-labeled collagen-degradation assay [18] showed no changes in matrix

Table 1 Flow cytometric cell cycle fractionation analysis of PC-3ML cells treated with BIRM for 24 h. The distributions of cells in the various cell cycle phases were calculated from the DNA content of propidium iodide-labeled cells using the MODFIT program. Values are mean ± SE percentages from three independent experiments. Similar results were obtained from the cell cycle fractionation analysis of LNCaP cells exposed to BIRM

Treatment	G_0/G_1 phase	Difference (%)[a]	S phase	Difference (%)[a]	G_2/M phase	Difference (%)[a]
Control	56.37 ± 0.9		28.9 ± 2.1		14.6 ± 1.2	
BIRM (10 µl/ml)	67.93 ± 2.1	+20.5	19.5 ± 2.4	−32.5	12.5 ± 0.28	−15
BIRM (25 µl/ml)	75.46 ± 2.2	+33.8	13.1 ± 2.9	−54.6	11.39 ± 0.29	−22

[a]Calculated as [(% of cells in respective phase of untreated samples−% of cells in respective phase in BIRM-treated samples)/(% of cells in respective phase in untreated control)]×100
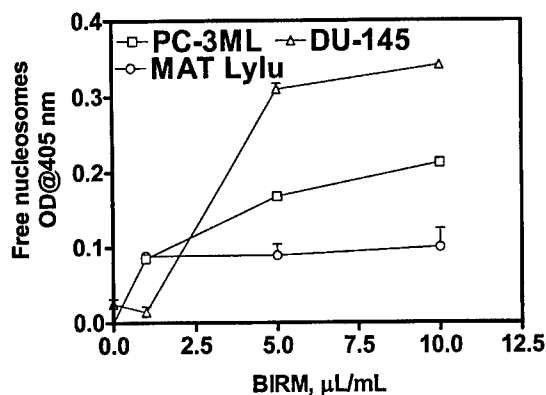
Fig. 3 BIRM kills tumor cells by induction of apoptosis. PC-3ML, DU-145 and Mat Lylu CaP cells cultured in growth medium (1×10^4 cells/well; 48-well plates) with or without BIRM at various concentrations for 24 h were analyzed for apoptotic activity using the Cell Death ELISA Plus assay kit, which allowed measurement of soluble nucleosomes by spectrophotometry. The data presented as means ± SEM from three independent experiments

Fig. 5 Effect of daily dosing of BIRM on growth and metastasis of Dunning MAT LyLu tumors in rats. Tumor growth in rats with subcutaneous tumor implant with EGFP-MAT Lylu cells (1×10^5 cells/animal). The data are presented as means ± SEM of each treatment group over time. Data from the control group include measurements from six tumor bearing rats, whereas the BIRM-treated group had only four animals; the other two animals in this group did not develop tumors

Characterization of active ingredients in BIRM solution

BIRM retained its full cytotoxic activity after boiling for 5 min or digestion with proteinase K, indicating that reactive species present in BIRM most likely are heat-stable proteinase-resistant compounds. Similarly, charcoal-dextran extraction also did not result in any loss in the cytotoxic activity associated with BIRM, suggesting that the active species present in BIRM are not lipid-soluble compounds such as alkaloids or steroids. No loss in cytotoxic activity was found upon ultrafiltration through a 3.5-kDa membrane barrier. However, a 40% loss in activity was observed after ultrafiltration through 10-kDa and 30-kDa membranes (Fig. 8). These results indicate that BIRM contains at least two species with different molecular mass, i.e. one with a molecular mass between 3500 and 10,000 and a second with a molecular mass of ≥30,000, with cytotoxic activity against CaP cells. The possibility of the growth-inhibitory activity being associated with carbohydrate derivatives was investigated using the Bitter and Muir modified carbazole assay to measure glycosaminoglycans and proteoglycans containing D-glucuronic acid (i.e. uronate) [23]. The results showed that BIRM is rich in uronate-containing carbohydrates (19.5 mg/ml). Gel filtration chromatography on a Sephadex G-50 column also showed two active fractions (fraction nos. 28 and 42, Fig. 9).
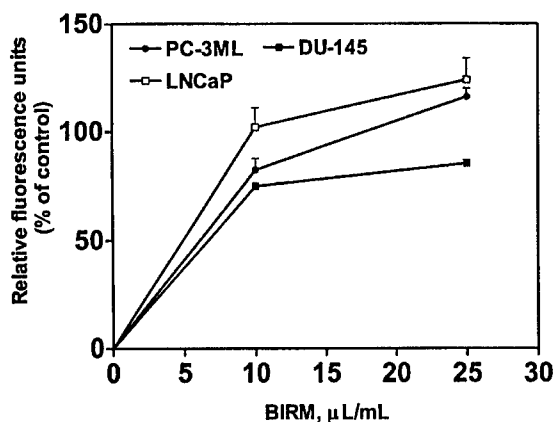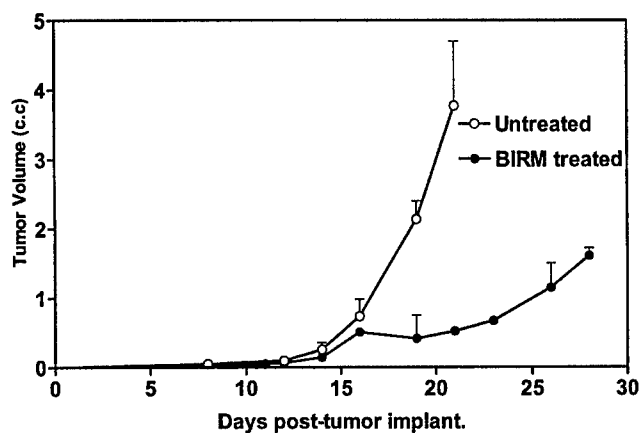

Fig. 4 BIRM induced increases in caspase activity. CaP cells were treated with BIRM for 4 to 24 h and the total activities of cell death-associated caspases were measured using a kit that employed a rhodamine110-conjugated peptide substrate common to all cell death-related caspases. The results are presented as means ± SEM from three independent experiments in each of which cell lysates incubated with BIRM for 24 h were used for caspase activity determination. Caspase activity in untreated control cultures was detectable, but was typically ten times less than the activity detected in the positive controls provided with the assay kit

metalloproteinase activity following BIRM treatment (data not shown). We next examined whether BIRM could inhibit the activity of HYAL1-type HAase. We have previously shown that HYAL1 is the major HAase expressed in cancers of the prostate and bladder [21, 22]. Furthermore, invasive tumor cells express high levels of HYAL1 [5, 21, 22]. As shown in Fig. 7, BIRM potently inhibited HAase activity. BIRM inhibited the HAase activity present in the culture-conditioned medium of DU-145 cells (a good source of HYAL-1 [21]) and the activity of partially purified HYAL1, in a dose-dependent manner (IC_{50} 0.25 µl/ml).

Discussion

A systematic investigation of promising plant products has led to the discovery and development of antineoplastic agents with unique modes of action and striking efficacy (e.g. paclitaxel, vinblastine, etoposide, etc) [7]. In

Fig. 6A, B EGFP-MAT LyLu
rat prostate tumors metastatic
to lungs. The figure shows rat
lungs with fluorescent tumor
foci (*arrows*). **A** Control
animals (×40); **B** a typical
tumor metastatic to the lung in
a BIRM-treated animal (×20).
Tumor foci in the lungs of
BIRM-treated animals were
typically ten times smaller or
absent

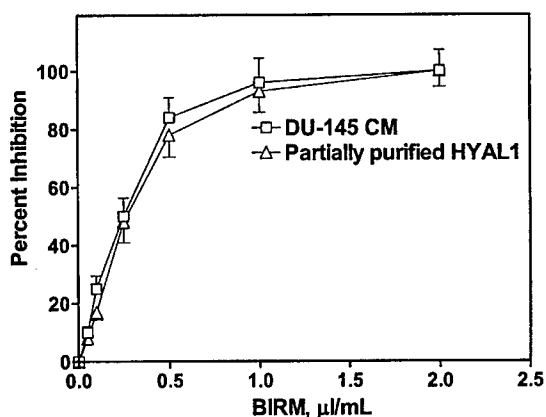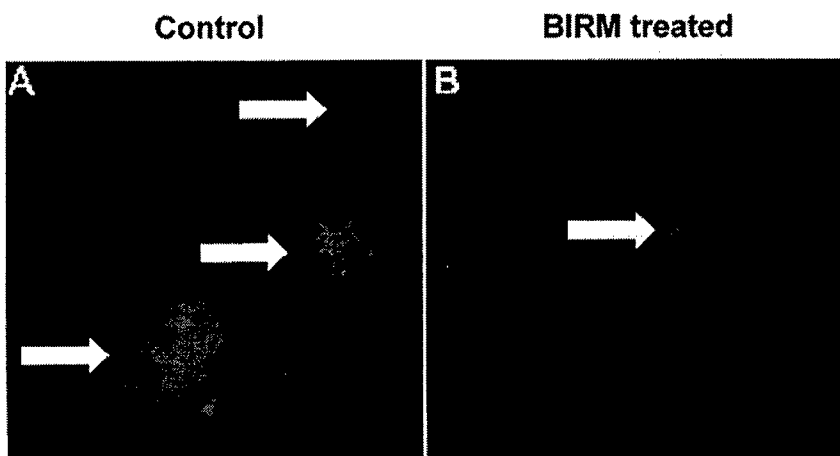**Control**   **BIRM treated**

Fig. 7 BIRM inhibits tumor-derived HAase. Effect of BIRM on the
HAase activity present in DU-145 cell-conditioned medium and
partially purified preparation of HYAL1 was carried out using an
HAase ELISA-like assay as described in Materials and methods.
The data shown are from a typical experiment. Similar results were
obtained in three other experiments using LNCaP cells (data not
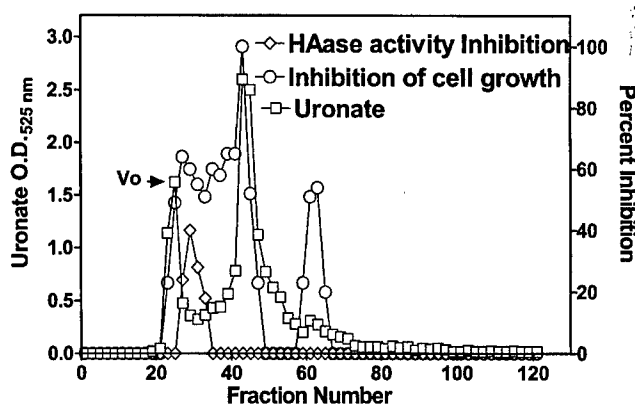shown)

Fig. 9 Fractionation of antineoplastic ingredients present in BIRM
by gel filtration chromatography. Clarified BIRM (5 ml) was
fractionated on a Sephadex G-50 column. The column fractions
were assayed for protein ($A_{280\ nm}$), uronate concentration (Bitter
and Muir assay), HAase activity (HAase activity ELISA) and
cytotoxicity (MTT assay). A single protein peak was detected in
fraction no. 20, which had neither cytotoxic activity nor HAase-
inhibitory activity
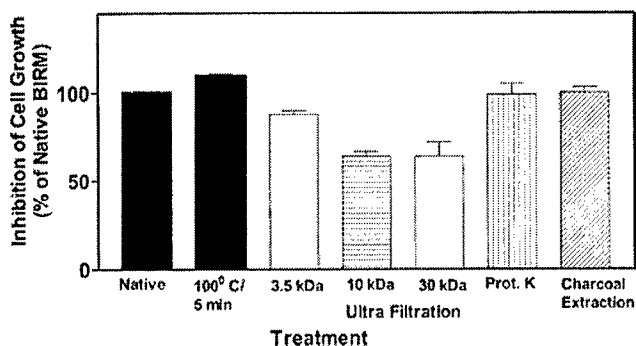
Fig. 8 Cytotoxicity of modified BIRM as assayed by MTT assay
and compared with unmodified BIRM. BIRM solution was treated
with proteinases (proteinase K), heated for 5 min in a bath of
boiling water or subjected to ultrafiltration as described in
Materials and methods. Following treatment, untreated and
treated BIRM solutions were tested for cytotoxic activity in PC3-
ML cells by MTT assay, as described in Materials and methods
(*vertical bars* means ± SEM from four independent assays)

this report, we present evidence of the antineoplastic
activity of a plant-derived nutritional supplement,
BIRM. The medicinal value of BIRM is believed to be
associated only with the Amazonian variety of the plant
Dulcamara, where the micronutrients present in the soil
of the Upper Amazon basin promote the synthesis of
medicinal compounds in the plant. BIRM inhibited cell
proliferation and clonogenic survival (Figs. 1 and 2) and
caused apoptotic cell death via the caspase activation
pathway (Figs. 3 and 4). In vivo studies on the growth
and metastasis of Dunning MAT LyLu tumors sug-
gested that oral dosing with BIRM resulted in lower
tumor incidence, slower tumor growth and reduced
spontaneous metastasis to the lungs (Figs. 5 and 6). A
preliminary biochemical characterization and size-
exclusion chromatography suggested that there were at
least four active species present in BIRM, three with
cytotoxic activity and one with HAase-inhibitory activ-
ity. We have not yet determined whether the three

cytotoxic species present in BIRM have the same chemical composition but different polymer length. Nonetheless, all four active ingredients were heat-stable and unlikely to be proteins or lipid-soluble compounds.

Inhibition of tumor growth in the rat CaP model following the oral administration of BIRM clearly suggests that the active ingredient(s) of BIRM are absorbed in the gastrointestinal tract. The reduction in tumor incidence (33%) and the number of tumor foci in the lungs (>80%) in BIRM-treated animals suggest that BIRM may exert both antiproliferative and antimetastatic activities. It is estimated that 20–40% of patients initially diagnosed with local CaP have either locally advanced disease (stage C) or metastatic disease (stage D) [10, 16], and the cure of metastatic disease still remains a challenge. Our observation that CaP cell cultures treated with BIRM showed a significant reduction in cell proliferation and undergo apoptosis (Figs. 1, 2, and 3) indicates that the active ingredients present in BIRM have potential for use in controlling advanced hormone-refractory prostate cancer. We investigated whether the BIRM-induced cytotoxic effect was due to inhibition of mitotic spindle separation. This would lead to mitotic inhibition and arrest of cells in the G_2/M phase. Contrary to our expectation, incubation with BIRM arrested CaP cells in G_0/G_1, which was compensated for by a significant decrease (i.e. −56%) in the proportion of cells in S phase and a modest decrease in G_2/M, indicating lack of mitotic arrest or cytokinesis (Table 1). This finding is novel in the sense that most plant-derived compounds used in cancer therapy interfere with tubulin polymerization (e.g. vinblastine and vincristine) or depolymerization (paclitaxel), or inhibit topoisomerase I activity (e.g. irinotecan, topotecan, 9-aminocamptothecin and 9-nitrocamptothecin) [6] or topoisomerase II activity, leading to cell cycle arrest in the G_2/M phase (e.g. paclitaxel, etoposide and teniposide) [24].

Apoptotic cell death may be one of the mechanisms involved in BIRM-induced cytotoxicity. BIRM increased the apoptosis in three CaP cell lines (Fig. 3). Furthermore, induction of apoptosis in BIRM-treated CaP cells was coincident with activation of cell-death caspases (Fig. 4). In addition to its cytotoxic effects, BIRM appeared to be a potent inhibitor of metastasis. Although, the mechanism by which it may inhibit metastasis is unknown at present, our results suggests that BIRM is a potent inhibitor of HAase, a class of matrix-degrading enzymes whose levels have been shown to correlate with CaP progression [20, 22].

The recommended minimum dose of BIRM for human consumption is 4 ml/day (as indicted on the bottle label), a significantly lower dose than that used in the current study. We based the dosage to rats on the observed efficacy in vitro. We found no observable systemic toxicity in rats at a dose of 4 ml/kg. Given its effect on tumor growth and metastasis and no systemic toxicity, inclusion of BIRM as an adjuvant to standard therapy has potential to reduce/halt disease progression.

In summary, our study demonstrated that BIRM shows cytotoxic activity against both androgen-dependent and androgen-independent CaP cells in vitro. More importantly, it reduced tumor incidence, delayed tumor growth and caused a significant reduction in metastasis in an experimental model of late-stage CaP. Furthermore, no systemic toxicity was seen following continuous administration of BIRM in an in vivo rat model. These useful properties of BIRM indicate that further investigation of its mechanism of action and clinical trials involving its use in advanced CaP are warranted.

References

1. BIRM Carbohydrate of low molecular weight ECA10-142 controls AIDS (1994) Tenth International Conference on AIDS (Yokohama, Japan). Abstracts, vol 2 (abstract no. 0291)
2. Bitter T, Muir H (1966) Mucopolysaccharides of whole human spleens in generalized amyloidosis. J Clin Invest 45:963–975
3. Cevallos EA (1994) Binational experience in the treatment of AIDS with a low molecular weight natural carbohydrate (ECA-10-142), as a stimulant of the immune system. Tenth International Conference on AIDS (Yokohama, Japan). Abstracts, vol 1 (abstract no. 0294)
4. Cevallos EA (1996) "BIRM: La estrategia terapeuticadel futuro". Abstract of Congresso Mundial de SIDA en Vancouver
5. Delpech B, Girard N, Bertrand P (1997) Hyaluronan: fundamental principles and applications in cancer. J Intern Med 242:41–48
6. Dennis RAM, Adriana BN, Rocha DA, Gilberto S (2000) Anti-cancer drug discovery and development in Brazil: targeted plant collection as a rational strategy to acquire candidate anti-cancer compound. Oncologist 5:185–198
7. Donehower RC, Rowinsky EK (1993) Anticancer drugs derived from plants. In: DeVita VT Jr, Hellman S, Rosenberg SA (eds) Principles and practice of oncology, 4th edn. Lippincott, New York
8. Dudak SD, Lopez A, Block NL, Lokeshwar BL (1996) Enhancement of radiation response of prostatic carcinoma by lonidamine. Anticancer Res 16:3665–3671
9. Eisel D, Fertig G, Fischer B, Manzow S, Schmelig K (eds) (2000) Guide to cell proliferation and apoptosis methods, 2nd edn (technical manual). Roche Applied Science, Mannheim, Germany
10. Harris K, Reese DM (2001) Treatment options in hormone-refractory prostate cancer: current and future approaches. Drugs 61:2177–2192
11. Horoszewicz JS, Leong SS, Kawinski E, Karr JP, Rosenthal H, Chu TM, Mirand EA, Murphy GP (1983) LNCaP model of human prostatic carcinoma. Cancer Res 43:1809–1818
12. Jacobson JS, Chetty AP (2001) Complementary and alternative medicine in prostate cancer. Curr Oncol Rep 3:448–452
13. Jamel A, Thomas A, Murray T, Thun M (2002) Cancer statistics 2000. CA Cancer J Clin 52:23–47
14. Jones HA, Metz JM, Devine P, Hahn SM, Whittington R (2002) Rates of unconventional medical therapy use in patients with prostate cancer: standard history versus directed questions. Urology 59:272–276
15. Kaighn ME, Narayan KS, Ohnuki Y, Lechner JF, Jones LW (1979) Establishment and characterization of a human prostatic carcinoma cell line (PC-3). Invest Urol 17:16–23

16. Kojima M, Troncoso P, Babaian RJ (1995) Use of prostate-specific antigen and tumor volume in predicting needle biopsy grading error. Urology 45:807–812

17. Korenchuk S, Lehr JE, Mclean L, Lee YG, Whitney S, Vessella R, Lin DL, Pienta KJ (2001) VCaP, a cell-based model system of human prostate cancer. In Vivo 15:163–168

18. Lokeshwar BL, Selzer MG, Block NL, Gunja-Smith Z (1993) Secretion of matrix metalloproteinases and their inhibitors (tissue inhibitor of metalloproteinases) by human prostate in explant cultures: reduced tissue inhibitor of metalloproteinase secretion by malignant tissues. Cancer Res 53:4493–4498

19. Lokeshwar BL, Selzer MG, Zhu BQ, Block NL, Golub LM (2002) Inhibition of cell proliferation, invasion, tumor growth and metastasis by an oral non-antimicrobial tetracycline analog (COL-3) in a metastatic prostate cancer model. Int J Cancer 98:297–309

20. Lokeshwar VB, Lokeshwar BL, Pham HT, Block NL (1996) Association of elevated levels of hyaluronidase, a matrix-degrading enzyme, with prostate cancer progression. Cancer Res 56:651–657

21. Lokeshwar VB, Young MJ, Goudarzi G, Iida N, Yudin AI, Cherr GN, Selzer MG (1999) Identification of bladder tumor-derived hyaluronidase: its similarity to HYAL1. Cancer Res 59:4464–4470

22. Lokeshwar VB, Rubinowicz D, Schroeder GL, Forgacs E, Minna JD, Block NL, Nadji M, Lokeshwar BL (2001) Stromal and epithelial expression of tumor markers hyaluronic acid and hyaluronidase in prostate cancer. J Biol Chem 276:11922–11932

23. Mickey DD, Stone KR, Wunderli H, Mickey H, Paulson DF (1980) Characterization of a human prostate adenocarcinoma cell line (DU 145) as a monolayer culture and as a solid tumor in athymic mice. Prog Clin Biol Res 37:67–84

24. Pienta KJ, Naik HN, Jeffrey EL (1996) Effect of estramustine, etoposide and taxol on prostate cancer cell growth in vitro and in vivo. Urology 48:164–170

25. Roche Applied Science (2002) Homogeneous caspases assay, fluorimetric (pack insert/product instruction). Roche Applied Science, Mannheim Germany

26. Smith M, Mills EJ (2001) Select complementary/alternative therapies for prostate cancer: the benefits and risks. Cancer Pract 9:253–255

27. Wang M, Stearns ME (1991) Isolation and characterization of PC-3 human prostatic sublines, which preferentially metastasize to select organs in S.C.I.D. mice. Differentiation 48:115–125

28. Wenger AS, Mickey DD, Hall M, Silverman LM, Mickey GH, Fried A (1984) In vitro characterization of MAT LyLu: a Dunning rat prostate adenocarcinoma tumor subline. J Urol 131:1232–1236

29. Yamamura Y, Rodriguez N, Schwartz A, Eylar E, Bagwell B, Yano N (1995) A new flow cytometric method for quantitative assessment of lymphocyte mitogenic potentials. Cell Mol Biol (Noisy-le-grand) 41:121–132

COMPARISON OF THE PROGNOSTIC POTENTIAL OF HYALURONIC ACID, HYALURONIDASE (HYAL-1), CD44V6 AND MICROVESSEL DENSITY FOR PROSTATE CANCER

Sinan Ekici[1], Wolfgang H. Cerwinka[1], Robert Duncan[2], Pablo Gomez[1], Francisco Civantos[1], Mark S. Soloway[1] and Vinata B. Lokeshwar[1,3,4]*

[1]*Department of Urology, University of Miami School of Medicine, Miami, FL, USA*
[2]*Department of Epidemiology, University of Miami School of Medicine, Miami, FL, USA*
[3]*Sylvester Comprehensive Cancer Center, University of Miami School of Medicine, Miami, FL, USA*
[4]*Department of Cell Biology and Anatomy, University of Miami School of Medicine, Miami, FL, USA*

Despite the development of nomograms designed to evaluate a prostate cancer (PCa) patient's prognosis, the information has been limited to PSA, clinical stage, Gleason score and tumor volume estimates. We compared the prognostic potential of 4 histologic markers, hyaluronic acid (HA), HYAL-1-type hyaluronidase (HAase), CD44v6 and microvessel density (MVD) using immunohistochemistry. HA is a glycosaminoglycan that promotes tumor metastasis. CD44 glycoproteins serve as cell surface receptors for HA, and the CD44v6 isoform is associated with tumor metastasis. HYAL-1-type HAase is expressed in tumor cells and, like other HAases, degrades HA into angiogenic fragments. Archival PCa specimens (n = 66) were obtained from patients who underwent radical prostatectomy for clinically localized PCa and had a minimum follow-up of 72 months (range 72–131 months, mean 103 months). For HA, HYAL-1 and CD44v6 staining and MVD determination, a biotinylated HA-binding protein, an anti-HYAL-1 IgG, an anti-CD44v6 IgG and an anti-CD34 IgG were used, respectively. HA and HYAL-1 staining was classified as either low- or high-grade. CD44v6 staining and MVD were evaluated quantitatively and then grouped as either low- or high-grade. Using 72 months as the cut-off limit for evaluating biochemical recurrence, HA, HYAL-1, combined HA–HYAL-1, CD44v6 and MVD staining predicted progression with 96%, 84%, 84%, 68% and 76% sensitivity, respectively. Specificity was, 61% (HA), 80.5% (HYAL-1), 87.8% (HA–HYAL-1), 56.1% (CD44v6) and 61% (MVD). Sensitivity and specificity values for each marker did not change significantly in a subset of 45 patients for whom follow-up of longer than 112 months was available. In univariate analysis using the Cox proportional hazards model, preoperative PSA, Gleason sum, margin status, seminal vesicle, extraprostatic extension (EPE), HA, HYAL-1, HA–HYAL-1 and MVD, but not CD44v6, age and clinical stage, were significant in predicting biochemical recurrence (p < 0.05). In multivariate analysis using stepwise selection, only preoperative PSA (hazard ratio/unit PSA change = 1.086, p < 0.0001), EPE (hazard ratio = 6.22, p = 0.0016) and HYAL-1 (hazard ratio = 8.196, p = 0.0009)/HA–HYAL-1 (hazard ratio = 5.191, p = 0.0021) were independent predictors of biochemical recurrence. HA was an independent predictor of prognosis if HYAL-1 staining inference was not included in the multivariate model. In our retrospective study with 72- to 131-month follow-up, EPE, preoperative PSA and HYAL-1 either alone or together with HA (i.e., combined HA–HYAL-1) were independent prognostic indicators for PCa.
© 2004 Wiley-Liss, Inc.

Over the last decade, the number of curable PCa cases has significantly increased due to the widespread use of PSA.[1,2] However, despite careful selection of patients, the disease recurs in a substantial percentage of localized PCa cases undergoing curative treatment modalities (*i.e.*, radical prostatectomy and radiotherapy).[3–6] Accurate prediction of the risk of progression would be useful in choosing the type and timing of the most appropriate treatment. Although existing parameters, such as Gleason sum or preoperative PSA, provide some prognostic information, it is dif-

ficult to estimate prognosis in PCa patients since two-thirds of them have Gleason sum of 5–7 and serum PSA levels of 4–10 ng/ml.[6–11] Furthermore, all patients with the same pathologic stage and/or grade do not have the same prognosis. Thus, there is a need for accurate prognostic markers to identify the biologic behavior of the tumor. Previously, we showed that HYAL-1-type HAase, either alone or in combination with HA, appears to be an independent predictor of biochemical recurrence among radical prostatectomy patients.[12]

HA is a nonsulfated glycosaminoglycan made up of repeated disaccharide units, D-glucuronic acid and N-acetyl-D-glucosamine.[13] HA maintains the osmotic balance of tissues and regulates cellular processes such as adhesion, migration and proliferation.[13] The biologic functions of HA are mediated by different HA receptors, including CD44.[14] The concentration of HA is elevated in several tumor types, and in some tumors (*e.g.*, breast, colon), high-level HA expression in tumor-associated stroma and/or tumor cells predicts poor survival.[15–19] Increased urinary HA levels serve as an accurate diagnostic marker for bladder cancer, regardless of tumor grade and stage.[20] However, in PCa, HA is not an independent predictor for prognosis.[12,19]

HYAL-1-type HAase is present in serum and produced by bladder, prostate and head-and-neck cancer cells.[21–24] The HAase class of enzymes degrades HA into small fragments, some of which (3–25 disaccharide units) induce angiogenesis.[25,26] Angiogenic HA fragments stimulate endothelial cell proliferation, adhesion and migration by activating focal adhesion kinase and mitogen-activated protein kinase pathways.[26] We have previously shown the presence of angiogenic HA fragments in PCa tissues and in the urine and saliva of bladder and head-and-neck cancer patients, respectively.[22,24,27] Given the observations that HYAL-1

is the major tumor-derived HAase expressed and secreted by tumor cells and that it is active at pH $\leq$ 4.5, it is possible that in the tumor microenvironment, where the pH is acidic, secreted HYAL-1 degrades the HA present in the extracellular matrix into angiogenic HA fragments.[22,24,27,28] In a retrospective study with a minimum of 5-year follow-up, we showed that HYAL-1 staining predicts progression with 84% sensitivity and 80% specificity.[12] Furthermore, high HYAL-1 staining was an independent predictor for prognosis.

CD44 belongs to a family of cell surface transmembrane glycoproteins involved in cell-to-cell and cell-to-extracellular matrix interactions.[29,30] Alternative splicing of CD44 mRNA in 10 of the 20 exons generates several variant CD44 isoforms.[30,31] The standard form of CD44 (*i.e.,* CD44s) is an HA receptor expressed in a variety of normal and tumor cell types.[29,32] We have previously shown that an isoform of CD44 (ex14/v10) is involved in HA-mediated endothelial cell proliferation.[33] The correlation between tumor progression and CD44s and/or its isoforms is unclear. We and others have shown that the androgen-insensitive PCa line PC-3 and primary PCa cells express CD44s and CD44 variants (*e.g.,* CD44v3 and CD44v6); however, the androgen-sensitive, poorly metastatic line LNCaP does not express CD44.[34–36] Contrary to these findings, it has been shown that overexpression of CD44v6 in a rat PCa line decreases metastasis.[37] Ekici *et al.*[38] showed that decreased expression of CD44v6 could be a predictor of poor prognosis in clinically localized PCa. Aaltomaa *et al.*[39] reported similar results.

Angiogenesis is an essential process for tumor growth and metastasis.[40–42] The clinical significance of angiogenesis, measured as MVD, has been demonstrated for several tumor types, including gastrointestinal, breast, bladder and renal cell carcinomas.[43–46] Studies that compared various endothelial cell markers (*i.e.,* CD31, CD34 and factor VIII) have shown that CD34 is a sensitive endothelial cell marker for measuring MVD.[47,48] At the present time, the clinical significance of MVD as an independent predictor of pathologic stage and recurrence in PCa remains unclear.[47–52]

We compared the prognostic potential of markers HA, CD44v6, HYAL-1 and MVD with regard to clinically localized PCa. Since HYAL-1 degrades HA and generates angiogenic fragments and CD44 acts as a cell surface receptor for both HA and HA fragments, we examined whether these biologically linked molecules are accurate prognostic indicators for PCa and whether they influence each other's prognostic capability.

MATERIAL AND METHODS

Specimens and study patients

Sixty-six randomly selected PCa specimens were obtained from patients who underwent radical retropubic prostatectomy for clinically localized PCa between 1992 and 1995 at the University of Miami. Patients neither received neoadjuvant hormonal therapy nor had metastasis to regional pelvic lymph nodes. The minimum available follow-up on all patients was 72 months. The study was conducted under a protocol approved by the University of Miami's Institutional Review Board. Of the 66 patients, 25 had biochemical or clinical recurrence before 72 months (mean time to recurrence 21.3 months, range 3–61) and 41 were free of disease recurrence (mean follow-up 103 months, range 72–131). Biochemical recurrence was defined as a PSA level $\geq$ 0.4 ng/ml in 2 successive measurements after the operation, in which case the first date an elevated PSA level was recorded was considered the date of failure. Patient characteristics including age, preoperative PSA and tumor (*i.e.,* Gleason sum, stage, margin, EPE and seminal vesicle invasion) are shown in Table I.

IHC and slide grading

For all specimens, paraffin-embedded blocks containing PCa tissues representing the major Gleason score were selected by a pathologist. From each block, 8 slides were prepared. Four slides were used for HA, HYAL-1, CD44v6 and anti-CD34 (for MVD determination) staining. The remaining slides were used either for determining nonspecific staining corresponding to each staining reagent or for repeating the staining to evaluate its consistency. For all staining procedures, specimen slides were deparaffinized, rehydrated and treated with an antigen retrieval solution (Dako, Copenhagen, Denmark).

HA and HYAL-1 staining. IHC for localizing HA and HYAL-1 in PCa tissues was carried out as described previously.[12,22] HA was localized in PCa tissues using a biotinylated HA-binding protein purified from bovine nasal cartilage, as described previously by Tengblad.[53] HYAL-1 was localized using a rabbit polyclonal anti-HYAL-1 IgG, which was generated against a peptide sequence present in the HYAL-1 protein (amino acids 321–338).[12,22]

Staining for HA and HYAL-1 was graded as 0 (no staining), 1+, 2+ and 3+. For HA staining, both the tumor-associated stroma and tumor cells were graded in each slide. The overall staining grade for each slide was assigned based on the staining intensity of the majority of the tumor tissue in the specimen. However, if 50% of the tumor tissue stained as 1+ and the other 50% as 3+, the overall staining grade was 2+. If 50% of the tumor stained as 2+ and the remaining as 3+, the overall staining inference was assigned as 3+. The staining scale was further subcategorized into low- and high-grade. For HA staining, low-grade staining included 0, 1+ and 2+ staining and high-grade staining included 3+ intensity. For HA staining, high-grade staining in tumor-associated stroma and/or tumor cells was considered as high-grade. HA staining was graded as low only when both the tumor-associated stroma and tumor cells showed low-grade staining. Therefore, in cases (*n* = 2) where stromal tissues showed low-grade staining but the tumor cells stained as 3+, the overall

TABLE I – PRE- AND POSTOPERATIVE PARAMETERS OF STUDY PATIENTS

Progression	Preoperative parameters			Postoperative parameters			
	Age (years)	PSA (ng/ml)	Clinical stage	Gleason sum	EPE	Margin	Seminal vesicle invasion
Biochemical recurrence (*n* = 25)	Median: 64	Median: 9.0	T1c: 10	6 = 2	(+) = 21	(+) = 18	(+) = 14
	Mean: 65.1	Mean: 14.04	T2a: 5 T2b: 10	7 = 14 8 = 6 9 = 3	(−) = 4	(−) = 7	(−) = 11
No biochemical or clinical recurrence (*n* = 41)	Median: 65	Median: 6	T1c: 22	5 = 7	(+) = 4	(+) = 9	(+) = 3
	Mean: 62.98	Mean: 8.1	T2a: 5 T2b: 14	6 = 9 7 = 20 8 = 5	(−) = 37	(−) = 32	(−) = 38
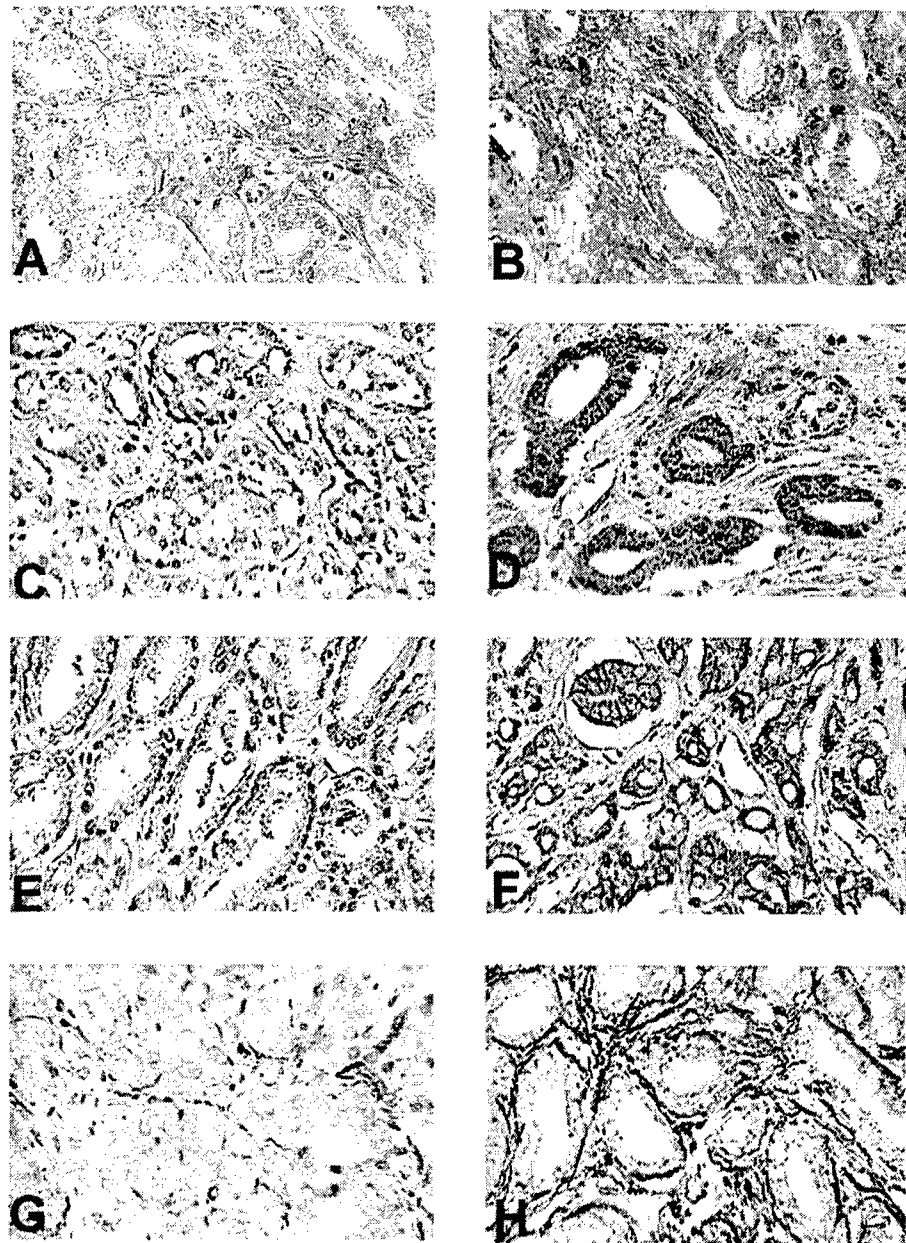
FIGURE 1 – Localization of HA, HYAL-1, CD44v6 and MVD in PCa tissues. Histologic markers were localized in PCa tissues from a nonprogressed patient *(a,c,e,g)* and a progressed patient *(b,d,f,h)*. *(a,b)* HA was localized in PCa tissues using a biotinylated HA-binding protein. *(c,d)* HYAL-1 was localized in PCa tissues using an anti-HYAL-1 antibody. *(e,f)* CD44v6 was localized in PCa tissues using an anti-CD44v6 MAb. *(g,h)* MVD was visualized using an anti-CD34 MAb. Magnification ×400.

HA staining was considered as high-grade. For HYAL-1, high-grade staining represented 2+ and 3+ staining, whereas low-grade staining included 0 and 1+ staining. For the combined HA–HYAL-1 staining, a positive result was indicated only when both HA (stromal, tumor cells or both) and HYAL-1 staining intensities were of high grade. Any other combination was considered negative. All slides were reviewed out of order, to prevent direct comparison of individual cases for HA and HYAL-1. Two readers independently evaluated all slides in a blinded fashion. Of the 132 total slides (*i.e.*, 66 each for HA and HYAL-1), there was discrepancy in 5 HA slides and 4 HYAL-1 slides. These discrepancies were resolved by both readers reexamining the slides simultaneously. In addition, to check for the repeatability of the evaluation system, a third reader randomly picked 35 slides each from the HA and HYLA1 sets and graded them for staining intensity. The discrepancy in slide evaluations by the third reader was <10%.

*CD34 staining.*Following the antigen retrieval step (as described above), slides were incubated with a mouse antihuman hematopoietic progenitor cell CD34 MAb (dilution 1:20; Dako) at 4°C for 15 hr. Slides were then incubated with a biotinylated antimouse antibody and an avidin-peroxidase conjugate solution (Vectastain ABC Kit; Vector, Burlingame, CA). To visualize peroxidase binding sites, slides were incubated with a DAB chromogen substrate solution (Dako) for 10 min. Slides were counterstained with hematoxylin, dehydrated and mounted.

The method described by Weidner *et al.*[49] was used for scoring the microvessels stained with CD34. The area of the highest MVD in each tissue specimen was localized under ×40 magnification and designated as a "hot spot". Microvessels in the hot spots were counted under ×400 magnification. Any vessel with lumen and endothelial cells or an endothelial cell cluster stained positively for CD34 was considered to be a single countable microvessel. MVD

TABLE II – SENSITIVITY, SPECIFICITY, ACCURACY, PPV AND NPV OF HA, HYAL-1, COMBINED HA–HYAL-1, CD34 AND CD44V6 STAINING INFERENCES

Parameter	HA, HYAL-1 and HA–HYAL-1								
	HA (%)				HYAL-1 (%)				HA-HYAL-1 (%)
	72 months	84 months	100 months	112 months	72 months	84 months	100 months	112 months	72 months
Sensitivity	96 (24/25)	96 (24/25)	92.3 (24/26)	92.6 (25/27)	84 (21/25)	84 (21/25)	84.6 (22/26)	85.2 (23/27)	84 (21/25)
Specificity	61 (25/41)	61.1 (22/36)	65.4 (17/26)	80.6 (16/18)	80.5 (33/41)	80.6 (29/36)	84.6 (22/26)	94.4 (17/18)	87.8 (36/41)
Accuracy	74.2 (49/66)	75.4 (46/61)	78.8 (41/52)	91.1 (41/45)	81.8 (54/66)	82 (50/61)	84.6 (44/52)	88.9 (40/45)	86.4 (57/66)
PPV	60 (24/40)	63.2 (24/38)	77.4 (24/31)	92.6 (25/27)	70 (21/30)	75 (21/28)	84.6 (22/26)	95.8 (23/24)	80.8 (21/26)
NPV	96.1 (25/26)	95.7 (22/23)	89.5 (17/19)	80.6 (16/18)	89.3 (34/37)	87.9 (29/33)	84.6 (22/26)	81 (17/21)	90 (36/40)

count was defined as the mean value of the counts obtained in 3 separate, contiguous but not overlapping areas within the hot spot. A cut-off value was determined using the ROC curve, and according to this value, 2 groups (low and high MVD) were assigned. Microvessels were examined and counted by the 3 readers (S.E., V.B.L. and W.H.C.) independently and without the knowledge of the clinical and pathologic status of the patients. Sections were reviewed out of order, to prevent direct comparison of individual cases for CD34.

CD44v6 staining. Following antigen retrieval, slides were incubated with a mouse antihuman CD44v6 MAb (dilution 1:50; Bender Med Systems, Vienna, Austria) at 4°C for 15 hr. Sections were then incubated with a biotinylated secondary antibody and an avidin-peroxidase conjugate solution (Vectastain ABC Kit). To visualize peroxidase binding sites, slides were incubated with DAB chromogen substrate solution for 10 min. Slides were counterstained with hematoxylin, dehydrated and mounted.

Slides for CD44v6 were scored as described by Ekici *et al.*[38] All sections included normal prostate tissue and/or benign prostatic hyperplasia glands as internal controls. Intensity of staining was graded as 0 for no staining, 1 for weak, 2 for moderate and 3 for strong. A combined staining score based on an estimate of the percentage of tumor cells stained and the intensity of staining was developed. Areas of tumor cells stained with maximum intensity (primary area) and with lesser intensity (secondary area) were determined in percentage values. The combined score was obtained by adding the scores of the primary and secondary areas. Staining intensities were examined and scored by 2 readers (S.E., V.B.L.) independently and in a blinded fashion. A cut-off value was determined from the ROC curve, and according to this value, 2 groups (low and high CD44v6 staining) were assigned.

Statistical analysis

Interassay variability regarding staining intensity was determined by Pearson's correlation analysis. Spearman's bivariate correlation coefficients were 0.85, 0.9, 0.98 and 0.95 for HA, HYAL-1, CD34 and CD44v6 staining, respectively. For all markers, high-grade staining was considered to be a true positive if the patient had biochemical recurrence. Consequently, low-grade staining was considered to be a true negative if the patient had no biochemical recurrence. The sensitivity, specificity, accuracy, PPV and NPV for HA, HYAL-1, HA–HYAL-1, CD34 and CD44v6 staining inferences were calculated using a 2 × 2 contingency table (high-grade/low-grade staining and progressed/nonprogressed PCa patients) at 72, 84, 100 and 112 month cut-off limits. For CD44v6 and MVD, ROC curves were developed for determining the optimal cut-off limits that yielded the best possible sensitivity and specificity values. The cut-off limits for CD44v6 and MVD were 180 and 41, respectively. Sensitivity was defined as true positive (*i.e.,* number of recurred patients predicted by a marker/total number of recurred patients). Specificity was defined as true negative (*i.e.,* number of nonrecurred patients predicted by a marker/total number of nonrecurred patients). Accuracy was determined as follows: (number of true positives + number of true negatives)/total number of PCa patients. PPV was determined as follows: number of true positives/(number of true positives + number of false positives). NPV was determined as follows: number of true negatives/(number of true negatives + number of false negatives). Data on various biochemical, surgical and pathologic

parameters, as well as HA, HYAL-1, HA–HYAL-1, CD34 and CD44v6 staining inferences, were analyzed by the Cox proportional hazards model, using single-variable analysis (univariate analysis) or step-wise selection analysis. Stratified Kaplan-Meier analyses were performed on the variables found to be significant in the multivariate Cox proportional hazards model. For PSA subset analysis, Mantel-Haenszel χ^2 analysis or Student's *t*-test were used to determine statistical significance. Statistical analysis was carried out using the SAS software program (version 8.02; SAS Institute, Cary, NC).

RESULTS

IHC of tissue markers

The HA, HYAL-1, CD44v6 and CD34 antigens were localized in 66 archival PCa specimens obtained from patients who underwent radical retropubic prostatectomy for clinically localized disease. An increase in PSA levels ≥0.4 ng/ml was taken as an indicator of biochemical recurrence. Figure 1 shows IHC localization of HA, HYAL-1, CD44v6 and MVD in 2 Gleason 7 PCa specimens, one each from a nonrecurred (Fig. 1*a,c,e,g*) and a recurred (Fig. 1*b, d,f,h*) patient.

As shown in Figure 1*a,* very little HA staining was seen in PCa tissue from a patient who did not progress within 72 months. Among the 41 PCa specimens from nonrecurred patients, 25 showed low-grade staining. Figure 1*b* shows high-grade HA staining in a PCa specimen from a patient who had biochemical recurrence before 72 months (median time to recurrence 19 months, mean 21.3 months). HA staining was seen mainly in tumor-associated stroma. However, high-grade HA staining was also seen in tumor cells in 8 of 25 specimens from patients who had biochemical recurrence. Among these 8 specimens, 6 showed high-grade staining in tumor-associated stroma. Of the 25 patients who had recurred, 24 showed high-grade HA staining and only 1 showed low-grade staining in both tumor-associated stroma and tumor cells.

An anti-HYAL-1 peptide IgG was used to localize HYAL-1. As shown in Figure 1*c,* little HYAL-1 staining was seen in the PCa tissue from a nonrecurred patient. Of the 41 nonrecurred patients, PCa specimens from 33 had low-grade staining. In the PCa specimen from a patient who later recurred, high-grade HYAL-1 staining was seen (Fig. 1*d*). HYAL-1 expression was seen exclusively in tumor cells. Of the 25 patients who recurred within 72 months, 21 had high-grade HYAL-1 staining.

CD44v6 was localized using an anti-CD44v6 mouse MAb. Contrary to some earlier reports,[38,39] low-grade CD44v6 staining was observed in the PCa specimen from a nonrecurred patient (Fig. 1*e*) and high-grade CD44v6 staining, in the PCa tissue from a recurred patient (Fig. 1*f*). CD44v6 staining was mostly associated with the plasma membrane of tumor cells. We also observed CD44v6 in non-neoplastic epithelial cells in normal prostate and benign prostatic hyperplasia glands. However, the staining intensity of CD44v6 in non-neoplastic cells was less than that in tumor cells. There was a great degree of heterogeneity in CD44v6 staining. For these reasons, we used a semiquantitative method to grade CD44v6 staining.[38] Using a cut-off limit of 180 on the scoring scale, 23 of 41 PCa specimens from nonrecurred patients showed low-grade staining, whereas of the 25 patients who recurred, 17 showed high-grade staining.

| H, HYAL-1 and HA-HYAL-1 | | | CD34 and CD44v6 | | | | | | | |
| HA-HYAL-1 (%) | | | MVD (%) | | | | CD44v6 (%) | | | |
84 months	100 months	112 months	72 months	84 months	100 months	112 months	72 months	84 months	100 months	112 months
84 (21/25)	80.8 (21/26)	81.5 (22/27)	76 (19/25)	76 (19/25)	76.9 (20/26)	77.8 (21/27)	68 (17/25)	68 (17/25)	65.4 (17/26)	62.9 (17/27)
88.9 (32/36)	88.5 (23/26)	94.4 (17/18)	61 (25/41)	61.1 (22/36)	65.4 (17/26)	77.8 (14/18)	56.1 (23/41)	52.8 (19/36)	50 (13/26)	61.1 (11/18)
86.9 (53/61)	84.6 (44/52)	86.7 (39/45)	66.7 (44/66)	67.2 (41/61)	71.1 (37/52)	77.8 (35/45)	57.6 (38/66)	59 (36/61)	57.7 (30/52)	62.2 (28/45)
84 (21/25)	87.5 (21/24)	95.7 (22/23)	54.3 (19/35)	57.6 (19/33)	69 (20/29)	84 (21/25)	48.6 (17/35)	50 (17/34)	56.7 (17/30)	70.8 (17/24)
88.9 (32/36)	85.2 (23/27)	77.3 (17/22)	80.6 (25/31)	78.6 (22/28)	73.4 (17/23)	70 (14/20)	74.2 (23/31)	70.4 (19/27)	59 (13/22)	52.4 (11/21)

It has been shown that visualization and scoring of microvessels using anti-CD34 staining are both sensitive and specific.[47,48,54] We therefore used an anti-CD34 MAb to visualize microvessels in PCa tissues. As shown in Figure 1g, MVD was low in the PCa tissue from a nonrecurred patient. As determined from the ROC curve, a cut-off limit of 41 was set to score low or high MVD. Of the 41 nonrecurred patients, PCa tissues from 25 patients had low MVD. However, MVD was high in 19 of 25 PCa tissues obtained from patients who had a recurrence. Figure 1h shows high MVD in the PCa specimen from a patient who later recurred.

Determination of sensitivity, specificity, accuracy, PPV and NPV

In all patients, a minimum 72-month follow-up was available (mean 103 months, median 104.2 months, range 72–131 months). Therefore, we determined the sensitivity, specificity, accuracy, PPV and NPV of HA, HYAL-1, combined HA–HYAL-1, CD44v6 and MVD at 72, 84, 100 and 112 months of follow-up. As shown in Table II, at 72 months the sensitivity of HA, HYAL-1, combined HA–HYAL-1, CD44v6 and MVD for predicting PCa recurrence was 96%, 84%, 84%, 76% and 68%, respectively. The specificity of HA (61%), CD44v6 (56.1%) and MVD (61%) was lower than that of HYAL-1 (80.5%) and combined HA–HYAL-1 (87.8%). Accuracy was highest for HA–HYAL-1 (86.4%), followed by HYAL-1 (81.8%), HA (74.2%), MVD (66.7%) and CD44v6 (57.6%). Due to higher specificity, the PPV of combined HA–HYAL-1 (80.8%) and HYAL-1 (70%) was high. However, the PPV of CD44v6 was the lowest (48.6%), followed by MVD (54.3%) and HA (60%). Due to high sensitivity, the NPV of HA staining (96.1%) was the highest, followed by HA–HYAL-1 (90%), HYAL-1 (89.3%), MVD (80.6%) and CD44v6 (74.2%) (Table II).

At 84-month follow-up, the cohort consisted of 61 patients (mean follow-up 107.9 months, median 112 months, range 85–131 months), of whom 36 were in the nonrecurred group. Thus, the sensitivity values of all markers remained unchanged at 84 months compared to 72 months (Table II). There was also no significant change in the specificity, accuracy, PPV and NPV values for HA (61.1%, 75.4%, 63.2%, 95.7%), HYAL-1 (80.6%, 82%, 75%, 87.9%), combined HA–HYAL-1 (88.9%, 86.9%, 84%, 88.9%), MVD (61.1%, 67.2%, 57.6%, 78.6%) and CD44v6 (52.8%, 59%, 50% and 70.4%), respectively. At 100 months, follow-up information was available on 52 patients (mean follow-up 117.1 months, median 117.8 months, range 101.6–131 months). Of these 52 patients, one who had been in the nonrecurred category up to the 84-month follow-up showed biochemical recurrence. Interestingly, this patient was scored as a false positive on HYAL-1 and CD34 at 72- and 84-month follow-up. Thus, the sensitivity of both HYAL-1 (84.6%) and CD34 (76.9%) increased slightly, whereas that of HA (92.3%), combined HA–HYAL-1 (80.8%) and CD44v6 (65.4%) decreased (Table II).

Follow-up information beyond 112 months was available for 45 patients (mean follow-up 121 months, median 120.2 months, range 112–131 months). At 112 months, one patient who was a false positive on HA, HYAL-1, combined HA–HYAL-1 and MVD markers up to 100 months showed biochemical recurrence. Thus, the sensitivity of HA, HYAL-1, combined HA–HYAL-1, MVD and CD44v6 was 92.6%, 85.2%, 81.5%, 77.8% and 62.9%, respectively. At final analysis, both HYAL-1 and combined HA–HYAL-1 had the best specificity (94.4%, 94.4%), accuracy

TABLE III – UNIVARIATE ANALYSIS OF PRE- AND POSTOPERATIVE PROGNOSTIC PARAMETERS AND IHC STAINING INFERENCES

Parameter	χ^2	p	Hazard ratio	95% CI[1]
Age	0.4332	0.5104	1.019	0.963–1.078
PSA	11.648	0.0006[1]	1.048	1.02–1.077
Gleason sum (overall)	14.19	0.0002[1]	2.5	1.552–4.024
Gleason ≥7	5.744	0.0165[1]	5.827	1.379–24.633
Clinical stage	1.226	0.2683	1.262	0.836–1.905
EPE	25.411	<0.0001	12.781	4.746–34.42
Surgical margin positivity	13.355	0.0003[1]	4.5	2.008–10.079
Seminal vesicle invasion	22.268	<0.0001	6.56	3.002–14.317
HA	11.319	0.0008[1]	12.091	2.831–51.648
HYAL-1	22.054	<0.0001[1]	13.192	4.5–38.716
HA–HYAL-1	25.364	<0.0001[1]	10.749	4.266–27.087
MVD	10.0314	0.0015[1]	4.36	1.753–10.845
CD44v6	2.277	0.131	1.826	0.835–3.994

[1]Statistically significant. CI, confidence interval. Cox proportional hazards model and single-parameter analysis were used to determine the prognostic significance of preoperative (age, preoperative PSA and clinical stage) and postoperative (Gleason sum overall and ≥ or ≤ 7, margin, EPE, seminal vesicle invasion) parameters and HA, HYAL-1, HA–HYAL-1, MVD and CD44v6 staining inferences.

(88.9%, 86.7%), PPV (95.8%, 95.7%) and NPV (81%, 77.3%), followed by HA (80.6%, 91.1%, 92.6%, 80.6%), MVD (77.8%, 77.8%, 84%, 70%) and CD44v6 (61.1%, 62.2%, 70.8%, 52.4%).

Evaluation of the prognostic capability of pre- and postoperative parameters and histologic markers

Univariate analysis. Since the patients in this cohort had variable follow-up between 72 and 131 months, we used the Cox proportional hazards model and single-parameter analysis to determine the prognostic significance of each of the preoperative (i.e., age, PSA and clinical stage) and postoperative (i.e., Gleason sum, margin, EPE, seminal vesicle invasion) parameters, as well as staining inferences of HA, HYAL-1, combined HA–HYAL-1, CD44v6 and MVD. As shown in Table III, age (p = 0.5104, hazard ratio = 1.019), clinical stage (p = 0.2683, hazard ratio = 1.2620) and CD44v6 staining (p = 0.131, hazard ratio = 1.826) were not significant in predicting biochemical recurrence. However, preoperative PSA (p = 0.0006, hazard ratio/unit PSA change = 1.048), Gleason sum overall (p = 0.0002, hazard ratio = 2.5), margin status (p = 0.0003, hazard ratio = 4.5), EPE (p < 0.0001, hazard ratio = 12.781), seminal vesicle invasion (p < 0.0001, hazard ratio = 6.56), HA staining (p = 0.0008, hazard ratio = 12.091), HYAL-1 staining (p < 0.0001, hazard ratio = 13.192), HA–HYAL-1 staining (p < 0.0001, hazard ratio = 10.749) and MVD (p = 0.0015, hazard ratio = 4.36) significantly predicted biochemical recurrence (Table III). Patients with Gleason sum ≥7 have a greater risk of progression.[42] In single-parameter analysis, the hazard of developing biochemical recurrence in Gleason sum ≥7 patients (p = 0.0165, hazard ratio = 5.827) increased 2.3-fold when all Gleason sums were analyzed together (Table III).

Multivariate analysis. To determine the smallest number of variables that could jointly predict biochemical recurrence in this

TABLE IV – MULTIVARIATE ANALYSIS OF PRE- AND POSTOPERATIVE PROGNOSTIC PARAMETERS AND IHC STAINING INFERENCES

Parameters	HA and HYAL-1 separate				HA–HYAL-1 combined			
	χ^2	p	Hazard ratio	95% CI[1]	χ^2	p	Hazard ratio	95% CI
PSA	16.857	<0.0001[1]	1.086	1.044–1.130	14.127	0.0002[1]	1.077	1.036–1.12
EPE	9.939	0.0016[1]	6.222	1.997–19.384	10.998	0.0009[1]	6.906	2.204–21.640
HYAL-1	11.094	0.0009[1]	8.196	2.377–26.259	9.428	0.0021[1]	5.191	1.814–14.854

Cox proportional hazards model and stepwise selection were used to determine which of the preoperative (*i.e.*, age, PSA and clinical stage) and postoperative (*i.e.*, Gleason sum overall and ≥ or ≤ 7, EPE, margin and seminal vesicle invasion) parameters and HA, HYAL-1, HA–HYAL-1, MVD and CD44v6 staining inferences had independent prognostic significance. Significant parameters (p > 0.05) selected by the model are shown.
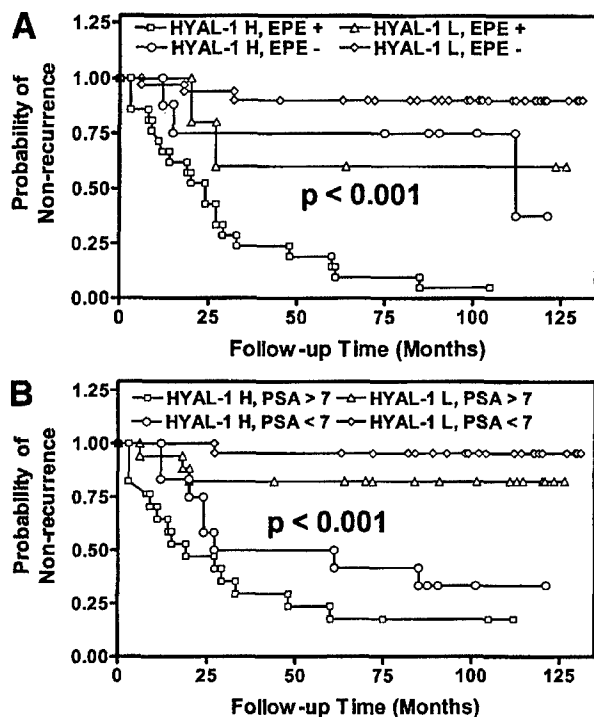[1]Statistically significant. CI, confidence interval.

FIGURE 2 – Kaplan-Meier analysis was performed after stratifying the data as (a) HYAL-1 high (H)/low (L) and EPA[+]/EPA[−] and (b) HYAL-1 high (H)/low (L) and PSA < or > 7 ng/ml.

cohort of patients, we used the Cox proportional hazards model and step-wise selection analysis. When age, preoperative PSA, clinical stage, Gleason sum (overall or ≥7), EPE, seminal vesicle invasion and staining inferences of HA, HYAL-1, CD44v6 and MVD were included in the model, only preoperative PSA (p < 0.0001, hazard ratio/unit PSA change = 1.086), EPE (p = 0.0016, hazard ratio = 6.222) and HYAL-1 (p = 0.0009, hazard ratio = 8.1896) reached statistical significance in predicting biochemical recurrence (Table IV).

To demonstrate the joint effect of HYAL-1 and EPE or HYAL-1 and PSA on biochemical recurrence, we performed Kaplan-Meier analysis. As shown in Figure 2a, the probability of biochemical recurrence was highest when HYAL-1 was high and EPE was positive, and a patient had the lowest probability of recurrence when HYAL-1 was low and EPE was negative. Since PSA was a continuous estimate, with values ranging from 0.5 to 62 ng/ml, for the entire cohort (*n* = 66), we divided the cohort into those with PSA levels <7 and >7 ng/ml, 7 ng/ml PSA being used as the cut-off limit since that was the median value for the entire cohort. As shown in Figure 2b, individuals with HYAL-1 high and PSA > 7 ng/ml had the highest probability of recurrence, followed by

those with HYAL-1 high and PSA < 7 ng/ml. Individuals with low HYAL-1 staining and PSA < 7 ng/ml had the lowest probability of recurrence. These data explain why multivariate analysis selected HYAL-1, EPE and PSA as independent prognostic indicators.

Inclusion of the combined HA–HYAL-1 staining inference instead of HA and HYAL-1 staining inferences in the multiple regression model again showed that preoperative PSA (p = 0.0002, hazard ratio/unit PSA change = 1.077), EPE (p = 0.0009, hazard ratio = 6.906) and HA–HYAL-1 (p = 0.0021, hazard ratio = 5.191) were significant in predicting biochemical recurrence (Table IV). None of the other preoperative (PSA, clinical stage) and postoperative (Gleason sum overall or Gleason stratification ≥ or ≤ 7 and seminal vesicle) parameters or CD44v6 and MVD staining inferences reached statistical significance in the multivariate model (p > 0.05 in each case). Kaplan-Meier analysis using HA–HYAL-1 and EPE or HA–HYAL-1 and PSA demonstrated that individuals with high HA–HYAL-1 and positive EPE or high HA–HYAL-1 and PSA > 7 ng/ml had the highest probability of biochemical recurrence (data not shown).

When HYAL-1 was omitted in the model during stepwise analysis, HA (p = 0.0065, hazard ratio = 8.658) together with preoperative PSA (p = 0.0006, hazard ratio/unit PSA change = 1.079) and EPE (p < 0.0001, hazard ratio = 9.073) were significant in predicting biochemical recurrence. Similarly, when PSA was omitted in the model, margin status reached independent prognostic significance together with EPE and HYAL-1 or HA–HYAL-1 (data not shown).

PSA subgroup analysis. It has been suggested that biochemical recurrence before 24 months indicates systemic disease, whereas biochemical recurrence beyond 24 months suggests local recurrence. To test whether any of the pre- and postoperative parameters as well as IHC markers under study distinguish between these groups, we performed Mantel-Haenszel χ^2 analysis (for testing Gleason sum, Gleason sum ≥ 7, EPE, margin status, seminal vesicle invasion, HA, HYAL-1, combined HA–HYAL-1 CD34 and CD44v6) or Student's *t*-test (for age and preoperative PSA). As shown in Table V, margin status could distinguish between PSA recurrence before and after 24 months (p = 0.269, χ^2 = 4.894); however, none of the other parameters or markers reached statistical significance in this comparison.

DISCUSSION

We compared the prognostic potential of histologic markers HA, HYAL-1, CD44v6 and MVD for predicting biochemical recurrence in PCa patients since their biologic functions are interrelated. For example, HA, an extracellular matrix component, is a high-affinity ligand for CD44.[14,29] HA–CD44 interaction promotes cell adhesion, migration and proliferation.[14,29] HAase degrades HA into small fragments that promote angiogenesis, and MVD is an indicator of angiogenesis.[25,26,41] In addition to their biologic relatedness, each of these histologic markers has shown potential to predict prognosis for PCa patients.[12,19,38,39,47–52]

The prognostic capability of HA staining in tumors varies depending on the tissue where the cancer originates. HA staining in

TABLE V – PSA SUBGROUP ANALYSIS

Parameter	Variable	p
Age	0.66^1	0.513
PSA	1.06^1	0.298
Gleason sum (overall)	0.133^2	0.453
Gleason $\geq$ 7	0.15^2	0.699
Clinical stage	1.903^2	0.168
EPE	0.736^2	0.391
Surgical margin positivity	4.894^2	0.0269*
Seminal vesicle invasion	0.122^2	0.7265
HA	0.15^2	0.699
HYAL-1	0.280^2	0.596
HA–HYAL-1	0.0437^2	0.834
MVD	1.322^2	0.25
CD44v6	1.102^2	0.294

[1]The ability of PSA and age to predict PSA recurrence within 24 months was determined using the t-test (since these were continuous variables).– [2]Mantel-Haenszel χ^2 analysis was used to evaluate the ability of clinical stage, post- operative parameters and IHC staining markers to predict PSA recurrence within 24 months.

tumor-associated stroma and/or tumor cells has prognostic capability in breast, colon and gastrointestinal cancers; however, it does not have independent prognostic capability in PCa.[13–19] We found that the HA staining had 92.3% sensitivity and 80.6% specificity to predict biochemical recurrence within 112 months. Interestingly, the specificity of HA staining to predict biochemical recurrence increased from 61% at 72-month follow-up to 80.6% at 112-month follow-up. We have previously shown that at 64-month follow-up, although HA staining had high sensitivity (96%), the specificity of this marker to predict biochemical recurrence was even lower (55.5%) compared to that at 72 months.[12] These results indicate that positive HA staining in PCa tissues means that the patient could have a recurrence within 112 months. In this and a previous study, we found that HA staining shows prognostic capability in univariate analysis; however, it is not an independent predictor of biochemical recurrence. Interestingly, however, if HYAL-1 staining inference is not included in the Cox proportional hazards model during stepwise analysis, HA together with preoperative PSA and EPE reaches independent prognostic significance. These results indicate that HYAL-1 provides all of the prognostic information supplied by HA staining, as well as some additional information. However, although there was <10% discrepancy between 3 readers who evaluated the HA and HYAL-1 staining, at present we do not know the repeatability of the staining evaluation system in another laboratory. Therefore, more studies need to be conducted to verify that HYAL-1 is a better prognostic indicator than HA in predicting biochemical recurrence for PCa patients. Nonetheless, the evaluation system, which involves grading of HA staining as high when tumor-associated stroma and/or tumor cells show high-grade staining and as low when tumor-associated stroma and/or tumor cells show low-grade staining, appears to be accurate. This is because the prognostic significance of HA staining, and consequently of HA–HYAL-1 staining, in both univariate and multivariate analyses remained unchanged when the 2 specimens in which HA staining was low-grade in tumor-associated stroma but high-grade in tumor cells were graded as low-grade instead of high-grade (unpublished results).

The prognostic significance of the CD44 standard form and its variant isoforms (e.g., CD44v6) is unclear. Contrary to our finding that CD44v6 expression was elevated in patients who later had biochemical recurrence, 2 reports showed that a decrease in CD44v6 expression correlated with increased Gleason sum and disease progression.[38,39] For example, Ekici et al.[38] showed that CD44v6 expression inversely correlates with pathologic stage and disease progression and positively correlates with PSA-free survival. However, in that study, CD44v6 was not an independent predictor of prognosis. Contrary to the findings of Ekici et al.,[38] Aaltomaa et al.[39] found that CD44v6 is an independent predictor of survival. In the present study, increased CD44v6 expression had

reasonable sensitivity to predict prognosis at 72-month (68%) or 112-month (62.9%) follow-up. However, among all of the markers, it had the lowest specificity (56.1% at 72 months and 61.1% at 112 months) to predict biochemical recurrence. This low specificity may explain why CD44v6 staining is not significant in predicting biochemical recurrence in both univariate and multivariate analyses. A likely explanation of why different studies report conflicting results regarding CD44v6 staining and prognosis for PCa is that PCa tissues have a high degree of heterogeneity with respect to CD44v6 staining. Aaltomaa et al.[39] reported variability in CD44v6 staining intensity and in the number of tumor cells that were positive for CD44v6. Similarly, Ekici et al.[38] reported the heterogeneous nature of CD44v6 expression and developed a semiquantitative method for scoring CD44v6 staining. We used this scoring method to evaluate CD44v6 staining. Nonetheless, it is likely that the heterogeneous nature of CD44v6 will limit its prognostic significance.

Determination of MVD in PCa tissues, using anti-CD34 antibodies, is sensitive and accurate in predicting prognosis.[47,48,54] Although problems exist in the methods of counting the vessels and in setting a universally accepted cut-off limit for MVD to predict recurrence, MVD has been correlated with Gleason sum, pathologic stage and outcome.[47–49] However, other studies have shown that MVD does not correlate with tumor grade, stage and clinical outcome.[50–52] In our study, MVD at a cut-off limit of 41 showed reasonably high sensitivity at both 72-month (76%) and 112-month (77.8%) follow-up. The specificity of MVD to predict biochemical recurrence increased from 61% at 72-month follow-up to 77.8% at 112-month follow-up, suggesting that in some false-positive patients high MVD may be indicative of biochemical recurrence before 112 months. Although in the univariate analysis MVD showed prognostic significance (Table III), in the multivariate analysis it had no additional prognostic significance. MVD did not reach independent prognostic significance even when HA alone, in the absence of HYAL-1, was included in the Cox model. It is possible that since HA, HYAL-1 and MVD are biologically related, all of the prognostic information provided by MVD inferences is contained in either HA or HYAL-1 staining inferences.

In our study, HYAL-1 staining alone had high sensitivity both at 72-month (84%) and at or beyond 112-month (85.2%) follow-up. Indeed, it had either the same or slightly higher sensitivity to predict biochemical recurrence as the combined HA–HYAL-1 staining inference (84% at 72 months and 81.5% at 112 months). The specificity of HYAL-1 staining inference (80.5%) at 72-month follow-up was slightly lower than that of HA–HYAL-1 (87.8%). However, HYAL-1 and HA–HYAL-1 staining inferences had the same specificity (94.4%) to predict biochemical recurrence at 112 months and beyond. Therefore, HYAL-1 either has the same or slightly better PPV and NPV to predict biochemical recurrence. Thus, contrary to our earlier report that combined HA–HYAL-1 has slightly better prognostic capability than HYAL-1 staining alone at 64 months,[12] our present study suggests that HYAL-1 alone is sufficiently accurate to predict biochemical recurrence at 72 months and beyond.

In the multivariate analysis, among all of the pre- and postoperative parameters and histologic markers, only preoperative PSA and EPE had additional prognostic significance if HYAL-1 (or HA–HYAL-1) was included in the analysis. In an earlier study, we found that EPE, margin status and HYAL-1 (or HA–HYAL-1) were independent predictors of prognosis. The difference between that study[12] and this is that in the earlier study we used 64-month follow-up as a cut-off limit and performed Wald's forward stepwise regression analysis, whereas in the present study we used the Cox proportional hazards model and stepwise selection to calculate the hazard of biochemical recurrence over the entire period of follow-up (i.e., up to 131 months). Interestingly, when preoperative PSA was not included in the model, margin status reached independent prognostic significance together with EPE and

HYAL-1 (or HA–HYAL-1), suggesting that preoperative PSA provides all of the prognostic information related to margin status plus some additional information. Nonetheless, HYAL-1 appears to be an independent prognostic indicator for predicting biochemical recurrence.

As is the case for HA expression in tumor tissues, the prognostic significance of HYAL-1 expression may also vary based on the origin of cancer tissue. For example, in bladder cancer, HYAL-1 expression correlates with tumor grade.[21] Also, HAase levels are elevated in brain metastases of carcinomas compared to primary glioblastomas.[55] Furthermore, brain metastasis-derived cell lines have 1,000-fold more HAase than glioma-derived cell lines.[55] HYAL-1 levels are also elevated in the saliva of patients with squamous cell carcinoma of the head and neck.[24] However, HA accumulation without HAase activation has been associated with aggressiveness of ovarian cancer.[56] Similarly, HYAL-1 expression suppresses tumor growth in a rat colon carcinoma model.[57] However, HYAL-1 expression in PC-3 cells (a PCa cell line) increases their metastatic potential.[58] Thus, HYAL-1 expression is associated with PCa progression.

The major dilemma for clinicians in the management of PCa is the identification of the site of disease recurrence, which ultimately guides therapy decisions. It is generally accepted that PSA recurrence within 1–2 years relates to a higher risk of developing metastatic disease.[9,59] However, it is not understood whether existing pre- and postoperative parameters as well as histologic markers can distinguish between patients who will recur within 24 months and those who will not. In our study, PSA subset analysis showed that, except for margin status, none of the markers (*i.e.,* HA, HYAL-1, HA–HYAL-1, MVD and CD44v6) and preoperative (*i.e.,* age, clinical stage and preoperative PSA) and postoperative (*i.e.,* Gleason sum overall or ≥ 7, EPE, seminal vesicle invasion) was able to distinguish between patients who recurred within 24 months and those who did not. In this cohort, we had 25 patients who recurred within 72 months, of whom 17 (68%) recurred within 24 months and 3 more recurred at 27 months (mean time to recur for the entire cohort 21.3 months). Thus, the ability of various clinical and pathologic parameters as well as histologic markers to predict biochemical recurrence within 24 months may need to be studied in a larger group of biochemically recurred patients.

Nearly two-thirds of PCa patients have preoperative PSA levels of 4–10 ng/ml, stage T1C disease and a biopsy Gleason of 5–7.[2,10,11] For such patients, one or a combination of accurate prognostic indicators could improve the physicians' ability to identify PCas that are aggressive and will progress so that individualized treatments could be offered. In our study, although preoperative PSA was an independent predictor for prognosis, neither the overall Gleason sum nor Gleason sum $\leq$ or ≥ 7 was an independent predictor for prognosis. Among the 4 potential prognostic indicators for PCa that we compared, HYAL-1 appears to be an accurate and independent predictor.

ACKNOWLEDGEMENTS

REFERENCES

1. Khan MA, Han M, Partin AW, Epstein JI, Walsh PC. Long-term cancer control of radical prostatectomy in men younger than 50 years of age: update 2003. Urology 2003;62:86–92.
2. Draisma G, Boer R, Otto SJ, van der Cruijsen IW, Damhuis RA, Schröder FH, de Koning HJ. Lead times and overdetection due to prostate-specific antigen screening: estimates from the European Randomized Study of Screening for Prostate Cancer. J Natl Cancer Inst 2003;95:868–78.
3. Palisaar RJ, Graefen M, Karakiewicz PI, Hammerer PG, Huland E, Haese A, Fernandez S, Erbersdobler A, Henke RP, Huland H. Assessment of clinical and pathologic characteristics predisposing to disease recurrence following radical prostatectomy in men with pathologically organ-confined prostate cancer. Eur Urol 2002;41:155–61.
4. Pound CR, Partin AW, Epstein JI, Walsh PC. Prostate-specific antigen after anatomic radical retropubic prostatectomy. Patterns of recurrence and cancer control. Urol Clin North Am 1997;24:395–406.
5. Neulander EZ, Soloway MS. Failure after radical prostatectomy. Urology 2003;61:30–6.
6. Symon Z, Griffith KA, McLaughlin PW, Sullivan M, Sandler HM. Dose escalation for localized prostate cancer: substantial benefit observed with 3D conformal therapy. Int J Radiat Oncol Biol Phys 2003;57:384–90.
7. Syed S, Petrylak DP, Thompson IM. Management of high-risk localized prostate cancer: the integration of local and systemic therapy approaches. Urol Oncol 2003;21:235–43.
8. Moul JW. Variables in predicting survival based on treating "PSA-only" relapse. Urol Oncol 2003;21:292–304.
9. Swindle PW, Kattan MW, Scardino PT. Markers and meaning of primary treatment failure. Urol Clin North Am 2003;30:377–401.
10. Blute ML, Bergstralh EJ, Iocca A, Scherer B, Zincke H. Use of Gleason score, prostate specific antigen, seminal vesicle and margin status to predict biochemical failure after radical prostatectomy. J Urol 2001;165:119–25.
11. Pettaway CA. Prognostic markers in clinically localized prostate cancer. Tech Urol 1998;4:35–42.
12. Posey JT, Soloway MS, Ekici S, Sofer M, Civantos F, Duncan RC, Lokeshwar VB. Evaluation of the prognostic potential of hyaluronic acid and hyaluronidase (HYAL-1) for prostate cancer. Cancer Res 2003;63:2638–44.
13. Tammi MI, Day AJ, Turley EA. Hyaluronan and homeostasis: a balancing act. J Biol Chem 2002;277:4581–4.
14. Turley EA, Noble PW, Bourguignon LY. Signaling properties of hyaluronan receptors. J Biol Chem 2002;277:4589–92.
15. Setälä LP, Tammi MI, Tammi RH, Eskelinen MJ, Lipponen PK, Ågren UM, Parkkinen J, Alhava EM, Kosma V-M. Hyaluronan expression in gastric cancer cells is associated with local and nodal spread and reduced survival rate. Br J Cancer 1999;79:1133–8.
16. Auvinen P, Tammi R, Parkkinen J, Tammi M, Ågren U, Johansson R, Hirvikoski P, Eskelinen M, Kosma V-M. Hyaluronan in peritumoral stroma and malignant cells associates with breast cancer spreading and predicts survival. Am J Pathol 2000;156:529–36.
17. Knudson W. Tumor-associated hyaluronan. Providing an extracellular matrix that facilitates invasion. Am J Pathol 1996;148:1721–6.
18. Ropponen K, Tammi M, Parkkinen J, Eskelinen M, Tammi R, Lipponen P, Ågren U, Alhava E, Kosma V-M. Tumor cell–associated hyaluronan as an unfavorable prognostic factor in colorectal cancer. Cancer Res 1998;58:342–7.
19. Lipponen P, Aaltomaa S, Tammi R, Tammi M, Ågren U, Kosma V-M. High stromal hyaluronan level is associated with poor differentiation and metastasis in prostate cancer. Eur J Cancer 2001;37:849–56.
20. Lokeshwar VB, Öbek C, Pham HT, Wei D, Young MJ, Duncan RC, Soloway MS, Block NL. Urinary hyaluronic acid and hyaluronidase: markers for bladder cancer detection and evaluation of grade. J Urol 2000;163:348–56.
21. Hautmann SH, Lokeshwar VB, Schroeder GL, Civantos F, Duncan RC, Gnann R, Friedrich MG, Soloway MS. Elevated tissue expression of hyaluronic acid and hyaluronidase validates the HA-HAase urine test for bladder cancer. J Urol 2001;165:2068–74.
22. Lokeshwar VB, Rubinowicz D, Schroeder GL, Forgacs E, Minna JD, Block NL, Nadji M, Lokeshwar BL. Stromal and epithelial expression of tumor markers hyaluronic acid and HYAL-1 hyaluronidase in prostate cancer. J Biol Chem 2001;276:11922–32.
23. Csoka AB, Frost GI, Stern R. The six hyaluronidase-like genes in the human and mouse genomes. Matrix Biol 2001;20:499–508.
24. Franzmann EJ, Schroeder GL, Goodwin WJ, Weed DT, Fisher P, Lokeshwar VB. Expression of tumor markers hyaluronic acid and hyaluronidase (HYAL-1) in head and neck tumors. Int J Cancer 2003;106:438–45.
25. West DC, Hampson IN, Arnold F, Kumar S. Angiogenesis induced by degradation products of hyaluronic acid. Science 1985;228:1324–6.
26. Lokeshwar VB, Selzer MG. Differences in hyaluronic acid–mediated functions and signaling in arterial, microvessel, and vein-derived human endothelial cells. J Biol Chem 2000;275:27641–9.
27. Pham HT, Block NL, Lokeshwar VB. Tumor-derived hyaluronidase: a diagnostic urine marker for high-grade bladder cancer. Cancer Res 1997;57:778–83.
28. Kumar S, West DC, Ponting JM, Gattamaneni HR. Sera of children with renal tumours contain low-molecular-mass hyaluronic acid. Int J Cancer 1989;44:445–8.

29. Lesley J, Hascall VC, Tammi M, Hyman R. Hyaluronan binding by cell surface CD44. J Biol Chem 2000;275:26967–75.
30. Cichy J, Pure E. The liberation of CD44. J Cell Biol 2003;161:839–43.
31. Naor D, Nedvetzki S, Golan I, Melnik L, Faitelson Y. CD44 in cancer. Crit Rev Clin Lab Sci 2002;39:527–79.
32. Lokeshwar VB, Fregien N, Bourguignon LY. Ankyrin-binding domain of CD44(GP85) is required for the expression of hyaluronic acid–mediated adhesion function. J Cell Biol 1994;126:1099–109.
33. Lokeshwar VB, Iida N, Bourguignon LY. The cell adhesion molecule, GP116, is a new CD44 variant (ex14/v10) involved in hyaluronic acid binding and endothelial cell proliferation. J Biol Chem 1996;271:23853–64.
34. Lokeshwar BL, Lokeshwar VB, Block NL. Expression of CD44 in prostate cancer cells: association with cell proliferation and invasive potential. Anticancer Res 1995;15:1191–8.
35. Welsh CF, Zhu D, Bourguignon LY. Interaction of CD44 variant isoforms with hyaluronic acid and the cytoskeleton in human prostate cancer cells. J Cell Physiol 1995;164:605–12.
36. Iczkowski KA, Bai S, Pantazis CG. Prostate cancer overexpresses CD44 variants 7–9 at the messenger RNA and protein level. Anticancer Res 2003;23:3129–40.
37. Gao AC, Lou W, Sleeman JP, Isaacs JT. Metastasis suppression by the standard CD44 isoform does not require the binding of prostate cancer cells to hyaluronate. Cancer Res 1998;58:2350–2.
38. Ekici S, Ayhan A, Kendi S, Özen H. Determination of prognosis in patients with prostate cancer treated with radical prostatectomy: prognostic value of CD44v6 score. J Urol 2002;167:2037–41.
39. Aaltomaa S, Lipponen P, Ala-Opas M, Kosma V-M. Expression and prognostic value of CD44 standard and variant v3 and v6 isoforms in prostate cancer. Eur Urol 2001;39:138–44.
40. Sato Y. Molecular diagnosis of tumor angiogenesis and anti-angiogenic cancer therapy. Int J Clin Oncol 2003;8:200–6.
41. Sullivan DC, Bicknell R. New molecular pathways in angiogenesis. Br J Cancer 2003;89:228–31.
42. Folkman J, Browder T, Palmblad J. Angiogenesis research: guidelines for translation to clinical application. Thromb Haemost 2001;86:23–33.
43. Sauer G, Deissler H. Angiogenesis: prognostic and therapeutic implications in gynecologic and breast malignancies. Curr Opin Obstet Gynecol 2003;15:45–9.
44. Goddard JC, Sutton CD, Furness PN, O'Byrne KJ, Kockelbergh RC. Microvessel density at presentation predicts subsequent muscle invasion in superficial bladder cancer. Clin Cancer Res 2003;9:2583–6.
45. Poon RT, Fan ST, Wong J. Clinical significance of angiogenesis in gastrointestinal cancers: a target for novel prognostic and therapeutic approaches. Ann Surg 2003;238:9–28.
46. Zhang X, Yamashita M, Uetsuki H, Kakehi Y. Angiogenesis in renal cell carcinoma: evaluation of microvessel density, vascular endothelial growth factor and matrix metalloproteinases. Int J Urol 2002;9:509–14.
47. de la Taille A, Katz AE, Bagiella E, Buttyan R, Sharir S, Olsson CA, Burchardt T, Ennis RD, Rubin MA. Microvessel density as a predictor of PSA recurrence after radical prostatectomy. A comparison of CD34 and CD31. Am J Clin Pathol 2000;113:555–62.
48. Bono AV, Celato N, Cova V, Salvadore M, Chinetti S, Novario R. Microvessel density in prostate carcinoma. Prostate Cancer Prostatic Dis 2002;5:123–7.
49. Weidner N, Carroll PR, Flax J, Blumenfeld W, Folkman J. Tumor angiogenesis correlates with metastasis in invasive prostate carcinoma. Am J Pathol 1993;143:401–9.
50. Silberman MA, Partin AW, Veltri RW, Epstein JI. Tumor angiogenesis correlates with progression after radical prostatectomy but not with pathologic stage in Gleason sum 5 to 7 adenocarcinoma of the prostate. Cancer 1997;79:772–9.
51. Gettman MT, Bergstralh EJ, Blute M, Zincke H, Bostwick DG. Prediction of patient outcome in pathologic stage T2 adenocarcinoma of the prostate: lack of significance for microvessel density analysis. Urology 1998;51:79–85.
52. Rubin MA, Buyyounouski M, Bagiella E, Sharir S, Neugut A, Benson M, de la Taille A, Katz AE, Olsson CA, Ennis RD. Microvessel density in prostate cancer: lack of correlation with tumor grade, pathologic stage, and clinical outcome. Urology 1999;53:542–7.
53. Tengblad A. Affinity chromatography on immobilized hyaluronate and its application to the isolation of hyaluronate binding properties from cartilage. Biochim Biophys Acta 1979;578:281–99.
54. Norrby K, Ridell B. Tumour-type-specific capillary endothelial cell stainability in malignant B-cell lymphomas using antibodies against CD31, CD34 and factor VIII. APMIS 2003;111:483–9.
55. Delpech B, Laquerriere A, Maingonnat C, Bertrand P, Freger P. Hyaluronidase is more elevated in human brain metastases than in primary brain tumours. Anticancer Res 2002;22:2423–7.
56. Hiltunen EL, Anttila M, Kultti A, Ropponen K, Penttinen J, Yliskoski M, Kuronen AT, Juhola M, Tammi R, Tammi M, Kosma VM. Elevated hyaluronan concentration without hyaluronidase activation in malignant epithelial ovarian tumors. Cancer Res 2002;62:6410–3.
57. Jacobson A, Rahmanian M, Rubin K, Heldin P. Expression of hyaluronan synthase 2 or hyaluronidase 1 differentially affect the growth rate of transplantable colon carcinoma cell tumors. Int J Cancer 2002;102:212–9.
58. Patel S, Turner PR, Stubberfield C, Barry E, Rohlff CR, Stamps A, McKenzie E, Young K, Tyson K, Terrett J, Box G, Eccles S, Page MJ. Hyaluronidase gene profiling and role of hyal-1 overexpression in an orthotopic model of prostate cancer. Int J Cancer 2002;97:416–24.
59. Canto EI, Shariat SF, Slawin KM. Biochemical staging of prostate cancer. Urol Clin North Am 2003;30:263–77.

HYAL1 Hyaluronidase: A Molecular Determinant of Bladder Tumor Growth and Invasion

Vinata B. Lokeshwar,[1,2,4] Wolfgang H. Cerwinka,[1] and Bal L. Lokeshwar[1,3,4]

Departments of [1]Urology, [2]Cell Biology and Anatomy, and [3]Radiation Oncology and [4]Sylvester Comprehensive Cancer Center, University of Miami Miller School of Medicine, Miami, Florida

Abstract

Hyaluronic acid and HYAL1-type hyaluronidase show high accuracy in detecting bladder cancer and evaluating its grade, respectively. Hyaluronic acid promotes tumor progression; however, the functions of hyaluronidase in cancer are largely unknown. In this study, we stably transfected HT1376 bladder cancer cells with HYAL1-sense (HYAL1-S), HYAL1-antisense (HYAL1-AS), or vector cDNA constructs. Whereas HYAL1-S transfectants produced 3-fold more HYAL1 than vector transfectants, HYAL1-AS transfectants showed ~90% reduction in HYAL1 production. HYAL1-AS transfectants grew four times slower than vector and HYAL1-S transfectants and were blocked in the G_2-M phase of the cell cycle. The expression of cdc25c and cyclin B1 and cdc2/p34-associated H1 histone kinase activity also decreased in HYAL1-AS transfectants. HYAL1-S transfectants were 30% to 44% more invasive, and HYAL1-AS transfectants were ~50% less invasive than the vector transfectants *in vitro*. In xenografts, there was a 4- to 5-fold delay in the generation of palpable HYAL1-AS tumors, and the weight of HYAL1-AS tumors was 9- to 17-fold less than vector and HYAL1-S tumors, respectively ($P < 0.001$). Whereas HYAL1-S and vector tumors infiltrated skeletal muscle and blood vessels, HYAL1-AS tumors resembled benign neoplasia. HYAL1-S and vector tumors expressed significantly higher amounts of HYAL1 (in tumor cells) and hyaluronic acid (in tumor-associated stroma) than HYAL1-AS tumors. Microvessel density in HYAL1-S tumors was 3.8- and 9.5-fold higher than that in vector and HYAL1-AS tumors, respectively. These results show that HYAL1 expression in bladder cancer cells regulates tumor growth and progression and therefore serves as a marker for high-grade bladder cancer. (Cancer Res 2005; 65(6): 2243–50)

Introduction

Bladder tumors, particularly transitional cell carcinomas, show heterogeneity in their ability to invade and metastasize (1–4). For example, low-grade bladder tumors rarely progress, whereas about two-thirds of high-grade tumors are detected at stages $\geq$T1 (i.e., invading lamina propria and beyond; ref. 5). Muscle invasion by a bladder tumor indicates poor prognosis, as 50% of patients develop metastases within 2 years and 60% die within 5 years regardless of treatment (6). Certain molecular markers, such as hyaluronidase, have been identified as highly sensitive and specific markers for detecting high-grade (i.e., grade 2 and 3) bladder cancer (7, 8).

However, the functions of hyaluronidase (if any) in bladder tumor growth and/or invasion are unknown.

Hyaluronic acid is the substrate of hyaluronidase. It is a glycosaminoglycan made up of repeating disaccharide units, D-glucuronic acid, and N-acetyl-D-glucosamine (9). Hyaluronic acid is normally present in tissues and body fluids. Hyaluronic acid keeps tissues hydrated in an osmotically balanced environment (10). It also regulates cell proliferation, migration, and adhesion by interacting with cell surface hyaluronic acid receptors, such as CD44 (11). Concentrations of hyaluronic acid are elevated in cancers of the breast, colon, prostate, bladder, etc. (8, 12–18). In tumor tissues, elevated hyaluronic acid is mostly localized to tumor stroma; however, in some tumors, including bladder cancer, it is also expressed in tumor cells (12–18). We have shown previously that hyaluronic acid levels are elevated in the urine of bladder cancer patients regardless of the tumor grade (8, 19). Thus, the measurement of urinary hyaluronic acid levels (hyaluronic acid test) has 83% sensitivity and 90% specificity for detecting bladder cancer (8). In tumor tissues, hyaluronic acid swells on hydration and opens up spaces for tumor cell migration, and tumor cells migrate on hyaluronic acid–rich matrix by interacting with hyaluronic acid receptors (10, 11). A hyaluronic acid coat around tumor cells causes a partial loss of contact-mediated growth and migration and offers protection against immune surveillance (20–23). Small fragments of hyaluronic acid (i.e., 3-25 disaccharide units) are angiogenic (24, 25). We have isolated previously such small fragments from the urine of grade 2/3 bladder cancer patients, high-grade prostate cancer tissues, and saliva of head and neck cancer patients (18, 19, 26).

Small fragments of hyaluronic acid are generated by limited digestion of the hyaluronic acid polymer with hyaluronidase. Hyaluronidase levels have been shown to be elevated in cancers of the prostate, bladder, and head and neck cancer and in breast tumors and malignant glioma (7, 19, 26–32). For example, we have shown that urinary hyaluronidase levels measured using an ELISA-like assay (hyaluronidase test) is a highly sensitive (81% sensitivity) and specific (83.8% specificity) marker for detecting grade 2 and 3 bladder tumors (7, 8). Elevated hyaluronidase levels also seem to be a sensitive marker for detecting head and neck cancer (26). We partially purified and characterized the first tumor-derived hyaluronidase from the urine of high-grade bladder cancer patients and showed its identity to HYAL1 (33). Subsequently, we showed HYAL1 expression in several invasive bladder, prostate, and head and neck tumor cell lines (18, 26, 33). For example, we analyzed HYAL1 expression and hyaluronidase secretion in 11 bladder cancer cell lines (33). Among these, HT1376 cells secrete the highest amount of hyaluronidase activity (32 ± 2.4 mU/mg protein) in their conditioned medium, and HYAL1 is the major hyaluronidase expressed in these cells. We showed recently that HYAL1 expression in radical prostatectomy specimens is an independent predictor of biochemical recurrence in prostate cancer patients

(27, 34). In tumor cells, the expression of enzymatically active HYAL1 seems to be regulated by alternative mRNA splicing (35–37).

Jacobson et al. reported recently that overexpression of HYAL1 in a rat colon cancer line suppresses tumor growth in xenografts (38). Contrarily, Victor et al. showed that passage of a human breast cancer line CAL 51 from the primary state to metastatic stage increases hyaluronidase production (39). Expression of HYAL1 in a prostate cancer line that produces little hyaluronidase did not affect tumor growth but caused a slight increase in lung metastasis (40). Thus, the functional significance of HYAL1 expression in human tumor cells, which normally express HYAL1, is still unknown.

At present, it is also unknown whether HYAL1 is only a marker for more aggressive bladder cancer or it also functions as one of the molecular determinants that control bladder tumor growth and invasion. In this study, we examined the function of HYAL1 in bladder tumor growth, invasion, and angiogenesis using HYAL1-antisense (HYAL1-AS) transfection to block HYAL1 expression and HYAL1-sense (HYAL1-S) cDNA transfection to overexpress HYAL1.

Materials and Methods

Construction of HYAL1-S and HYAL1-AS cDNA Constructs. HYAL1 cDNA containing the entire coding region was amplified by reverse transcription-PCR analysis and cloned into a eukaryotic expression vector, pcDNA3.1/v5-His TOPO, using a TOPO-TA cloning kit (Invitrogen, Carlsbad, CA; ref. 35). The TOPO-TA cloning allowed bidirectional cloning of the HYAL1 cDNA insert with respect to the cytomegalovirus promoter (i.e., HYAL1-S and HYAL1-AS cDNA constructs). HYAL1-S, HYAL1-AS, and vector cDNA constructs were used for transfection studies.

Generation of HYAL1 Transfectants. HT1376, a transitional cell carcinoma of the bladder cell line, was cultured in RPMI 1640 containing 10% fetal bovine serum and gentamicin (growth medium). HT1376 cells (2×10^5 per 6 cm dish) were transfected with 5 µg of vector, HYAL1-S, or HYAL1-AS cDNA constructs using the Superfect transfection reagent (Qiagen, Valencia, CA). The transfectants were selected in growth medium containing 200 µg/mL geneticin (Invitrogen).

Analysis of Hyaluronidase Activity by Hyaluronidase ELISA-Like Assay. Hyaluronidase activity in serum-free conditioned medium of transfectants (1×10^6 cells) was assayed using the hyaluronidase ELISA-like assay (7, 8, 33). Hyaluronidase activity (mU/mL) was normalized to total protein concentration (mg/mL) and was expressed as mU/mg.

Substrate (Hyaluronic Acid)-Gel Assay. Conditioned media from HT1376 transfectants (secreted by 5×10^4 cells, ~10 µg total protein) were separated on a substrate (hyaluronic acid)-gel. Following incubation in a hyaluronidase assay buffer, the gel was stained and destained to visualize active hyaluronidase species (7, 18).

Immunoblot Analysis. Conditioned media from the transfectant clones (5×10^4 cells, ~10 µg total protein) were immunoblotted using an anti-HYAL1 peptide IgG (i.e., anti-HYAL1 IgG) as described previously (18, 33). Cell lysates (4×10^4 cells per transfectant) were subjected to immunoblot analysis using the following primary antibodies: 1 µg/mL mouse anti–cyclin B1 IgG (clone GNS1, Neomarkers, Labvision, Fremont, CA), 1 µg/mL mouse anti-cdc2/p34 IgG (clone A27.1.1 with POH-1), or 0.2 µg/mL rabbit anti-cdc25c IgG (C-20, Santa Cruz Biotechnology, Inc., Santa Cruz, CA). Protein loading was evaluated by reprobing the blots with mouse anti-actin IgG (Neomarkers).

Cell Proliferation Assay. HT1376 transfectants (2×10^4 cells per well) were plated on 24-well culture plates in growth medium with geneticin. Every 24 hours for a total period of 5 days (0-120 hours), cells were trypsinized and counted following trypan blue staining. Counts were obtained from triplicate wells in two independent experiments.

Cell Cycle Analysis. HT1376 transfectant cultures (60% confluence) were lysed in a propidium iodide dye solution (0.1% sodium citrate, 0.4% NP40, and 25 µg/mL propidium iodide) and analyzed in an EPICS XL flow cytometer equipped with a long pass red filter, FL3 (630 nm). The FL3 histograms were analyzed for estimating cell cycle phase distribution by

Modift Easy (Lite) program (Veritas Software, Mountainview, CA; ref. 41). All samples were assayed in duplicates in two independent experiments.

Immunoprecipitation and Kinase Assay. HT1376 transfectant cells (1×10^6) were solubilized in a lysis buffer and immunoprecipitated using 2 µg/mL mouse anti-cdc2/p34 IgG and protein A agarose (Sigma-Aldrich, St. Louis, MO). In control samples, the primary antibody was excluded. The immunoprecipitates were incubated with histone H1 in a hot kinase solution (2.5 µg H1 histone, 5 µmol/L ATP, 5 µCi [γ-^{32}P]ATP in kinase buffer) at 37°C for 30 minutes. Histone H1 was analyzed by 12% SDS-PAGE and autoradiography (42).

Analysis of Apoptosis. Forty-eight-hour cultures of transfectants (10^5 cells per 24-well plate) were lysed and the cell lysates were tested for free nucleosome release using the Cell Death ELISA kit (Roche Diagnostics, Pleasanton, CA). All samples were assayed in triplicates in two independent experiments.

Matrigel Invasion Assay. The membranes in 12-well Transwell plates (Corning-Costar, Corning, NY) were coated with Matrigel (100 µg/cm^2) or Matrigel with hyaluronic acid (50 µg/mL) in serum-free medium. HT1376
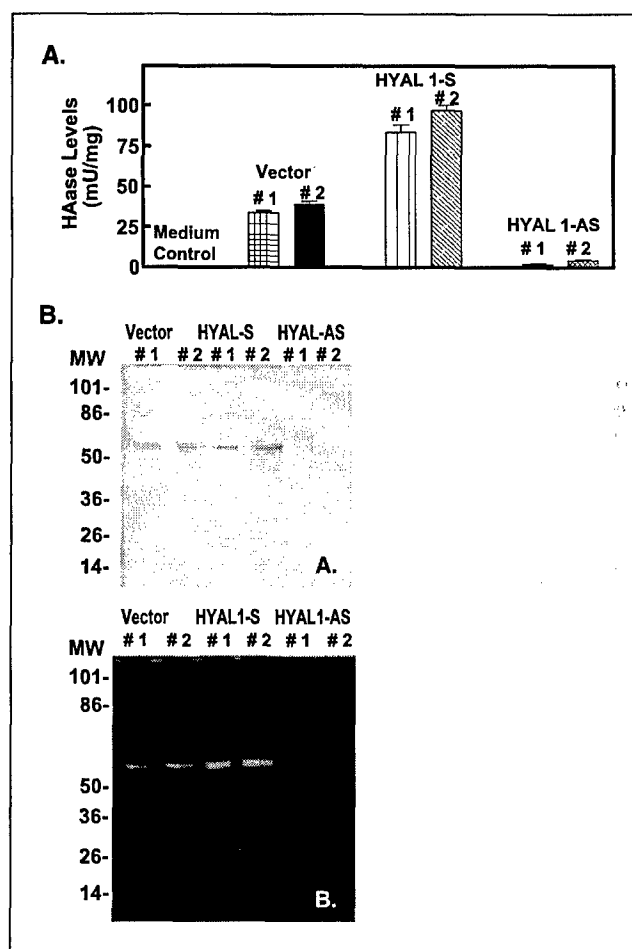

Figure 1. Analysis of HYAL1 expression in HT1376 transfectants. *A,* measurement of hyaluronidase (*HAase*) activity. *Columns,* mean hyaluronidase activity (mU/mg) from three separate experiments; *bars,* SE. *B,* immunoblot analysis using anti-HYAL1 IgG. Conditioned media (10 µg protein; conditioned medium of 5×10^4 cells) from each transfectant clone were subjected to anti-HYAL1 IgG immunoblotting as described in Materials and Methods. *C,* substrate (hyaluronic acid)-gel assay. Conditioned media (10 µg protein; conditioned medium of 5×10^4 cells) from each transfectant clone were analyzed by substrate (hyaluronic acid)-gel. In the absence of a specific and well-accepted protein loading control for secreted protein, we used cell number and total protein for normalizing the total amount of conditioned medium for each transfectant, for HYAL1 immunoblot analysis, and for substrate (hyaluronic acid)-gel assay.
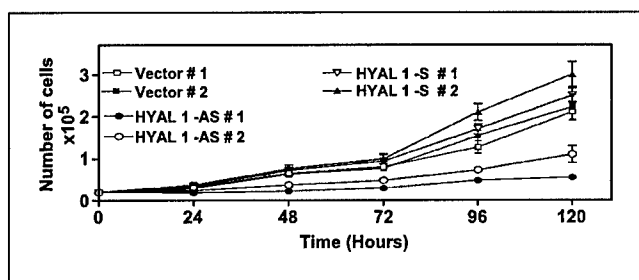
Figure 2. Determination of the proliferation rate of HT1376 transfectants. *Points,* mean cell count from triplicate measurements in two independent measurements; *bars,* SD.

transfectants (3×10^5 cells per well) were plated on the upper chamber in serum-free medium. The bottom chamber contained growth medium with geneticin. Following 48-hour incubation, invasion of cells through Matrigel into the bottom chamber was quantified using the 3-(4,5-dimethylthiazol-2-yl)-2,5-diphenyltetrazolium bromide assay (41). Invasion of cells was calculated as (cells in the bottom chamber) / (cells in upper and bottom chambers) $\times$ 100. Invasion by vector transfectants was normalized as 100% (control). Invasive activity of each clone was determined in triplicates in two independent experiments.

Pericellular Matrix (Coat) Assay. Pericellular matrices (coats) around transfectants were visualized using a particle exclusion assay involving formaldehyde fixed human erythrocytes as described previously (43, 44). Cells were counted in 10 fields (127-155 cells per transfectant) per dish and in two dishes per transfectant. Cells, which showed a phase bright region around the entire periphery, with an average width greater than or equal to the diameter of one erythrocyte, were counted as having a pericellular matrix. Results were expressed as percentage ± SD of cells with pericellular matrix.

Tumor Xenografts. HT1376 transfectants (2×10^6 or 4×10^6 cells per animal, 10 animals per group) were s.c. implanted on the right dorsal flank of 6-week-old female athymic mice. After tumors became palpable, tumor size was measured twice weekly and tumor volume was calculated assuming an ellipsoid shape. At day 30, all 10 animals from vector and HYAL1-S transfectants and 5 animals from HYAL1-AS groups were euthanzied. The remaining 5 mice in HYAL1-AS group were euthanized at day 60. Difference in tumor growth rate (i.e., generation of palpable tumors) and tumor weight at day 30 were statistically evaluated by Tukey-Kramer multiple comparisons test. The experiment was repeated once. Tumor histology was done at Charles River Laboratories (Wilmington, MA).

Immunohistochemistry: Hyaluronic Acid and HYAL1 Localization. Hyaluronic acid and HYAL1 were localized in tumor xenograft specimens by immunohistochemistry using a biotinylated bovine nasal cartilage hyaluronic acid–binding protein and the rabbit anti-HYAL1 IgG as described previously (17, 18, 27, 34). The hyaluronic acid– and HYAL1-stained slides were graded with respect to staining intensity 0 or 1+ (weak), 2+ (moderate), and 3+ (high) staining. All the authors read the slides independently.

Microvessel Density Determination. To visualize microvessels, slides containing tumor specimens were incubated with 3.1 μg/mL rat anti-mouse CD34 IgG (BD PharMingen, San Diego, CA) at 4°C for 18 hours. The slides were then sequentially incubated with a biotinylated rabbit anti-rat IgG, an avidin-biotin peroxidase conjugate solution (anti-rat ABC kit, Vector Laboratories, Burlingame, CA), and 3,3'-diaminobenzidine substrate solution (DAKO Laboratories, Carpinteria, CA). The slides were counterstained with hematoxylin and the microvessel density (MVD) was determined by counting the anti-CD34-stained microvessels (34). MVD was determined by two readers independently by choosing the hotspots and counting the microvessels. MVD was expressed as mean ± SD.

Results

Analysis of HYAL1 Expression in HT1376 Transfectants. Because HT1376 cells secrete the highest amount of hyaluronidase activity among the 11 bladder cancer cell lines (33), we chose HT1376 cell line to generate HYAL1-S (hyaluronidase-overproducing) and HYAL1-AS (hyaluronidase-non-producing) stable transfectants. We analyzed 25 to 30 stable clones of each transfectant type for analysis, and data on two clones from each category are presented. As shown in Fig. 1*A*, hyaluronidase activity (mU/mg) secreted by HYAL1-S (1: 83.5 ± 4.5 and 2: 94.5 ± 3.5) transfectants is ~2.5-fold when compared with the vector (1: 33.5 ± 1.5 and 2: 38.5 ± 2.5) transfectants. There is >90% reduction in the amount of hyaluronidase secreted by HYAL1-AS (1: 2.0 ± 0.5 and 2: 4.3 ± 0.4) transfectants when compared with vector transfectants (Fig. 1*A*). The amount of hyaluronidase activity secreted by HYAL1-AS transfectants is similar to that secreted by noninvasive bladder cancer cell lines, such as RT4 (33). As shown in Fig. 1*B*, a ~60-kDa HYAL1 protein is detected in the conditioned medium of vector (1 and 2) and HYAL1-S (1 and 2) transfectants. However, this protein is not detected HYAL1-AS (1 and 2) transfectant conditioned medium. The substrate (hyaluronic acid)-gel analysis confirms the presence of a ~60-kDa active hyaluronidase species in the conditioned medium of both vector and HYAL1-S transfectants. As expected, the active hyaluronidase species is not detected in the conditioned medium of HYAL1-AS transfectants (Fig. 1*C*).

Effect of HYAL1 Expression on Cell Proliferation, Cell Cycle, and Apoptosis. The growth rate of vector and HYAL1-S transfectants is comparable (Fig. 2). The doubling time of both vector transfectant clones is ~30 hours and that of HYAL1-S 1 and HYAL1-S 2 transfectants is 26 and 24 hours, respectively. HYAL1-AS transfectants, however, grew ~4 times slower when compared with vector and HYAL1-S transfectants (doubling time, 1: 96 hours and 2: 80 hours; Fig. 2).

As shown in Table 1, HYAL1 expression seems to affect the G_2-M phase of the cell cycle. There is a 200% and ≥500% increase in the

Table 1. Cell cycle analysis of HT1376 transfectants: HYAL1-S, HYAL1-AS, and vector transfectant clones subjected to flow cytometry for cell cycle analysis

Phase	Vector 1 (%)	Vector 2 (%)	HYAL1-S 1 (%)	HYAL1-S 2 (%)	HYAL1-AS 1 (%)	HYAL1-AS 2 (%)
G_0-G_1	56.7	55.8	55.2	54.2	55.9	57.1
S	37.7	38.4	42.4	44.3	31.4	32.7
G_2-M	5.6	5.8	2.4	1.5	12.7	10.2

NOTE: Percentages of cells in G_0-G_1, S, and G_2-M phases of the cell cycle are shown. Average of duplicates from two independent experiments. SD ≤ 5%.

number of HYAL1-AS transfectants in G_2-M phase when compared with the vector and HYAL1-S transfectants, respectively (<0.001; Tukey-Kramer multiple comparisons test). Correspondingly, the percentage of HYAL1-AS cells in S phase decreases when compared with vector and HYAL1-S cells. HYAL1 expression does not affect the G_0-G_1 phase (Table 1).

We next analyzed the expression of G_2-M regulators (i.e., cdc25c, cyclin B1, and cdc2/p34 proteins) in HT1376 transfectant clones. There is a 3- to 4-fold decrease in the expression of cdc25c and cyclin B1 in HYAL1-AS transfectant clones when compared with that in vector and HYAL1-S transfectants, respectively (Fig. 3A). The expression of cdc2/p34 in HYAL1-AS transfectants does not change in HYAL1-AS transfectants when compared with the vector transfectants but decreases ~1.5-fold when compared with HYAL1-S transfectants (Fig. 3A). There is also a ~2- and ~4-fold decrease in the cdc2/p34-associated H1 histone kinase activity in HYAL1-AS transfectant clones when compared with the vector and HYAL1-S transfectants, respectively (Fig. 3B). These results show that HYAL1-AS transfectants are arrested in the G_2-M phase of the cell cycle.

We also determined whether HYAL1 expression affects apoptosis. As shown in Table 2, there are no significant differences in apoptosis among vector, HYAL1-S, and HYAL1-AS clones. This was further confirmed by using Annexin V binding to study outward transloca-tion of plasma membrane phosphatidylserine among HYAL1 trans-fectants. No differences in phosphatidylserine translocation were observed among vector (1 and 2), HYAL1-S (1 and 2), and HYAL1-AS (1 and 2) transfectants. These results show that inhibition of HYAL1 expression affects cell cycle progression but not apoptosis.

Effect of HYAL1 Expression on Invasion. The invasive activity of vector transfectant clones (28.8 ± 2.3%) was normalized as 100%. As shown in Fig. 4A, HYAL1-AS transfectants 1 and 2 are 40% and 45% less invasive than the vector transfectant clones. Contrarily, HYAL1-S transfectants are 140% (1) and 159% (2) more invasive than vector transfectants. Incorporation of hyaluronic acid in Matrigel does not influence the invasive properties of various HT1376 transfectants (Fig. 4B). These results show that blocking of

HYAL1 expression significantly reduces the invasive activity of bladder cancer cells.

Effect of HYAL1 Expression on Hyaluronic Acid–Dependent Pericellular Matrix Formation. As shown in Fig. 5, the vector and HYAL1-S clones do not exhibit pericellular matrices, as the erythrocytes closely abut the surface of each cell and in some cases cover the cells. However, HYAL1-AS cells exhibit a pericellular matrix, as the erythrocytes do not penetrate the matrix and a clear coat surrounds the cells. The percentage of cells with pericellular matrix was elevated in HYAL1-AS transfectants (1: 85.6 ± 15.9 and 2: 86.7 ± 14.3) when compared with the vector (1: 56.3 ± 16.7 and 2: 47.8 ± 15.3) and HYAL1-S (1: 21.7 ± 16.25 and 2: 19.61 ± 14.83) transfectants. The differences among HYAL1-AS and vector, HYAL1-AS and HYAL1-S, and HYAL1-S and vector were statistically significant ($P < 0.001$). Thus, hyaluronic acid is an important component of the pericellular matrix that surrounds bladder cancer cells.

Effect of HYAL1 Expression on Tumor Xenografts. As shown in Fig. 5A, when injected at 2×10^6 cells per site density, there was a 4- to 5-fold delay in the generation of palpable tumors in

Table 2. Analysis of apoptosis in HT1376 transfectants

Transfectant	Free nucleosome A_{405}	% of Control
Vector 1 (control)	1.8 ± 0.05	100
Vector 2	1.5 ± 0.25	83.3
HYAL1-S 1	1.79 ± 0.21	99.4
HYAL1-S 2	1.91 ± 0.37	106
HYAL1-AS 1	1.46 ± 0.16	81.1
HYAL1-AS 2	1.83 ± 0.2	102

NOTE: Apoptotic activity in vector, HYAL1-S, and HYAL1-AS trans-fectant clones was determined. Apoptotic activity in vector 1 clone was considered as 100% (control). Average ± SE A_{405} from duplicate measurements in two independent experiments.
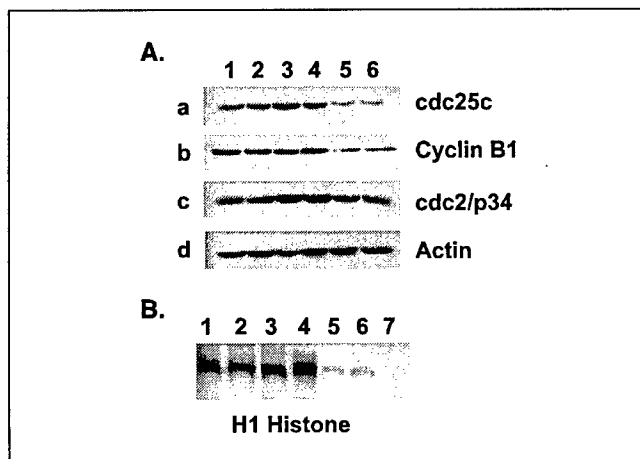

Figure 3. Analysis of G_2-M cell cycle regulators in HT1376 transfectants. *A*, cell lysates of HT1376 transfectants were analyzed by immunoblotting using anti-cdc25c (*a*), anti-cyclin B1 (*b*), anti-cdc2/p34 (*c*), and β-actin (*d*) antibodies. Lanes 1 and 2, vector clones 1 and 2; lanes 3 and 4, HYAL1-S clones 1 and 2; lanes 5 and 6, HYAL1-AS clones 1 and 2. *B*, H1 histone kinase-associated activity of cdc2/p34 was measured as described in Materials and Methods. Lanes 1 and 2, vector clones 1 and 2; lanes 3 and 4, HYAL1-S clones 1 and 2; lanes 5 and 6, HYAL1-AS clones 1 and 2; lane 7, negative control.
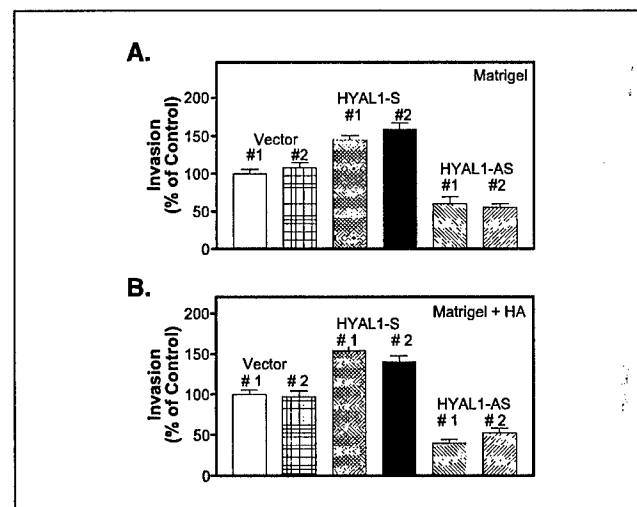

Figure 4. Determination of the invasive activity of HT1376 transfectants *in vitro*. Invasive activity was tested in Matrigel alone (*A*) or Matrigel + hyaluronic acid (*B*). Invasive activity of vector transfectant clone 1 (control) was considered as 100%. *Columns*, mean from triplicate determinations in two independent experiments; *bars*, SD.
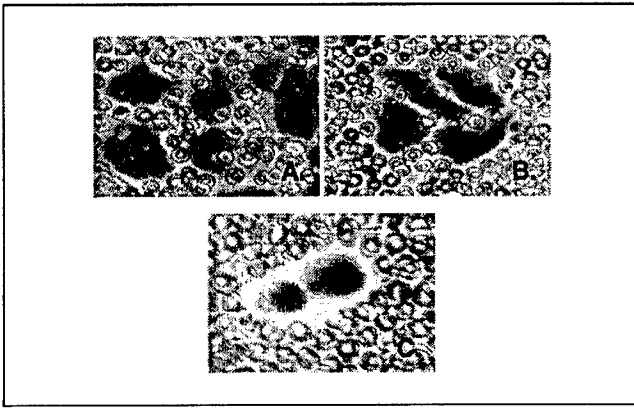
Figure 5. Examination of pericellular matrix in HT1376 transfectants: pericellular matrices surrounding various HT1376 transfectants were visualized using the particle exclusion assay. Human erythrocytes surrounding tumor cells: (*A*) vector 2, (*B*) HYAL1-S 2, and (*C*) HYAL1-AS 2.

animals injected with HYAL1-AS transfectant (40 ± 3 days) when compared with animals injected with HYAL1-S (7 days) and vector (10 ± 2 days) transfectants, respectively (*P* < 0.001). The weight of HYAL1-AS transfectant tumors is 9.1-fold less than that of vector tumors and 17.3-fold less than that of HYAL1-S tumors, respectively (Fig. 5*B*; *P* < 0.001). The 1.9-fold increase in the weight of HYAL1-S tumors compared with vector tumors is also statistically significant (*P* < 0.05). The picture of two representative tumors from each transfectant group shows that HYAL1-AS tumors are indeed much smaller than the vector and HYAL1-S tumors (Fig. 5*C*).

We also injected various transfectants at 4 × 10⁶ cells per site. As shown in Fig. 5*D*, the weight of HYAL1-AS tumors is still 10- and 17.7-fold less when compared with the weights of vector and HYAL1-S tumors, respectively (*P* < 0.001). Therefore, blocking HYAL1 expression decreases tumor growth regardless of the initial tumor inoculum.

Tumor histology report provided by Charles River Laboratories stated that vector and HYAL1-S tumors grew by infiltrating surrounding tissues, including skeletal muscle. The tumors also contained numerous blood vessels. On the contrary, HYAL1-AS tumor growth was described as resembling benign neoplasm. Figure 6 shows the photomicrographs of representative tumor histology corresponding to vector, HYAL1-S, and HYAL1-AS tumors. As shown in Fig. 6*A*, clusters of tumor cells have infiltrated the skeletal muscle, and two blood vessels are present at the periphery. At higher magnification, tumor cells are adjacent to skeletal muscle fibers. A blood vessel is also present close to tumor cells at the lower left (Fig. 6*D*). In the HYAL1-S tumor specimen, the skeletal muscle fibers are entrapped in tumor cells, as are the blood vessels (Fig. 6*B*). At higher magnification, tumor cells are present at the edge of a blood vessel, indicating infiltration. The tumor cells are surrounding the skeletal muscle fibers and also show a high number of mitotic figures (Fig. 6*E*). As shown in Fig. 6*C*, the HYAL1-AS tumor has a discrete margin and there is no evidence of infiltration into skeletal muscle. In addition, no large vessels are present in the specimen. At higher magnification, the specimen does not contain any skeletal muscle fibers and only a single capillary is present in the center (Fig. 6*F*). These results show that HYAL1 expression influences the invasive phenotype of bladder tumor cells *in vivo*.

Expression of Hyaluronic Acid, HYAL1, and Microvessel Density. To determine whether tumor cells in vector, HYAL1-S, and

HYAL1-AS tumor specimens retain their phenotype, we localized HYAL1 and hyaluronic acid in tumor xenografts. Tumor cells in the vector specimen show moderate expression of HYAL1 (2+ staining intensity), whereas tumor cells in HYAL1-S specimen show high level of HYAL1 expression (3+ staining intensity; Fig. 7*a-c*). None to very little HYAL1 staining is observed in HYAL1-AS tumor specimen (0 to 1+ staining intensity). In the vector tumor specimen, there is moderate (2+ staining intensity) hyaluronic acid expression in the tumor-associated stroma, but tumor cells are negative for hyaluronic acid expression (Fig. 7*A, d*). There is high level of hyaluronic acid expression in tumor-associated stroma in HYAL1-S tumor specimen (Fig. 7*A, e*). Interestingly, very low hyaluronic acid expression is observed in the stromal compartment in HYAL1-AS tumor specimens (Fig. 7*A, f*).

As shown in Fig. 7*B*, MVD in HYAL1-S tumor specimens (127.2 ± 29.23; range, 97-196) is 3.8-fold higher than that in vector tumor specimens (33.86 ± 5.55; range, 27-45) and 9.5-fold higher than that in HYAL1-AS specimens (13.43 ± 5.09; range, 6-22; *P* < 0.001; Tukey-Kramer multiple comparisons test; Fig. 8).
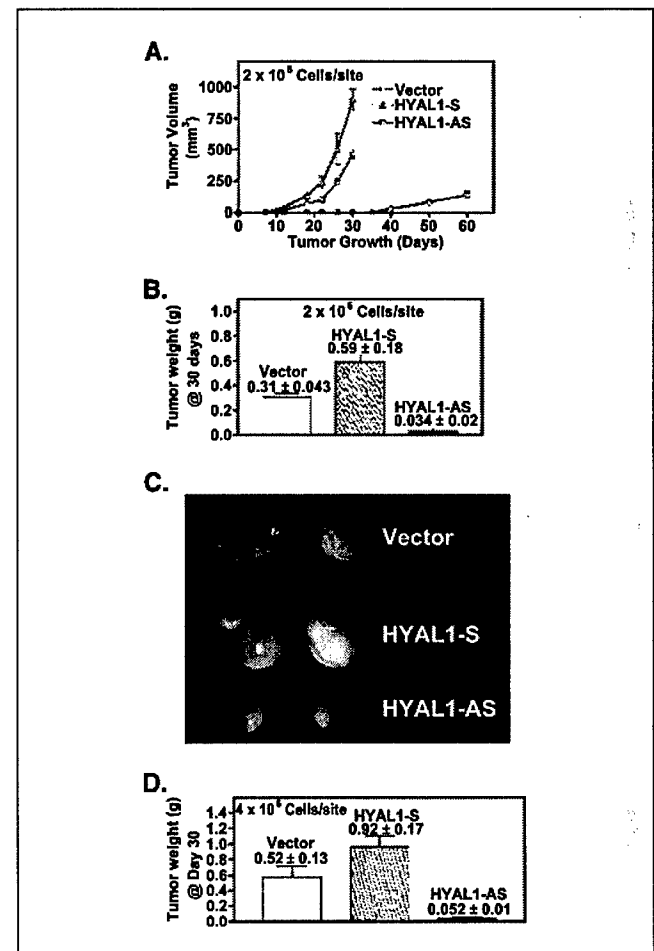
Figure 6. Examination of the growth of HT1376 transfectant tumors in xenografts. Vector 2, HYAL1-S 2, and HYAL1-AS 2 transfectant clones were injected s.c. in athymic mice (10 animals per group) at 2 × 10⁶ cells per site density. *A, points,* mean tumor volume; *bars,* SD. *B, columns,* mean tumor weight (g); *bars,* SD. *C,* two representative tumors from each group (i.e., vector, HYAL1-S, and HYAL1-AS) taken at necropsy. *D,* vector 2, HYAL1-S 2, and HYAL1-AS 2 transfectant clones were injected s.c. in athymic mice at 4 × 10⁶ cells per site density. *Columns,* mean tumor weight (g); *bars,* SD.

Figure 7. Examination of histology of transfectant tumors. Charles River Laboratories provided the tumor histology pictures (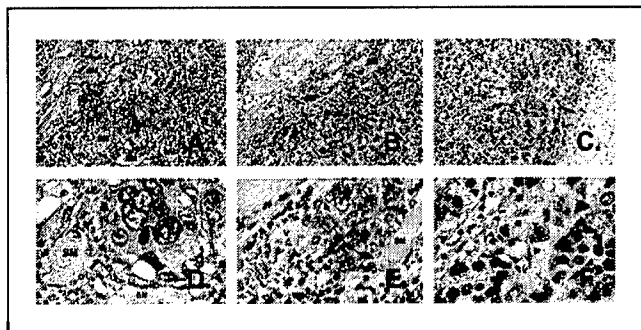*A-F*). *A-C*, magnification, ×100. *D-F*, magnification, ×400. *SM*, skeletal muscle fiber; *T*, tumor or tumor cells; *V*, blood vessel; *WBC*, leukocytes. *Arrows*, entrapment of skeletal muscle fibers by tumor.

Discussion

Our results show that blocking HYAL1 expression in a bladder cancer line results in a 4-fold decrease in cell growth rate, suggesting that HYAL1 expression by tumor cells is required for cell proliferation. The proliferation rate of HYAL1-S transfectants, however, is not significantly higher than that of the vector transfectants. Because HYAL1-S transfectants secrete only ~2.5-fold more HYAL1 than vector transfectants, moderate over-expression of HYAL1 in a bladder cancer cell line that already produces significantly higher amounts of HYAL1 (30 mU/mg) may not appreciably alter the cell proliferation rate. Our results, which show that blocking of HYAL1 expression induces cell cycle arrest, are consistent with a report that HYAL1 expression in an oral squamous cell carcinoma line induces S-phase entry (45). Based on the analysis of cell cycle and G_2-M regulators, HYAL1 expression very likely affects cell proliferation by regulating cell cycle.

Our finding that HYAL1-AS transfectants are ~50% less invasive than vector transfectants and that HYAL1-S transfectants are more invasive than vector transfectants are consistent with our previous observations that HYAL1 levels are elevated in high-grade bladder tumor tissues and in patients' urine (8, 17). Most high-grade tumors given sufficient time will invade bladder muscle and metastasize and therefore present with poor prognosis (1–4).

In addition to the effect of HYAL1 on tumor growth, its effects on tumor infiltration into skeletal muscle are interesting. HYAL1-S and vector tumors infiltrated skeletal muscle. HYAL1-AS tumors were benign and did not invade the muscle. Muscle invasion by bladder tumor is independent of tumor volume and is ominous, as 60% of patients have distant metastasis within 2 years and 50% die within 5 years (1–6). The observations of this study suggest that HYAL1 plays a role in promoting the invasive potential of bladder tumor cells. It may also explain why urinary hyaluronidase levels serve as an accurate marker for detecting high-grade bladder cancer but are not elevated in patients with low-grade tumors (1–4). HYAL1 is also an independent prognostic indicator for predicting biochemical recurrence in prostate cancer and increases metastatic potential of a prostate cancer line (29, 34, 40). Taken together, HYAL1 seems to function in bladder tumor growth and invasion.

In tumor xenografts, hyaluronic acid was exclusively localized in tumor-associated stroma, whereas HYAL1 was expressed by tumor cells. We have shown previously such dichotomy of hyaluronic acid and HYAL1 expression in prostate cancer (18). There is also a synergy between hyaluronic acid and HYAL1 expression. For example, there was considerably less hyaluronic acid in the stroma in HYAL1-AS tumors than there was in vector and HYAL1-S tumors. These observations are consistent with the expression of hyaluronic acid and HYAL1 in human bladder tumors. For example, there is low expression of hyaluronic acid and HYAL1 in grade 1 tumors when compared with grade 2 and 3 tumors, respectively (17). The synergy between stromal hyaluronic acid and tumor cell-HYAL1 expression suggests that one or both of these molecules may influence each other's synthesis in the tumor microenvironment.

One of the well-studied functions of the hyaluronic acid and hyaluronidase system is the generation of angiogenic hyaluronic acid fragments (24, 25). These angiogenic hyaluronic acid fragments have been shown to induce endothelial cell proliferation, migration, and adhesion (46–48). The secretion of hyaluronidase by tumor cells has been shown to induce angiogenesis (32), whereas
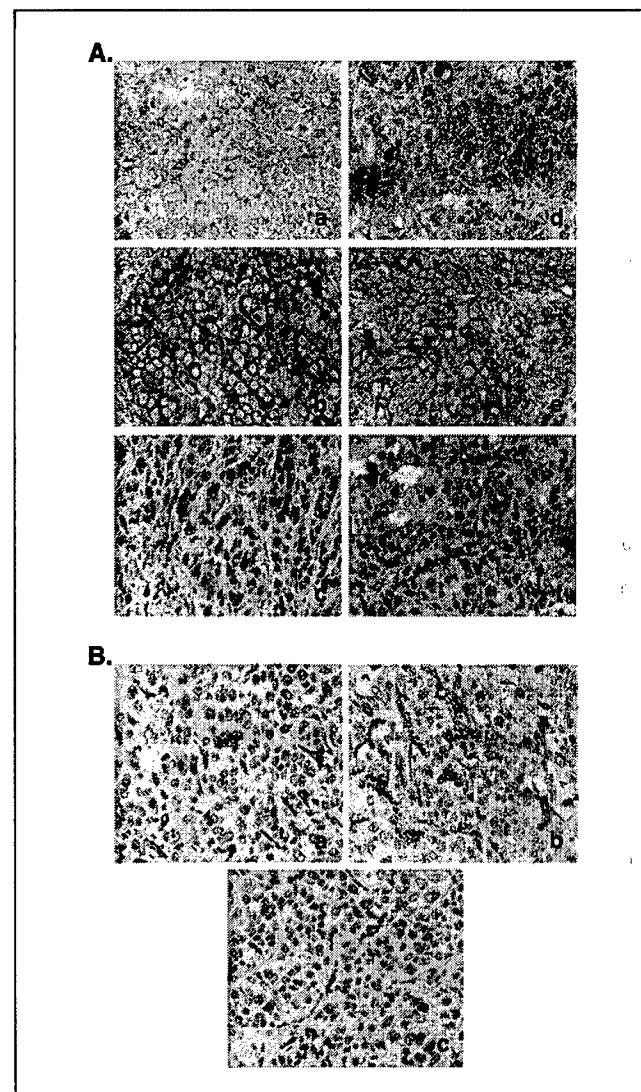
Figure 8. Localization of HYAL1, hyaluronic acid, and microvessels in tumor tissues. *A*, localization of HYAL1 and hyaluronic acid. *a-c*, HYAL1 localization; *d-f*, hyaluronic acid localization; *a* and *d*, vector transfectant; *b* and *e*, HYAL1-S transfectant; *c* and *f*, HYAL1-AS transfectant. *B*, localization of microvessels. Areas of the highest MVD from each type of tumor specimen. Magnification, ×400. *a*, vector tumor; *b*, HYAL1-S tumor; *c*, HYAL1-AS tumor.

hyaluronic acid causes avascularity (49). Angiogenic hyaluronic acid fragments are present in the urine of grade 2 and 3 bladder cancer patients, suggesting that the hyaluronic acid and HYAL1 system is active in bladder cancer (19). Our observations that HYAL1-S tumors have a significantly higher MVD than vector tumors and HYAL1-AS tumors have the lowest MVD among the three tumor groups are consistent with the function of the tumor associated hyaluronic acid-hyaluronidase system. Jacobson et al. also observed increased MVD in HYAL1-overexpressing rat colon carcinoma xenografts (38).

At present, the role of hyaluronidase as a tumor promoter or a repressor has been controversial. The results presented in this study show that blocking HYAL1 expression reduces tumor growth and invasion. HYAL1 levels in various cancers are associated with high-grade invasive tumors (7, 8, 26, 27, 34). However, chromosome region 3p21.3 that contains *HYAL1*, *HYAL2*, and *HYAL3* genes is deleted in some cancer lines (50–53). Although the tumor suppressor gene in 3p21.3 is not *HYAL1*, *HYAL2*, or *HYAL3*, it originally gave rise to the idea that hyaluronidase is a tumor suppressor (54). Jacobson et al. found that the overexpression of HYAL1 by cDNA transfection in a rat colon carcinoma line decreases tumor growth, although the tumors are angiogenic (38). It is noteworthy that HYAL1-overexpressing transfectants in that study secreted 4- to 5-fold more hyaluronidase activity than the HYAL1-S transfectants in our study. Shuster et al. injected a large dose (300 or 75 units/injection × 4 injections) of bovine testicular hyaluronidase in MDA435 breast cancer xenografts and observed a reduction in tumor volume over a period of 4 days; however, the effect was not studied beyond 4 days (55). Thus, it is possible that the effect of HYAL1 (and possibly other hyaluronidases) on tumor growth and invasion is concentration dependent. Although moderate HYAL1 expression in tumor cells increases their proliferative and invasive potentials, the lack of HYAL1 expression as well as very high HYAL1 expression decreases tumor growth and invasion perhaps

by completely degrading the tumor-associated hyaluronic acid matrix. It is also noteworthy that other proteins related to hyaluronic acid synthesis (hyaluronic acid synthase 2 and 3) and hyaluronic acid-receptor RHAMM are also involved in tumor growth and metastasis. For example, blocking hyaluronic acid synthase 3 expression in prostate cancer cells decreases cell growth *in vitro* and tumor growth *in vivo*. Hyaluronic acid synthase 2 expression induces mesenchymal and transformed properties in normal epithelial cells (56–58). Interestingly, hyaluronic acid synthase 2 expression in the absence of hyaluronidase decreases tumor growth in glioma cells. Interaction between RHAMM and hyaluronic acid fragments is known to induce the mitogen-activated protein kinase pathway, and overexpression of RHAMM is a useful prognostic indicator for breast cancer. These results show that the hyaluronic acid-hyaluronidase system is involved in the regulation of tumor growth and invasion.

Taken together, our study shows that HYAL1 is one of the molecular determinants of bladder tumor growth and invasion; therefore, it is a sensitive and specific marker for detecting high-grade bladder cancer.

Acknowledgments

References

1. Lee R, Droller MJ. The natural history of bladder cancer. Implications for therapy. Urol Clin North Am 2000;27:1–13; vii.
2. Heney NM. Natural history of superficial bladder cancer. Prognostic features and long-term disease course. Urol Clin North Am 1992;19:429–33.
3. Droller MJ. Cancer heterogeneity and its biologic implications in the grading of urothelial carcinoma. J Urol 2001;165:696–7.
4. Hassen W, Droller MJ. Current concepts in assessment and treatment of bladder cancer. Curr Opin Urol 2000;10:291–9.
5. Soloway MS, Sofer M, Vaidya A. Contemporary management of stage T1 transitional cell carcinoma of the bladder. J Urol 2002;167:1573–83.
6. Vaidya A, Soloway MS, Hawke C, Tiguert R, Civantos F. De novo muscle invasive bladder cancer: is there a change in trend? J Urol 2001;165:47–50; discussion 50.
7. Pham HT, Block NL, Lokeshwar VB. Tumor-derived hyaluronidase: a diagnostic urine marker for high-grade bladder cancer. Cancer Res 1997;57:778–83. Erratum in: Cancer Res 1997;57:1622.
8. Lokeshwar VB, Obek C, Pham HT, et al. Urinary hyaluronic acid and hyaluronidase: markers for bladder cancer detection and evaluation of grade. J Urol 2000;163:348–56.
9. Tammi MI, Day AJ, Turley EA. Hyaluronan and homeostasis: a balancing act. J Biol Chem 2002; 277:4581–4.
10. Delpech B, Girard N, Bertrand P, Courel MN, Chauzy C, Delpech A. Hyaluronan: fundamental principles and applications in cancer. J Intern Med 1997;242:41–8.
11. Turley EA, Noble PW, Bourguignon LY. Signaling properties of hyaluronan receptors. J Biol Chem 2002;277:4589–92.
12. Setälä LP, Tammi MI, Tammi RH, et al. Hyaluronan expression in gastric cancer cells is associated with local and nodal spread and reduced survival rate. Br J Cancer 1999;79:1133–8.
13. Auvinen P, Tammi R, Parkkinen J, et al. Hyaluronan in peritumoral stroma and malignant cells associates with breast cancer spreading and predicts survival. Am J Pathol 2000;156:529–36.
14. Knudson W. Tumor-associated hyaluronan. Providing an extracellular matrix that facilitates invasion. Am J Pathol 1996;148:1721–6.
15. Ropponen K, Tammi M, Parkkinen J, et al. Tumor cell-associated hyaluronan as an unfavorable prognostic factor in colorectal cancer. Cancer Res 1998;58:342–7.
16. Lipponen P, Aaltomaa S, Tammi R, Tammi M, Ågren U, Kosma V-M. High stromal hyaluronan level is associated with poor differentiation and metastasis in prostate cancer. Eur J Cancer 2001;37:849–56.
17. Hautmann SH, Lokeshwar VB, Schroeder GL, et al. Elevated tissue expression of hyaluronic acid and hyaluronidase validates the HA-HAase urine test for bladder cancer. J Urol 2001;165:2068–74.
18. Lokeshwar VB, Rubinowicz D, Schroeder GL, et al. Stromal and epithelial expression of tumor markers hyaluronic acid and HYAL1 hyaluronidase in prostate cancer. J Biol Chem 2001;276:11922–32.
19. Lokeshwar VB, Obek C, Soloway MS, Block NL. Tumor-associated hyaluronic acid: a new sensitive and specific urine marker for bladder cancer. Cancer Res 1997;57:773–7. Erratum in: Cancer Res 1998;58:3191.
20. Liu N, Lapcevich RK, Underhill CB. Metastatin: a hyaluronan-binding complex from cartilage that inhibits tumor growth. Cancer Res 2001;61:1022–8.
21. Hayen W, Goebeler M, Kumar S, Riessen R, Nehls V. Hyaluronan stimulates tumor cell migration by modulating the fibrin fiber architecture. J Cell Sci 1999;112:2241–51.
22. Hobarth K, Maier U, Marberger M, et al. Topical chemoprophylaxis of superficial bladder cancer by mitomycin C and adjuvant hyaluronidase. Eur Urol 1992;21:206–10.
23. Itano N, Atsumi F, Sawai T, et al. Abnormal accumulation of hyaluronan matrix diminishes contact inhibition of cell growth and promotes cell migration. Proc Natl Acad Sci 2002;99:3609–14.
24. Lees VC, Fan TP, West DC. Angiogenesis in a delayed revascularization model is accelerated by angiogenic oligosaccharides of hyaluronan. Lab Invest 1995;73:259–66.
25. West DC, Hampson IN, Arnold F, Kumar S. Angiogenesis induced by degradation products of hyaluronic acid. Science 1985;228:1324–6.
26. Franzmann EJ, Schroeder GL, Goodwin WJ, Weed DT, Fisher P, Lokeshwar VB. Expression of tumor markers hyaluronic acid and hyaluronidase (HYAL1) in head and neck tumors. Int J Cancer 2003;106:438–45.
27. Posey JT, Soloway MS, Ekici S, et al. Evaluation of the prognostic potential of hyaluronic acid and

hyaluronidase (HYAL1) for prostate cancer. Cancer Res 2003;63:2638–44.

28. Lokeshwar VB, Lokeshwar BL, Pham HT, Block NL. Association of elevated levels of hyaluronidase, a matrix-degrading enzyme, with prostate cancer progression. Cancer Res 1996;56:651–7.

29. Madan AK, Yu K, Dhurandhar N, Cullinane C, Pang Y, Beech DJ. Association of hyaluronidase and breast adenocarcinoma invasiveness. Oncol Rep 1999;6:607–9.

30. Bertrand P, Girard N, Duval C, et al. Increased hyaluronidase levels in breast tumor metastases. Int J Cancer 1997;73:327–31.

31. Delpech B, Laquerriere A, Maingonnat C, Bertrand P, Freger P. Hyaluronidase is more elevated in human brain metastases than in primary brain tumours. Anticancer Res 2002;22:2423–7.

32. Liu D, Pearlman E, Diaconu E, et al. Expression of hyaluronidase by tumor cells induces angiogenesis *in vivo*. Proc Natl Acad Sci U S A 1996;93:7832–7.

33. Lokeshwar VB, Young MJ, Goudarzi G, et al. Identification of bladder tumor-derived hyaluronidase: its similarity to HYAL1. Cancer Res 1999;59:4464–70.

34. Ekici S, Cerwinka W, Ducan RC, et al. Comparison of the prognostic potential of hyaluronic acid, hyaluronidase (HYAL-1), CD44v6 and microvessel density for prostate cancer. Int J Cancer 2004;112:121–9.

35. Lokeshwar VB, Schroeder GL, Carey RI, Soloway MS, Iida N. Regulation of hyaluronidase activity by alternative mRNA splicing. J Biol Chem 2002;277:33654–63.

36. Junker N, Latini S, Petersen LN, Kristjansen PE. Expression and regulation patterns of hyaluronidases in small cell lung cancer and glioma lines. Oncol Rep 2003;10:609–16.

37. Frost GI, Mohapatra G, Wong TM, Csoka AB, Gray JW, Stern R. HYAL1LUCA-1, a candidate tumor suppressor gene on chromosome 3p21.3, is inactivated in head and neck squamous cell carcinomas by aberrant splicing of pre-mRNA. Oncogene 2000;19:870–7.

38. Jacobson A, Rahmanian M, Rubin K, Heldin P. Expression of hyaluronan synthase 2 or hyaluronidase 1 differentially affect the growth rate of transplantable colon carcinoma cell tumors. Int J Cancer 2002;102:212–9.

39. Victor R, Chauzy C, Girard N, et al. Human breast-cancer metastasis formation in a nude-mouse model: studies of hyaluronidase, hyaluronan and hyaluronan-binding sites in metastatic cells. Int J Cancer 1999;82:77–83.

40. Patel S, Turner PR, Stubberfield C, et al. Hyaluronidase gene profiling and role of hyal-1 overexpression in an orthotopic model of prostate cancer. Int J Cancer 2002;97:416–24. Erratum in: Int J Cancer 2002;98:957.

41. Lokeshwar BL, Selzer MG, Zhu BQ, Block NL, Golub LM. Inhibition of cell proliferation, invasion, tumor growth and metastasis by an oral non-antimicrobial tetracycline analog (COL-3) in a metastatic prostate cancer model. Int J Cancer 2002;98:297–309.

42. Agarwal C, Singh RP, Dhanalakshmi S, et al. Silibinin upregulates the expression of cyclin-dependent kinase inhibitors and causes cell cycle arrest and apoptosis in human colon carcinoma HT-29 cells. Oncogene 2003;22:8271–82.

43. Deyst KA, Toole BP. Production of hyaluronan-dependent pericellular matrix by embryonic rat glial cells. Brain Res Dev Brain Res 1995;88:122–5.

44. Zoltan-Jones A, Huang L, Ghatak S, Toole BP. Elevated hyaluronan production induces mesenchymal and transformed properties in epithelial cells. J Biol Chem 2003;278:45801–10.

45. Lin G, Stern R. Plasma hyaluronidase (Hyal-1) promotes tumor cell cycling. Cancer Lett 2001;163:95–101.

46. Slevin M, Kumar S, Gaffney J. Angiogenic oligosaccharides of hyaluronan induce multiple signaling pathways affecting vascular endothelial cell mitogenic and wound healing responses. J Biol Chem 2002;277:41046–59.

47. Lokeshwar VB, Selzer MG. Differences in hyaluronic acid-mediated functions and signaling in arterial, microvessel, and vein-derived human endothelial cells. J Biol Chem 2000;275:27641–9.

48. Feinberg RN, Beebe DC. Hyaluronate in vasculogenesis. Science 1983;220:1177–9.

49. Senchenko V, Liu J, Braga E, et al. Deletion mapping using quantitative real-time PCR identifies two distinct 3p21.3 regions affected in most cervical carcinomas. Oncogene 2003;22:2984–92.

50. Senchenko VN, Liu J, Loginov W, et al. Discovery of frequent homozygous deletions in chromosome 3p21.3 LUCA and AP20 regions in renal, lung and breast carcinomas. Oncogene 2004 [Epub ahead of print].

51. Csoka AB, Frost GI, Stern R. The six hyaluronidase-like genes in the human and mouse genomes. Matrix Biol 2001;20:499–508.

52. Kashuba VI, Li J, Wang F, et al. RBSP3 (HYA22) is a tumor suppressor gene implicated in major epithelial malignancies. Proc Natl Acad Sci U S A 2004; 101:4906–11.

53. Ji L, Nishizaki M, Gao B, et al. Expression of several genes in the human chromosome 3p21.3 homozygous deletion region by an adenovirus vector results in tumor suppressor activities *in vitro* and *in vivo*. Cancer Res 2002;62:2715–20.

54. Csoka TB, Frost GI, Heng HH, Scherer SW, Mohapatra G, Stern R. The hyaluronidase gene HYAL1 maps to chromosome 3p21.2-p21.3 in human and 9F1-F2 in mouse, a conserved candidate tumor suppressor locus. Genomics 1998;48:63–70.

55. Shuster S, Frost GI, Csoka AB, Formby B, Stern R. Hyaluronidase reduces human breast cancer xenografts in SCID mice. Int J Cancer 2002;102:192–7.

56. Simpson MA, Wilson CM, McCarthy JB. Inhibition of prostate tumor cell hyaluronan synthesis impairs subcutaneous growth and vascularization in immuno-compromised mice. Am J Pathol 2002;161:849–57.

57. Enegd B, King JA, Stylli S, Paradiso L, Kaye AH, Novak U. Overexpression of hyaluronan synthase-2 reduces the tumorigenic potential of glioma cells lacking hyaluronidase activity. Neurosurgery 2002;50: 1311–8.

58. Wang C, Thor AD, Moore DH II, et al. The overexpression of RHAMM, a hyaluronan-binding protein that regulates ras signaling, correlates with overexpression of mitogen-activated protein kinase and is a significant parameter in breast cancer progression. Clin Cancer Res 1998;4:567–76.

Research Article

HYAL1 Hyaluronidase in Prostate Cancer: A Tumor Promoter and Suppressor

Vinata B. Lokeshwar,[1,2,4] Wolfgang H. Cerwinka,[1] Tadahiro Isoyama,[1] and Bal L. Lokeshwar[1,3,4]

Departments of [1]Urology, [2]Cell Biology and Anatomy, and [3]Radiation Oncology, and [4]Sylvester Comprehensive Cancer Center, Miller School of Medicine, University of Miami, Miami, Florida

Abstract

Hyaluronidases degrade hyaluronic acid, which promotes metastasis. HYAL1 type hyaluronidase is an independent prognostic indicator of prostate cancer progression and a biomarker for bladder cancer. However, it is controversial whether hyaluronidase (e.g., HYAL1) functions as a tumor promoter or as a suppressor. We stably transfected prostate cancer cells, DU145 and PC-3 ML, with HYAL1-sense (HYAL1-S), HYAL1-antisense (HYAL1-AS), or vector DNA. HYAL1-AS transfectants were not generated for PC-3 ML because it expresses little HYAL1. HYAL1-S transfectants produced ≤42 milliunits (moderate overproducers) or ≥80 milliunits hyaluronidase activity (high producers). HYAL1-AS transfectants produced <10% hyaluronidase activity when compared with vector transfectants (18-24 milliunits). Both blocking HYAL1 expression and high HYAL1 production resulted in a 4- to 5-fold decrease in prostate cancer cell proliferation. HYAL1-AS transfectants had a G_2-M block due to decreased cyclin B1, cdc25c, and cdc2/p34 expression and cdc2/p34 kinase activity. High HYAL1 producers had a 3-fold increase in apoptotic activity and mitochondrial depolarization when compared with vector transfectants and expressed activated proapoptotic protein WOX1. Blocking HYAL1 expression inhibited tumor growth by 4- to 7-fold, whereas high HYAL1 producing transfectants either did not form tumors (DU145) or grew 3.5-fold slower (PC-3 ML). Whereas vector and moderate HYAL1 producers generated muscle and blood vessel infiltrating tumors, HYAL1-AS tumors were benign and contained smaller capillaries. Specimens of high HYAL1 producers were 99% free of tumor cells. This study shows that, depending on the concentration, HYAL1 functions as a tumor promoter and as a suppressor and provides a basis for anti-hyaluronidase and high-hyaluronidase treatments for cancer. (Cancer Res 2005; 65(17): 7782-9)

Introduction

Hyaluronidase is an endoglycosidase that degrades hyaluronic acid. Hyaluronic acid is a glycosaminoglycan made up of repeating disaccharide units D-glucuronic acid and N-acetyl-D-glucosamine (1, 2). In addition to maintaining hydration status and osmotic balance in tissues, hyaluronic acid interacts with cell surface receptors, such as CD44 and receptor for hyaluronic acid–mediated motility, and regulates cell adhesion, migration, and proliferation (1–3). Hyaluronic acid concentration is elevated in several tumors, including carcinomas of breast, colon, prostate, and bladder (4–8). We have shown that increased urinary hyaluronic acid levels serve as an accurate marker for detecting bladder cancer, regardless of the tumor grade (9, 10). In prostate cancer tissues, hyaluronic acid is mainly produced by tumor-associated stroma; however, ~ 40% of tumor cells express hyaluronic acid (11, 12). Tumor-associated hyaluronic acid promotes tumor cell migration, aids in the loss of contact inhibition, and offers protection against immune surveillance (13–15). Small hyaluronic acid fragments (3-25 disaccharide units), generated by hyaluronidase, are angiogenic (16, 17). We have detected such fragments in prostate cancer tissues, in bladder cancer patients' urine, and in the saliva of head and neck cancer patients (7, 9, 18).

Hyaluronidase is crucial for the spread of bacterial infections, toxins, and venoms (19, 20). The human genome contains six hyaluronidase genes, found on two chromosomes: 3p 21.3 (HYAL1, HYAL2, and HYAL3) and 7q 21.3 (HYAL4, PH20, and HYALP1; ref. 21). PH20 or testicular hyaluronidase induces the acrosomal reaction during ovum fertilization (22). HYAL1 is present in human serum and urine and has a pH optimum of ~ 4.2. HYAL1 is 50% active at pH 4.5 (7, 23, 24). Lack of functional HYAL1 causes a mild disorder called type IX mucopolysaccharidosis (25). It is also the major hyaluronidase expressed in cancers of the prostate, bladder, and head and neck, and is secreted by tumor cells (7, 11, 18, 26). In bladder cancer, increased hyaluronidase levels (i.e., HYAL1) serve as an accurate marker for detecting high-grade tumors (6, 9, 10). Using radical prostatectomy specimens from patients with a 6- to 10-year follow-up, we found that HYAL1 is an independent predictor of biochemical recurrence (i.e., disease progression; refs. 11, 12). Hyaluronidase levels also increase in breast cancer cells when they become metastatic (27, 28). We recently showed that blocking HYAL1 expression in an invasive bladder cancer line decreases tumor growth by 9- to 17-fold, inhibits tumor infiltration, and decreases microvessel density 4- to 9-fold (29). Expression of HYAL1 in PC-3 prostate cancer cells that produce low levels of hyaluronidase causes a slight increase in lung metastasis (30). These observations show that hyaluronidases in general, and HYAL1 in particular, are tumor promoters.

Contrary to the tumor growth- and metastasis-promoting effects of HYAL1, the chromosomal locus (i.e., 3p 21.3) that encodes the HYAL-1, HYAL-2, and HYAL-3 genes is deleted in some epithelial tumors at high frequency, although the tumor suppressor gene in this locus is not one of the hyaluronidase genes (31–33). HYAL2 levels are also slightly decreased in high-grade B-cell non-Hodgkin's lymphomas (34). Overexpression of HYAL1 in a rat colon carcinoma line inhibits tumor growth and generates necrotic tumors (35). Administration of super high concentrations of bovine testicular hyaluronidase (300 units) causes a 50% regression of breast tumor xenografts (36).

Furthermore, transient expression of HYAL1 and HYAL2 in L929 mouse fibroblasts or treatment of these cells with super high concentrations of bovine testicular hyaluronidase (100 units/mL) increases tumor necrosis factor–mediated cytotoxicity by inducing the expression of a proapoptotic protein WOX1 (a ww domain–containing oxidoreductase; refs. 37–40). In these cells, WOX1 induces apoptosis following its activation by phosphorylation on Tyr-33 residue (WOX1-^{P}Tyr-33) and its translocation to mitochondria and then into the nucleus (38). These observations suggest that hyaluronidases, including HYAL1, are tumor suppressors.

At present, no studies have been conducted to explain the contradictory findings about HYAL1 function in tumor growth and invasion. To discern the tumor-promoting and tumor-suppressing functions of HYAL1, we stably transfected androgen-independent prostate cancer cell lines DU145 and PC-3 ML to generate moderate HYAL1 producers, high HYAL1 producers, and no/little HYAL1 producers. Our results show that HYAL1 is both a tumor promoter and a suppressor, depending on its concentration.

Materials and Methods

Generation of HYAL1-S and HYAL1-AS stable transfectants. The HYAL1 coding region was cloned into a eukaryotic expression vector, pcDNA3.1/v5-His TOPO, in the sense (HYAL1-S) and antisense (HYAL1-AS) orientation, with respect to the cytomegalovirus promoter (29). DU145 and PC-3 ML cells (1 × 10^5/6-cm dish) were transfected with vector, HYAL1-S, or HYAL1-AS cDNA constructs (1 μg DNA) using Effectene (Qiagen). Transfectant clones were selected in a growth medium (RPMI 1640 + 10% fetal bovine serum + gentamicin) plus geneticin (Invitrogen, Carlsbad, CA).

Analysis of hyaluronidase activity and HYAL1. Hyaluronidase activity secreted by transfectants into serum-free conditioned media was measured using a hyaluronidase ELISA-like assay and expressed as milliunits per 10^6 cells (41). Both the active hyaluronidase species and HYAL1 were identified in the transfectant conditioned media (secreted by 5 × 10^4 cells, ∼10 μg total protein) with substrate (hyaluronic acid)-gel electrophoresis and immunoblot analysis, using a rabbit anti-HYAL1 immunoglobulin G (IgG), respectively (26).

Immunoblot analysis and kinase assay. Cell lysates (4 × 10^4 cells) were immunoblotted using anti-cyclin B1 IgG, anti-cdc2/p34 IgG, anti-cdc25c IgG, or anti-actin IgG (Lab Vision Corp./Neomarkers, Fremont, CA; ref. 29). cdc2/p34 kinase was immunoprecipitated from cell lysates (1 × 10^6 cells/ transfectant) using an anti-cdc2/p34 antibody. Immunoprecipitates were used for the cdc2/p34-associated H1 histone kinase activity assay using H1 histone (29). Cell lysates were also immunoblotted using rabbit anti-WOX1 and rabbit anti-WOX1 phosphospecific Tyr-33 IgG (1:3,000 dilution; EMD Biosciences, San Diego, CA).

Cell proliferation assay. Transfectant clones were cultured on 24-well plates in growth medium + geneticin. Cells were counted in duplicate wells every 24 hours, for a total period of 120 hours, in two independent experiments.

Cell cycle analysis. Cell cycle phase distribution in actively growing transfectant cultures was estimated by propidium iodide staining of DNA and flow cytometry using an EPICS XL flow cytometer (29). FL3 histograms were analyzed using the Modfit Easy (Lite) Program (Veritas Software ME). Samples were assayed in duplicate in two independent experiments.

Apoptosis assays. Ninety-six-hour cultures of transfectants (10^5 cells/24-well plate) were lysed and the cell lysates were tested for free nucleosome release using the Cell Death ELISA kit (Roche Diagnostics, Pleasanton, CA). Annexin V binding was examined in 96-hour cultures of transfectants (∼3 × 10^5 cells/6-cm dish) using the ApoAlert Annexin V-enhanced green fluorescent protein kit (BD Clontech Labs, Mountain View, CA) and flow cytometry. Median fluorescence intensity (Annexin V binding to phosphatidylserine) was compared among the transfectants in the green fluorescence

channel (log FL1). Mitochondrial depolarization was examined by incubating actively growing cultures of transfectants with a mitochondria-specific dye, JC-1, for 15 minutes followed by flow cytometry. An increase in the green fluorescence intensity was approximated as a decrease in mitochondrial membrane potential ($\Delta\Psi$; ref. 42).

Matrigel invasion assay. Transfectants (3 × 10^5 cells) were plated on the upper chamber of a Matrigel-coated transwell plate in serum-free medium. The bottom chamber contained growth medium. After 48 hours, invasion of cells through the Matrigel into the bottom chamber was quantified using the 3-(4,5-dimethylthiazol-2-yl)-2,5-diphenyltetrazolium bromide assay. Cell invasion was calculated as (cells in the bottom chamber ÷ cells in upper + bottom chambers) × 100 (29).

Pericellular matrix assay. Formaldehyde-fixed human erythrocytes were overlaid on transfectants, which were cultured for 24 hours (10^4 cells/ 6-cm dish). Cells showing a bright region around the entire periphery with width equal to or greater than the diameter of an erythrocyte (i.e., pericellular matrix) were counted in 10 fields. Results were expressed as percentage of cells with pericellular matrix ± SD (29, 43).

Tumor xenografts and histology. Transfectants (2 × 10^6 cells) were s.c. implanted on the dorsal flank of 5-week-old male athymic mice (10/clone). After the tumors became palpable, the tumor size was measured twice weekly. Tumor volume was approximated to an ellipsoid (44). Following euthanasia (DU145: 42 day; PC-3 ML: 28 day), the tumors were weighed. Tukey's multiple comparison test was used to evaluate the differences in tumor growth rate and tumor weight. Tumor histology was done at Charles River Laboratories (Wilmington, MA).

Hyaluronic acid, HYAL1 localization, and microvessel density determination. Hyaluronic acid and HYAL1 were localized in tumor xenograft specimens by immunohistochemistry using a biotinylated hyaluronic acid–binding protein and the anti-HYAL1 IgG, respectively (29). Microvessel density was evaluated using CD34 staining (rat anti-mouse CD34 IgG; BD PharMingen, Mountain View, CA; ref. 29). Microvessel density was determined by two readers independently counting microvessels in 10 fields and expressed as mean ± SD. The length of the microvessels was measured using a Nikon H550L microscope with a video screen camera equipped with measuring tools.

Results

Analysis of HYAL1 expression in DU145 and PC-3 ML transfectants. Whereas DU145 cells secrete hyaluronidase activity into their conditioned media, PC-3 ML cells secrete very little hyaluronidase (7). We generated HYAL1-S (hyaluronidase overproducing) transfectants of both DU145 and PC-3 ML cells, but only HYAL1-AS transfectants of DU145. We analyzed 25 to 30 clones of each transfectant type for hyaluronidase production and HYAL1 expression. We selected two types of HYAL-S transfectants, moderate hyaluronidase overproducing and high hyaluronidase overproducing. Data on two clones from each type are shown. As shown in Fig. 1A-a, when compared with vector #1 and #2 clones, DU145 HYAL1-S clones #1 and #2 secrete 1.5- to 2.3-fold more hyaluronidase activity (moderate overproducers). HYAL1-S #3 and #4 clones (high producers) secrete 3.8- to 7.3-fold more hyaluronidase activity than the vector clones (Fig. 1A-a). There is >90% reduction in hyaluronidase secretion in HYAL1-AS clones. PC-3 ML HYAL1-S clones #1 and #2 secrete 10-fold more hyaluronidase activity than that secreted by PC-3 ML vector clones (Fig. 1A-b). HYAL1-S #3 and #4 clones secrete 80 to 100 milliunits hyaluronidase activity, which is similar to that secreted by DU145 #3 and #4 clones.

Anti-HYAL1 immunoblot analysis shows that a ∼60 kDa HYAL1 protein is secreted in the conditioned media of DU145 vector and HYAL1-S clones but not in HYAL1-AS clones (Fig. 1B-a). In PC-3 ML clones, HYAL1 protein is detected in the conditioned media of HYAL1-S transfectants but not in vector clones. The amount of
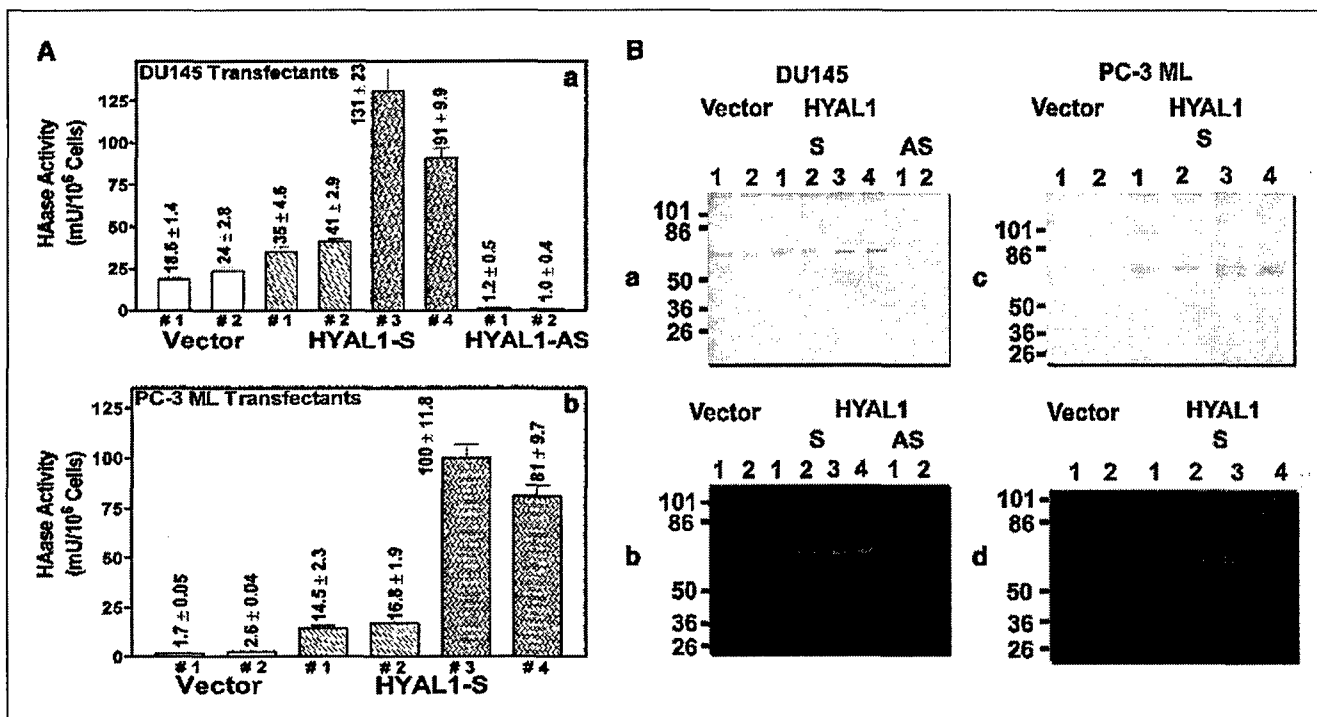
Figure 1. Analysis of hyaluronidase activity in DU145 and PC-3 ML transfectants. *A*, hyaluronidase activity (milliunits per milligram) was measured using an ELISA-like assay. *Columns,* mean (triplicates in three experiments); *bars,* SD. *B,* detection of HYAL1 expression by immunoblot and substrate (hyaluronic acid)-gel assay. *A* and *C,* immunoblot analysis. Conditioned media (10 μg protein; conditioned media of 50,000 cells) were subjected to anti-HYAL1 IgG immunoblotting. *B* and *D,* substrate (hyaluronic acid)-gel assay. Conditioned media (10 μg protein; conditioned media of 50,000 cells) were analyzed by substrate (hyaluronic acid)-gel electrophoresis.

HYAL1 protein detected in HYAL1-S clones #3 and #4 is higher than that detected in HYAL1-S #1 and #2 clones (Fig. 1*B-b*). The substrate (hyaluronic acid)-gel analysis confirms immunoblot results and detects a ~60 kDa active hyaluronidase species in the conditioned media of DU145 vector and HYAL1-S clones and in PC-3 ML HYAL1-S clones (Fig. 1*B-c* and *B-d*).

Effect of HYAL1 expression on cell proliferation and cell cycle. The growth rates of DU145 vector and HYAL1-S #1 and #2 transfectants are comparable (doubling time, ~26-28 hours; Fig. 2*A*). However, both HYAL1-AS clones and HYAL1-S #3 and #4 clones (which secrete ≥100 milliunits/10^6 hyaluronidase activity) grow 4- to 5-fold slower than vector clones (doubling time, ~90-96 hours). PC-3 ML HYAL1-S #1 and HYAL1-S #2 clones grow 1.5- to 2-fold faster than the vector clones; however, the high HYAL1 producing clones, HYAL1-S #3 and #4, grow 2- to 2.5-fold slower than the vector clones (Fig. 2*B*).

Cell cycle analysis showed that the decreased growth rate of HYAL1-AS transfectants was due to cell cycle arrest in the G_2-M phase. There was a 200% to 300% increase in the number of HYAL1-AS #1 and #2 cells in G_2-M phase (22.3% and 31.3%, respectively) when compared with vector (#1: 11.5%, #2: 12.4%) and all HYAL1-S transfectant (9.7-12.1%) clones. This increase in the G_2-M phase was statistically significant ($P < 0.001$, Tukey's test). Correspondingly, the percentage of HYAL1-AS cells in S phase was lower (#1: 28.8%, #2: 24.8%) when compared with vector (#1: 35.9%; #2: 37.2%) and HYAL1-S (#1: 36.4%; #2: 38.5%) cells. There was no change in the percentage of cells in G_0-G_1 phase in any of the transfectants. In PC-3 ML transfectants, HYAL1 expression also increased the number of cells in the S phase with a corresponding decrease in the number of cells in G_2-M phase (data not shown).

The expression of G_2-M regulators (i.e., cdc25c, cyclin B1, and cdc2/p34 proteins) was analyzed in various clones by immunoblotting. As shown in Fig. 2*C*, both cdc25c bands, plausibly representing phosphorylated (slow-moving) and native forms, are detected in all DU145 transfectants. There is an ~3-fold decrease in the expression cdc25c and cyclin B1, as well as a 2-fold decrease in cdc2/p34 expression in HYAL1-AS transfectants, when compared with the vector and HYAL1-S transfectant clones (Fig. 2*C*). A 2.5- and 3-fold decrease in cdc2/p34-associated H1 histone kinase activity is observed in HYAL1-AS transfectant clones when compared with vector and all HYAL1-S transfectants (Fig. 2*C*). These results show that the slow proliferation rate of HYAL1-AS transfectants is due to G_2-M arrest.

Effect of HYAL1 expression on apoptosis. Next we determined whether the slower growth of HYAL1-S #3 and #4 clones of DU145 and PC-3 ML cells was due to a high rate of apoptosis. As shown in Fig. 3*A*, there was a 3-fold increase in the intracellular levels of free nucleosomes (i.e., increased apoptotic activity) in DU145 HYAL1-S #3 and HYAL1-S #4 clones when compared with vector, HYAL1-S #1 and #2, as well as HYAL1-AS clones. Similar results were obtained for PC-3 ML transfectants.

To confirm the induction of apoptosis, we measured the outward translocation of plasma membrane phosphatidylserine by Annexin V binding. As shown in Fig. 3*B*, there is a distinct increase in enhanced green fluorescent protein-Annexin V binding to the surface of HYAL1-S #3 and #4 cells when compared with vector control (i.e., right shift in log FL1; median peak log FL1: vector, 1.21; HYAL1-S #3, 2.37; HYAL1-S #4, 2.83).

We next examined mitochondrial involvement in high-HYAL1-mediated increase in apoptosis using the JC-1 dye binding assay
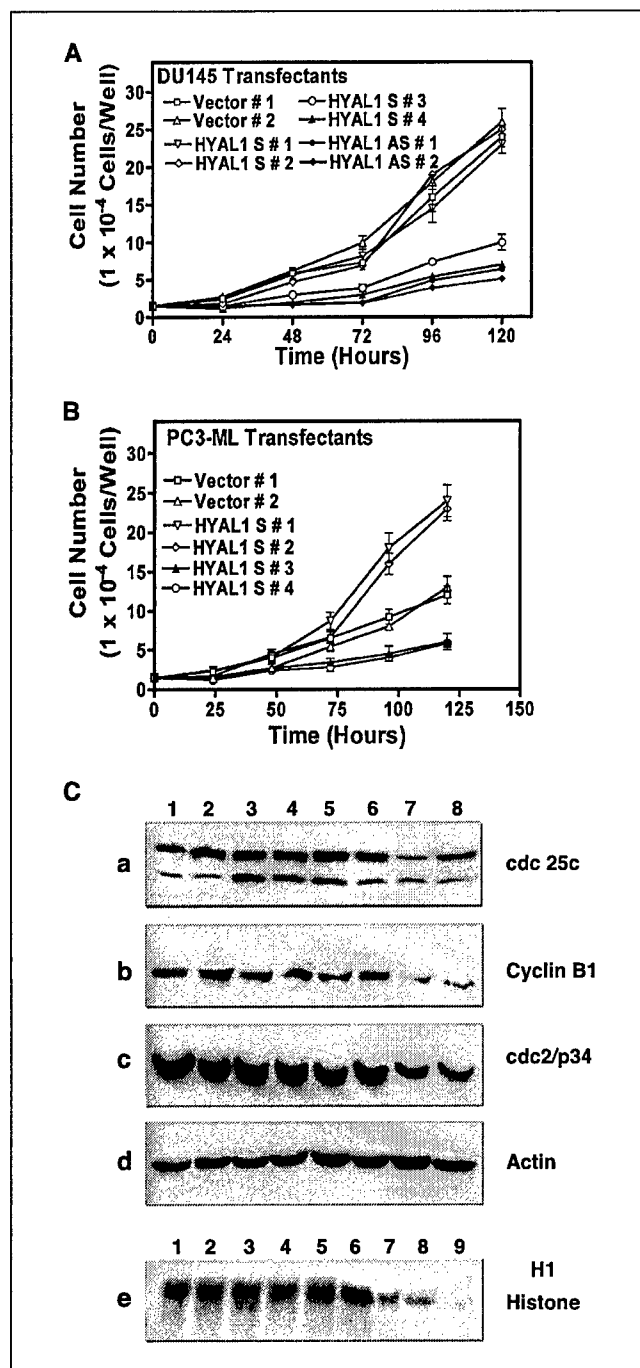
A

DU145 Transfectants
- Vector # 1
- Vector # 2
- HYAL1 S # 1
- HYAL1 S # 2
- HYAL1 S # 3
- HYAL1 S # 4
- HYAL1 AS # 1
- HYAL1 AS # 2

B

PC3-ML Transfectants
- Vector # 1
- Vector # 2
- HYAL1 S # 1
- HYAL1 S # 2
- HYAL1 S # 3
- HYAL1 S # 4

C

a — cdc 25c
b — Cyclin B1
c — cdc2/p34
d — Actin
e — H1 Histone

Figure 2. *A* and *B*, determination of proliferation rate of transfectants. *Points,* mean from duplicate measurements (three independent experiments); *bars,* SD. *A,* DU145; *B,* PC-3 ML. *C,* analysis of G_2-M cell cycle regulators. Cell lysates of DU145 transfectants were analyzed by immunoblotting using anti-cdc25c (*a*), anti-cyclin B1 (*b*), anti-cdc2/p34 (*c*), and β-actin (*d*) antibodies. *Lanes 1* and *2,* vector clones #1 and #2; *lanes 3* to *6,* HYAL1-S clones #1 to #4; *lanes 7* and *8,* HYAL1-AS clones #1 and #2. *e,* measurement of H1 histone kinase-associated activity. *Lanes 1* to *8,* the same as described above; *lane 9,* negative control.

(42). As shown in Fig. 3*C,* HYAL1-S #3 and HYAL1-S #4 transfectants exhibit a 200% increase in log FL1, indicating a decrease in $\Delta\Psi$ (i.e., increased mitochondrial permeabilization) when compared with vector and moderate HYAL1 overexpressing clones.

A

Apoptosis Index ($O.D._{450}/10^4$ Cells)

Vector #1 #2   HYAL1-S #1 #2 #3 #4   HYAL1-AS #1 #2

B

Vector # 1
HYAL1 # 3
HYAL1 # 4

Log FL1

C

Log FL1 (Mean Fluorescence Intensity)

Vector #1   HYAL1-S #1 #3 #4

D

a

MW 101 86 50 36 26 14

1 2 3 4 5 6 7 8

b

MW 101 86 50 36 26 14

1 2 3 4 5 6 7 8
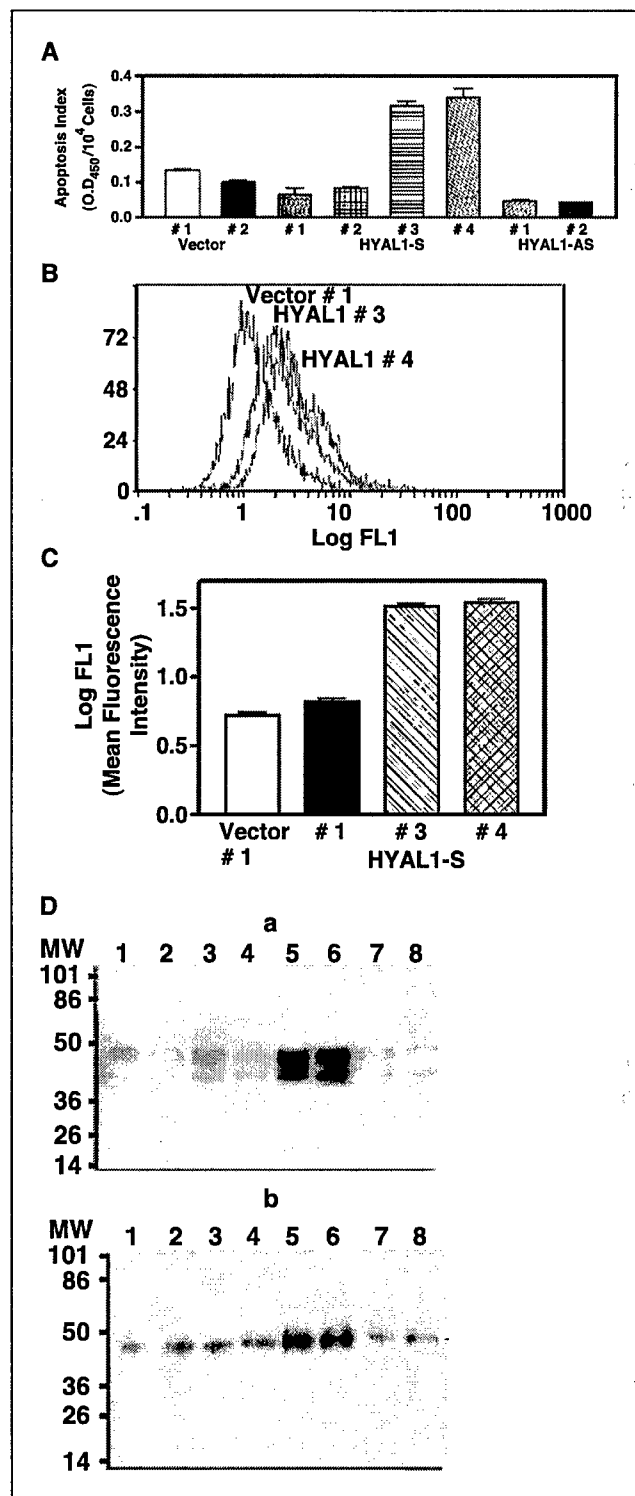
Figure 3. Examination of apoptosis. *A,* apoptotic activity in various transfectants was evaluated using the Cell Death ELISA Plus assay kit. *Columns,* mean (triplicates in two experiments); *bars,* SD. *B,* cell surface enhanced green fluorescent protein-Annexin V binding to translocated phosphatidylserine was analyzed in transfectants using flow cytometry. Experiment was repeated twice. *C,* mitochondrial depolarization was analyzed by JC-1 dye binding assay using flow cytometry. *Columns,* mean; *bars,* SD. *D,* cell lysates of DU145 transfectants were analyzed by immunoblotting using anti-WOX1 (*a*) and anti-WOX1 phosphospecific Tyr-33 antibodies (*b*). *Lanes 1* and *2,* vector clones #1 and #2; *lanes 3* to *6,* HYAL1-S clones #1 to #4; *lanes 7* and *8,* HYAL1-AS clones #1 and #2.

Figure 4. Examination of pericellular matrix in DU145 transfectants. Pericellular matrices surrounding DU145 transfectants were visualized using the particle exclusion assay. A, vector #1; B, HYAL1-S #1; C, HYAL1-S #4; D, HYAL1-AS #2.

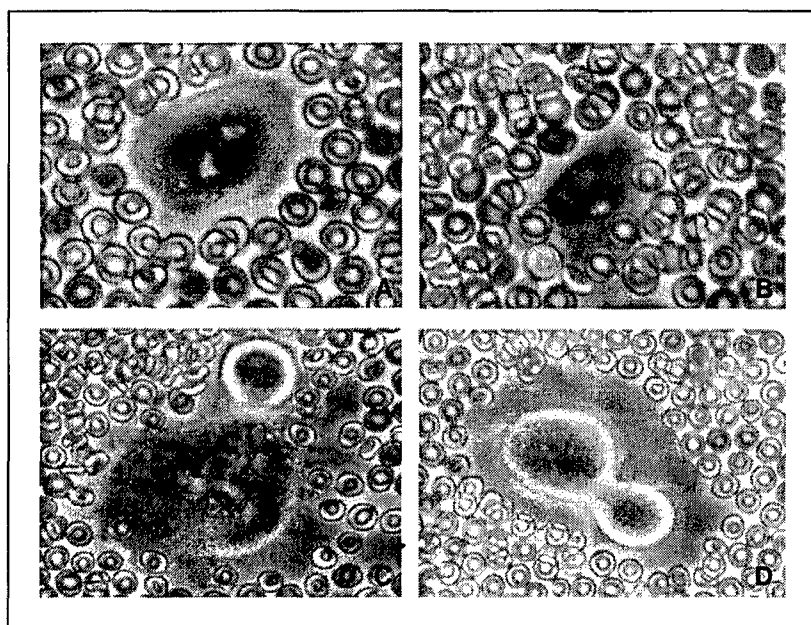We then examined the expression of the proapoptotic protein WOX1 and its activated form, WOX1-^{P}Tyr-33, in various transfectants. As shown in Fig. 3D, the major WOX1 isoform expressed in DU145 transfectants is 46 kDa WOX1-v1, although some expression of the 41 kDa WOX1-v2 isoform is also observed (Fig. 3D-a). The expression of both WOX1 isoforms is increased >3-fold in HYAL1-S #3 and #4 clones, when compared with vector, moderate HYAL1 expressing clones, and HYAL1-AS clones. The expression of the activated form of WOX1-v1 (WOX1-^{P}Tyr-33) is also increased >3-fold in HYAL1-S #3 and #4 clones. This suggests that increased apoptosis in high HYAL1 producing clones involves mitochondria and is possibly mediated by increased WOX1 expression and its activation.

Effect of HYAL1 expression on *in vitro* invasion. In the Matrigel invasion assay, the invasive activity of DU145 vector #1 clone (22.3 ± 4.3%) was normalized as 100%. The invasive activity of all HYAL1-S clones (#1-#4) varied between 109% and 118% and was not statistically different from that of vector clones ($P > 0.05$). However, the invasive activity of HYAL1-AS clones (28.2 ± 1.7% and 31.5 ± 1.5%) was 3-fold less when compared with vector clones ($P < 0.001$, Tukey's test). HYAL1 expression increased the invasive activity of PC-3 ML transfectants by 3- to 3.5-fold when compared with vector clones ($P < 0.001$). These results show that HYAL1 expression increases the invasive activity of prostate cancer cells.

Effect of HYAL1 expression on pericellular matrix formation. As shown in Fig. 4, vector #1 and HYAL1-S clones (#1 and #3) do not exhibit pericellular matrices as the erythrocytes closely abut the surface of each cell. However, HYAL1-AS cells (clone #1) exhibit a clear pericellular matrix. In 10 randomly selected fields (120-150 cells), the percentage of cells with pericellular matrix was 3- and 4.6-fold higher in the HYAL1-AS transfectants (#1: 94.2 ± 8.6%; #2: 86.3 ± 9.0%) when compared with vector (#1: 27.8 ± 18%; #2: 35.5 ± 11.1%), moderate HYAL1 overproducing (HYAL1-S #1: 25.5 ± 13.2%; #2: 31.2 ± 18%), and high HYAL1 overproducing (HYAL1-S #3: 22.3 ± 16.1%; #4: 17.2 ± 13.2%) transfectants, respectively ($P < 0.001$). Thus, hyaluronic acid is an important component of the pericellular matrix of prostate cancer cells and it is degraded by HYAL1.

Effect of HYAL1 expression on tumor xenografts. In xenografts, there is a 4- to 5-fold delay in the generation of palpable tumors in animals injected with DU145 HYAL1-AS transfectants (33 ± 4 days) when compared with vector and moderate HYAL1 overproducing transfectants (6-8 days; Fig. 5A, $P < 0.001$). Interestingly, high HYAL1 producers did not form palpable tumors even on day 40 when necropsy was done. Weights
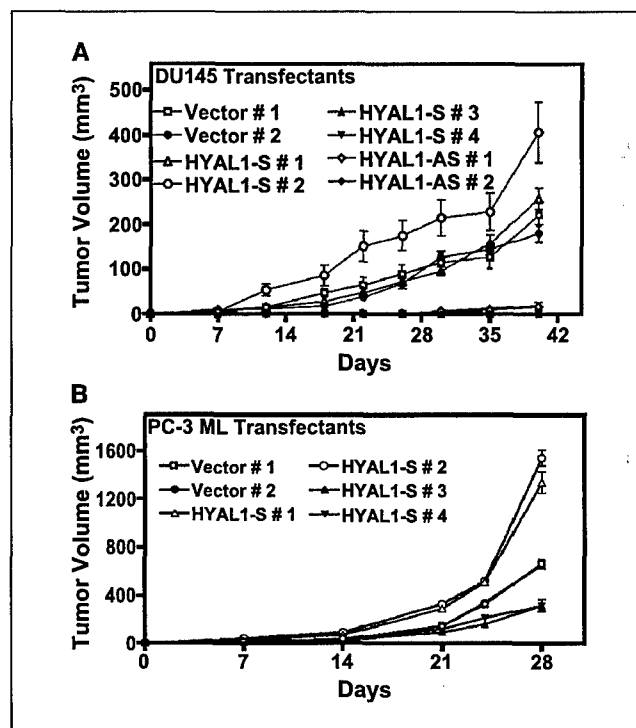

Figure 5. Examination of the growth of DU145 and PC-3 ML transfectant tumors in xenografts. DU145 and PC-3 ML transfectants were injected s.c. in athymic mice (10 animals/group) and tumor volume was measured as described in Materials and Methods. Columns, mean; bars, SD. A, DU145; B, PC-3 ML.

(in grams) of tumors generated by vector clones (#1: 0.17 ± 0.05; #2: 0.14 ± 0.04) and moderate HYAL1 overproducers (HYAL1-S #1: 0.21 ± 0.06; #2: 0.27 ± 0.14) were 4- to 7-fold higher than HYAL1-AS tumors (#1: 0.03 ± 0.01; #2: 0.04 ± 0.01), respectively ($P < 0.001$). HYAL1-S #1 and #2 tumors also showed the presence of large blood vessels. None of the animals injected with HYAL1-S #3 or #4 transfectants had visible evidence of tumor, although in some animals a Matrigel pluglike material was visible. Two additional high HYAL1 producing transfectants generated in a second transfection experiment also did not form palpable tumors (data not shown).

Moderate HYAL1 producing PC-3 ML tumors (HYAL1-S #1 and #2) grow about 2-fold faster, whereas high HYAL1 producing tumors grow 2- to 2.5-fold slower than vector tumors (Fig. 5B). At day 28, the weights (in grams) of moderate HYAL1 producing tumors (#1: 0.57 ± 0.12; #2: 0.6 ± 0.14) were ~2-fold higher than vector tumors (#1: 0.28 ± 0.06; #2: 0.29 ± 0.04) and 3.5-fold higher than high HYAL1 producing tumors (#3: 0.16 ± 0.03; #4: 0.14 ± 0.05; $P < 0.001$). Interestingly, PC-3 ML cells cultured from HYAL1-S #3 and #4 tumor tissues did not secrete any hyaluronidase activity and had lost HYAL1 expression. This suggests that *in vivo*, in the absence of a selecting agent (i.e., geneticin), HYAL1-S #3 and #4 transfectants reverted to wild-type, and therefore formed tumors (although the tumors were smaller than vector tumors).

Histology reports and photomicrographs show that DU145 vector and moderate HYAL1 producing tumors show high mitotic figures, invade skeletal muscle and lymph nodes, and infiltrate lymphatic and blood vessels. However, the tumors generated by HYAL1-AS transfectants are noninvasive (Fig. 6A). The Matrigel pluglike material removed from HYAL1-S #3 and #4 animals is ≥99% free of tumor cells and no mitotic figures are observed (Fig. 6A). Therefore, whereas blocking HYAL1 production significantly reduces tumor growth, its overproduction also decreases tumor growth and may even inhibit tumor incidence.

HYAL1, hyaluronic acid expression, and microvessel density in tumor xenografts. Tumor cells in vector and HYAL1-S #1 and #2 xenografts express significant levels of HYAL1, but HYAL1-AS cells do not secrete HYAL1 (Fig. 6B). Interestingly, as we observed in bladder cancer xenografts (29), hyaluronic acid production is increased in the tumor-associated stroma of vector and HYAL1-S #1 tumor specimens when compared with HYAL1-AS #1 tumor specimens (Fig. 6B). Microvessel density in vector (39.09 ± 4.6; #2: 36.5 ± 6.5) and moderate HYAL1 producing (HYAL1-S #1: 47.64 ± 13; #2: 51.3 ± 12.5) tumors is slightly higher than HYAL1-AS (#1: 34.3 ± 17.6; #2: 27.3 ± 12.1) tumors ($P > 0.05$). However, the

length of the capillaries (in micrometers) in vector (817.4 ± 141.5) and HYAL1-S (#1: 1,031 ± 262.5; #2: 817.9 ± 305.3) tumors is 4- to 5-fold greater than the capillaries found in HYAL1-AS tumors (#1: 218.1 ± 103.4; #2: 247.1 ± 96.1; Fig. 6C).
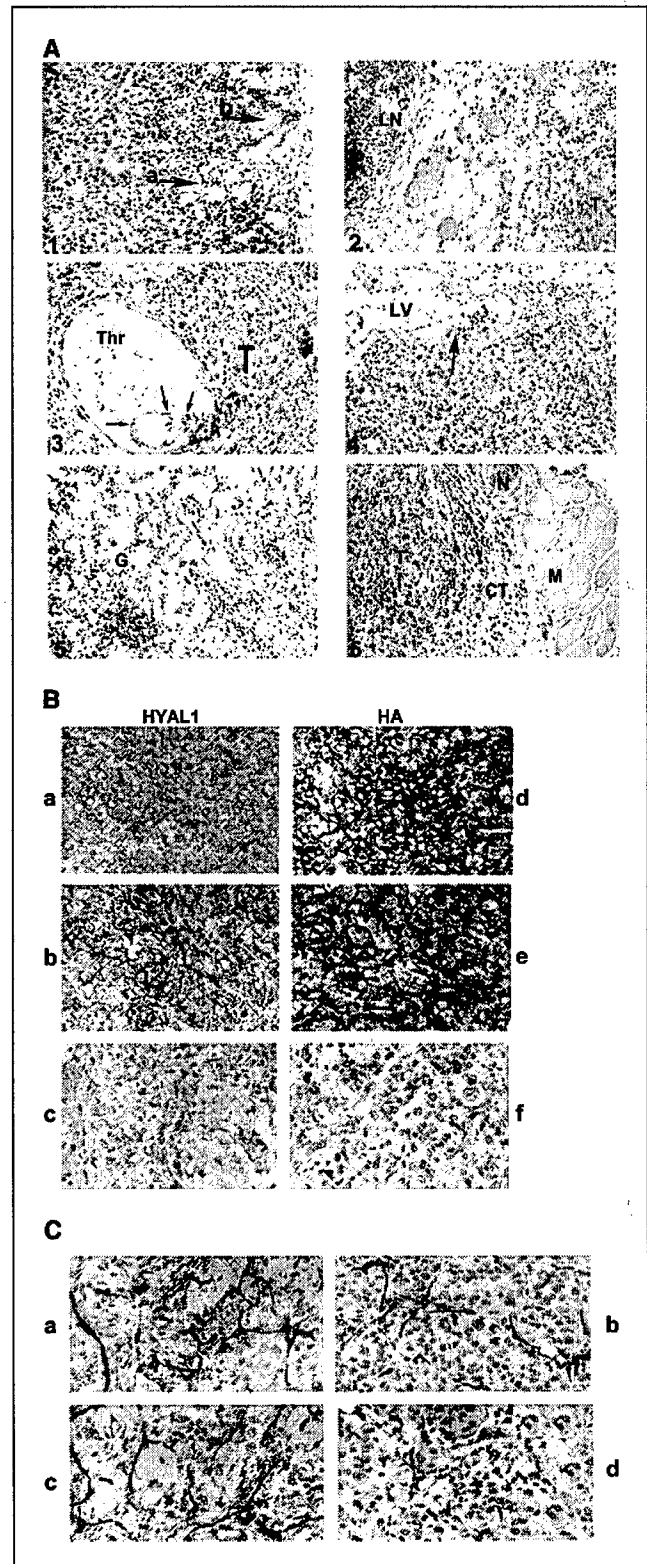

Figure 6. Examination of tumor histology. *A*, photomicrographs of H&E-stained tumor specimens are shown at ×100 magnification. *1*, vector #1: muscle fibers are surrounded by tumor cells (*arrow a*) and the tumor impinges on an adjacent nerve (*arrow b*). *2*, vector #2: tumor (*T*) approaches a lymph node (*LN*). Between the tumor and the lymph node is adipose tissue containing several blood vessels. *3*, HYAL1-S #1: a thrombus (*Thr*) fills a blood vessel at the periphery of the tumor (*T*). Tumor cells (*arrows*) have infiltrated the blood vessel. *4*, HYAL1-S #2: tumor cells (*arrow*) have infiltrated a lymphatic vessel (*LV*). *5*, HYAL1-S #4: clusters of cells, mostly leukocytes, are scattered in pale-staining Matrigel (*G*). *6*, HYAL1-AS #1: the tumor (*T*) does not invade skeletal muscle (*M*) or a nerve (*N*) as connective tissue (*CT*) separates them. *B*, HYAL1 and hyaluronic acid localization. *a-c*, HYAL1 localization; *d-f*, hyaluronic acid localization. *a* and *d*, vector #1; *b* and *e*, HYAL1-S #1; *c* and *f*, HYAL1-AS #1. *C*, localization of microvessels. The areas of the highest microvessel density from each type of tumor specimen are presented; magnification, ×400. *a*, vector #1; *b*, HYAL1-S #1; *c*, HYAL1-S #2; *d*, HYAL1-AS #1. HYAL1-S #3 and #4 were not stained for hyaluronic acid, HYAL1, or microvessels as the specimen was tumor cell–free.

Discussion

The results of our study help to explain contradictory findings about the role of HYAL1 as a tumor promoter or suppressor. Whereas in some cancers hyaluronidase (i.e., HYAL1 or PH20) serves as a diagnostic or prognostic indicator, in others, hyaluronidase levels slightly decrease in high-grade tumors (6, 9–12, 18, 45–47). In bladder cancer, blocking HYAL1 expression decreases tumor growth, invasion, and angiogenesis, but in a rat colon cancer line, HYAL1 expression suppresses tumor growth and induces necrosis (29, 35). Two possibilities can explain these contradictory results: (*a*) hyaluronidases (and HYAL1 in particular) function either as tumor promoters or suppressors depending on the tumor type; (*b*) tumor promoter and suppressor functions of hyaluronidase/HYAL1 are concentration dependent.

Our data on two prostate cancer lines show that in the same tumor cell system, HYAL1 acts as a tumor suppressor and as a tumor promoter, depending on its concentration. For example, as is the case in bladder cancer (29), HYAL1-AS transfectants of prostate cancer cells grow 4-fold slower *in vitro*, are blocked in the G_2-M phase of the cell cycle, are less invasive, and generate small, less angiogenic, noninvasive tumors. HYAL1 expression in PC-3 cells has also been shown to increase their metastatic potential (30). Therefore, HYAL1 is necessary for tumor growth, invasion, and angiogenesis.

Mean hyaluronidase levels in high-grade prostate cancer tissues (~ 36 milliunits/mg protein) are comparable to the hyaluronidase activity (14-40 milliunits/10^6 cells) secreted by vector and moderately overproducing HYAL1 transfectants of DU145 and PC-3 ML cells (7). This suggests that the hyaluronidase concentration found in tumor tissues is in the range that is stimulatory to tumor growth, invasion, and angiogenesis.

Our data show that hyaluronidase levels of ≥ 80 to 100 milliunits/10^6 cells slow tumor cell growth *in vitro*, inhibit tumor generation by DU145 transfectants, and decrease growth of PC-3 ML tumors. Consistent with these observations, in the study that reported HYAL1 expression suppresses tumor growth in a rat colon carcinoma cell model, the transfectants expressed 220 to 360 milliunits hyaluronidase activity/10^6 cells (35). In the study involving bladder cancer cells in which we showed HYAL1 enhances tumor growth, invasion, and angiogenesis, HYAL1-S transfectants produced only 2- to 2.5-fold more hyaluronidase activity than vector transfectants (29). It is possible that in that study, high HYAL1 producing transfectants grew extremely slowly and did not form clones. Our results show that high HYAL1 producing prostate cancer cells undergo apoptosis. Furthermore, partially purified HYAL1 induces apoptosis in DU145 vector and

HYAL1-S #1 and #2 clones.[5] This finding may be important in cancer treatment, as tumor cells which either do not express or moderately overexpress HYAL1 can be induced to undergo apoptosis by exposing them to HYAL1 concentration of >100 milliunits/mL.

Although the mechanism by which HYAL1 induces apoptosis in tumor cells is not fully understood, our data show that high HYAL1 expression-induced apoptosis in prostate cancer cells involves mitochondria and is possibly mediated by increased WOX1 expression and its activation. WOX1-induced apoptosis involves a mitochondrial pathway, resulting in mitochondrial permeabilization (38). Increased WOX1 expression has been shown in benign prostatic hyperplasia, prostate cancer, and metastasis (48). WOX1 may also be activated by androgens in an androgen receptor-independent manner (48). However, the functional significance of these observations is unknown.

Nearly a decade ago, it was shown that treatment with testicular hyaluronidase overcomes acquired drug resistance displayed by tumor cells growing in multicellular spheroids (49). Similarly, a clinical study conducted a few years ago showed that infusion of high doses of bovine testicular hyaluronidase (>100,000 units/kg) improves the efficacy of cytotoxic drugs (50). In these studies, it was believed that hyaluronidase played a passive role by improving drug penetration. However, such high levels of hyaluronidase may also aid in controlling tumor growth by inducing apoptosis.

Taken together, our study helps to resolve the contradiction about the role of HYAL1 as a tumor promoter and a suppressor. This study may also provide a basis for possible anti-hyaluronidase (hyaluronidase inhibition) and high-hyaluronidase treatments for controlling cancer growth and progression.

Acknowledgments

---

[5] Unpublished results.

References

1. Toole BP. Hyaluronan: from extracellular glue to pericellular cue. Nat Rev Cancer 2004;4:528–39.
2. Tammi MI, Day AJ, Turley EA. Hyaluronan and homeostasis: a balancing act. Biol Chem 2002;277:4581–4.
3. Turley EA, Noble PW, Bourguignon LY. Signaling properties of hyaluronan receptors. J Biol Chem 2002; 277:4589–92.
4. Setälä LP, Tammi MI, Tammi RH, et al. Hyaluronan expression in gastric cancer cells is associated with local and nodal spread and reduced survival rate. Br J Cancer 1999;79:1133–8.

5. Auvinen P, Tammi R, Parkkinen J, et al. Hyaluronan in peritumoral stroma and malignant cells associates with breast cancer spreading and predicts survival. Am J Pathol 2000;156:529–36.
6. Hautmann SH, Lokeshwar VB, Schroeder GL, et al. Elevated tissue expression of hyaluronic acid and hyaluronidase validates the HA-HAase urine test for bladder cancer. J Urol 2001;165:2068–74.
7. Lokeshwar VB, Rubinowicz D, Schroeder GL, et al. Stromal and epithelial expression of tumor markers hyaluronic acid and HYAL1 hyaluronidase in prostate cancer. J Biol Chem 2001;276:11922–32.
8. Lipponen P, Aaltomaa S, Tammi R, Tammi M, Ågren U, Kosma VM. High stromal hyaluronan level is associated

with poor differentiation and metastasis in prostate cancer. Eur J Cancer 2001;37:849–56.
9. Lokeshwar VB, Obek C, Soloway MS, Block NL. Tumor-associated hyaluronic acid: a new sensitive and specific urine marker for bladder cancer. Cancer Res 1997;57:773–7. Erratum in: Cancer Res 1998;58:3191.
10. Lokeshwar VB, Obek C, Pham HT, et al. Urinary hyaluronic acid and hyaluronidase: markers for bladder cancer detection and evaluation of grade. J Urol 2000; 163:348–56.
11. Posey JT, Soloway MS, Ekici S, et al. Evaluation of the prognostic potential of hyaluronic acid and hyaluronidase (HYAL1) for prostate cancer. Cancer Res 2003;63: 2638–44.

---

12. Ekici S, Cerwinka WH, Duncan R, et al. Comparison of the prognostic potential of hyaluronic acid, hyaluronidase (HYAL-1), CD44v6 and microvessel density for prostate cancer. Int J Cancer 2004;112:121–9.
13. Hayen W, Goebeler M, Kumar S, Riessen R, Nehls V. Hyaluronan stimulates tumor cell migration by modulating the fibrin fiber architecture. J Cell Sci 1999;112:2241–51.
14. Hobarth K, Maier U, Marberger M. Topical chemoprophylaxis of superficial bladder cancer with mitomycin C and adjuvant hyaluronidase. Eur Urol 1992;21:206–10.
15. Itano N, Atsumi F, Sawai T, et al. Abnormal accumulation of hyaluronan matrix diminishes contact inhibition of cell growth and promotes cell migration. Proc Natl Acad Sci 2002;99:3609–14.
16. Lees VC, Fan TP, West DC. Angiogenesis in a delayed revascularization model is accelerated by angiogenic oligosaccharides of hyaluronan. Lab Invest 1995;73:259–66.
17. West DC, Hampson IN, Arnold F, Kumar S. Angiogenesis induced by degradation products of hyaluronic acid. Science 1985;228:1324–6.
18. Franzmann EJ, Schroeder GL, Goodwin WJ, Weed DT, Fisher P, Lokeshwar VB. Expression of tumor markers hyaluronic acid and hyaluronidase (HYAL1) in head and neck tumors. Int J Cancer 2003;106:438–45.
19. Girish KS, Shashidharamurthy R, Nagaraju S, Gowda TV, Kemparaju K. Isolation and characterization of hyaluronidase a "spreading factor" from Indian cobra (*Naja naja*) venom. Biochemie 2004;86:193–202.
20. Kuhn-Nentwig L, Schaller J, Nentwig W. Biochemistry, toxicology and ecology of the venom of the spider *Cupiennius salei* (*Ctenidae*). Toxicon 2004;43:543–53.
21. Csoka AB, Frost GI, Stern R. The six hyaluronidase-like genes in the human and mouse genomes. Matrix Biol 2001;20:499–508.
22. Cherr GN, Yudin AI, Overstreet JW. The dual functions of GPI-anchored PH-20: hyaluronidase and intracellular signaling. Matrix Biol 2001;20:515–25.
23. Csoka AB, Frost GI, Wong T, Stern R. Purification and microsequencing of hyaluronidase isozymes from human urine. FEBS Lett 1997;417:307–10.
24. Frost GI, Csoka AB, Wong T, Stern R. Purification, cloning, and expression of human plasma hyaluronidase. Biochem Biophys Res Commun 1997;236:10–5.
25. Triggs-Raine B, Salo TJ, Zhang H, Wicklow BA, Natowicz MR. Mutations in HYAL1, a member of a tandemly distributed multigene family encoding disparate hyaluronidase activities, cause a newly described lysosomal disorder, mucopolysaccharidosis IX. Proc Natl Acad Sci U S A 1999;96:6296–300.
26. Lokeshwar VB, Young MJ, Goudarzi G, et al. Identification of bladder tumor-derived hyaluronidase: its similarity to HYAL1. Cancer Res 1999;59:4464–70.
27. Victor R, Chauzy C, Girard N, et al. Human breast-cancer metastasis formation in a nude-mouse model: studies of hyaluronidase, hyaluronan and hyaluronan-binding sites in metastatic cells. Int J Cancer 1999;82:77–83.
28. Madan AK, Yu K, Dhurandhar N, Cullinane C, Pang Y, Beech DJ. Association of hyaluronidase and breast adenocarcinoma invasiveness. Oncol Rep 1999;6:607–9.
29. Lokeshwar VB, Cerwinka WH, Lokeshwar BL. HYAL1 hyaluronidase: a molecular determinant of bladder cancer growth and progression. Cancer Res 2005;65:2243–50.
30. Patel S, Turner PR, Stubberfield C, et al. Hyaluronidase gene profiling and role of hyal-1 overexpression in an orthotopic model of prostate cancer. Int J Cancer 2002;97:416–24. Erratum in: Int J Cancer 2002;98:957.
31. Junker N, Latini S, Petersen LN, Kristjansen PE. Expression and regulation patterns of hyaluronidases in small cell lung cancer and glioma lines. Oncol Rep 2003;10:609–16.
32. Csoka AB, Frost GI, Heng HH, Scherer SW, Mohapatra G, Stern R. The hyaluronidase gene HYAL1 maps to chromosome 3p21.2-p21.3 in human and 9F1-F2 in mouse, a conserved candidate tumor suppressor locus. Genomics 1998;48:63–70.
33. Ji L, Nishizaki M, Gao B, et al. Expression of several genes in the human chromosome 3p21.3 homozygous deletion region by an adenovirus vector results in tumor suppressor activities *in vitro* and *in vivo*. Cancer Res 2002;62:2715–20.
34. Bertrand P, Courel MN, Maingonnat C, Jardin F, Tilly H, Bastard C. Expression of HYAL2 mRNA, hyaluronan and hyaluronidase in B-cell non-Hodgkin lymphoma: relationship with tumor aggressiveness. Int J Cancer 2005;113:207–12.
35. Jacobson A, Rahmanian M, Rubin K, Heldin P. Expression of hyaluronan synthase 2 or hyaluronidase 1 differentially affect the growth rate of transplantable colon carcinoma cell tumors. Int J Cancer 2002;102:212–9.
36. Shuster S, Frost GI, Csoka AB, Formby B, Stern R. Hyaluronidase reduces human breast cancer xenografts in SCID mice. Int J Cancer 2002;102:192–7.
37. Chang NS. Hyaluronidase activation of c-Jun N-terminal kinase is necessary for protection of L929 fibrosarcoma cells from staurosporine-mediated cell death. Biochem Biophys Res Commun 2001;283:278–86.
38. Chang NS, Doherty J, Ensign A, et al. Molecular mechanisms underlying WOX1 activation during apoptotic and stress responses. Biochem Pharmacol 2003;66:1347–54.
39. Chang NS, Pratt N, Heath J, et al. Hyaluronidase induction of a WW domain-containing oxidoreductase that enhances tumor necrosis factor cytotoxicity. J Biol Chem 2001;276:3361–70.
40. Chang NS. Transforming growth factor-β1 blocks the enhancement of tumor necrosis factor cytotoxicity by hyaluronidase Hyal-2 in L929 fibroblasts. BMC Cell Biol 2002;3:8.
41. Pham HT, Block NL, Lokeshwar VB. Tumor-derived hyaluronidase: a diagnostic urine marker for high-grade bladder cancer. Cancer Res 1997;57:778–83. Erratum in: Cancer Res 1997;57:1622.
42. Lokeshwar BL, Selzer MG, Zhu BQ, Block NL, Golub LM. Inhibition of cell proliferation, invasion, tumor growth and metastasis by an oral non-antimicrobial tetracycline analog (COL-3) in a metastatic prostate cancer model. Int J Cancer 2002;98:297–309.
43. Zoltan-Jones A, Huang L, Ghatak S, Toole BP. Elevated hyaluronan production induces mesenchymal and transformed properties in epithelial cells. J Biol Chem 2003;278:45801–10.
44. Dandekar DS, Lokeshwar BL. Inhibition of cyclooxygenase (COX)-2 expression by Tet-inducible COX-2 antisense cDNA in hormone-refractory prostate cancer significantly slows tumor growth and improves efficacy of chemotherapeutic drugs. Clin Cancer Res 2004;10:8037–47.
45. Beech DJ, Madan AK, Deng N. Expression of PH-20 in normal and neoplastic breast tissue. J Surg Res 2002;103:203–7.
46. Tuhkanen H, Anttila M, Kosma VM, et al. Genetic alterations in the peritumoral stromal cells of malignant and borderline epithelial ovarian tumors as indicated by allelic imbalance on chromosome 3p. Int J Cancer 2004;109:247–52.
47. Hiltunen EL, Anttila M, Kultti A, et al. Elevated hyaluronan concentration without hyaluronidase activation in malignant epithelial ovarian tumors. Cancer Res 2002;62:6410–3.
48. Chang NS, Schultz L, Hsu LJ, Lewis J, Su M, Sze CI. 17β-Estradiol up-regulates and activates WOX1/WWOXv1 and WOX2/WWOXv2 *in vitro*: potential role in cancerous progression of breast and prostate to a premetastatic state *in vivo*. Oncogene 2005;24:714–23.
49. Croix BS, Rak JW, Kapitain S, Sheehan C, Graham CH, Kerbel RS. Reversal by hyaluronidase of adhesion-dependent multicellular drug resistance in mammary carcinoma cells. J Natl Cancer Inst 1996;88:1285–96.
50. Klocker J, Sabitzer H, Raunik W, Wieser S, Schumer J. Hyaluronidase as additive to induction chemotherapy in advanced squamous cell carcinoma of the head and neck. Cancer Lett 1998;131:113–5.

NOT FOR
PUBLIC RELEASE

Differential selectivity of hyaluronidase inhibitors toward acidic and basic hyaluronidases

Tadahiro Isoyama[1,3], Dwayne Thwaites[1,3],
Marie G. Selzer[3], Robert I. Carey[3], Rolando Barbucci[4],
and Vinata B. Lokeshwar[2,3,5,6]

[3]Department of Urology, University of Miami Miller School of Medicine, Miami, FL 33136; [4]Department of Chemical and Biosystem Sciences and Technologies and C.R.I.S.M.A., University of Siena, Siena, Italy; [5]Department of Cell Biology and Anatomy, University of Miami Miller School of Medicine, Miami, FL 33136; and [6]Sylvester Comprehensive Cancer Center, University of Miami Miller School of Medicine, Miami, FL 33136

Hyaluronidase (HAase), a class of enzymes which degrade hyaluronic acid (HA), are involved in the spread of infections/toxins, ovum fertilization, and cancer progression. Thus, HAase inhibitors may have use in disease treatments. We evaluated 21 HAase inhibitors against HYAL-1, testicular, honeybee, and Streptomyces HAases. Among these inhibitors, polymers of poly (styrene-4-sulfonate) (PSS) (i.e., molecular weight 1400–990,000 or PSS 1400–PSS 990,000) and O-sulfated HA (sHA) derivatives (sHA2.0, 2.5, and 2.75) were the most effective. HYAL-1 and bee HAases were the most sensitive, followed by testicular HAase; Streptomyces HAase was resistant to all inhibitors, except PSS 990,000 and VERSA-TL 502 (i.e., PSS 10^6 dalton). The length of the PSS polymer determined their potency (e.g., IC_{50} for HYAL-1, PSS 990,000: 0.0096 μM; PSS 210 no inhibition; IC_{50} for testicular HAase, PSS 990,000: 0.042 μM; PSS 210 no inhibition). The presence, but not the number, of sulfate groups on the sHA molecule determined its potency (e.g., IC_{50} for HYAL-1: sHA2.0, 0.019 μM; sHA2.75, 0.0083 μM). Other known HAase inhibitors, such as gossypol, sodium-aurothiomalate, 1-tetradecane sulfonic acid, and glycerrhizic acid, were not effective. Both PSS and sHA inhibited HAases by a mixed inhibition mechanism (i.e., competitive + uncompetitive) and were 5- to 17-fold better as uncompetitive inhibitors than as competitive inhibitors. These results demonstrate that HAase inhibitors show selectivity toward the different types of HAases, which could be exploited to inhibit specific HAases involved in a variety of pathophysiologic conditions.

Key words: bee hyaluronidase/HYAL1/hyaluronic acid/hyaluronidase inhibitors/hyaluronidase/Streptomyces hyaluronidase/testicular hyaluronidase

[1]These authors contributed equally to this work.
[2]To whom correspondence should be addressed; e-mail: vlokeshw@med.miami.edu

Introduction

Extracelluar matrix synthesis and its degradation not only regulate several normal physiologic functions but are also involved in disease processes, such as tumor metastasis, angiogenesis, and atherosclerosis. Inhibitors of extracelluar matrix degrading enzymes (e.g., matrix-metalloproteinases) are useful in the treatment of gingivitis, dry eye syndrome, and cancer (Lokeshwar, 1999; Woessner, 1999; Dursun et al., 2002). Inhibitors of hyaluronidase (HAase) may be useful as contraceptives, because these inhibit the acrosomal reaction initiated by testicular HAase (Anderson et al., 2000, 2002; Zaneveld et al., 2002).

Hyaluronic acid (HA) is a glycosaminoglycan made up of repeating disaccharide units, D-glucuronic acid and N-acetyl-D-glucosamine. In addition to maintaining the tissues hydrated and osmotically balanced, HA regulates cell adhesion, migration, and proliferation (Laurent and Fraser, 1992; Delpech et al., 1997; Tammi et al., 2002). Concentrations of HA are elevated in cancer tissues, where it most likely promotes tumor metastasis (Delpech et al., 1997; Setala et al., 1999; Auvinen et al., 2000; Lokeshwar et al., 2000, 2001; Pirinen et al., 2001; Toole et al., 2002; Posey et al., 2003). Elevated urinary HA levels serve as an accurate marker for detecting bladder cancer regardless of the tumor grade (Lokeshwar et al., 2000, 2002b). The high molecular mass HA ($>10^5$ daltons) is anti-angiogenic, whereas small fragments of HA (3–25 disaccharide units) are angiogenic (Rooney et al., 1995; Trochon et al., 1997; Slevin et al., 1998; Lokeshwar and Selzer, 2000).

HAase cleaves internal β-N-acetyl-D-glucosaminidic linkages in the HA polymer. Exhaustive digestion of HA by HAase yields tetrasaccharides, whereas limited digestion yields angiogenic HA fragments (Roden et al., 1989). In humans, six HAase genes cluster into two tightly linked triplets on chromosomes 3p21.3 (HYAL-1, HYAL-2, and HYAL-3) and 7q31.3 (HYAL-4, HYALP1, and PH20) (Csoka et al., 2001). PH20, that is, the testicular HAase, is present on the sperm cell surface and is required for penetration through the follicle cell layer (Cherr et al., 2001; Vines et al., 2001). It has a broad pH spectrum (pH 3.2–9.0) (Vines et al., 2001; Franzmann et al., 2003). HYAL-1 type HAase is present in human serum and urine (Csoka et al., 1997; Frost et al., 1997). However, we have shown that HYAL-1 is the major tumor-derived HAase expressed in prostate, bladder, and head and neck cancer cells (Lokeshwar et al., 1999; 2001; Franzmann et al., 2003). Elevated HYAL-1 levels serve as an accurate marker for detecting intermediate- and high-grade bladder cancer and as a prognostic indicator for predicting prostate cancer progression (Lokeshwar et al., 2000; Posey et al., 2003). We have recently shown that expression of

HYAL-1 in tissues is regulated by alternative mRNA splicing (Lokeshwar *et al.*, 2002a).

Historically, HAases were considered "spreading factors," because they are crucial for the spread of bacterial infections and toxins present in various venoms (Tu and Hendon, 1983; Henrissat, 1991; Gmachl and Kreil, 1993; Kreil, 1995; Henrissat and Bairoch, 1996; Stern, 2004). Determination of the crystal structure of honeybee (bee) venom HAase has helped in the understanding of HA catalysis by mammalian HAases, since these HAases share ~30% sequence identity with bee HAase (Markovic-Housley *et al.*, 2000). Many pathogenic streptococci such as *Streptomyces hyaluronlyticus* and even phages of group A streptococci produce HAase (Baker *et al.*, 2002). HAase production by streptococci is related to their virulence. Streptomyces HAase is often used as a standard in HAase assays (Stern and Stern, 1992; Lokeshwar *et al.*, 2000, 2001). We have recently shown that HYAL1-type HAase promotes bladder tumor growth, muscle invasion, and angiogenesis (Lokeshwar *et al.*, 2005b). Therefore, potent HAase inhibitors would be useful as contraceptives, anti-tumor agents and possibly have anti-bacterial and anti-venom/toxin properties.

Many synthetic and naturally occurring compounds act as HAase inhibitors. These include high molecular mass poly (styrene-4-sulfonate) (PSS), gossypol, sodium aurothiomalate, fenoprofen, glycerrhizic acid, fatty acids, plant-derived compounds, heparin, and O-sulfated HA (sHA) (Balazs *et al.*, 1951; Perreault *et al.*, 1980; Wolf *et al.*, 1984; Joyce *et al.*, 1986; Yuan *et al.*, 1995; Furuya *et al.*, 1997; Toida *et al.*, 1999; Anderson *et al.*, 2000, 2002; Mio and Stern, 2002; Zaneveld *et al.*, 2002; Yingprasertchai *et al.*, 2003). For example, more than half a century ago, Balazs *et al.* (1951) reported that sHA and heparin inhibit testicular HAase. HAase inhibitors such as high molecular mass PSS and sodium cellulose sulfate (Ushercell) are being tested as vaginal contraceptives, because they inhibit the activity of testicular HAase (Anderson *et al.*, 2002). These compounds also inhibit sexually transmitted disease-causing bacteria but not the normal vaginal flora (Anderson *et al.*, 2000; 2002; Zaneveld *et al.*, 2002). Similarly, sodium aurothiomalate has been shown to reduce local tissue damage and prolong survival time in mice injected with different venoms (Yingprasertchai *et al.*, 2003). The anti-inflammatory agent glycerrhizic acid from licorice has been shown to inhibit testicular HAase (Furuya *et al.*, 1997). O-Sulfated derivatives of HA inhibit urinary HAase, which is identical to HYAL1 (Csoka *et al.*, 1997; Frost *et al.*, 1997; Lokeshwar *et al.*, 1999; Toida *et al.*, 1999).

Although several inhibitors of HAase are known, it is unknown whether these inhibitors show variability in inhibiting the activity of different types of HAases (i.e., testicular, HYAL-1, bacterial, and venom-derived [e.g., bee venom]). If different HAases show differential sensitivity toward various HAase inhibitors, HAase inhibitors can be selected to inhibit the activity of one type of HAase without inhibiting others. Such selectivity may help in designing HAase inhibitors as therapeutics for diseases, contraceptives, and venom antidotes, without significantly affecting HAase functions that are required in normal physiology.

In this study, we compared the sensitivity of HYAL-1, testicular, bee, and Streptomyces HAases with 21 HAase

inhibitors, using the HAase enzyme-linked immunosorbent assay (ELISA)-like assay and enzyme kinetic analysis.

Results

Effect of PSS compounds on HAase activity

To study the effect of PSS compounds on HYAL-1, testicular, Streptomyces, and bee HAases, we used an activity-based HAase ELISA-like assay. All four HAases were assayed at their optimum pH, and the pH optimum value for each HAase was determined by generating pH activity profile curves (14, 26, and data not shown). HAase activity is usually expressed as the number of glycosidic linkages split per time unit. It is noteworthy that although the HAase ELISA-like assay is specific and allows assaying of several specimens simultaneously, it does not give information on the number of glycosidic linkages split per time unit. Therefore, all of the constants, that is, IC_{50}, K_m, V_{max}, and K_i values reported in this study should be considered as apparent. In addition, the molecular weights of each compound (e.g., 990,000 dalton for PSS 990,000, 1400 dalton for PSS 1400) were used in the calculations of IC_{50} values and other constants.

As shown in Figure 1A, PSS 990,000 inhibits the activity of all four HAases in a dose-dependent manner. However,
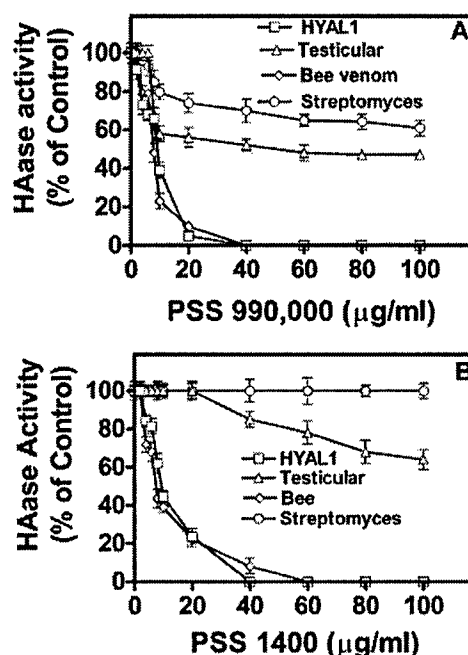
Fig. 1. Effect of PSS 990,000 and PSS 1400 on HAase activity. Approximately 40 mU/mL of HYAL-1, bee, testicular, or Streptomyces HAase were incubated on an HA-coated microtiter well plate in the presence or absence of various concentrations of PSS 990,000 (A) or PSS 1400 (B). The HAase ELISA-like assay was performed as described in *Materials and methods*. HAase activity, in the absence of any inhibitor, was considered as 100% (control), and the data are expressed as % of control.

HYAL-1 and bee HAases are more sensitive to inhibition by PSS 990,000 than testicular and Streptomyces HAases. From the inhibition curves, we determined the IC_{50} values for each inhibitor. The IC_{50} values of PSS 990,000 for testicular HAase (0.042 µM) and Streptomyces HAase (0.39 µM) are 4.2-fold and 40-fold higher than the IC_{50} values for HYAL-1 (0.0096 µM) and bee HAase (0.0091 µM), respectively (Table I). VERSA-TL 502 is the sodium salt of PSS of molecular weight ~10^6 dalton, which was used by Anderson et al. (2000) to demonstrate that PSS inhibits testicular HAase activity and blocks fertilization. As summarized in Table I, IC_{50} values of VERSA-TL 502 for HYAL-1 (0.0088 µM), bee (0.0081 µM), testicular HAase (0.042 µM), and Streptomyces HAase (0.32 µM) mirror those for PSS 990,000.

Next, we determined whether the length of the PSS polymer affects its ability to inhibit the activity of different HAases. All four HAases showed a progressive decrease in susceptibility to inhibition by PSS polymers of decreasing lengths, when IC_{50} values were calculated on the real molecular weight basis. In addition, the HAases also showed differential sensitivity to various PSS inhibitors. For example, PSS 210 (a monomer) does not inhibit the activity of any of the four HAases (Table I). As shown in Figure 1B and Table I, although HYAL-1 and bee HAase

are inhibited completely with PSS 1400 (IC_{50} = 8.2 and 6.6 µM, respectively), the activity of testicular HAase is blocked only partially (IC_{50} = 68 µM). The activity of Streptomyces HAase is not inhibited by PSS 1400. PSS 4300 and PSS 6800 also show differences in their ability to inhibit HYAL-1 (IC_{50} = 3.3 and 2.0 µM), bee (IC_{50} = 2.6 and 1.9 µM), testicular (IC_{50} = 4.9 and 6.7 µM), and Streptomyces (no inhibition) HAases. The IC_{50} values for HYAL-1 and bee HAases closely resemble those for testicular HAase for PSS compounds between PSS 17,000 and PSS 150,000 (Table I). It is noteworthy that although significant differences were observed in the sensitivity of testicular HAase to higher molecular mass PSS compounds, when compared with PSS1400, there appears to be very little difference in the inhibitory power of PSS compounds when the IC_{50} values for HYL1 and bee HAases are calculated on a weight concentration basis.

Effect of sHA on HAase activity

O-Sulfation of glycosaminoglycans, including O-sHA and heparin, inhibit both urinary and testicular HAases (Balazs et al., 1951; Wolf et al., 1984; Toida et al., 1999). In fact, the anti-HAase activities of sHA and heparin against testicular HAase were compared as early as 1951 by Balazs et al.

Table I. IC_{50} values of 21 HAase inhibitors for HYAL-1, bee, testicular, and Streptomyces HAases

Inhibitors	HYAL1 IC_{50} (µM)	Bee venom HAase IC_{50} (µM)	Testicular HAase IC_{50} (µM)	Streptomyces HAase IC_{50} (µM)
990,000	0.0096	0.0091	0.042[a]	0.39[a]
VERSA-TL 502	0.00876	0.0081	0.0416[a]	0.316[a]
350,000	0.037	0.013	0.074	1.5
150,000	0.07	0.047	0.074	NI
77,000	0.19	0.13	0.39	NI
49,000	0.31	0.34	0.23	NI
32,000	0.42	0.53	0.54	NI
17,000	0.89	1.0	0.89	NI
6800	3.3	2.6	4.9	NI
4300	1.97	1.9	6.7	NI
1400	8.2	6.6	67.6[a]	NI
PSS 210	NI	NI	NI	NI
sHA2.0	0.019	0.019	0.078[a]	NI
sHA2.5	0.017	0.018	0.049[a]	NI
sHA2.75	0.0083	0.012	0.038[a]	NI
Heparin	0.39	0.41	17[a]	NI
Gossypol	NI	NI	NI	NI
Fenoprofen	NI	NI	NI	NI
1-Tetradecane sulfonic acid	63[a]	NI	NI	NI
Glycerrhizic acid	39.4[a]	NI	NI	NI
Sodium aurothiomalate	NI	NI	94[a]	NI

NI, no inhibition.

The IC_{50} values for each of the 21 inhibitors were calculated by generating an inhibition curve for each inhibitor, as shown in Figures 1 and 3 for PSS and sHA compounds, respectively.

[a]The differences in the IC_{50} values of a particular HAase inhibitor among different HAases are statistically significant ($P < 0.05$; unpaired t test).

T. Isoyama et al.

(1951). Therefore, we tested the effect of sHA and heparin on the activity of HYAL-1, testicular, bee, and Streptomyces HAases. We also determined whether the number of sulfate groups on sHA affected its ability to inhibit HAase activity.

sHA compounds containing varying degrees of sulfation were prepared using the tributylamine salt of HA and various amounts of SO_3– pyridine, as reported by one of us (i.e., Barbucci et al., 1995). Depending on the sulfate content, we designated these sHA species as sHA2.0, sHA2.5, and sHA2.75. To determine the degrees of sulfation in each of the sHA compounds, we performed %S and %N analysis. As summarized in Table II, based on our previously described procedure, we are able to obtain sHA species with increasing degrees of sulfation by increasing the SO_3– pyridine to the tributylamine HA ratio. The %S in sHA2.0 (9.74%) is close to the theoretical %S value (i.e., 10.3%) calculated from a sHA disaccharide (molecular weight = 620 dalton) that contains two sulfate groups; the experimental and theoretical values for %N are identical (i.e., 2.2%). The %S in sHA2.5 (i.e., 11.8%) is slightly lower than the theoretical %S value (i.e., 12.2%), and the %N value in sHA2.5 is slightly higher (i.e., 2.2%) than the theoretical %N value (i.e., 2.1%). These differences may be because of experimental variation, which was about 10%. sHA2.5 (molecular weight of the disaccharide = 656 dalton) means that 50% of disaccharides in the HA molecule most likely contain two sulfate groups and the remaining 50% contain three sulfate groups. Nonetheless, the degree of sulfation in sHA2.5 is higher than that in sHA2.0. In case of sHA2.75 (disaccharide molecular weight = 680 dalton), the %S value (12.5%) is closer to the theoretical value 12.9%, and the %N value is almost the same (2.01%) as that of the theoretical value (2.05%). This suggest that in the sHA2.75 polymer, 75% of the HA oligosaccharides contain three sulfate groups and the remaining 25% contain two sulfate groups. As summarized in Table II, increasing the SO_3– pyridine to the tributylamine HA to 15:1 does not result in a further increase in HA sulfation.

We also confirmed the presence of sulfate groups in each sHA compound using the dimethylmethylene blue (DMMB) assay and the HA ELISA-like assay. Sulfated glycosaminoglycans, but not HA, are detected by the DMMB assay. As shown in Figure 2A, HA is not detected
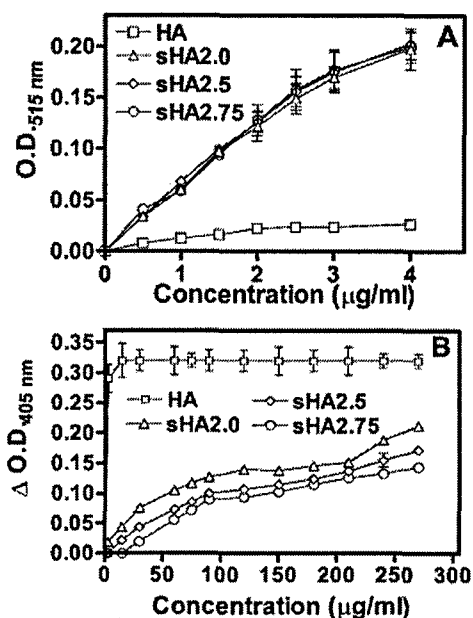
Table II. Elemental analysis of sHA compounds.

Compound	SO_3– pyridine ratio: tributylamine HA (w/w)	%N	%S	Nitrogen/ sulfur ratio
HA	—	3.41	0.68	5.0
sHA2.0	4.2:1	2.2	9.74	0.23
sHA2.5	8.4:1	2.2	11.8	0.19
sHA2.75	10:1/15:1	2.01/1.98	12.5/12.6	0.16/0.16

sHA compounds were prepared by adding various amounts of SO_3– pyridine to the tributylamine salt of HA. The %S was determined by inductively coupled plasma atomic emission spectroscopy (ICP-AES) analysis after dissolution. %N was determined by micro combustion and micro titration analyses. Each analysis was carried out in duplicate. The variation in duplicate %S analyses was $\leq 2.3\%$, and in %N analyses, it was $\leq 9.1\%$.

Fig. 2. Characterization of sHA compounds. (A) DMMB assay. Various concentrations of HA and sHA compounds were mixed with DMMB reagent, and the O.D. was measured at 515 nm. (B) HA ELISA-like assay. Various concentrations of HA and sHA compounds were measured by the HA ELISA-like assay, as described in *Materials and methods*.

by the DMMB assay. However, sHA derivatives, sHA2.0, sHA2.5, and sHA2.75, are detected by the DMMB assay, and the optical density increases in a dose-dependent manner. Furthermore, sHA derivatives are detected by the DMMB assay in a manner very similar to that of other sulfated glycosaminoglycans assayed by the DMMB method (data not shown). As shown in Figure 2B, HA is detected by the HA ELISA-like assay; and the maximum limit of HA detection by the ELISA-like assay is 10 ng/mL of HA. However, none of the sHA compounds are detected by the HA ELISA-like assay at that concentration. Furthermore, even at >100,000-fold excess concentration (i.e., 100–300 µg/mL), the detection of sHA2.0, sHA2.5, or sHA2.75 in the HA ELISA-like assay is <50% of the maximum optical density reading obtained at 10 ng/mL concentration of HA. It is noteworthy that sulfated glycosaminoglycans are also not detected by the HA ELISA-like assay. These three analytical analyses establish that we have synthesized sulfated derivatives of HA.

We tested the effects of sHA2.0, sHA 2.5, and sHA 2.75 on HAase activity using the HAase ELISA-like assay. As shown in Figure 3A, sHA2.0 inhibits the activity of HYAL-1, bee, and testicular HAases in a dose-dependent manner. However, the activity of Streptomyces HAase is not inhibited by sHA2.0. The IC_{50} value of sHA2.0 to inhibit testicular HAase (0.078 µM) is four times higher than that for HYAL-1 (0.019 µM) and bee HAase (0.019 µM), respectively (Table I). sHA2.5 has similar inhibition profile as that for sHA2.0, that is, HYAL-1 and bee HAases are inhibited to a greater degree than the testicular HAase (Figure 3B; Table I). Streptomyces HAase is not inhibited by sHA2.5
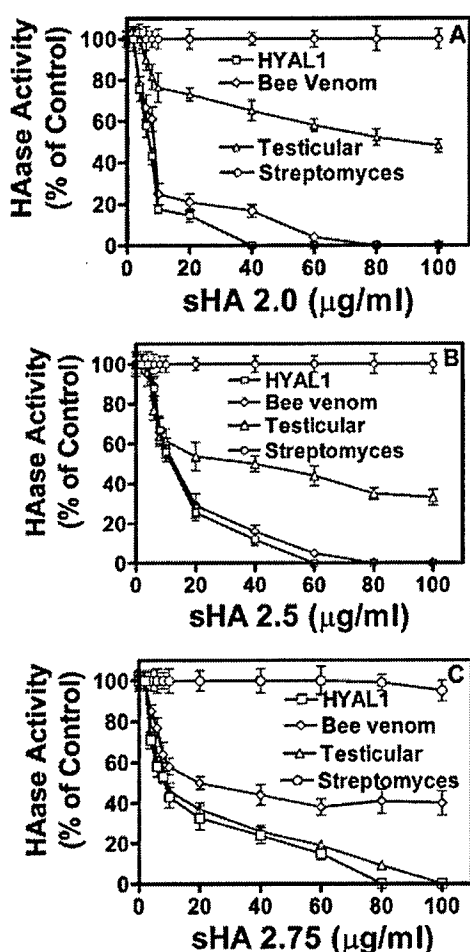
Fig. 3. Effect of sHA on HAase activity. Approximately 40 mU/mL of HYAL-1, bee, testicular, or Streptomyces HAase were incubated on an HA-coated microtiter well plate in the presence or absence of various concentrations of sHA2.0 (A), sHA2.5 (B), or sHA2.75 (C). The HAase ELISA-like assay was performed as described in *Materials and methods*. HAase activity, in the absence of any inhibitor was considered as 100% (control), and the data are expressed as % of control.

even at a concentration of 100 µg/mL (Figure 3B). sHA2.75 is slightly more inhibitory to HYAL-1, bee, and testicular HAase than to sHA2.0 and sHA2.5 (Figure 3C). In fact, Streptomyces HAase is slightly inhibited (~5%) by sHA2.75 at the 100 µg/mL concentration. The IC_{50} values for HYAL-1 (0.0083 µM) and bee (0.012 µM) HAases are ~2.8- to 4.6-fold higher than the IC_{50} values for testicular HAase (0.038 µM), respectively (Table I). It is noteworthy that in the same assay system, HA alone even at high concentration (i.e., 100 µg/mL) did not inhibit the activity of any of the four HAases (data not shown). Because sHA derivatives are hygroscopic and the molecular weight of sHA2.0 (774,000 dalton), sHA2.5 (818,000 dalton), and sHA2.75 (848,000 dalton) are estimates, the IC_{50} values presented in Table I for each sHA compound may be off by a factor of 2 (or 50% error).

As summarized in Table I, both HYAL-1 and bee HAases can be inhibited by heparin with IC_{50} values of 0.39 µM for HYAL-1 and 0.41 µM for bee HAase, respectively. However, the IC_{50} of heparin for testicular (IC_{50} = 17 µM) is ~40 times higher, and Streptomyces HAase is resistant to inhibition by heparin.

Effect of small molecular weight inhibitors on HAase activity

As summarized in Table I, gossypol and fenoprofen do not inhibit the activity of any of the four HAases when tested up to a concentration of 100 µg/mL. Both 1-tetradecane sulfonic acid (IC_{50} = 63 µM) and glycerrhizic acid (IC_{50} = 39 µM) weakly inhibit HYAL-1 activity (Table I). Sodium aurothiomalate inhibited only testicular HAase with an IC_{50} of 94 µM (Table I).

The results described above demonstrate that among the 21 HAase inhibitors that were tested, PSS and sHA are the two categories of inhibitors that are the most effective in inhibiting HYAL-1, bee HAases and to a lesser degree testicular HAase. The activity of Streptomyces HAase is not inhibited by all but two (i.e., PSS 990,000 and VERSA-TL 502) HAase inhibitors.

Enzyme kinetic studies

To determine the mechanism by which PSS and sHA compounds inhibit the activity of HYAL-1, bee, and testicular HAases, we performed enzyme kinetic studies. For kinetic studies, we slightly modified the ELISA-like assay by coating microtiter wells with HA at concentrations from 0.5 to 10 µg/mL. This range of substrate concentration was chosen to be in the linear range of product formation.

Figures 4 and 5 show Lineweaver-Burke plots for HA degradation by HYAL-1 (Figure 4) and testicular (Figure 5) HAases in the presence of four different concentrations of PSS 990,000, PSS 1400, and sHA2.5. As shown in Figure 4A–C, the double reciprocal plots for HA degradation by HYAL-1 in the presence or absence of PSS 990,000, PSS 1400, and sHA2.5 are linear, indicating that none of the HAase inhibitors induce any cooperativity. However, in the presence of each of these inhibitors, the slopes and extrapolated Y- and X-intercepts increase, suggesting that PSS 990,000, PSS 1400, and sHA2.5 inhibit HYAL-1 through a mixed inhibition mechanism (i.e., competitive and uncompetitive inhibition). Both sHA2.0 and sHA2.75 also inhibit HYAL-1 activity through a mixed inhibition mechanism. As summarized in Table III, the K_m of HYAL1 to degrade HA, in the absence of any inhibitor, is 0.28 µM, and it either increases or decreases slightly when PSS 990,000 (K_m = 0.4 µM), PSS 1400 (K_m = 0.33 µM), sHA2.0 (K_m = 0.35 µM), sHA2.5 (K_m = 0.31 µM), and sHA2.75 (K_m = 0.25 µM) are added in the enzyme reaction. Although not statistically significant (Tukey's multiple comparison test), this consistent increase or decrease in K_m is characteristic of a mixed inhibition. As summarized in Table III, the V_{max} also decreases in the presence of various inhibitors, and this decrease in V_{max} when compared with no inhibitor, is statistically significant (Tukey's multiple comparison test; $P >$ 0.05, in each case). The K_i(s) of PSS 990,000 for competitive and uncompetitive components are 0.03 µM and 0.035 µM, respectively, suggesting that PSS 990,000 is equally effective
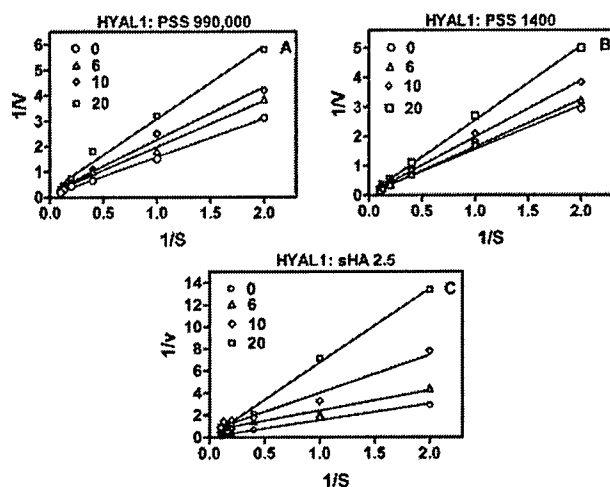
Fig. 4. Lineweaver-Burke (double reciprocal) analysis of HA degradation by HYAL-1 in the presence of HAase inhibitors. HYAL-1 (~20 mU/mL) was incubated on a HA-coated (0.5–10 µg/mL) microtiter well plate in the presence or absence of four different concentrations of PSS 990,000 (A), PSS 1400 (B), or sHA2.5 (C). The HAase ELISA-like assay was performed, as described in *Materials and methods*. The initial velocity *V* was defined as pmol of HA degraded per min, during incubation. S is the substrate concentration (µg/mL) used to coat the micro titer wells.
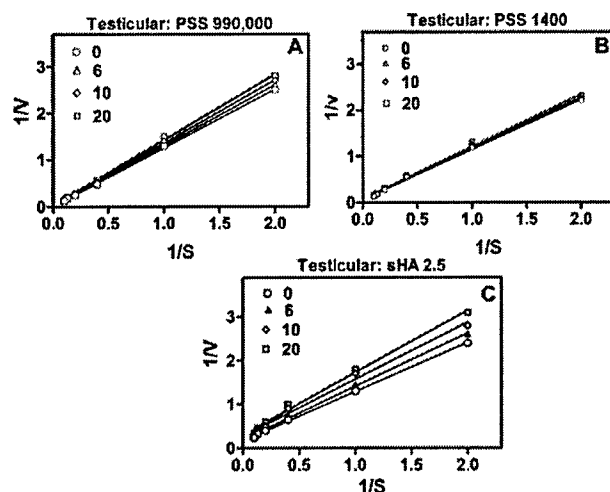

Fig. 5. Lineweaver-Burke (double reciprocal) analysis of HA degradation by testicular HAase in the presence of HAase inhibitors. Testicular HAase (~20 mU/mL) was incubated in a HA-coated (0.5–10 µg/mL) microtiter well plate in the presence or absence of four different concentrations of HAase inhibitors PSS 990,000 (A), PSS 1400 (B), or sHA2.5 (C). The HAase ELISA-like assay was performed, as described in *Materials and methods*. The initial velocity *V* was defined as pmol of HA degraded per min, during incubation. S is the substrate concentration (µg/mL) used to coat the micro titer wells.

as a competitive and uncompetitive inhibitor. However, because the Ki(s) of PSS 1400 and all three sHA compounds as competitive inhibitors are 15- to 23-fold higher than their Ki(s) as uncompetitive inhibitors, these compounds are

more effective as uncompetitive inhibitors. As in the case of IC_{50} values, the Ki values obtained for each sHA compound may be off by a factor of 2 (or 50% error).

As summarized in Table III, both testicular and bee HAases also appear to be inhibited by PSS and sHA compounds through a mixed inhibition mechanism. Except for PSS 1400, the other inhibitors are equally good as competitive and uncompetitive inhibitors of testicular HAase (Table III). For bee HAase, except for PSS 990,000, the Ki(s) of PSS 1400, sHA2.0, sHA2.5, and sHA2.75 as competitive inhibitors are ~25-fold higher than the Ki(s) of the same inhibitors as uncompetitive inhibitors, suggesting that these compounds are better uncompetitive inhibitors.

Discussion

HAases are expressed in both prokaryotes and eukaryotes and are involved in bacterial pathogenesis, spread of toxins and venoms, acrosomal reaction/ovum fertilization, and cancer progression (Tu and Hendon, 1983; Henrissat, 1991; Gmachl and Kreil, 1993; Kreil, 1995; Henrissat and Bairoch, 1996; Anderson *et al.*, 2000, 2002; Lokeshwar *et al.*, 2000, 2001, 2002b, 2005b; Zaneveld *et al.*, 2002; Stern, 2004). Thus, inhibition of HAase activity by HAase inhibitors could be used as an antidote for toxins/venoms, contraceptives, and anti-tumor therapy. For example, using bladder and prostate cancer model systems, we have recently shown that HYAL1 is a molecular determinant of tumor growth, invasion, and angiogenesis (Lokeshwar *et al.*, 2005a,b). Lack of HYAL1 arrests cells in the G2-M phase of the cell cycle, and the tumors generated are 10-fold smaller, less angiogenic, and resemble benign neoplasia. Thus, if an HAase inhibitor is more specific for HYAL1, it could be used to design anti-cancer therapies. Several reports have shown that the sodium salt of PSS, sodium cellulose sulfate, and other HAase inhibitors have a broad spectrum of anti-microbial activity against organisms which cause sexually transmitted diseases and are effective as both contraceptive agents and as antidotes for cobra and pit viper venoms (Anderson *et al.*, 2000, 2002; Zaneveld *et al.*, 2002; Yingprasertchai *et al.*, 2003). The availability of selective inhibitors, which target one type of HAase, without affecting other HAases, is desirable because HAases have normal physiologic functions. These examples suggest a practical value for surveying HAase inhibitors for specific clinical uses.

In this study, we show that there is some selectivity among the different inhibitors with respect to blocking the activity of different HAases. For example, we found that HYAL-1 and bee HAases show similar sensitivity to all but two HAase inhibitors (i.e., 1-tetradecane sulfonic acid and glycerrhizic acid). HYAL-1 and bee HAases have an acidic pH optimum and share a 27.2% amino acid identity. However, the amino acid identity cannot explain the similarity and differences of various HAases to inhibition by different HAase inhibitors. For example, testicular HAase is more resistant than HYAL-1 and bee HAase to inhibition by 20 of the 21 HAase inhibitors that were tested in this study. Similarly, Streptomyces HAase, which has a pH optimum at 5.0, is resistant to all but two (PSS 990,000 and VERSA-TL

Table III. Effect of PSS and sHA on HAase activity

Inhibitor	HYAL1				Bee venom HAase				Testicular HAase			
	Competitive (K_i μM)	Uncompetitive (K_i μM)	V_{max} pmol/min	K_m (μM)	Competitive (K_i μM)	Uncompetitive (K_i μM)	V_{max} pmol/min	K_m (μM)	Competitive (K_i μM)	Uncompetitive (K_i μM)	V_{max} pmol/min	K_m (μM)
None	—	—	0.45 ± 0.22	0.28 ± 0.07	—	—	0.38 ± 0.13	0.35 ± 0.06	—	—	0.16 ± 0.04	0.41 ± 0.10
PSS 990,000	0.03 ± 0.01	0.04 ± 0.02	0.03 ± 0.01	0.40 ± 0.13	0.03 ± 0.01	0.02 ± 0.01	0.03 ± 0.01	0.48 ± 0.11	0.57 ± 0.24	0.41 ± 0.10	0.08 ± 0.02	0.53 ± 0.06
PSS 1400	91 ± 7	3.5 ± 2.1	0.18 ± 0.04	0.33 ± 0.09	95 ± 12	3.8 ± 1.4	0.17 ± 0.03	0.37 ± 0.14	290 ± 50	72 ± 9	0.11 ± 0.01	0.62 ± 0.16
SHA2.0	0.08 ± 0.03	0.004 ± 0.002	0.03 ± 0.01	0.35 ± 0.14	0.04 ± 0.01	0.002 ± 0.001	0.04 ± 0.02	0.05 ± 0.01	0.16 ± 0.06	0.05 ± 0.02	0.08 ± 0.01	0.55 ± 0.04
SHA2.5	0.04 ± 0.01	0.002 ± 0.001	0.02 ± 0.01	0.31 ± 0.15	0.04 ± 0.01	0.002 ± 0.001	0.03 ± 0.02	0.65 ± 0.15	0.05 ± 0.02	0.04 ± 0.02	0.07 ± 0.02	1.02 ± 0.21
SHA2.75	0.03 ± 0.02	0.002 ± 0.001	0.02 ± 0.01	0.25 ± 0.08	0.04 ± 0.01	0.002 ± 0.001	0.03 ± 0.01	0.53 ± 0.12	0.04 ± 0.02	0.04 ± 0.01	0.04 ± 0.02	0.67 ± 0.20

Kinetic data were generated for PSS 990,000, PSS 1400, sHA2.0, sHA2.5, and sHA2.75 from the double reciprocal plots for each inhibitor as have been presented for PSS 990,000, PSS 1400, and sHA2.5 for HYAL-1 (Figure 4) and testicular (Figure 5) HAases. The K_m and V_{max} values (mean ± SD) for each enzyme are calculated assuming the molecular mass of HA as 500,000 dalton. K_i values for each inhibitor are calculated using the molecular mass of each inhibitor.

T. Isoyama *et al.*

502) of the HAase inhibitors tested in this study. Thus, although the reason is unknown at this time, it appears that HAases active at pH ≥5.0 are resistant to several different classes of HAase inhibitors. However, consistent with our conclusion that different HAase inhibitors have different selectivity toward HAases, Botzki *et al.* (2004) showed that L-ascorbic acid 6-hexadeconoate is 14- to 25-fold more potent in inhibiting HAase from *Streptococcus agalactiae* than it is for inhibiting *Streptococcus pneumoniae* and testicular HAase. Because sodium-PSS, cellulose sulfate, heparin, and gossypol have been shown to inhibit the acrosomal reaction, it is important to bear in mind that when used clinically, these inhibitors will inhibit HYAL-1 which is present in serum (Wolf *et al.*, 1984; Yuan *et al.*, 1995; Lokeshwar *et al.*, 1999; Anderson *et al.*, 2000, 2002; Zaneveld *et al.*, 2002).

At this time, it is unknown why the bacterial HAase (i.e., Streptomyces HAase) is resistant to all but two HAase inhibitors that were tested. Because the sequence of *Streptomyces hyaluronlyticus* is unknown, we performed an amino acid sequence alignment between HYAL-1 (GenBank Accession number BC035695.1) and *Streptomyces griseus* HAase (GenBank Accession number AB028210.1). Although, there is ~26% amino acid identity between these two proteins, the identical amino acids occur randomly in both sequences. In addition, large stretches of amino acid sequences present in one protein are absent in the other and vice versa. Similar observations were made when we aligned the Streptomyces HAase sequence with either PH20 (GenBank accession number NM003117.3) or bee HAase (GenBank accession number A47477; Markovic-Housley *et al.*, 2000). It is noteworthy that we have identified a 30 amino acid sequence that is well conserved in all six human HAases and in bee HAase. This sequence is required for HAase activity (Lokeshwar *et al.*, 2002a). We noted that within this 30 amino acid sequence, identical or conserved amino acid substitutions are present at positions 2, 3, 6, 7, 14, 15, and 17–22 in all mammalian and bee HAases. However, this 30 amino acid sequence is not well conserved in Streptomyces HAase. These observations suggest that higher eukaryotic HAases have significantly diverged from bacterial HAases, and this may explain why the bacterial HAase is resistant to most of the HAase inhibitors that were tested in this study. The crystal structures of *S. agalactiae*, testicular HAase, bee venom HAase and chondroitin ABC lyase have been deciphered recently (Markovic-Housley *et al.*, 2000; Huang *et al.*, 2003; Botzki *et al.*, 2004). These structures show notable similarities and differences in the catalytic sites of these glycosaminoglycan-degrading enzymes. Because many of the HAase inhibitors are uncompetitive inhibitors, it appears that they most likely do not bind directly to the catalytic domain. The sequences of these enzymes in other parts of the molecule are less conserved, suggesting that it may be possible to identify natural compounds or synthesize new ones that specifically inhibit a particular glycosaminoglycan-degrading enzyme.

It has been previously shown that fully O-sHA can inhibit urinary HAase activity. In this study, we find that modification of HA with two sulfate groups is as effective in inhibiting HAase activity as is the sHA with a mixture of HA disaccharides with two and three sulfate groups. It is interesting that although theoretically HA disaccharides can contain up to four sulfate groups, experimentally we could not achieve this degree of sulfation even after increasing the SO_3- pyridine to the tributylamine HA ratio from 1:10 to 1:15. We could not increase this ratio further, because of the solubility of SO_3^- pyridine, at higher concentrations. It is noteworthy that Balazs *et al.* (1951) reported 13.2% S content in their sHA preparation. This experimental %S value is also less than the theoretical %S value (13.8%) for a HA disaccharide that contains three sulfate groups, suggesting that maximally sHA polymer is most likely a mixture of disaccharides containing two or three sulfate groups. In the case of PSS compounds, the length of the polymer is the factor that decides the efficacy of HAase inhibition. Therefore, if these or cellulose-sulfate compounds are to be used as contraceptives, the optimum concentration will depend upon the length of the polymer and how it inhibits testicular HAase.

It has been previously reported that fully O-sHA inhibits urinary HAase activity through both competitive and noncompetitive mechanisms (Toida *et al.*, 1999). Since in that study, the K_m values in the absence or presence of inhibitor were not reported, it is unclear whether the authors observed a non-competitive or uncompetitive inhibition. In our study, most inhibitors caused a slight increase in the K_m, suggesting a mixed inhibition consisting of competitive and uncompetitive mechanisms. Since both sHA and PSS compounds are more effective as uncompetitive inhibitors than as competitive inhibitors, these would be effective *in vivo*, as their efficacy will be independent of the HA concentration present in target tissues and tissue fluids. This finding is particularly important for designing anti-HAase treatments for cancer, because in many tumor tissues HA concentration is elevated (Setala *et al.*, 1999; Auvinen *et al.*, 2000; Lokeshwar *et al.*, 2000, 2001, 2002b; Pirinen *et al.*, 2001; Posey *et al.*, 2003).

Taken together, our study demonstrates that although all HAases degrade HA, they show differences in their sensitivity to different classes of HAase inhibitors. HAase inhibitors displaying mixed inhibition may prove to be effective in inhibiting HAase activity in various pathophysiologic conditions.

Materials and methods

Materials

Sodium salts of PSS of molecular weight 210 (PSS 210), 1400 (PSS 1400), 4300 (PSS 4300), 6800 (PSS 6800), 17,000 (PSS 17,000), 32,000 (PSS 32,000), 49,000 (PSS 49,000), 77,000 (PSS 77,000), 150,000 (PSS 150,000), 350,000 (PSS 350,000), and 990,000 (PSS 990,000) were purchased from Fluka Biochemicals (Switzerland). VERSA-TL 502, a PSS of molecular weight 1×10^6 dalton was kindly provided by Alco Chemicals, a Division of National Starch Company (Chattanooga, TN). Gossypol, fenoprofen, 1-tetradecane sulfonic acid, glycerrhizic acid, and heparin were purchased from Sigma Chemicals (St. Louis, MO).

sHA derivatives sHA2.0, sHA2.5, and sHA2.75 were prepared as discussed previously (Barbucci *et al.*, 1995) with the following modifications: 100 mg of human umbilical

cord HA– sodium salt was dissolved in distilled water and desalted on a Celex-P matrix (BioRad, Hercules, CA). HA was then mixed with three molar equivalents of tributylamine at room temperature for 2 h. Following incubation, the HA solution was alkalinated (~pH 8.0), dialyzed extensively against distilled water, and lyophilized. Hundred milligrams of the HA-tributylamine salt was suspended in anhydrous dimethylformamide and mixed with various amounts of anhydrous SO_3^- pyridine under a stream of nitrogen. The amount of SO_3^- pyridine determines the number of O-sulfated groups in the sHA polymer (Barbucci et al., 1995). The sHA was then precipitated, dialyzed against water, and lyophilized. The molecular mass of the various sHA compounds was determined using a Sepharose S-300 gel filtration column (1.5 × 120 cm) eluted with phosphate-buffered saline + 0.05% Tween 20; 1.6 mL/fraction. The column was calibrated using HA species of various molecular mass (2.0×10^6 D to 8 kD; Genzyme, MA). The elution volume for sHA2.0 derivatives was similar to 0.5×10^6 D HA, whereas that of sHA2.75 was closer to the 1.0×10^6 D HA standard. Based on the degree of sulfation, and the molecular weight of HA, the molecular weights of sHA2.0, sHA2.5, and sHA2.75 were approximated to 774,000, 818,000, and 848,000 dalton, respectively. These molecular weights were used for calculating Ki values.

Elemental analysis

Percentages of nitrogen and sulfur per disaccharide unit of sHA2.0, sHA2.5, and sHA2.75 were determined by elemental analysis performed by Mikroanalytisches Labor Pascher, Remagen-Bandorf, Germany. Nitrogen analysis was carried out by micro combustion and micro titration, and sulfur analysis was performed by inductively coupled plasma atomic emission spectroscopy (ICP-AES).

HAases

HYAL-1 was partially purified from the conditioned medium of HT1376 bladder cancer cells stably transfected with HYAL-1 cDNA encoding the full-length protein (Lokeshwar et al., 2005b). Briefly, a stable HYAL1 clone expressing ~40 mU/mL activity was expanded in T-75 cm^2 flasks. At ~60% confluence, cultures were washed three times in phosphate-buffered saline and incubated in RPMI 1640 medium containing insulin, transferrin, and selenium. Following 48-h incubation, the conditioned medium was collected and HYAL-1 was partially purified, as described previously (Lokeshwar et al., 1999). Bovine testicular HAase and Streptomyces HAase were purchased from MP Biomedicals (Irvine, CA). Lyophilized bee venom was purchased from Sigma Chemicals.

HAase ELISA-like assay

The HAase ELISA-like assay was performed, as described earlier (Stern and Stern, 1992; Lokeshwar et al., 2000, 2001). Microtiter well plates coated with human umbilical cord HA (MP Biomedicals) were incubated with ~40 mU/mL of HYAL-1, testicular, bee, or Streptomyces HAase in the presence or absence of various HAase inhibitors in respective assay buffers. For the HYAL-1 activity assay, we used 0.1 M sodium formate, 0.15 M NaCl, 0.02% bovine serum albumin buffer, pH 4.2. Testicular HAase assay buffer contains 0.1 sodium acetate, 0.15 M NaCl, 0.02% bovine serum albumin, pH 5.5. Bee HAase was assayed in the same buffer as that used for HYAL-1, whereas Streptomyces HAase was assayed in 0.1 M sodium acetate, 0.15 M NaCl, 0.02% bovine serum albumin, pH 5.0.

The effect of HAase inhibitors on the activity of HYAL-1, testicular, bee, and Streptomyces HAases was tested at 0, 1, 2, 4, 6, 8, 10, 20, 40, 60, 80, and 100 µg/mL concentrations of each inhibitor. The plate was incubated at 37°C for 16 h. Following incubation, the degraded HA was washed off, and the HA remaining on the microtiter plate was determined using a biotinylated HA-binding protein and an avidin-biotin detection system (Vector Laboratories, Burlingame, CA) (Lokeshwar et al., 2001). Each plate was developed for 3 min, and the reaction was terminated by adding 3 N HCl. HAase activity (mU/mL) was calculated from a standard graph, prepared by plotting known amounts of Streptomyces HAase (10^{-4} U/mL), versus (control [no enzyme] O.D.$_{405 nm}$ – sample O.D.$_{405 nm}$). IC$_{50}$ for each inhibitor was calculated as the concentration (µM) of an inhibitor required to inhibit 50% of the activity of the HAase tested. Molecular weights of each compound (e.g., 990,000 dalton for PSS 990,000, 1400 dalton for PSS 1400, 774,000 for sHA2.0) were used in the calculations of IC$_{50}$ values in µM. About 100% activity was defined as the enzyme activity obtained in the absence of any inhibitor. The data presented are mean ± SEM from duplicate measurements in two independent experiments.

Enzyme kinetic assays

Microtiter plates were coated with 100 µL of 0, 0.5, 1, 2.5. 5, 7.5, and 10 µg/mL of human umbilical cord HA at 37°C for 4 h. Following incubation, each well received ~20 mU/mL of HYAL-1, Streptomyces, testicular, or bee HAase and 0, 6, 10 or 20 µg/mL of an inhibitor, in a total volume of 100 µL of an appropriate HAase assay buffer (as described above). Control wells received inhibitor at a particular concentration but no enzyme. The plate was incubated at 37°C for 4 h and then developed as described above. The amount of product (i.e., HA degraded) was calculated by subtracting the amount of HA remaining on the well from the amount of HA that was used to coat the wells. The amount of HA remaining on the wells was calculated from O.D.$_{405 nm}$ in control wells (i.e., wells containing no enzyme) and O.D.$_{405 nm}$ in sample wells (i.e., wells containing enzyme + inhibitor). K_m, V_{max}, and Ki (for both competitive and uncompetitive inhibition) were calculated by plotting Lineweaver-Burke double reciprocal plots. The K_m value was expressed in µM by assuming the molecular mass of HA to be 500,000 dalton. The molecular mass of HA was determined by gel filtration chromatography performed on a Sepharose S-300 column. The V_{max} was expressed as pmole/min. The graphs were plotted using the GraphPad Prism Software Program (version 3.1), and Ki values for each inhibitor were calculated from the extrapolated X- and Y-intercepts and the slope. Ki for the competitive inhibition component of mixed inhibition was calculated from the equation: $\alpha = 1 + I/Ki$, where $\alpha = 1/V_{max}$. The Ki for the uncompetitive inhibition component of mixed inhibition was

calculated as $\alpha' = 1 + I/Ki$, where $\alpha' = $ Y-intercept $\times V_{max}$. The Ki values were expressed as µM concentration of the inhibitor and were calculated from the molecular mass of the inhibitor.

DMMB assay

Various concentrations of HA and sHA in a final volume of 0.1 mL were mixed with 0.5 mL of DMMB reagent. The optical density of the color developed was determined at 515 nm (Farndale *et al.*, 1982).

HA ELISA-like assay

HA ELISA-like assay was performed, as described previously (Lokeshwar *et al.*, 2000, 2001). Briefly, 25 µg/mL human umbilical cord HA was coated on microtiter wells of a 96-well plate. Following the blocking of nonspecific sites using 1% bovine serum albumin, various concentrations of HA or sHA compounds were incubated in HA-coated wells in phosphate-buffered saline, containing 0.05% Tween 20 and 1 µg/mL biotinylated HA-binding protein. The incubation was continued for 16 h at room temperature. Following incubation, the unbound HA-binding protein was washed off, and the HA-binding protein bound to microtiter wells was measured using an avidin–biotin detection system (Vector Laboratories). HA present in each sample (ng/mL) was determined from a standard graph plotted as (control $O.D._{405\ nm}$ – sample $O.D._{405\ nm}$) versus concentration.

Acknowledgments

Abbreviations

DMMB, dimethylmethylene blue; ELISA, enzyme-linked immunosorbent assay; HA, hyaluronic acid; HAase, hyaluronidase; PSS, poly (styrene-4-sulfonate); sHA, sulfated HA.

References

Anderson R.A., Feathergill, K., Diao, X., Cooper, M., Kirkpatrick, R., Spear, P., Waller, D.P., Chany, C., Doncel, G.F., Herold, B., and Zaneveld, L.J. (2000) Evaluation of poly (styrene-4-sulfonate) as a preventive agent for conception and sexually transmitted diseases. *J. Androl.*, **21**, 862–875.

Anderson, R.A., Feathergill, K.A., Diao, X.H., Cooper, M.D., Kirkpatrick, R., Herold, B.C., Doncel, G.F., Chany, C.J., Waller, D.P., Rencher, W.F., and Zaneveld, L.J. (2002) Preclinical evaluation of sodium cellulose sulfate (Ushercell) as a contraceptive antimicrobial agent. *J. Androl.*, **23**, 426–438.

Auvinen, P., Tammi, R., Parkkinen, J., Tammi, M., Agren, U., Johansson, R., Hirvikoski, P., Eskelinen, M., and Kosma, V.M., (2000) Hyaluronan in peritumoral stroma and malignant cells associates with Breast cancer spreading and predicts survival. *Am. J. Pathol.*, **156**, 529–536.

Baker, J.R., Dong, S., and Pritchard, D.G. (2002) The hyaluronan lyase of Streptococcus pyogenes bacteriophage H4489A. *Biochem. J.*, **365**, 317–322.

Balazs, E.A., Hogberg, B., and Laurent, T.C. (1951) The biological activity of hyaluron sulfuric acid. *Acta Physiol. Scand.*, **23**, 168–178.

Barbucci, R., Magnani, A., Casolaro, M., Marchettini, N., and Rossi, C. (1995) Modification of hyaluronic acid by insertion of sulphate groups to obtain a heparin-like molecule. Part 1. Characterisation and behaviour in aqueous solution towards H^+ and Ca^{2+} ions. *Gazz. Chim. Ital.*, **125**, 169–180.

Botzki, A., Rigden, D.J., Braun, S., Nukui, M., Salmen, S., Hoechstetter, J., Bernhardt, G., Dove, S., Jedrzejas, M.J., and Buschauer, A. (2004) L-Ascorbic acid, 6-hexadecanoate, a potent hyaluronidase inhibitor. X-ray structure and molecular modeling of enzyme-inhibitor complexes. *J. Biol. Chem.*, **279**, 45990–45997.

Cherr, G.N., Yudin, A.I., and Overstreet, J.W. (2001) The dual functions of GPI-anchored PH-20: hyaluronidase and intracellular signaling. *Matrix Biol.*, **20**, 515–525.

Csoka, A.B., Frost, G.I., Wong, T., and Stern, R. (1997) Purification and microsequencing of hyaluronidase isozymes from human urine. *FEBS Lett.*, **417**, 307–310.

Csoka, A.B., Frost, G.I., and Stern, R. (2001) The six hyaluronidase-like genes in the human and mouse genomes. *Matrix Biol.*, **20**, 499–508.

Delpech, B., Girard, N., Bertrand, P., Courel, M.N., Chauzy, C., and Delpech, A. (1997) Hyaluronan: fundamental principles and applications in cancer. *J. Intern. Med.*, **242**, 41–48.

Dursun, D., Wang, M., Monroy, D., Li, D.Q., Lokeshwar, B.L., Stern, M., and Pflugfelder, S.C. (2002) Experimentally induced dry eye produces ocular surface inflammation and epithelial disease. *Adv. Exp Med. Biol.*, **506**, 647–655.

Farndale, R.W., Sayers, C.A., and Barrett, A.J. (1982) A direct spectrophotometric microassay for sulfated glycosaminoglycans in cartilage cultures. *Connect Tissue Res.*, **9**, 247–248.

Franzmann, E.J., Schroeder, G.L., Goodwin, W.J., Weed, D.T., Fisher, P., and Lokeshwar, V.B. (2003) Expression of tumor markers hyaluronic acid and hyaluronidase (HYAL1) in head and neck tumors. *Int. J. Cancer.*, **106**, 438–445.

Frost, G.I., Csoka, A.B., Wong, T., and Stern, R. (1997) Purification, cloning, and expression of human plasma hyaluronidase. *Biochem. Biophys. Res. Commun.*, **236**, 10–15.

Furuya, T., Yamagata, S., Shimoyama, Y., Fujihara, M., Morishima, N., and Ohtsuki, K. (1997) Biochemical characterization of glycyrrhizin as an effective inhibitor for hyaluronidases from bovine testis. *Biol. Pharm. Bull.*, **20**, 973–977.

Gmachl, M. and Kreil, G. (1993) Bee venom hyaluronidase is homologous to a membrane protein of mammalian sperm. *Proc. Natl. Acad. Sci. U. S. A.*, **90**, 3569–3573.

Henrissat, B. (1991) A classification of glycosyl hydrolases based on amino acid sequence similarities. *Biochem. J.*, **280**, 309–316.

Henrissat, B. and Bairoch, A. (1996) Updating the sequence-based classification of glycosyl hydrolases. *Biochem. J.*, **316**, 695–696.

Huang, W., Lunin, V.V., Li, Y., Suzuki, S., Sugiura, N., Miyazono, H., and Cygler, M. (2003) Crystal structure of Proteus vulgaris chondroitin sulfate ABC lyase I at 1.9A resolution. *J. Mol. Biol.*, **328**, 623–634.

Joyce, C.L., Mack, S.R., Anderson, R.A., and Zaneveld, L.J. (1986) Effect of hyaluronidase, beta-glucuronidase and beta-N-acetylglucosaminidase inhibitors on sperm penetration of the mouse oocyte. *Biol. Reprod.*, **35**, 336–346.

Kreil, G. (1995) Hyaluronidases – a group of neglected enzymes. *Protein Sci.*, **4**, 1666–16669.

Laurent, T.C. and Fraser, J.R. (1992) Hyaluronan. *FASEB J.*, **6**, 2397–2404.

Lokeshwar, B.L. (1999) MMP inhibition in prostate cancer. *Ann. N. Y. Acad. Sci.*, **878**, 271–289.

Lokeshwar, V.B. and Selzer, M.G. (2000) Bladder tumor markers for monitoring recurrence and screening: comparison of HA-HAase and BTA-Stat tests. *J. Biol. Chem.*, **265**, 27641–27649.

Lokeshwar, V.B., Young, M.J., Goudarzi, G., Iida, N., Yudin, A.I., Cherr, G.N., and Selzer, M.G. (1999) Identification of bladder tumor-derived hyaluronidase: its similarity to HYAL1. *Cancer Res.*, **59**, 4464–4470.

Lokeshwar, V.B., Obek, C., Pham, H.T., Wei, D., Young, M.J., Duncan, R.C., Soloway, M.S., and Block, N.L. (2000) Urinary hyaluronic acid

and hyaluronidase: markers for bladder cancer detection and evaluation of grade. *J. Urol.*, **163**, 348–356.

Lokeshwar, V.B., Rubinowicz, D., Schroeder, G.L., Forgacs, E., Minna, J.D., Block, N.L., Nadji, M., and Lokeshwar, B.L. (2001) Stromal and epithelial expression of tumor markers hyaluronic acid and HYAL1 hyaluronidase in prostate cancer. *J. Biol. Chem.*, **276**, 11922–11932.

Lokeshwar, V.B., Schroeder, G.L., Carey, R.I., Soloway, M.S., and Iida, N. (2002a) Regulation of hyaluronidase activity by alternative mRNA splicing. *J. Biol. Chem.*, **277**, 33654–33663.

Lokeshwar, V.B., Schroeder, G.L., Selzer, M.G., Hautmann, S.H., Posey, J.T., Duncan, R.C., Watson, R., Rose, L., Markowitz, S., and Soloway, M.S. (2002b) Bladder tumor markers for monitoring recurrence and screening comparison of hyaluronic acid-hyaluronidase and BTA-Stat tests. *Cancer*, **95**, 61–72.

Lokeshwar, V.B., Cerwinka, W.H., Isoyama, T., and Lokeshwar, B.L. (2005a) HYAL1 hyaluronidase in prostate cancer: a tumor promoter and suppressor. *Cancer Res.*, **65**, 7782–7789.

Lokeshwar, V.B., Cerwinka, W.H., and Lokeshwar, B.L. (2005b) HYAL1 hyaluronidase: a molecular determinant of bladder tumor growth and invasion. *Cancer Res.*, **65**, 2243–2250.

Markovic-Housley, Z., Miglierini, G., Soldatova, L., Rizkallah, P.J., Muller, U., and Schirmer, T. (2000) Crystal structure of hyaluronidase, a major allergen of bee venom. *Structure Fold. Des.*, **8**, 1025–1035.

Mio, K. and Stern, R. (2002) Inhibitors of the hyaluronidases. *Matrix Biol.*, **21**, 31–37.

Perreault, S., Zaneveld, L.J., and Rogers, B.J. (1980) Inhibition of fertilization in the hamster by sodium aurothiomalate, a hyaluronidase inhibitor. *J. Reprod. Fertil.*, **60**, 461–467.

Pirinen, R., Tammi, R., Tammi, M., Hirvikoski, P., Parkkinen, J.J., Johansson, R., Bohm, J., Hollmen, S., and Kosma, V.M. (2001) Prognostic value of hyaluronan expression in non-small-cell lung cancer: increased stromal expression indicates unfavorable outcome in patients with adenocarcinoma. *Int. J. Cancer*, **95**, 12–17.

Posey, J.T., Soloway, M.S., Ekici, S., Sofer, M., Civantos, F., Duncan, R.C., and Lokeshwar, V.B. (2003) Evaluation of the prognostic potential of hyaluronic acid and hyaluronidase (HYAL1) for prostate cancer. *Cancer Res.*, **63**, 2638–2644.

Roden, L., Campbell, P., Fraser, J.R., Laurent, T.C., Pertoft, H., and Thompson, J.N. (1989) Enzymatic pathways of hyaluronan catabolism. *Ciba Found. Symp.*, **143**, 60–86.

Rooney, P., Kumar, S., Ponting, J., and Wang, M. (1995) The role of hyaluronan in tumour neovascularization (review). *Int. J. Cancer.*, **60**, 632–636.

Setala, L.P., Tammi, M.I., Tammi, R.H., Eskelinen, M.J., Lipponen, P.K., Agren, U.M., Parkkinen, J., Alhava, E.M., and Kosma, V.M. (1999) Hyaluronan expression in gastric cancer cells is associated with

local and nodal spread and reduced survival rate. *Br. J. Cancer*, **79**, 1133–1138.

Slevin, M., Krupinski, J., Kumar, S., and Gaffney, J. (1998) Angiogenic oligosaccharides of hyaluronan induce protein tyrosine kinase activity in endothelial cells and activate a cytoplasmic signal transduction pathway resulting in proliferation. *Lab. Invest.*, **78**, 987–1003.

Stern, R. (2004) Hyaluronan catabolism: a new metabolic pathway. *Eur. J. Cell Biol.*, **83**, 317–325.

Stern, M. and Stern, R. (1992) An ELISA-like assay for hyaluronidase and hyaluronidase inhibitors. *Matrix*, **12**, 397–403.

Tammi, M.I., Day, A.J., and Turley, E.A. (2002) Hyaluronan and homeostasis: a balancing act. *J. Biol. Chem.*, **277**, 4581–4584.

Toida, T., Ogita, Y., Suzuki, A., Toyoda, H., and Imanari, T. (1999) Inhibition of hyaluronidase by fully O-sulfonated glycosaminoglycans. *Arch. Biochem. Biophys.*, **370**, 176–182.

Toole, B.P., Wight, T.N., and Tammi, M.I. (2002) Hyaluronan–cell interactions in cancer and vascular disease. *J. Biol. Chem.*, **277**, 4593–4596.

Trochon, V., Mabilat-Pragnon, C., Bertrand, P., Legrand, Y., Soria, J., Soria, C., Delpech, B., and Lu, H. (1997) Hyaluronectin blocks the stimulatory effect of hyaluronan-derived fragments on endothelial cells during angiogenesis in vitro. *FEBS Lett.*, **418**, 6–10.

Tu, A.T. and Hendon, R.R. (1983) Characterization of lizard venom hyaluronidase and evidence for its action as a spreading factor. *Comp. Biochem. Physiol. B.*, **76**, 377–383.

Vines, C.A., Li, M.W., Deng, X., Yudin, A.I., Cherr, G.N., and Overstreet, J.W. (2001) Identification of a hyaluronic acid (HA) binding domain in the PH-20 protein that may function in cell signaling. *Mol. Reprod. Dev.*, **60**, 542–552.

Woessner, J.F. Jr. (1999) Matrix metalloproteinase inhibition. From the Jurassic to the third millennium. *Ann. N. Y. Acad. Sci.*, **878**, 388–403.

Wolf, R.A., Glogar, D., Chaung, L.Y., Garrett, P.E., Ertl, G., Tumas, J., Braunwald, E., Kloner, R.A., Feldstein, M.L., and Muller, J.E. (1984) Heparin inhibits bovine testicular hyaluronidase activity in myocardium of dogs with coronary artery occlusion. *Am. J. Cardiol.*, **53**, 941–944.

Yingprasertchai, S., Bunyasrisawat, S., and Ratanabanangkoon, K. (2003) Hyaluronidase inhibitors (sodium cromoglycate and sodium auro-thiomalate) reduce the local tissue damage and prolong the survival time of mice injected with Naja kaouthia and Calloselasma rhodostoma venoms. *Toxicon*, **42**, 635–646.

Yuan, Y.Y., Shi, Q.X., and Srivastava, P.N. (1995) Inhibition of rabbit sperm acrosomal enzymes by gossypol. *Mol. Reprod. Dev.*, **40**, 228–232.

Zaneveld, L.J., Waller, D.P., Anderson, R.A., Chany, C. 2nd, Rencher, W.F., Feathergill, K., Diao, X.H., Doncel, G.F., Herold, B., and Cooper, M. (2002) Efficacy and safety of a new vaginal contraceptive antimicrobial formulation containing high molecular weight poly (sodium 4-styrenesulfonate). *Biol. Reprod.*, **66**, 886–894.

CYCLOOXYGENASE-2 (COX-2) EXPRESSION IS AN INDEPENDENT PREDICTOR OF PROSTATE CANCER RECURRENCE

Brian L. Cohen[*,1], Pablo Gomez[*1], Yohei Omori[1], Robert C. Duncan[2], Mark S. Soloway[1], Vinata B. Lokeshwar[1,3,4] and Bal L. Lokeshwar[1,4,5¥]

Departments of Urology (1), Epidemiology and Public Health (2), Cell Biology & Anatomy (3), Sylvester Comprehensive Cancer Center (4), Radiation Oncology (5), Miller School of Medicine, University of Miami, Miami, Florida-33101

Running Title: COX-2 expression predicts prostate cancer recurrence

* Both authors (BLC and PG) contributed equally to this work.

¥Address for Correspondence:

Bal L. Lokeshwar, Ph.D.
Department of Urology (M-800)
P.O. Box 016960
Miami, Florida, 33101

Phone No. 305-243-1012; FAX NO. 305-243-6893

E-mail: blokeshw@med.miami.edu.

Key words:

Abbreviations used: COX-2: Cyclooxygenase-2; EPE: Extraprostatic extension; IHC: Immunohistochemistry; PSA: Prostate specific antigen; RP: radical prostatectomy; SV: Seminal vesicle

Text words (including abstract): 3425; Abstract words: 250; Figures: 2; Tables: 4; References: 59

ABSTRACT

Introduction: Lack of reliable prognostic markers hinders accurate prediction of disease progression in prostate cancer. The inducible pro-inflammatory enzyme Cyclooxygenase-2 (COX-2) is implicated in prostate carcinogenesis, but its role in cancer progression is less clear. We examined whether COX-2 expression evaluated by immunohistochemistry (IHC) in radical prostatectomy (RP) specimens can predict biochemical recurrence.

Experimental Design: Archival prostate cancer specimens (n=60) were obtained from patients who underwent RP, but had not received neo-adjuvant hormonal therapy. 23 patients had biochemical or clinical recurrence (mean time of recurrence: 38.2 months), and 37 patients were recurrence free (mean follow-up: 95 months). COX-2 expression was determined by IHC using an anti-COX-2 antibody. Three individuals scored the staining independently, as high- or low-expression.

Results: COX-2 was expressed in prostate cancer cells, and in adjacent normal glands, in specimens from patients who later progressed. At 62-months follow-up, COX-2 staining predicted progression with 82.4% sensitivity and 81.3% specificity. Sensitivity (86.4%) and specificity (86.7%) improved at $\geq$ 100-month follow-up. In univariate analysis, Gleason score, pre-operative PSA, extra-prostatic extension, margin, seminal vesicle invasion, and high COX-2 expression were significant predictors of biochemical recurrence ($P<0.05$). In multivariate analysis, pre-operative PSA (Hazard ratio/unit PSA change 1.080; $P = 0.0036$) and COX-2 expression (Hazard ratio 16.442; $P < 0.0001$) were independent prognostic indicators. Patients with PSA> 7 ng/ml and high COX-2 expression had the highest probability of recurrence (Kaplan-Meier analysis).

Conclusion: COX-2 expression is an independent predictor of prostate cancer progression following RP and underscores the significance of inflammatory factors in this process.

INTRODUCTION

Cyclooxygenase-1 (COX-1) and Cyclooxygenase-2 (COX-2) are prostaglandin endoperoxide synthases that are rate limiting enzymes in the conversion of the fatty acid arachidonic acid into physiologically active eicosanoids such as prostaglandin, thromboxane, and prostacyclin [1]. COX-2 is the inducible form of COX that is frequently elevated in cancer tissues [2-4]. Although the mechanism of COX-2 action in carcinogenesis or progression is not well established, COX-2 inhibitors have been shown to be chemopreventive in cancer, specifically in colorectal cancer [5-7].

The expression and role of COX-2 in prostate cancer has been a topic of several reports over the decade [reviewed in 8, 9]. There exists some controversy over the expression, detection and the putative role of COX-2 in prostate carcinogenesis and progression. While early studies reported high-level expression of COX-2 in prostate, findings from subsequent studies have been mixed [10-12]. Typically, later studies reported low or no expression in normal, benign prostatic hyperplasia or low-grade cancer tissues but elevated levels in prostatic intraepithelial neoplasia (PIN) and high-grade cancer [13-26]. A prominent study however discounted COX-2 specific staining in all epithelial tissues and claimed that COX-2 is expressed only in infiltrating lymphocytes and proliferative inflammatory atrophy [27]. Nonetheless, several studies using experimental models and established prostate cancer cell lines have established a chemopreventive and anti-tumor activity of COX-2 inhibitors, implying the putative role of COX-2 in prostate carcinogenesis [28-35].

A direct demonstration of potential role of COX-2 in advanced prostate cancer was recently demonstrated by one of us [36]. Using an anti-sense COX-2 cDNA construct (tetracycline-inducible model) to suppress COX-2 expression in PC-3ML cell line (a highly metastatic androgen unresponsive prostate cancer line) we demonstrated tumor-enhancing function of COX-2. In a related study we also showed chemosensitization of prostate tumor xenografts by a COX-2 inhibitor celecoxib, indicating a potential role of COX-2 in both carcinogenesis and resistance to treatment [37].

Until recently, elevated COX-2 levels were shown to be related to carcinogenesis but not progression as illustrated by its elevated levels in pre-neoplastic colon polyps, inflammatory atrophy and prostatic intraepithelial neoplasia. Moreover, the significance of the elevated expression of COX-2 was believed to be secondary to the elevation of several COX-2 inducing signaling mechanisms, notably the activated levels of Akt (phospho-AKT) [38, 39]) and nuclear-factor kappa B (NFkB) which activates COX-2 promoter and transcription [40-42]. The significance of COX-2 over-expression in disease progression, especially in prostate cancer, has evaded rigorous testing until now. This ambivalence is due to earlier studies that showed uneven labeling of COX-2 in prostate cancer tissues in archival samples. However, if COX-2 expression in prostate cancer specimens correlates with disease recurrence/progression, it may explain the conflicting results reported in various studies regarding COX-2 expression [10-27]. Investigating such a correlation is also important to understand prostate cancer progression because at least in experimental models of prostate cancer, COX-2 over-expression leads to increase in aggression of tumor cells, higher secretion of angiogenic factors and metastasis [43, 44]. In this study, we investigated COX-2 expression in archival radical prostatectomy specimens from 60 prostate cancer patients on whom a minimum 62-month follow-up was available. Our results show that COX-2 expression in

prostate cancer cells is an independent prognostic indicator for predicting biochemical recurrence.

MATERIALS AND METHODS
Specimens and study patients:

Sixty randomly selected prostate cancer specimens were obtained from patients who underwent radical retropubic prostatectomy between 1992 and 1995 at the University of Miami Medical Center, Miami, Florida. These patients did not receive neo-adjuvant hormonal therapy and 58 patients were node negative. The minimum available follow-up on all patients was 62 months. The study was conducted under a protocol approved by University of Miami's Institutional Review Board for human subjects' research. Of the 60 patients, 23 patients had biochemical or clinical recurrence (mean time to recurrence: 38.2 months; range: 1 to 121 months), and 37 patients were free of disease recurrence (mean follow-up: 95 months; range: 62 - 142 months). Biochemical recurrence was defined as a PSA level $\geq$ 0.4 ng/ml in 2 successive measurements after radical prostatectomy, in which case the first date of elevated PSA level was considered as the date of recurrence. The patient characteristics with respect to age, preoperative PSA, and tumor (i.e., Gleason sum, stage, margin, extra-prostatic extension (EPE) and seminal vesicle (SV) invasion) are shown in Table 1.

Immunohistochemistry and slide grading:

For all specimens, paraffin embedded blocks containing prostate cancer tissues representing the major Gleason score was selected. From each block, 6 slides were prepared and 2 were used for COX-2 staining. The other slides were used to either optimize COX-2 antibody concentration for staining, for determining non-specific staining, for repeating the staining in case of any discrepancy or for comparing COX-2 staining using antibodies from different companies (as discussed below). The specimen slides were de-paraffinized, rehydrated and treated with an antigen retrieval solution (Dako Laboratories). The slides were incubated with a rabbit polyclonal anti-human COX-2 IgG, PG-27b (200-fold dilution of the antiserum; Oxford Biomedical Res., Oxford, MI) at 4^0 C for 16 hours. Following incubation the slides were washed and incubated with a linking solution containing a biotinylated swine anti-rabbit IgG (Dako LSAB kit) at room temperature for 30 min. The slides were then treated with streptavidin peroxidase and DAB chromogen. The slides were counterstained with hematoxylin, dehydrated and mounted.

Initially about 20 specimens were stained with anti-COX-2 antibodies from Santa Cruz Biotechnology (Santa Cruz, CA) and Cayman Chemical (Ann Arbor, MI) along with the PG-27b antibody to evaluate the specificity of different antibodies. We also evaluated 10 specimens for COX-2 staining using a non-biotin-based Envision kit, as per the manufacturer's protocol (DAKO Laboratories).

Slide grading: COX-2 staining of tumor cells in each slide was initially graded as 0 to 3+. To account for heterogeneity in staining, the overall staining grade for each slide was assigned based on the staining intensity of the majority of the tumor tissue in the specimen. However, if $\sim$ 50% of the tumor cells in the section were assigned +1 staining, and the other 50% as 3+, the overall staining grade was 2+. If the staining distribution was, $\sim$ 50% of the tumor cells staining 2+ and the remaining staining as 3+, the overall staining inference assigned were 3+. The staining was later grouped as low- and high-grade staining. High-grade staining represented 2+ and 3+ staining, whereas low-grade staining included 0 and 1+ staining intensities. Normal-benign tissues near and away from tumor cells were also evaluated for staining intensity and graded as low- and high-staining. Two readers independently evaluated all slides in a blinded fashion. Out of the total 60 stained slides, there was discrepancy in 8 slides. These discrepancies were resolved by both readers reexamining those slides simultaneously. In

addition, to check for the repeatability of the evaluation system, a 3rd reader, after familiarizing with the grading system, randomly picked 40 slides and graded them for staining intensity. The discrepancy in slide evaluations by the 3rd reader was < 10%.

Statistical Analysis:

For COX-2 staining, high-grade staining was considered as a true positive if the patient had biochemical recurrence. Consequently, low-grade staining was considered as a true negative, if the patient had no biochemical recurrence. The sensitivity, specificity, accuracy, positive predictive value (PPV), and negative predictive value (NPV) for COX-2 staining inferences were calculated using the 2 x 2 contingency table (high-grade/low-grade staining and progressed/non-progressed CaP patients) at 62, 72, and 100 month cut-off limits [45]. The data on various, biochemical, surgical, and pathologic parameters, as well as COX-2 staining inferences, were analyzed by Cox proportional hazard model, using single variable analysis (univariate analysis) or step-wise selection (multivariate) analysis. Stratified Kaplan-Meier analyses were performed on the variables that were found to be significant in the multivariate Cox Proportional Hazard model. For PSA subset analysis, Mantael-Haenszel Chi-square analysis or Student's t test were used to determine statistical significance. Statistical analysis was carried out using the SAS Software Program (version 8.02; SAS Institute, Cary, NC).

RESULTS:

Localization of COX-2 in prostate cancer tissues:

Previous studies on the localization of COX-2 in prostate cancer cells or tissues have used anti-COX-2 antibodies from at least 3 different commercial sources (i.e., Oxford Biomedical Research; Cayman Chemical and Santa Cruz Biotechnology [13, 17, and 19]). Among these antibodies, a 1:200 dilution of the PG-27b anti-COX-2 antibody from Oxford Biomedical Research was specific in localizing COX-2 in prostate cancer tissues and yielded optimal staining intensity. As reported previously, we also determined the ability of PG27b to localize COX-2 in archival prostate tissues using a non-biotin based immunohistochemical method (Envision Plus; [13]). However, this method yielded only weak to no staining in any prostate glands (i.e., normal-benign or cancer) from recurred or non-recurred patients. Therefore, we used PG27b antibody at 1: 200 dilution to stain all of the 60 archival prostate cancer tissues.

The 60 archival tissues used in this study were from patients with prostate cancer, who either had biochemical recurrence or did not, in a mean follow-up of up to 95 months. As shown in **Figure 1A**, very little COX-2 staining is observed in prostate cancer cells from two patients with either Gleason 7 (panel a̲) or Gleason 8 (panel c̲) prostate cancer, and who had no biochemical recurrence within 62 months. Among 43 patients with prostate cancer, who did not have biochemical recurrence in 62 months, specimens from 35 patients showed low-grade staining. **Figure 1A** also shows high-grade staining in prostate cancer cells of two different patients with either Gleason 7 (panel b̲) or Gleason 8 (panel d̲) prostate cancer, and who had biochemical recurrence within 62 months (mean time to recur 38 months). Among the 17 patients who had biochemical recurrence within 62 months, 14 had high-grade staining in their specimens.

We next examined COX-2 staining in normal-benign glands. As shown in **Figure 1B**, normal-benign glands that are away from prostate cancer cells have low-grade staining, regardless of whether the specimen was obtained from a patient who did not recur (panel a̲) or recurred within 62 months (panel b̲). However, the normal-benign gland that is adjacent to tumor cells shows high-grade staining, if the specimen was obtained from a patient who recurred (panel d̲). The normal-benign glands adjacent to tumor cells do not stain for COX-2, if the

5

specimen was obtained from a patient who did not recur (panel c).   These results show that COX-2 expression in prostate cancer cells is related to disease progression and that normal prostate epithelial cells also express COX-2, if they are adjacent to prostate cancer cells which have malignant potential.

Determination of sensitivity, specificity, accuracy, PPV and NPV of COX-2 staining:

On all patients a minimum follow-up of 62 months was available (mean follow-up: 95 months; range: 62 - 142 months). We therefore determined the sensitivity, specificity, accuracy, PPV and NPV of COX-2 staining at 62 months, 72 months and 100 months of follow-up. As shown in Table 2, the sensitivity of COX-2 staining ranges from 82% to 86% between 62 and 100 months of follow-up. Out of the 23 patients who recurred, one recurred after 121 months and the COX-2 staining in the specimen was low-grade. Thus, the overall sensitivity for all 23 patients at 121 months is 82.6%. The specificity of COX-2 staining at 62 months is 81% but it increases to 84% and 86.7% at 72 and 100 months, respectively. The increased specificity is because, 5 of the patients who were false positive at 62-month follow-up had a biochemical recurrence within 62 to 100 month of follow-up (Table 2). Consequently, the accuracy of COX-2 staining also increases from 81.6% at 62 months to 86.5% at 100 months of follow-up. Similarly, the PPV of the COX-staining increases significantly from 62 months (PPV, 63.6%) to 100 months (PPV, 90.5%) of follow-up. The NPV of COX-2 staining decreases by about 10% at 100 months of follow-up, which might be due to the low number of patients in the non-recurred category for that follow-up.

Evaluating the prognostic potential of pre- and post-operative parameters and COX-2 staining in prostate specimens:

Univariate analysis: Since the patients in this cohort had variable follow-up between 62 and 142 months, we used the Cox proportional hazards model and single-parameter analysis to determine the prognostic significance of each of the preoperative (i.e., age, PSA and clinical stage) and postoperative (i.e., Gleason sum, margin, EPE, SV invasion) parameters, as well as staining inferences of COX-2. As shown in Table 3, age and clinical stage are not significant in predicting biochemical recurrence. However, pre-operative PSA, Gleason sum, margin status, EPE, SV invasion and COX-2 staining inferences significantly predict biochemical recurrence (Table 3).

Multivariate analysis: To determine the smallest number of variables that could jointly predict biochemical recurrence in this cohort of patients, we used the Cox proportional hazards model and step-wise selection analysis. When age, preoperative PSA, clinical stage, Gleason sum, EPE, SV invasion and COX-2 staining inference were included in the model, only preoperative PSA (P = 0.0036, hazard ratio/unit PSA change = 1.08), and COX-2 staining inference (P < 0.0001, hazard ratio = 16.442) reached statistical significance in predicting biochemical recurrence (Table 4).

To demonstrate the joint effect of COX-2 and pre-operative PSA on biochemical recurrence, we performed Kaplan-Meier analysis. Since PSA was a continuous estimate, with the median PSA level for the entire cohort of patients (n = 60) as 6.9 ng/ml, we divided the cohort into those with PSA levels ≤ 7 and > 7 ng/ml. As shown in Figure 2, individuals with COX-2 staining high and PSA > 7 ng/ml had the highest probability of recurrence, followed by those with COX-2 high and PSA ≤ 7 ng/ml. Individuals with low COX-2 staining and either PSA > 7 ng/ml or ≤ 7 ng/ml had the lowest probability of recurrence.

PSA subgroup analysis: It has been suggested that biochemical recurrence before 24 months indicates systemic disease, whereas biochemical recurrence beyond 24 months suggests local

6

recurrence [46]. By Mantel-Haenszel *chi-square* analysis we found that COX-2 staining inferences could distinguish between PSA recurrence before and after 24 months in a statistically significant manner (P < 0.0001; *chi-square*, 16.7812).

DISCUSSION

There are few reliable markers for accurate prediction of prostate cancer recurrence besides pre-operative PSA and Gleason sum [43]. However, nearly two thirds of patients diagnosed with prostate cancer have the preoperative PSA range 4 ng/ml to 10 ng/ml, with T1C disease and a biopsy Gleason score of 5 to 7 [47-49]. For such patients, one or a combination of accurate prognostic indicators could improve the physicians' ability to identify aggressive disease, so that more individualized treatments could be offered. In this study, pre-operative PSA level and COX-2 expression were found to provide independent prognostic information.

In specimens from prostate cancer patients who later progressed, normal-benign prostate glands adjacent to highly stained tumor cells also showed high-level COX-2 expression, indicating a paracrine mechanism of COX-2 induction. Therefore, it is likely that factors, which induce COX-2 enzyme, may also be potential markers for predicting progression. Identifying such a factor or factors is likely to be daunting because of the promiscuity of COX-2 induction. Several cytokines, chemokines and inflammatory enzymes are known to induce COX-2 expression [50-52].

The data analysis presented above for COX-2 staining intensity show for the first time that COX-2 expression, can independently predict prostate cancer recurrence. The sensitivity, specificity and accuracy of COX-2 staining to predict biochemical recurrence exceeded 80% at 62 to 100 month follow-up after radical prostatectomy. Furthermore, both univariate and multivariate analyses showed significant association of COX-2 over expression and biochemical recurrence. Kaplan-Meier analysis shows that prostate cancer patients with high COX-2 expression and PSA > 7 ng/ml have the highest probability of disease progression. This explains why the multivariate analysis selected COX-2 staining inference and pre-operative PSA as independent prognostic indicators. The data also show that prostate cancer patients with PSA > 7 ng/ml could be further classified based on the COX-2 staining in their prostate cancer specimens to predict biochemical recurrence. In this study, biochemical recurrence indicates the possibility of developing metastatic disease, since all of the study patients underwent radical prostatectomy, rising PSA levels would indicate either local or distant metastases. The high sensitivity, specificity and positive predictive value (63%-93%) of COX-2 expression point to the possibility that future treatment should consider inhibition of inflammatory pathways either at the time of initial treatment or together with androgen ablation during the treatment of residual disease [53].

The findings presented in this report are consistent with studies conducted on pre-clinical models of prostate cancer. For example, Fujita et al [41] reported that forced expression of COX-2 in a relatively indolent LNCaP tumor model increases tumor growth, angiogenesis and PSA secretion, without increasing androgen receptor levels or activity. Since, increased angiogenesis results in increased invasion and metastasis, increased COX-2 expression may be predictive of disease progression in prostate cancer patients. Our earlier work also showed that suppression of COX-2 by anti-sense cDNA transfection in an aggressive tumor model (PC-3ML) reduces tumor growth and increases apoptosis *in vivo* [37].

Earlier studies on IHC localization and semi-quantitative estimation of COX-2 expression concluded that COX-2 expression has limited association with stage, and disease severity (local

7

invasion) but it strongly associates with tumor grade [10-15]. On contrary, some reports have dismissed any association with tumor grade and have suggested that COX-2 is expressed by infiltrating lymphocytes and macrophage, which occurs during inflammatory atrophy of the prostate [13]. However, none of these reports analyzed COX-2 expression with respect to biochemical recurrence (i.e., disease progression). Consistent with earlier studies, we also did not find any correlation between COX-2 expression and tumor grade and stage (P > 0.05, *chi-square* analysis). In fact, the inclusion of COX-2 staining inferences in the multivariate model eliminated the prognostic significance of all clinical and pathologic parameters except pre-operative PSA.

Although, the expression of COX-2 with prostate cancer is controversial in several cancers COX-2 expression has been shown to associate with disease progression, poor response to treatment and survival. For example, in non-Hodgkin's lymphoma, high COX-2 expression correlates with increased stage, lower survival and lower complete response rate to therapy [54]. In breast cancer, COX-2 over-expression occurs in 43% of human invasive breast cancers and 63% of ductal carcinomas *in situ* [55]. Furthermore, high expression of COX-2 associates with decreased disease specific survival [56]. In gastric cancer, COX-2 is expressed not only in cancer cells but also in precancerous lesions such as metaplastic and adenomatous cells, suggesting that COX-2 over-expression is an early event in gastric cancer development [57]. In bladder cancer, COX-2 expression in carcinoma in situ significantly associates with disease recurrence and progression but it is not associated with survival [58, 59]. However, among bladder cancer patients who receive systemic chemotherapy, strong COX-2 expression significantly correlates with poor overall survival [59]. These studies support the notion that COX-2 expression and inflammatory processes are involved in cancer progression.

Taken together, this study shows that COX-2 expression in prostate cancer correlates with aggressive disease and is an independent prognostic indicator of biochemical recurrence. The results of our study also suggest that the inhibition of inflammatory processes may be an effective means of controlling prostate cancer progression.

REFERENCES

1. Vane JR, Bakhle YS, Botting RM. Cyclooxygenases 1 and 2. Annu Rev Pharmacol Toxicol. 1998;38:97-120.
2. Dubois RN, Abramson SB, Crawford L, et al. Cyclooxygenase in biology and disease. FASEB J 1998; 12: 1063-1073.
3. Fosslien, E. Molecular pathology of cyclooxygenase-2 in neoplasia Ann Clin Lab Sci 2000; **30:** 3-21.
4. Zha S, Yegnasubramanian V, Nelson WG, Isaacs WB, De Marzo AM. Cyclooxygenases in Cancer: progress and perspective. Cancer Lett 2004;215:1-20.
5. Steinbach G, Lynch PM, Phillips RK, Wallace MH, Hawk E, Gordon GB, Wakabayashi N, Saunders B, Shen Y, Fujimura T, Su LK, Levin B. The effect of celecoxib, a cyclooxygenase-2 inhibitor, in familial adenomatous polyposis. N Engl J Med. 2000 Jun 29;342(26):1946-52.
6. Gupta RA, Dubois RN. Colorectal cancer prevention and treatment by inhibition of cyclooxygenase-2.Nat Rev Cancer. 2001 Oct;1(1):11-21.
7. DuBois RN. Cyclooxygenase-2 and colorectal cancer. Prog Exp Tumor Res. 2003; 37:124-37.
8. O'Neill GP, Ford-Hutchinson AW. Expression of mRNA for cyclooxygenase-1 and cyclooxygenase-2 in human tissues. FEBS Lett. 1993 Sep 13;330(2):156-60.

9. Pruthi RS, Derksen E, Gaston K. Cyclooxygenase-2 as a potential target in the prevention and treatment of genitourinary tumors: a review. J Urol 2003; 169:2352-2359.
10. Gupta S, Srivastava M, Ahmad N, Bostwick DG, Mukhtar H. Over-expression of cyclooxygenase-2 in human prostate adenocarcinoma. Prostate. 2000 Jan;42(1):73-8.
11. Yoshimura R, Sano H, Masuda C, Kawamura M, Tsubouchi Y, Chargui J, Yoshimura N, Hla T, Wada S. Expression of cyclooxygenase-2 in prostate carcinoma. Cancer. 2000 Aug 1;89(3):589-96.
12. Uotila P, Valve E, Martikainen P, Nevalainen M, Nurmi M, Harkonen P. Increased expression of cyclooxygenase-2 and nitric oxide synthase-2 in human prostate cancer. Urol Res. 2001 Feb;29(1):23-8.
13. Zha S, Gage WR, Sauvageot J, Saria EA, Putzi MJ, Ewing CM, Faith DA, Nelson WG, De Marzo AM, Isaacs WB. Cyclooxygenase-2 is up-regulated in proliferative inflammatory atrophy of the prostate, but not in prostate carcinoma. Cancer Res. 2001 Dec 15;61(24):8617-23.
14. Hussain T, Gupta S, Mukhtar H. Cyclooxygenase-2 and prostate carcinogenesis. Cancer Lett. 2003 Mar 10;191(2):125-35.
15. Kirschenbaum A, Liotta DR, Yao S, Liu XH, Klausner AP, Unger P, Shapiro E, Leav I, Levine AC. Immunohistochemical localization of cyclooxygenase-1 and cyclooxygenase-2 in the human fetal and adult male reproductive tracts. J Clin Endocrinol Metab. 2000 Sep;85(9):3436-41.
16. Kirschenbaum A, Klausner AP, Lee R, Unger P, Yao S, Liu XH, Levine AC. Expression of cyclooxygenase-1 and cyclooxygenase-2 in the human prostate. Urology. 2000 Oct 1;56(4):671-6.
17. Subbarayan V, Sabichi AL, Llansa N, Lippman SM, Menter DG. Differential expression of cyclooxygenase-2 and its regulation by tumor necrosis factor-alpha in normal and malignant prostate cells. Cancer Res. 2001 Mar 15;61(6):2720-6.
18. Lee LM, Pan CC, Cheng CJ, Chi CW, Liu TY. Expression of cyclooxygenase-2 in prostate adenocarcinoma and benign prostatic hyperplasia. Anticancer Res. 2001 Mar-Apr;21(2B):1291-4.
19. Kirschenbaum A, Liu X, Yao S, Levine AC. The role of cyclooxygenase-2 in prostate cancer. Urology. 2001 Aug;58(2 Suppl 1):127-31.
20. Shappell SB, Manning S, Boeglin WE, Guan YF, Roberts RL, Davis L, Olson SJ, Jack GS, Coffey CS, Wheeler TM, Breyer MD, Brash AR. Alterations in lipoxygenase and cyclooxygenase-2 catalytic activity and mRNA expression in prostate carcinoma. Neoplasia. 2001 Jul-Aug;3(4):287-303.
21. Liu XH, Kirschenbaum A, Lu M, Yao S, Klausner A, Preston C, Holland JF, Levine AC. Prostaglandin E(2) stimulates prostatic intraepithelial neoplasia cell growth through activation of the interleukin-6/GP130/STAT-3 signaling pathway. Biochem Biophys Res Commun. 2002 Jan 11;290(1):249-55.
22. Fujita H, Koshida K, Keller ET, Takahashi Y, Yoshimito T, Namiki M, Mizokami A. Cyclooxygenase-2 promotes prostate cancer progression. Prostate. 2002 Nov 1;53(3):232-40.
23. Konig JE, Senge T, Allhoff EP, Konig W. Analysis of the inflammatory network in benign prostate hyperplasia and prostate cancer. Prostate. 2004 Feb 1;58(2):121-9.
24. Nye D, Che M, Zacharek A, Qiao Y, Li L, Li X, Lamberti M, Tang K, Cai Y, Guo Y, Grignon D, Honn KV. Differential expression of thromboxane synthase in prostate carcinoma: role in tumor cell motility. Am J Pathol. 2004 Feb;164(2):429-39.
25. Wang W, Bergh A, Damber JE. Chronic inflammation in benign prostate hyperplasia is associated with focal upregulation of cyclooxygenase-2, Bcl-2, and cell proliferation in the glandular epithelium. Prostate. 2004 Sep 15;61(1):60-72.

26. Di Lorenzo G, De Placido S, Autorino R, De Laurentiis M, Mignogna C, D'Armiento M, Tortora G, De Rosa G, D'Armiento M, De Sio M, Bianco AR, D'Armiento FP. Expression of biomarkers modulating prostate cancer progression: implications in the treatment of the disease. Prostate Cancer Prostatic Dis. 2005;8(1):54-9.

27. Zha S, Gage WR, Sauvageot J, Saria EA, Putzi MJ, Ewing CM, Faith DA, Nelson WG, De Marzo AM, Isaacs WB. Cyclooxygenase-2 is up-regulated in proliferative inflammatory atrophy of the prostate, but not in prostate carcinoma. Cancer Res. 2001 Dec 15; 61(24):8617-23.

28. Liu XH, Yao S, Kirschenbaum A, Levine AC. NS398, a selective cyclooxygenase-2 inhibitor, induces apoptosis and down-regulates bcl-2 expression in LNCaP cells. Cancer Res. 1998 Oct 1;58(19):4245-9.

29. Attiga FA, Fernandez PM, Weeraratna AT, Manyak MJ, Patierno SR. Inhibitors of prostaglandin synthesis inhibit human prostate tumor cell invasiveness and reduce the release of matrix metalloproteinases. Cancer Res. 2000 Aug 15;60(16):4629-37

30. Hong SH, Avis I, Vos MD, Martinez A, Treston AM, Mulshine JL. Relationship of arachidonic acid metabolizing enzyme expression in epithelial cancer cell lines to the growth effect of selective biochemical inhibitors. Cancer Res. 1999 May 1;59(9):2223-8.

31. Liu XH, Kirschenbaum A, Yao S, Lee R, Holland JF, Levine AC. Inhibition of cyclooxygenase-2 suppresses angiogenesis and the growth of prostate cancer in vivo. J Urol. 2000 Sep;164(3 Pt 1):820-5.

32. Narayanan BA, Condon MS, Bosland MC, Narayanan NK, Reddy BS. Suppression of N-methyl-N-nitrosourea/testosterone-induced rat prostate cancer growth by celecoxib: effects on cyclooxygenase-2, cell cycle regulation, and apoptosis mechanism(s). Clin Cancer Res. 2003 Aug 15;9(9):3503-13. Shappell SB, Olson SJ, Hannah SE, et al. Elevated expression of 12/15-lipoxygenase and cyclooxygenase-2 in a transgenic mouse model of prostate carcinoma. Cancer Res. 2003 May 1;63(9):2256-67.

33. Gupta S, Adhami VM, Subbarayan M, MacLennan GT, Lewin JS, Hafeli UO, Fu P, Mukhtar H. Suppression of prostate carcinogenesis by dietary supplementation of celecoxib in transgenic adenocarcinoma of the mouse prostate model. Cancer Res. 2004 May 1;64(9):3334-43.

34. Pruthi RS, Derksen JE, Moore D. A pilot study of use of the cyclooxygenase-2 inhibitor celecoxib in recurrent prostate cancer after definitive radiation therapy or radical prostatectomy. BJU Int. 2004 Feb;93(3):275-8.

35. Lieberman R. Chemoprevention of prostate cancer: current status and future directions. Cancer Metastasis Rev. 2002;21(3-4):297-309.

36. Dandekar DS, Lokeshwar BL. Inhibition of cyclooxygenase (COX)-2 expression by Tet-inducible COX-2 antisense cDNA in hormone-refractory prostate cancer significantly slows tumor growth and improves efficacy of chemotherapeutic drugs. Clin Cancer Res. 2004 Dec 1;10(23):8037-47.

37. Dandekar DS, Lopez M, Carey R, Lokeshwar BL. Cyclooxygenase-2 inhibitor celecoxib augments chemotherapeutic drug induced apoptosis by enhancing activation of caspase-3 and -9 in prostate cancer. Internatl J Cancer. 2005; 115:484-492.

38. Malik SN, Brattain M, Ghosh PM, Troyer DA, Prihoda T, Bedolla R, KreisbergJI. Immunohistochemical demonstration of phospho-Akt in high Gleason grade prostate cancer. Clin Cancer Res. 2002; 8(4):1168-71.

39. Kreisberg JI, Malik SN, Prihoda TJ, Bedolla RG, Troyer DA, Kreisberg S, Ghosh PM. Phosphorylation of Akt (Ser473) is an excellent predictor of poor clinical outcome in prostate cancer. Cancer Res. 2004;64(15):5232-6.

40. Hsu AL, Ching TT, Wang DS, Song X, Rangnekar VM, Chen CS. The cyclooxygenase-2 inhibitor celecoxib induces apoptosis by blocking Akt activation in human prostate cancer cells independently of Bcl-2. J Biol Chem. 2000 Apr 14;275(15):11397-403.

41. Smith WL, DeWitt DL, Garavito RM. Cyclooxygenases: structural, cellular, and molecular biology. Annu Rev Biochem. 2000;69:145-82.
42. St-Germain ME, Gagnon V, Parent S, Asselin E. Regulation of COX-2 protein expression by Akt in endometrial cancer cells is mediated through NF-kappaB/IkappaB pathway. Mol Cancer. 2004; 3(1):7.
43. Fujita H, Koshida K, Keller ET, et al. Cyclooxygenase-2 promotes prostate cancer progression. Prostate 2002; 53:232-240.
44. Tomozowa S, Tsuno NH, Sunami E, et al. Cyclooxygenase-2 overexpression correlates with tumor recurrence, especially haematogenous metastasis, of colorectal cancer. Br J Cancer 2000; 83 (3):324-328.
45. Eckici, S., Cerwinka, W.H., Duncan, R., Gomez, P., Civantos, F., Soloway, M.S., and Lokeshwar, V.B. Comparison of the prognostic potential of hyaluronic acid, hyaluronidase (HYAL-1), CD44v6 and microvessel density for prostate cancer. Int J Cancer, 112: 121 – 129, 2004.
46. Swindle PW, Kattan MW, Scardino PT. Markers and meaning of primary treatment failure. Urol Clin North Am 2003;30(2):377-401.
47. Draisma G, Boer R, Otto SJ et al. Lead times and overdetection of due to prostate-specific antigen screening: estimates from the European Randomized Study of Screening for Prostate Cancer (ERSCPC). J Natl Cancer Inst 2003; 95:868-78.
48. Blute ML, Bergstralh EJ, Iocca A, Scherer B, Zincke H. Use of Gleason score, prostate specific antigen, seminal vesicle and margin status to predict biochemical failure after radical prostatectomy. J Urol 2001; 165:119-25.
49. Pettaway CA. Prognostic markers in clinically localized prostate cancer. Tech Urol. 1998;4:35-48.
50. Canto EI, Shariat SF, Slawin KM. Biochemical staging of prostate cancer. Urol Clin North Am 2003; 30(2):263-77.
51. Wu KK. Control of cyclooxygenase-2 transcriptional activation by pro-inflammatory mediators. Prostaglandins Leukot Essent Fatty Acids. 2005 ;72(2):89-93.
52. Madaan S, Abel PD, Chaudhary KS, Hewitt R, Stott MA, Stamp GW, Lalani EN. Cytoplasmic induction and over-expression of cyclooxygenase-2 in human prostate cancer: implications for prevention and treatment. BJU Int. 2000; 86(6):736-41.
53. Dreicer R. The evolving role of hormone therapy in advanced prostate cancer. Cleve Clin J Med. 2000;67(10):720-2, 725-6.
54. Hazar B, Ergin M, Seyrek E, Erdogan S, Tuncer I, Hakverdi S. Cyclooxygenase-2 (Cox-2) expression in lymphomas. Leuk Lymphoma. 2004 Jul;45(7):1395-9.
55. Wang D, Dubois RN. Cyclooxygenase-2: a potential target in breast cancer. Semin Oncol. 2004 Feb;31(1 Suppl 3):64-73.
56. Sivula A, Talvensaari-Mattila A, Lundin J, et al. Association of cyclooxygenase-2 and matrix metalloproteinase-2 expression in human breast cancer. Breast Cancer Res Treat. 2005 Feb;89(3):215-20.
57. Lim HY, Joo HJ, Choi JH, Yi JW, Yang MS, Cho DY, Kim HS, Nam DK, Lee KB, Kim HC. Increased expression of cyclooxygenase-2 protein in human gastric carcinoma. Clin Cancer Res. 2000 Feb;6(2):519-25.
58. Shariat SF, Kim JH, Ayala GE, Kho K, Wheeler TM, Lerner SP. Cyclooxygenase-2 is highly expressed in carcinoma in situ and T1 transitional cell carcinoma of the bladder. J Urol. 2003 Mar;169(3):938-42.
59. Wulfing C, Eltze E, von Struensee D, Wulfing P, Hertle L, Piechota H. Cyclooxygenase-2 expression in bladder cancer: correlation with poor outcome after chemotherapy. Eur Urol. 2004 Jan;45(1):46-52.

Table 1: Pre- and postoperative parameters of the study patients. [1] EPE = extra-prostatic extension of tumor. [2] SV = seminal vesicle invasion. [3]Two patients who had biochemical recurrence had positive lymph nodes. [4] Three of the patients had only designation of tumor stage as T2.

Preoperative parameters				Postoperative parameters			
Progression	Age (yrs)	PSA (ng/ml)	Clinical Stage	Gleason sum	[1]EPE	Margin	[2]SV invasion
Biochemical recurrence (n = 23)[3]	Median: 66 Mean: 65.0	Median: 8.9 Mean: 12.1	T1c: 11 T2a: 3 T2b: 9	6 = 2 7 = 11 8 = 5 9 = 5	(+) = 17 (-) = 6	(+) = 15 (-) = 8	(+) = 9 (-) = 14
No biochemical or clinical recurrence (n = 37)	Median: 63 Mean: 62.8	Median: 6.3 Mean: 6.3	T1c: 23 T2a: 9 T2b: 2 [4]T2 : 3	4 = 1 5 = 4 6 = 8 7 = 21 8 = 2 9 = 1	(+) = 6 (-) = 31	(+) = 11 (-) = 26	(+) = 2 (-) = 35

Table 2: The sensitivity, specificity, accuracy, PPV and NPV of COX-2 staining inferences. Note that 62 months, 72 months, and 100 months were used a cut point for determining biochemical recurrence.

Parameter	62 Months (%)	72 Months (%)	100 Months (%)
Sensitivity	82.4 (14/17)	84.2 (16/19)	86.4 (19/22)
Specificity	81.3 (35/43)	84.6 (33/39)	86.7 (13/15)
Accuracy	81.6 (49/60)	84.5 (49/58)	86.5 (32/37)
PPV	63.6 (14/22)	72.7 (16/22)	90.5 (19/21)
NPV	92.1 (35/38)	91.6 (33/36)	81.3 (13/16)

Table 3: Univariate analysis of pre- and post-operative prognostic parameters and IHC staining inferences. *: Statistically significant. CI: Confidence Interval. Cox proportional hazard model and single parameter analysis was used to determine the prognostic significance of pre-operative (age, pre-operative PSA, and clinical stage) and post-operative (Gleason sum, margin +/-, EPE +/-, SV invasion +/-) parameters and COX-2 staining inferences.

Parameter	*Chi-square*	P-value	Hazard Ratio	95% CI
Gleason sum	14.9131	0.0001*	2.314	1.512-3.543
Age	1.5032	0.2202	1.045	0.974-1.120
Pre-operative PSA	22.1515	<0.0001*	1.138	1.078-1.201
Stage	1.2109	0.2712	1.584	0.698-3.593
EPE	18.9354	<0.0001*	8.054	3.147-20.612
Positive Surgical Margin	7.1743	0.0074*	3.240	1.371-7.660
SV invasion	14.1786	0.0002*	5.331	2.231-12.737
COX-2 Expression	23.4676	<0.0001*	20.868	6.104-71.338

Table 4: Multivariate analysis of pre- and post-operative prognostic parameters and IHC staining inferences. Cox proportional hazard model and step-wise selection was used to determine which of the pre-operative (i.e., age, PSA and clinical stage) and post-operative (i.e., Gleason sum, EPE, margin +/-, and SV invasion) parameters and Cox-2 staining inferences have independent prognostic significance. The significant parameters (P > 0.05) selected by the model are shown.

Parameter	*Chi-square*	P-value	Hazard Ratio	95% CI
Pre-op PSA	8.4813	0.0036	1.080	1.021-1.143
COX-2 Expression	45.4154	<0.0001	16.442	4.656-58.067

15

Figure Legends

Figure 1A: Localization of COX-2 in prostate cancer tissues. COX-2 was localized in prostate cancer tissues from non-progressed patients (panels a and c) and progressed patients (panels b and d) using anti-COX-2 antibody and immunohistochemistry. Panels a and b: Gleason sum 7 prostate cancer specimens. Panels c and d: Gleason 8 prostate cancer specimens. The each panel represents 400X magnification.

Figure 1B: Localization of COX-2 in normal-benign prostate glands. COX-2 expression was examined in normal-benign prostate glands, which are either adjacent to tumor or away from it. Panels a and b: Normal-benign glands away from tumor. Panels C and D: Normal-benign glands adjacent to tumor. Panels a and c: Specimen from a patient with Gleason sum 7 prostate cancer, who did not progress. Panels b and d: Specimen from a patient with Gleason sum 7 prostate cancer, who progressed.

Figure 2: Kaplan-Meier analysis. Kaplan-Meier analysis was performed after stratifying the data as COX-2 high (H)/Low (L), and PSA < or < 7 ng/ml.